

# CP Violation in the $B$ System and Relations to $K \rightarrow \pi\nu\bar{\nu}$ Decays

ROBERT FLEISCHER\*

*Deutsches Elektronen-Synchrotron DESY, Notkestr. 85,  
D-22607 Hamburg, Germany*

## Abstract

A review of CP violation in the  $B$  system and strategies to determine the unitarity triangle of the CKM matrix is given. We begin with an introduction to the description of CP violation in the Standard Model of electroweak interactions, and discuss the basic features of the theoretical framework to deal with non-leptonic  $B$  decays, which play the main rôle in this review. After a brief look at CP violation in the kaon system and a discussion of the rare decays  $K^+ \rightarrow \pi^+\nu\bar{\nu}$  and  $K_L \rightarrow \pi^0\nu\bar{\nu}$ , we turn to the formalism of  $B_{d,s}^0-\overline{B_{d,s}^0}$  mixing, allowing us to explore important  $B$ -factory benchmark modes and the  $B_s$ -meson system. We then focus on charged  $B$  decays,  $B \rightarrow \pi K$  modes and the phenomenology of  $U$ -spin related  $B$  decays, including the  $B_d \rightarrow \pi^+\pi^-$ ,  $B_s \rightarrow K^+K^-$  system. Finally, we discuss a particularly simple – but very predictive – scenario for new physics, which is provided by models with “minimal flavour violation”. In this framework, various bounds can be derived and interesting connections between the  $B$  system and the rare kaon decays  $K^+ \rightarrow \pi^+\nu\bar{\nu}$  and  $K_L \rightarrow \pi^0\nu\bar{\nu}$  arise.

(To appear in *Physics Reports*)

---

\*E-mail: Robert.Fleischer@desy.de



# Contents

<b>1</b>	<b>Introduction</b>	<b>1</b>
1.1	Motivation . . . . .	1
1.2	CP Violation in Cosmology and Beyond $K$ and $B$ Decays . . . . .	2
1.3	Outline . . . . .	3
<b>2</b>	<b>CP Violation in the Standard Model</b>	<b>4</b>
2.1	Charged-Current Interactions . . . . .	4
2.2	The Strong CP Problem . . . . .	5
2.3	Parametrizations of the CKM Matrix . . . . .	5
2.3.1	Standard Parametrization . . . . .	6
2.3.2	Fritzsch–Xing Parametrization . . . . .	7
2.3.3	Wolfenstein Parametrization . . . . .	7
2.4	Requirements for CP Violation . . . . .	9
2.5	The Unitarity Triangles of the CKM Matrix . . . . .	9
2.6	Towards an Allowed Range in the $\bar{\rho}$ – $\bar{\eta}$ Plane . . . . .	12
<b>3</b>	<b>Non-leptonic <math>B</math> Decays</b>	<b>16</b>
3.1	Preliminaries . . . . .	16
3.2	Classification . . . . .	16
3.3	Low-energy Effective Hamiltonians . . . . .	17
3.3.1	General Remarks . . . . .	17
3.3.2	Tree Decays . . . . .	18
3.3.3	Decays with Tree and Penguin Contributions . . . . .	22
3.4	Penguins with Internal Charm- and Up-Quark Exchanges . . . . .	25
3.5	Electroweak Penguin Effects . . . . .	27
3.6	Factorization of Hadronic Matrix Elements . . . . .	28
<b>4</b>	<b>A Brief Look at the Kaon System</b>	<b>29</b>
4.1	CP-violating Observables . . . . .	30
4.2	The Rare Decays $K^+ \rightarrow \pi^+ \nu \bar{\nu}$ and $K_L \rightarrow \pi^0 \nu \bar{\nu}$ . . . . .	32
<b>5</b>	<b>Time Evolution of Neutral <math>B</math> Decays</b>	<b>34</b>
5.1	Solution of the Schrödinger Equation . . . . .	34
5.2	Mixing Parameters and Decay Rates . . . . .	36
5.3	Determination of $R_t$ from $\Delta M_d$ . . . . .	37
5.4	CP-violating Asymmetries . . . . .	38
5.5	Impact of Physics Beyond the Standard Model . . . . .	40

<b>6</b>	<b>Important Benchmark Modes for the <math>B</math>-Factories</b>	<b>42</b>
6.1	The $B \rightarrow J/\psi K$ System . . . . .	42
6.1.1	Extracting $\beta$ from $B_d \rightarrow J/\psi K_S$ . . . . .	42
6.1.2	Isospin Relations between $B_d \rightarrow J/\psi K_S$ and $B^\pm \rightarrow J/\psi K^\pm$ . . . . .	45
6.1.3	New Physics in the $B \rightarrow J/\psi K$ Decay Amplitudes . . . . .	47
6.1.4	Observables for a General Analysis of New Physics . . . . .	49
6.1.5	Possible Scenarios . . . . .	50
6.1.6	$B_d \rightarrow J/\psi[\rightarrow \ell^+\ell^-]K^*[\rightarrow \pi^0 K_S]$ Decays . . . . .	52
6.2	The $B \rightarrow \phi K$ System . . . . .	53
6.2.1	Decay Amplitudes in the Standard Model . . . . .	54
6.2.2	Effects of Physics Beyond the Standard Model . . . . .	57
6.2.3	Observables for a General Analysis of New Physics . . . . .	59
6.2.4	Possible Scenarios . . . . .	59
6.3	The $B \rightarrow \pi\pi$ System . . . . .	60
6.3.1	Probing $\alpha$ through $B_d \rightarrow \pi^+\pi^-$ . . . . .	60
6.3.2	Isospin Relations between $B \rightarrow \pi\pi$ Amplitudes . . . . .	62
6.3.3	Extracting $\alpha$ from $B \rightarrow \rho\pi$ Modes . . . . .	64
6.3.4	Other Approaches to Extract $\alpha$ . . . . .	65
6.4	$B_d \rightarrow D^{(*)\pm}\pi^\mp$ Decays . . . . .	66
6.5	Summary . . . . .	68
<b>7</b>	<b>A Closer Look at the <math>B_s</math> System</b>	<b>70</b>
7.1	General Remarks and Differences to the $B_d$ System . . . . .	70
7.2	$\Delta M_s$ and Constraints in the $\bar{\rho}-\bar{\eta}$ Plane . . . . .	70
7.3	$\Delta\Gamma_s$ and Untagged Decay Rates . . . . .	72
7.4	Impact of New Physics . . . . .	73
7.5	Strategies using Pure Tree Decays of $B_s$ -Mesons . . . . .	74
7.6	The Golden Mode $B_s \rightarrow J/\psi\phi$ . . . . .	75
7.6.1	Structure of the Angular Distribution . . . . .	75
7.6.2	Structure of the Observables . . . . .	77
7.6.3	CP Asymmetries and Manifestation of New Physics . . . . .	77
7.7	Summary . . . . .	79
<b>8</b>	<b>CP Violation in Charged <math>B</math> Decays</b>	<b>79</b>
8.1	General Remarks . . . . .	80
8.2	Extracting $\gamma$ from $B^\pm \rightarrow K^\pm D$ Decays . . . . .	81
8.2.1	Triangle Relations and Experimental Problems . . . . .	81
8.2.2	Alternative Approaches and Constraints on $\gamma$ . . . . .	82
8.3	Extracting $\gamma$ from $B_c^\pm \rightarrow D_s^\pm D$ Decays . . . . .	84

8.3.1	Ideal Realization of Triangle Relations . . . . .	84
8.3.2	$U$ -Spin Relations and Experimental Remarks . . . . .	85
8.4	Impact of New Physics: $D^0$ - $\overline{D}^0$ Mixing enters the Stage . . . . .	86
8.5	Summary . . . . .	87
<b>9</b>	<b>Phenomenology of <math>B \rightarrow \pi K</math> Decays</b>	<b>88</b>
9.1	General Remarks and Experimental Status . . . . .	88
9.2	The $B_d \rightarrow \pi^\mp K^\pm$ , $B^\pm \rightarrow \pi^\pm K$ System . . . . .	90
9.2.1	Amplitude Structure and Isospin Relations . . . . .	90
9.2.2	A Simple Bound on $\gamma$ . . . . .	92
9.2.3	Impact of Rescattering Processes . . . . .	94
9.2.4	More Refined Strategies to Probe $\gamma$ . . . . .	97
9.3	The Charged and Neutral $B \rightarrow \pi K$ Systems . . . . .	99
9.3.1	Parametrization of Decay Amplitudes and Observables . . . . .	99
9.3.2	Theoretical Advantages . . . . .	100
9.3.3	Strategies to Probe $\gamma$ . . . . .	101
9.3.4	Constraints in the $\overline{\rho}$ - $\overline{\eta}$ Plane . . . . .	104
9.3.5	Bounds on Strong Phases . . . . .	105
9.4	Towards Calculations of $B \rightarrow \pi K, \pi\pi$ Decays . . . . .	107
9.5	Impact of New Physics . . . . .	111
9.6	Summary . . . . .	112
<b>10</b>	<b>Phenomenology of <math>U</math>-spin-related <math>B</math> Decays</b>	<b>113</b>
10.1	The $B_{s(d)} \rightarrow J/\psi K_S$ System . . . . .	114
10.1.1	Amplitude Structure . . . . .	114
10.1.2	Extraction of $\gamma$ . . . . .	115
10.1.3	Theoretical Uncertainties . . . . .	116
10.2	The $B_{d(s)} \rightarrow D_{d(s)}^+ D_{d(s)}^-$ and $B_{d(s)} \rightarrow K^0 \overline{K}^0$ Systems . . . . .	117
10.2.1	Extracting $\gamma$ from $B_{d(s)} \rightarrow D_{d(s)}^+ D_{d(s)}^-$ Decays . . . . .	117
10.2.2	Extracting $\gamma$ from $B_{d(s)} \rightarrow K^0 \overline{K}^0$ Decays . . . . .	119
10.3	The $B_d \rightarrow \pi^+ \pi^-$ , $B_s \rightarrow K^+ K^-$ System . . . . .	119
10.3.1	Extraction of $\beta$ and $\gamma$ . . . . .	119
10.3.2	Minimal Use of the $U$ -Spin Symmetry . . . . .	120
10.3.3	Theoretical Uncertainties . . . . .	122
10.3.4	Searching for New Physics . . . . .	124
10.3.5	Replacing $B_s \rightarrow K^+ K^-$ through $B_d \rightarrow \pi^\mp K^\pm$ . . . . .	124
10.4	The $B_{(s)} \rightarrow \pi K$ System . . . . .	128
10.5	Other $U$ -Spin Approaches . . . . .	130
10.6	Summary . . . . .	131

<b>11 Models with Minimal Flavour Violation</b>	<b>132</b>
11.1 General Remarks . . . . .	132
11.2 The Universal Unitarity Triangle . . . . .	134
11.3 Bounds on $\sin 2\beta$ . . . . .	137
11.4 $K \rightarrow \pi\nu\bar{\nu}$ Decays and Connections with $B$ Physics . . . . .	138
11.4.1 The Decay $K^+ \rightarrow \pi^+\nu\bar{\nu}$ . . . . .	139
11.4.2 Unitarity Triangle from $K_L \rightarrow \pi^0\nu\bar{\nu}$ and $K^+ \rightarrow \pi^+\nu\bar{\nu}$ . . . . .	139
11.4.3 $\text{BR}(K_L \rightarrow \pi^0\nu\bar{\nu})$ from $a_{\psi K_S}$ and $\text{BR}(K^+ \rightarrow \pi^+\nu\bar{\nu})$ . . . . .	140
11.4.4 Upper Bound on $\text{BR}(K_L \rightarrow \pi^0\nu\bar{\nu})$ from $\text{BR}(B \rightarrow X_s\nu\bar{\nu})$ . . . . .	143
11.4.5 Towards a Determination of $X$ . . . . .	144
11.5 Summary . . . . .	144
<b>12 Further Interesting Aspects of <math>B</math> Physics</b>	<b>145</b>
<b>13 Conclusions and Outlook</b>	<b>145</b>

# 1 Introduction

The violation of the CP symmetry, where C and P denote the charge-conjugation and parity-transformation operators, respectively, is one of the fundamental and most exciting phenomena in particle physics. Although weak interactions are not invariant under P (and C) transformations, as discovered in 1957, it was believed for several years that the product CP was preserved. Consider, for instance, the process

$$\pi^+ \rightarrow e^+ \nu_e \xrightarrow{C} \pi^- \rightarrow e^- \nu_e^C \xrightarrow{P} \pi^- \rightarrow e^- \bar{\nu}_e, \quad (1.1)$$

where the left-handed  $\nu_e^C$  state is not observed in nature; only after performing an additional parity transformation we obtain the usual right-handed electron antineutrino. Consequently, it appears as if CP was conserved in weak interactions. However, in 1964, it was then discovered through the observation of  $K_L \rightarrow \pi^+ \pi^-$  decays that weak interactions are *not* invariant under CP transformations [1].

## 1.1 Motivation

Since its discovery in 1964, CP violation has only been accessible in the kaon system, and we still have few experimental insights into this exciting phenomenon. However, a new era has just begun through the observation of CP violation in the  $B$  system [2, 3], which will provide several decisive tests of the Standard-Model description of CP violation. In this respect, it is obviously crucial to have CP-violating  $B$ -decay processes available that can be analysed reliably within the framework of the Standard Model. As an interesting by-product, strategies to explore CP violation with the help of  $B$  decays provide usually also valuable insights into hadron dynamics, including aspects such as “factorization” and final-state interaction effects. A remarkable bridge to the kaon system is provided by the loop-induced decays  $K^+ \rightarrow \pi^+ \nu \bar{\nu}$  and  $K_L \rightarrow \pi^0 \nu \bar{\nu}$ , which are very clean and exhibit interesting correlations with CP violation in the “gold-plated” channel  $B_d \rightarrow J/\psi K_S$ . These issues will be the main focus of this review. For a collection of basic references on CP violation and alternative reviews, the reader is referred to [4]–[8].

At present, we are still in the early stage of the  $B$ -factory era in particle physics: in the summer of 2000, the BaBar (SLAC) and Belle (KEK) collaborations reported their first results, and the CLEO-III detector (Cornell) started taking data. In the summer of 2001, BaBar and Belle could establish CP violation in the  $B$  system, and run II of the Tevatron (Fermilab) is expected to provide data soon, allowing – in addition to studies of  $B_u$ - and  $B_d$ -mesons – a promising exploration of the  $B_s$  system. Several interesting aspects will also be left for “second-generation”  $B$  experiments at hadron colliders, BTeV (Fermilab) and LHCb (CERN), which should enter the stage around 2005. Detailed studies of the  $B$ -physics potentials of BaBar, run II of the Tevatron, and

the LHC can be found in [9]. The rare kaon decays  $K^+ \rightarrow \pi^+ \nu \bar{\nu}$  and  $K_L \rightarrow \pi^0 \nu \bar{\nu}$  will be studied in dedicated experiments at Brookhaven, Fermilab and KEK. The experimental prospects for these modes were recently reviewed in [10].

The reason why studies of CP-violating effects are so exciting is very simple: physics beyond the Standard Model is usually associated with new sources for CP violation. Important examples are non-minimal supersymmetry, left-right-symmetric models, models with extended Higgs sectors, and many other scenarios for “new” physics [11]. Moreover, the indirect constraints on CP-violating effects in  $B$  decays that are implied by the CP violation in the kaon system and  $B_d^0-\bar{B}_d^0$  mixing may also be affected strongly by new physics which does not yield additional sources for CP violation, for instance by models with “minimal flavour violation” (MFV) [12, 13]. Then we would encounter discrepancies with the directly measured CP asymmetries in  $B$  decays. Therefore, explorations of CP violation may well indicate physics beyond the Standard Model, or may be very helpful to distinguish between various realizations of one particular kind of new physics after the corresponding new-physics particles have been observed directly. In this context, it is worth mentioning that the evidence for neutrino masses we got over the recent years points also towards physics beyond the Standard Model [14], raising – among other things – the question of CP violation in the neutrino sector [15]. In the more distant future, these fascinating topics may be studied at dedicated  $\nu$ -factories.

## 1.2 CP Violation in Cosmology and Beyond $K$ and $B$ Decays

Interestingly, indirect information on CP violation is also provided by cosmology. One of the characteristic features of our Universe is the dominance of matter over antimatter. From the observed baryon to photon number of the Universe, it can be concluded that there was, a few microseconds after the Big Bang, a very small excess of about  $10^{-10}$  of matter with respect to antimatter. As was pointed out by Sakharov [16], one of the necessary conditions to generate such an asymmetry of the Universe is – in addition to baryon number violation and deviations from thermal equilibrium – that the elementary interactions violate CP (and C) [17]. Model calculations indicate, however, that the CP violation present in the Standard Model is too small to generate the observed matter–antimatter asymmetry of  $\mathcal{O}(10^{-10})$  [18]. It is conceivable that the particular kind of new physics underlying the baryon asymmetry is associated with very short-distance scales. In this case, it could not be seen in CP-violating effects in weak meson decays. However, as we have noted above, there are also plenty of scenarios for physics beyond the Standard Model that would affect these processes. Moreover, we do not understand the observed patterns of quark and lepton masses, their mixings and the origin of flavour dynamics in general. It is likely that the new physics required to understand these features is also related to new sources for CP violation.



Let us note that not only  $K$ - and  $B$ -meson decays allow an exploration of CP violation in the laboratory. There are of course also other systems which are interesting in this respect, for example the  $D$ -meson system [19, 20], where CP-violating and mixing effects are very small in the Standard Model, electric dipole moments [21], or CP violation in hyperon decays [22]. However, apart from  $D^0$ - $\overline{D}^0$  mixing, which may also affect a certain  $B$ -physics approach to explore CP violation, we shall not consider these topics in further detail and refer the reader to the corresponding papers and references therein.

### 1.3 Outline

This review can be divided into three main parts, where Sections 2–5 set the stage for our discussion, Sections 6–8 give an up-dated presentation of various “standard” approaches, and Sections 9–12 deal with more recent developments.

To be more specific, the outline is as follows: in Section 2, we discuss the description of CP violation within the framework of the Standard Model, where the key elements are the quark-mixing matrix and the associated unitarity triangles. Since non-leptonic  $B$  decays play the main rôle for the exploration of CP violation in the  $B$  system, we discuss the basic features of the theoretical framework to deal with these transitions in Section 3. Before turning to CP-violating effects in  $B$  decays, we have a brief look at the present status of CP violation in the kaon system in Section 4, where we also give an introduction to the rare decays  $K^+ \rightarrow \pi^+ \nu \overline{\nu}$  and  $K_L \rightarrow \pi^0 \nu \overline{\nu}$ . In Section 5, we then discuss the formalism to describe the time evolution of neutral  $B$  decays, arising from  $B_{d,s}^0$ - $\overline{B}_{d,s}^0$  mixing, and introduce the corresponding CP-violating observables.

The formalism developed in Section 5 is applied to important  $B$ -factory benchmark modes in Section 6, where we present detailed discussions of the  $B \rightarrow J/\psi K$ ,  $B \rightarrow \phi K$  and  $B \rightarrow \pi\pi$  systems, as well as of  $B_d \rightarrow D^{(*)\pm} \pi^\mp$  decays. Because of its outstanding rôle for  $B$ -physics experiments at hadron machines, we have devoted a separate section to the  $B_s$  system: in Section 7, we discuss constraints on the unitarity triangles implied by  $B_s^0$ - $\overline{B}_s^0$  mixing, the width difference  $\Delta\Gamma_s$  between the  $B_s$  mass eigenstates, “untagged”  $B_s$  decay rates, and strategies to explore CP violation with pure tree decays and the “golden” mode  $B_s \rightarrow J/\psi\phi$ . In Section 8, we turn to CP-violating effects in decays of charged  $B$ -mesons. In the case of  $B_u^\pm \rightarrow K^\pm D$  and  $B_c^\pm \rightarrow D_s^\pm D$  modes, hadronic uncertainties can be eliminated with the help of certain amplitude relations, thereby allowing studies of CP violation. There we give also a brief discussion of  $D^0$ - $\overline{D}^0$  mixing.

Amplitude relations play also a key rôle in the subsequent two sections: in Section 9, we turn to the phenomenology of  $B \rightarrow \pi K$  decays, whereas we focus on certain  $U$ -spin-related decays in Section 10, including the  $B_{s(d)} \rightarrow J/\psi K_S$ ,  $B_{d(s)} \rightarrow D_{d(s)}^+ D_{d(s)}^-$ ,  $B_{d(s)} \rightarrow K^0 \overline{K}^0$  and  $B_d \rightarrow \pi^+ \pi^-$ ,  $B_s \rightarrow K^+ K^-$  systems, as well as  $B_{(s)} \rightarrow \pi K$  modes. The physics potential of  $B \rightarrow \pi K$  decays is particularly interesting for the  $B$ -factories,

while the  $U$ -spin-related modes – in particular the  $B_d \rightarrow \pi^+\pi^-$ ,  $B_s \rightarrow K^+K^-$  system – is very promising for run II of the Tevatron and ideally suited for BTeV and LHCb. Although general features of the impact of physics beyond the Standard Model on the decays listed above will be emphasized throughout this review in a model-independent way, in Section 11, we discuss a particularly simple – but very predictive – scenario for new physics in more detail, which is provided by models with “minimal flavour violation”. Within this framework, interesting bounds on CP violation in  $B_d \rightarrow J/\psi K_S$  decays can be derived, and remarkable connections with the rare kaon decays  $K^+ \rightarrow \pi^+\nu\bar{\nu}$  and  $K_L \rightarrow \pi^0\nu\bar{\nu}$  arise. Finally, we make a few remarks on further interesting aspects of  $B$  physics in Section 12, and give the conclusions and a brief outlook in Section 13.

## 2 CP Violation in the Standard Model

### 2.1 Charged-Current Interactions

In the framework of the Standard Model of electroweak interactions [23], which is based on the spontaneously broken gauge group

$$SU(2)_L \times U(1)_Y \xrightarrow{\text{SSB}} U(1)_{\text{em}}, \quad (2.1)$$

CP violation is related to the Cabibbo–Kobayashi–Maskawa (CKM) matrix [24, 25], connecting the electroweak eigenstates ( $d', s', b'$ ) of the down, strange and bottom quarks with their mass eigenstates ( $d, s, b$ ) through the following unitary transformation:

$$\begin{pmatrix} d' \\ s' \\ b' \end{pmatrix} = \begin{pmatrix} V_{ud} & V_{us} & V_{ub} \\ V_{cd} & V_{cs} & V_{cb} \\ V_{td} & V_{ts} & V_{tb} \end{pmatrix} \cdot \begin{pmatrix} d \\ s \\ b \end{pmatrix} \equiv \hat{V}_{\text{CKM}} \cdot \begin{pmatrix} d \\ s \\ b \end{pmatrix}. \quad (2.2)$$

The elements of the CKM matrix describe charged-current couplings, as can be seen easily by expressing the non-leptonic charged-current interaction Lagrangian in terms of the mass eigenstates appearing in (2.2):

$$\mathcal{L}_{\text{int}}^{\text{CC}} = -\frac{g_2}{\sqrt{2}} (\bar{u}_L, \bar{c}_L, \bar{t}_L) \gamma^\mu \hat{V}_{\text{CKM}} \begin{pmatrix} d_L \\ s_L \\ b_L \end{pmatrix} W_\mu^\dagger + \text{h.c.}, \quad (2.3)$$

where the gauge coupling  $g_2$  is related to  $SU(2)_L$ , and the  $W_\mu^{(\dagger)}$  field corresponds to the charged  $W$ -bosons. In Fig. 1, we show the  $b \rightarrow u W$  vertex and its CP conjugate. The important feature is that these processes are related by the replacement

$$V_{ub} \xrightarrow{CP} V_{ub}^*. \quad (2.4)$$

Consequently, in the Standard Model, CP violation is due to complex phases of CKM matrix elements. The origin of these phases, as the origin of quark mixing and flavour dynamics in general, lies of course beyond the Standard Model.

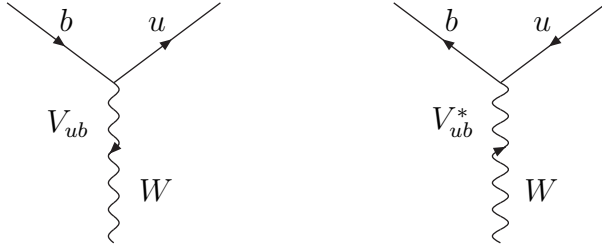


Figure 1: Charged-current interactions in the Standard Model.

## 2.2 The Strong CP Problem

The CP-violating effects discussed in this review are essentially due to phases appearing in the CKM matrix, i.e. they arise from weak interactions. However, there is also another source for CP violation in the Standard Model: in Quantum Chromodynamics (QCD), which is described by the gauge group  $SU(3)_C$ , topologically non-trivial quantum fluctuations, so-called instantons, induce a parity- and time-reversal-violating term of the QCD Lagrange density of the following form:

$$S_\theta = \theta \frac{g_s^2}{32\pi^2} G_{\mu\nu}^a \tilde{G}^{a\mu\nu}. \quad (2.5)$$

Here  $\theta$  is the “QCD vacuum angle”,  $g_s$  the QCD gauge coupling,  $G_{\mu\nu}^a$  the QCD field strength tensor, and  $\tilde{G}^{a\mu\nu}$  its dual. Observable quantities depend on the parameter

$$\bar{\theta} \equiv \theta - \arg(\det M_q), \quad (2.6)$$

where  $M_q$  is the non-diagonal quark-mass matrix in the electroweak basis. The experimental limits on the electric dipole moment of the neutron imply  $\bar{\theta} \lesssim 10^{-10}$ . Since QCD gauge invariance would perfectly allow a value of  $\bar{\theta} = \mathcal{O}(1)$ , we arrive at a very puzzling situation, suggesting a formidable fine tuning of the  $\theta$  parameter to yield such an extremely tiny value of  $\bar{\theta}$ . A detailed discussion of this “strong CP problem”, as well as ideas to overcome it, can be found, for instance, in [26].

## 2.3 Parametrizations of the CKM Matrix

As we have seen in (2.4), within the Standard Model, CP violation is related to complex phases of CKM matrix elements. However, the phase structure of the CKM matrix is not unique, as we may perform the phase transformations

$$V_{UD} \rightarrow \exp(i\xi_U) V_{UD} \exp(-i\xi_D), \quad (2.7)$$

which correspond to the following redefinitions of the up- and down-type quark fields:

$$U \rightarrow \exp(i\xi_U)U, \quad D \rightarrow \exp(i\xi_D)D. \quad (2.8)$$

Using these transformations, it can be shown that the general  $N$ -generation quark-mixing-matrix is described by  $(N - 1)^2$  parameters, consisting of

$$\frac{1}{2}N(N - 1) \quad (2.9)$$

Euler-type angles, and

$$\frac{1}{2}(N - 1)(N - 2) \quad (2.10)$$

complex phases. In the two-generation case [24], we have therefore to deal with a real matrix, involving just one Euler-type angle, and arrive at the well-known Cabibbo matrix

$$\hat{V}_C = \begin{pmatrix} \cos \theta_C & \sin \theta_C \\ -\sin \theta_C & \cos \theta_C \end{pmatrix}, \quad (2.11)$$

where  $\sin \theta_C = 0.22$  can be determined from semi-leptonic  $K \rightarrow \pi e^+ \nu_e$  decays.

### 2.3.1 Standard Parametrization

In the case of three generations, three Euler-type angles and one *complex phase* are needed to parametrize the CKM matrix. This complex phase allows us to accommodate CP violation in the Standard Model, as was pointed out by Kobayashi and Maskawa in 1973 [25]. In the ‘‘standard parametrization’’ [27], the three-generation CKM matrix takes the following form:

$$\hat{V}_{\text{CKM}} = \begin{pmatrix} c_{12}c_{13} & s_{12}c_{13} & s_{13}e^{-i\delta_{13}} \\ -s_{12}c_{23} - c_{12}s_{23}s_{13}e^{i\delta_{13}} & c_{12}c_{23} - s_{12}s_{23}s_{13}e^{i\delta_{13}} & s_{23}c_{13} \\ s_{12}s_{23} - c_{12}c_{23}s_{13}e^{i\delta_{13}} & -c_{12}s_{23} - s_{12}c_{23}s_{13}e^{i\delta_{13}} & c_{23}c_{13} \end{pmatrix}, \quad (2.12)$$

where  $c_{ij} \equiv \cos \theta_{ij}$  and  $s_{ij} \equiv \sin \theta_{ij}$ . Performing appropriate redefinitions of the quark-field phases, the real angles  $\theta_{12}$ ,  $\theta_{23}$  and  $\theta_{13}$  can all be made to lie in the first quadrant. The advantage of this parametrization is that the generation labels  $i, j = 1, 2, 3$  are introduced in such a way that the mixing between two chosen generations vanishes if the corresponding mixing angle  $\theta_{ij}$  is set to zero. In particular, for  $\theta_{23} = \theta_{13} = 0$ , the third generation decouples, and we arrive at a situation characterized by the Cabibbo matrix given in (2.11).

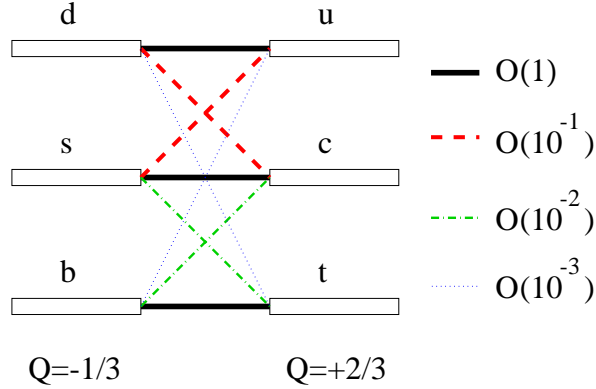


Figure 2: Hierarchy of the quark transitions mediated through charged currents.

### 2.3.2 Fritzsch–Xing Parametrization

Another interesting parametrization of the CKM matrix was proposed by Fritzsch and Xing [28]:

$$\hat{V}_{\text{CKM}} = \begin{pmatrix} s_u s_d c + c_u c_d e^{-i\varphi} & s_u c_d c - c_u s_d e^{-i\varphi} & s_u s \\ c_u s_d c - s_u c_d e^{-i\varphi} & c_u c_d c + s_u s_d e^{-i\varphi} & c_u s \\ -s_d s & -c_d s & c \end{pmatrix}. \quad (2.13)$$

It is inspired by the hierarchical structure of the quark-mass spectrum, and is particularly useful in the context of models for fermion masses and mixings. The characteristic feature of this parametrization is that the complex phase arises only in the  $2 \times 2$  submatrix involving the up, down, strange and charm quarks.

### 2.3.3 Wolfenstein Parametrization

In Fig. 2, we have illustrated the hierarchy of the strengths of the quark transitions mediated through charged-current interactions: transitions within the same generation are governed by CKM elements of  $\mathcal{O}(1)$ , those between the first and the second generation are suppressed by CKM factors of  $\mathcal{O}(10^{-1})$ , those between the second and the third generation are suppressed by  $\mathcal{O}(10^{-2})$ , and the transitions between the first and the third generation are even suppressed by CKM factors of  $\mathcal{O}(10^{-3})$ . In the standard parametrization (2.12), this hierarchy is reflected by

$$s_{12} = 0.222 \gg s_{23} = \mathcal{O}(10^{-2}) \gg s_{13} = \mathcal{O}(10^{-3}). \quad (2.14)$$

If we introduce a set of new parameters  $\lambda$ ,  $A$ ,  $\rho$  and  $\eta$  by imposing the relations [29, 30]

$$s_{12} \equiv \lambda = 0.222, \quad s_{23} \equiv A\lambda^2, \quad s_{13} e^{-i\delta_{13}} \equiv A\lambda^3(\rho - i\eta), \quad (2.15)$$

and go back to the standard parametrization (2.12), we obtain an *exact* parametrization of the CKM matrix as a function of  $\lambda$  (and  $A$ ,  $\rho$ ,  $\eta$ ). Now we can expand straightforwardly

each CKM element in the small parameter  $\lambda$ . Neglecting terms of  $\mathcal{O}(\lambda^4)$ , we arrive at the famous ‘‘Wolfenstein parametrization’’ of the CKM matrix [31]:

$$\hat{V}_{\text{CKM}} = \begin{pmatrix} 1 - \frac{1}{2}\lambda^2 & \lambda & A\lambda^3(\rho - i\eta) \\ -\lambda & 1 - \frac{1}{2}\lambda^2 & A\lambda^2 \\ A\lambda^3(1 - \rho - i\eta) & -A\lambda^2 & 1 \end{pmatrix} + \mathcal{O}(\lambda^4). \quad (2.16)$$

Since this parametrization makes the hierarchy of the CKM matrix explicit, it is very useful for phenomenological applications.

In several cases, next-to-leading order corrections in  $\lambda$  play an important rôle. Using the exact parametrization following from (2.15), they can be calculated in a similar manner by expanding each CKM element to the desired accuracy in  $\lambda$  [8, 30]:

$$\begin{aligned} V_{ud} &= 1 - \frac{1}{2}\lambda^2 - \frac{1}{8}\lambda^4 + \mathcal{O}(\lambda^6), & V_{us} &= \lambda + \mathcal{O}(\lambda^7), & V_{ub} &= A\lambda^3(\rho - i\eta), \\ V_{cd} &= -\lambda + \frac{1}{2}A^2\lambda^5 [1 - 2(\rho + i\eta)] + \mathcal{O}(\lambda^7), \\ V_{cs} &= 1 - \frac{1}{2}\lambda^2 - \frac{1}{8}\lambda^4(1 + 4A^2) + \mathcal{O}(\lambda^6), \\ V_{cb} &= A\lambda^2 + \mathcal{O}(\lambda^8), & V_{td} &= A\lambda^3 \left[ 1 - (\rho + i\eta) \left( 1 - \frac{1}{2}\lambda^2 \right) \right] + \mathcal{O}(\lambda^7), \\ V_{ts} &= -A\lambda^2 + \frac{1}{2}A(1 - 2\rho)\lambda^4 - i\eta A\lambda^4 + \mathcal{O}(\lambda^6), & V_{tb} &= 1 - \frac{1}{2}A^2\lambda^4 + \mathcal{O}(\lambda^6). \end{aligned} \quad (2.17)$$

It should be noted that here

$$V_{ub} = A\lambda^3(\rho - i\eta) \quad (2.18)$$

receives *by definition* no power corrections in  $\lambda$ . Introducing the following modified Wolfenstein parameters [30]:

$$\bar{\rho} \equiv \rho \left( 1 - \frac{1}{2}\lambda^2 \right), \quad \bar{\eta} \equiv \eta \left( 1 - \frac{1}{2}\lambda^2 \right), \quad (2.19)$$

we may simply write, up to corrections of  $\mathcal{O}(\lambda^7)$ ,

$$V_{td} = A\lambda^3(1 - \bar{\rho} - i\bar{\eta}). \quad (2.20)$$

Moreover, we have to an excellent accuracy

$$V_{us} = \lambda \quad \text{and} \quad V_{cb} = A\lambda^2, \quad (2.21)$$

as these CKM elements receive only corrections at the  $\lambda^7$  and  $\lambda^8$  levels, respectively. In comparison with other generalizations of the Wolfenstein parametrization found in the literature, the advantage of (2.17) is the absence of relevant corrections to  $V_{us}$  and  $V_{cb}$ , and that  $V_{ub}$  and  $V_{td}$  take similar forms as in (2.16).

Let us finally note that physical observables, for instance CP-violating asymmetries, cannot depend on the chosen parametrization of the CKM matrix, i.e. on the phase transformations given in (2.8).

## 2.4 Requirements for CP Violation

As we have seen in Subsection 2.3, at least three generations are required to accommodate CP violation in the Standard Model. However, still more conditions have to be satisfied for observable CP-violating effects. They can be summarized as follows [32, 33]:

$$(m_t^2 - m_c^2)(m_t^2 - m_u^2)(m_c^2 - m_u^2) \\ \times (m_b^2 - m_s^2)(m_b^2 - m_d^2)(m_s^2 - m_d^2) \times J_{\text{CP}} \neq 0, \quad (2.22)$$

where

$$J_{\text{CP}} = |\text{Im}(V_{i\alpha}V_{j\beta}V_{i\beta}^*V_{j\alpha}^*)| \quad (i \neq j, \alpha \neq \beta). \quad (2.23)$$

The factors in (2.22) involving the quark masses are related to the fact that the CP-violating phase of the CKM matrix could be eliminated through an appropriate unitary transformation of quark fields if any two quarks with the same charge had the same mass. Consequently, the origin of CP violation is not only closely related to the number of fermion generations, but also to the hierarchy of quark masses and cannot be understood in a deeper way unless we have insights into these very fundamental issues, usually referred to as the “flavour problem”.

The second ingredient of (2.22), the “Jarlskog Parameter”  $J_{\text{CP}}$  [32], can be interpreted as a measure of the strength of CP violation in the Standard Model. It does not depend on the chosen quark-field parametrization, i.e. is invariant under (2.8), and the unitarity of the CKM matrix implies that all combinations  $|\text{Im}(V_{i\alpha}V_{j\beta}V_{i\beta}^*V_{j\alpha}^*)|$  are equal. Using the Standard and Wolfenstein parametrizations, we obtain

$$J_{\text{CP}} = s_{12}s_{13}s_{23}c_{12}c_{23}c_{13}^2 \sin \delta_{13} = \lambda^6 A^2 \eta = \mathcal{O}(10^{-5}), \quad (2.24)$$

where we have taken into account the present experimental information on the Wolfenstein parameters in the quantitative estimate (see Subsection 2.6). Consequently, CP violation is a small effect in the Standard Model. Typically, new complex couplings are present in scenarios for new physics, yielding additional sources for CP violation.

## 2.5 The Unitarity Triangles of the CKM Matrix

Concerning tests of the Kobayashi–Maskawa picture of CP violation, the central targets are the “unitarity triangles” of the CKM matrix. The unitarity of the CKM matrix, which is described by

$$\hat{V}_{\text{CKM}}^\dagger \cdot \hat{V}_{\text{CKM}} = \hat{1} = \hat{V}_{\text{CKM}} \cdot \hat{V}_{\text{CKM}}^\dagger, \quad (2.25)$$

implies a set of 12 equations, consisting of 6 normalization relations and 6 orthogonality relations:

- Normalization relations:

$$|V_{ud}|^2 + |V_{cd}|^2 + |V_{td}|^2 = 1 \quad [1\text{st column}] \quad (2.26)$$

$$|V_{us}|^2 + |V_{cs}|^2 + |V_{ts}|^2 = 1 \quad [2\text{nd column}] \quad (2.27)$$

$$|V_{ub}|^2 + |V_{cb}|^2 + |V_{tb}|^2 = 1 \quad [3\text{rd column}] \quad (2.28)$$

$$|V_{ud}|^2 + |V_{us}|^2 + |V_{ub}|^2 = 1 \quad [1\text{st row}] \quad (2.29)$$

$$|V_{cd}|^2 + |V_{cs}|^2 + |V_{cb}|^2 = 1 \quad [2\text{nd row}] \quad (2.30)$$

$$|V_{td}|^2 + |V_{ts}|^2 + |V_{tb}|^2 = 1 \quad [3\text{rd row}]. \quad (2.31)$$

- Orthogonality relations:

$$V_{ud}V_{us}^* + V_{cd}V_{cs}^* + V_{td}V_{ts}^* = 0 \quad [1\text{st and 2nd column}] \quad (2.32)$$

$$V_{ud}V_{ub}^* + V_{cd}V_{cb}^* + V_{td}V_{tb}^* = 0 \quad [1\text{st and 3rd column}] \quad (2.33)$$

$$V_{us}V_{ub}^* + V_{cs}V_{cb}^* + V_{ts}V_{tb}^* = 0 \quad [2\text{nd and 3rd column}] \quad (2.34)$$

$$V_{ud}^*V_{cd} + V_{us}^*V_{cs} + V_{ub}^*V_{cb} = 0 \quad [1\text{st and 2nd row}] \quad (2.35)$$

$$V_{ub}^*V_{tb} + V_{us}^*V_{ts} + V_{ud}^*V_{td} = 0 \quad [1\text{st and 3rd row}] \quad (2.36)$$

$$V_{cd}^*V_{td} + V_{cs}^*V_{ts} + V_{cb}^*V_{tb} = 0 \quad [2\text{nd and 3rd row}]. \quad (2.37)$$

The orthogonality relations are of particular interest, since they can be represented as six “unitarity triangles” in the complex plane [34]. It should be noted that the set of equations (2.26)–(2.37) is invariant under the phase transformations specified in (2.7). If one performs such transformations, the triangles corresponding to (2.32)–(2.37) are rotated in the complex plane. However, the angles and sides of these triangles remain unchanged and are therefore physical observables. It can be shown that all six unitarity triangles have the same area [35], which is given by the Jarlskog parameter as follows:

$$A_{\Delta} = \frac{1}{2}J_{\text{CP}}. \quad (2.38)$$

The shape of the unitarity triangles can be analysed with the help of the Wolfenstein parametrization, implying the following structure for (2.32)–(2.34) and (2.35)–(2.37):

$$\mathcal{O}(\lambda) + \mathcal{O}(\lambda) + \mathcal{O}(\lambda^5) = 0 \quad (2.39)$$

$$\mathcal{O}(\lambda^3) + \mathcal{O}(\lambda^3) + \mathcal{O}(\lambda^3) = 0 \quad (2.40)$$

$$\mathcal{O}(\lambda^4) + \mathcal{O}(\lambda^2) + \mathcal{O}(\lambda^2) = 0. \quad (2.41)$$



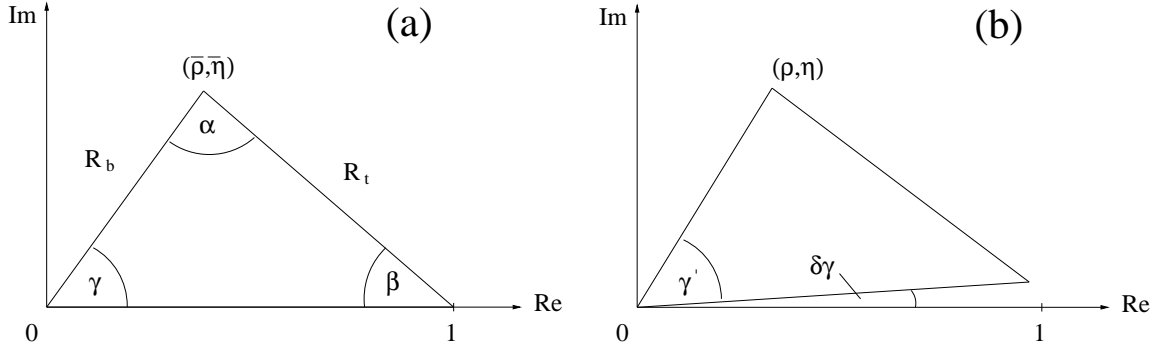


Figure 3: The two non-squashed unitarity triangles of the CKM matrix: (a) and (b) correspond to the orthogonality relations (2.33) and (2.36), respectively.

Consequently, only in the triangles corresponding to (2.33) and (2.36), all three sides are of comparable magnitude  $\mathcal{O}(\lambda^3)$ , while in the remaining triangles, one side is suppressed with respect to the others by  $\mathcal{O}(\lambda^2)$  or  $\mathcal{O}(\lambda^4)$ . The two “non-squashed” orthogonality relations (2.33) and (2.36) agree at the  $\lambda^3$  level and differ only through  $\mathcal{O}(\lambda^5)$  corrections. If we neglect these subleading contributions, we arrive at *the* unitarity triangle of the CKM matrix [35, 36], which appears usually in the literature. To be more specific, at leading non-vanishing order in  $\lambda$ , i.e.  $\mathcal{O}(\lambda^3)$ , (2.33) and (2.36) imply the triangle relation

$$(\rho + i\eta)A\lambda^3 + (-A\lambda^3) + (1 - \rho - i\eta)A\lambda^3 = 0. \quad (2.42)$$

If we now rescale all terms by  $A\lambda^3$ , the basis of the resulting triangle, which coincides with the real axis, is normalized to one, and its apex is given by  $(\rho, \eta)$ .

In the era of “second-generation”  $B$  experiments, the experimental accuracy will be so tremendous that we will also have to take into account the next-to-leading order terms of the Wolfenstein expansion, and will have to distinguish between the unitarity triangles described by (2.33) and (2.36). To this end, the generalized Wolfenstein parametrization introduced in Subsection 2.3.3 is particularly convenient. If we keep terms up to  $\mathcal{O}(\lambda^5)$  in the orthogonality relations (2.33) and (2.36), and rescale them as above by  $A\lambda^3$ , we arrive at the two unitarity triangles illustrated in Fig. 3, which differ at the  $\lambda^2$  level. In the unitarity triangle corresponding to (2.33), we have just to switch to the modified Wolfenstein parameters (2.19), i.e. the apex is given by  $(\bar{\rho}, \bar{\eta})$  instead of  $(\rho, \eta)$ . Consequently, here we have a straightforward generalization of *the* unitarity triangle, and whenever we refer to a unitarity triangle in the remainder of this review, we mean the one shown in Fig. 3 (a). On the other hand, in the case of (2.36), the apex is still given by  $(\rho, \eta)$ , whereas the angle  $\gamma'$  differs from  $\gamma$  through

$$\gamma - \gamma' \equiv \delta\gamma = \lambda^2\eta, \quad (2.43)$$

implying a small angle between the basis of the triangle and the real axis.

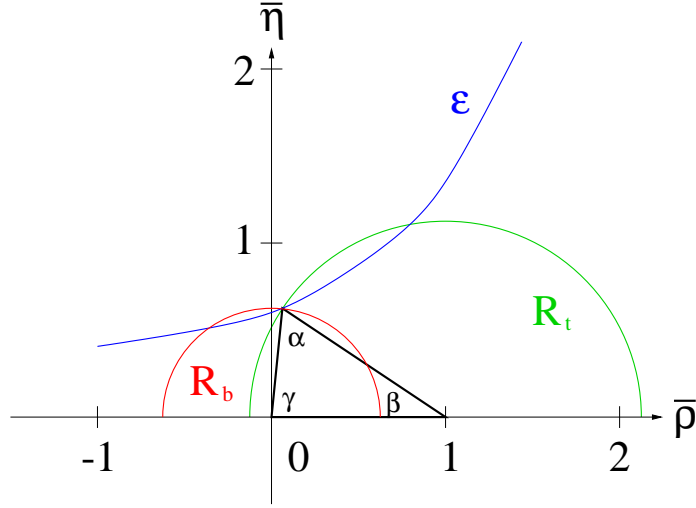


Figure 4: Contours to determine the unitarity triangle in the  $\bar{\rho}$ - $\bar{\eta}$  plane.

The angles  $\alpha$ ,  $\beta$ ,  $\gamma$  and  $\delta\gamma$  can be probed directly through CP-violating effects in  $B$  decays. Whereas  $\beta$  is very accessible and various promising strategies to extract  $\gamma$  were proposed, an experimentally feasible measurement of  $\alpha$  is unfortunately difficult. The small angle  $\delta\gamma$  plays a key rôle for CP violation in the  $B_s$ -meson system.

## 2.6 Towards an Allowed Range in the $\bar{\rho}$ - $\bar{\eta}$ Plane

Let us now discuss how the apex of the unitarity triangle can be constrained in the  $\bar{\rho}$ - $\bar{\eta}$  plane without using direct measurements of the angles  $\alpha$ ,  $\beta$  and  $\gamma$ . To accomplish this task, measurements of the sides  $R_b$  and  $R_t$  have to be performed. These quantities can be expressed in terms of CKM matrix elements as follows:

$$R_b \equiv \left| \frac{V_{ud}V_{ub}^*}{V_{cd}V_{cb}^*} \right| = \left( 1 - \frac{\lambda^2}{2} \right) \frac{1}{\lambda} \left| \frac{V_{ub}}{V_{cb}} \right| = \sqrt{\bar{\rho}^2 + \bar{\eta}^2} \quad (2.44)$$

$$R_t \equiv \left| \frac{V_{td}V_{tb}^*}{V_{cd}V_{cb}^*} \right| = \frac{1}{\lambda} \left| \frac{V_{td}}{V_{cb}} \right| = \sqrt{(1 - \bar{\rho})^2 + \bar{\eta}^2}, \quad (2.45)$$

and will show up at several places throughout this review. Other useful expressions are

$$V_{ub} = A\lambda^3 \left( \frac{R_b}{1 - \lambda^2/2} \right) e^{-i\gamma}, \quad V_{td} = A\lambda^3 R_t e^{-i\beta}, \quad (2.46)$$

since they make the dependence on  $\gamma$  and  $\beta$  explicit; they correspond to the phase convention chosen both in the standard parametrization (2.12) and in the generalized Wolfenstein parametrization (2.17). Moreover, taking into account (2.15), we obtain

$$\delta_{13} = \gamma. \quad (2.47)$$

Looking at (2.44) and (2.45), we observe that these expressions describe circles in the  $\bar{\rho}$ - $\bar{\eta}$  plane around  $(0, 0)$  and  $(1, 0)$  with radii  $R_b$  and  $R_t$ , respectively. Employing, moreover, an observable  $\varepsilon$ , which measures “indirect” CP violation in the neutral kaon system, as we will discuss in more detail in Section 4, a hyperbola in the  $\bar{\rho}$ - $\bar{\eta}$  plane can be fixed. These contours are sketched in Fig. 4; their intersection gives the apex of the unitarity triangle. As can be seen in Fig. 4, an upper bound on  $R_b$  implies [30]

$$(\sin \beta)_{\max} = R_b^{\max}, \quad (\sin 2\beta)_{\max} = 2R_b^{\max} \sqrt{1 - (R_b^{\max})^2}, \quad (2.48)$$

where the quantity  $\sin 2\beta$  is of particular interest, since it governs CP violation in the “gold-plated” decay  $B_d \rightarrow J/\psi K_S$ , as we will see in Subsection 6.1

The CKM matrix element  $|V_{cb}|$ , which is required – among other things – for the normalization of (2.44) and (2.45), can be extracted with the help of the “Heavy-Quark Effective Theory” (HQET) from semi-leptonic  $B$  decays into charmed mesons [37]. The key rôle is played by the decay  $\bar{B}_d^0 \rightarrow D^{*+} \ell^- \bar{\nu}_\ell$ , which is particularly clean. Measuring its differential rate at maximum  $q^2$ , which denotes the mass squared of the lepton-antineutrino system,  $|V_{cb}|$  can be extracted with corrections based on the HQET. An alternative strategy is provided by inclusive  $b \rightarrow c \ell^- \bar{\nu}_\ell$  decays. In a recent analysis [38], the following average over the presently available measurements performed by the CLEO and LEP collaborations was obtained:

$$|V_{cb}| = (41.0 \pm 1.6) \times 10^{-3} \quad \Rightarrow \quad A = 0.832 \pm 0.033, \quad (2.49)$$

where we have used (2.21) with  $\lambda = 0.222$  to evaluate the CKM parameter  $A$ .

In order to determine  $|V_{ub}|$ , semi-leptonic  $b \rightarrow u$  transitions are used. The CLEO collaboration has employed the exclusive decay  $\bar{B}_d^0 \rightarrow \rho^+ \ell^- \bar{\nu}_\ell$ , where the extraction of  $|V_{ub}|$  requires models for decay form factors [39]. On the other hand, the LEP collaborations have obtained a value for  $|V_{ub}|$  by developing algorithms to be sensitive to a large fraction of the inclusive  $b \rightarrow u \ell^- \bar{\nu}_\ell$  rate [40]. The corresponding results are given by

$$|V_{ub}| = \begin{cases} (32.5 \pm 2.9 \pm 5.5) \times 10^{-4} & \text{(CLEO [39])} \\ (41.3 \pm 6.3 \pm 3.1) \times 10^{-4} & \text{(LEP [40])}, \end{cases} \quad (2.50)$$

where the second uncertainty has a theoretical origin. In [38], the following average value has been obtained:  $|V_{ub}| = (35.5 \pm 3.6) \times 10^{-4}$ . On the other hand, in the review of the Particle Data Group [41], a more conservative uncertainty is given for  $|V_{ub}|$ , yielding  $|V_{ub}/V_{cb}| = 0.090 \pm 0.025$ . In this review, we shall follow [8], and take

$$|V_{ub}/V_{cb}| = 0.085 \pm 0.018 \quad \Rightarrow \quad R_b = 0.38 \pm 0.08, \quad (2.51)$$

which lies between these two “limiting” cases. Using (2.48), we obtain the bounds

$$\beta \lesssim 28^\circ, \quad \sin 2\beta \lesssim 0.82. \quad (2.52)$$

As we have just seen,  $R_b$  can be determined through semi-leptonic  $b \rightarrow u \ell^- \bar{\nu}_\ell$  and  $b \rightarrow c \ell^- \bar{\nu}_\ell$  decays. The second side  $R_t$  of the unitarity triangle shown in Fig. 3 (a) can be determined through  $B_{d,s}^0 - \overline{B}_{d,s}^0$  mixing, which will be discussed in Sections 5 and 7. The present data imply

$$R_t = \mathcal{O}(1). \quad (2.53)$$

In particular the experimental constraints on  $B_s^0 - \overline{B}_s^0$  mixing play an important rôle, excluding values for  $\gamma$  larger than  $90^\circ$  [42].

Because of theoretical and experimental uncertainties, things are not as simple as sketched in Fig. 4. Instead of contours, we have actually to deal with bands, whose intersection gives an allowed range in the  $\bar{\rho} - \bar{\eta}$  plane. Moreover, there are strong correlations between theoretical and experimental uncertainties. For instance, the circle and the hyperbola fixed through  $B_d^0 - \overline{B}_d^0$  mixing and  $\varepsilon$ , respectively, depend on  $|V_{cb}|$ , the top-quark mass, perturbative QCD corrections, and certain non-perturbative parameters, as we will see below. It is hence rather involved to convert the experimental information into an allowed range in the  $\bar{\rho} - \bar{\eta}$  plane, and various analyses can be found in the literature:

- The simple scanning approach, where experimental and theoretical parameters are both scanned independently within reasonable ranges (see, for example, [8]).
- The Gaussian approach, where experimental and theoretical input parameters are both treated with Gaussian errors (see, for instance, [42]).
- The “BaBar 95% Scanning Method” [43, 44], where one sets the theoretical input parameters to some fixed values and determines the 95% C.L. range in the  $\bar{\rho} - \bar{\eta}$  plane by using a Gaussian error analysis for the experimental input parameters. This procedure is repeated for all possible sets of theoretical input parameters lying within their allowed ranges, and an envelope of the 95% C.L. regions is obtained.
- The Bayesian approach [38], where the theoretical uncertainties are taken into account in a way similar to the experimental ones through probability distribution functions (p.d.f.). If the uncertainties are dominated by statistical effects or if there are many comparable contributions to the systematic error, a Gaussian model is chosen. On the other hand, a uniform p.d.f. is employed when the parameter can be assumed to lie (almost) certainly within a given range, with points that can be considered as being equally probable.
- The statistical approach developed in [45], allowing a non-Bayesian treatment of theoretical parameters and theoretical systematics of measurements. Using a likelihood function  $\mathcal{L}(y_{\text{mod}}) = \mathcal{L}_{\text{exp}}(x_{\text{exp}} - x_{\text{theo}}(y_{\text{mod}})) \mathcal{L}_{\text{theo}}(y_{\text{QCD}})$ ,  $\chi^2 \equiv -2 \ln \mathcal{L}(y_{\text{mod}})$  is minimized in the fitting procedure. The experimental likelihood  $\mathcal{L}_{\text{exp}}$  measures

the agreement between measurements  $x_{\text{exp}}$  and theoretical predictions  $x_{\text{theo}}$ , which are functions of model parameters  $y_{\text{mod}}$ . On the other hand, the theoretical likelihood  $\mathcal{L}_{\text{theo}}$  expresses the knowledge of QCD parameters  $y_{\text{QCD}} \in \{y_{\text{mod}}\}$ , where the allowed ranges are specified through the theoretical uncertainties. The agreement between theory and experiment is gauged by the global minimum  $\chi_{\text{min};y_{\text{mod}}}^2$ , which is determined by varying all model parameters  $y_{\text{mod}}$ . Besides a detailed discussion of the technicalities of this procedure, also comparisons with other approaches can be found in [45]. A similar comment applies to [38].

Group	$\alpha$	$\beta$	$\gamma$	$\sin 2\alpha$	$\sin 2\beta$
Buras [8]	78.8°–120°	15.1°–28.6°	37.9°–76.5°	−0.87–0.38	0.50–0.84
Ali & London [42]	77°–127°	14°–35°	34°–81°	−0.96–0.45	0.46–0.94
Höcker <i>et al.</i> [45]	80°–126°	14°–27°	34°–82°	−0.95–0.33	0.47–0.81

Table 1: Recent results of fits to the parameters of the unitarity triangle.

In Table 1, we have collected recent results, which agree rather well with one another. On the other hand, considerably narrower ranges are given by Ciuchini *et al.* in [38]:

$$\gamma = (54.8 \pm 6.2)^\circ, \quad \sin 2\alpha = -0.42 \pm 0.23, \quad \sin 2\beta = 0.698 \pm 0.066, \quad (2.54)$$

corresponding to

$$\bar{\rho} = 0.224 \pm 0.038, \quad \bar{\eta} = 0.317 \pm 0.040. \quad (2.55)$$

The question of combining the theoretical and experimental uncertainties in the “standard analysis” of the unitarity triangle illustrated in Fig. 4 in an optimal way and to obtain a realistic range in the  $\bar{\rho}$ - $\bar{\eta}$  plane will certainly continue to be a hot topic in the future. This is also reflected by the vast debate going on at present, dealing with the key issue of how to deal with the corresponding uncertainties (for instance, Bayesian [38] vs. non-Bayesian [45] approach). The importance of CP violation in  $B$  decays is related to the fact that such effects allow us to determine the angles of the unitarity triangle *directly*. Comparing the thus obtained values with the indirect ranges determined as sketched above, we may well encounter discrepancies, which may shed light on the physics beyond the Standard Model. In this context, non-leptonic  $B$ -meson decays play the key rôle.

We shall come back to the allowed range in the  $\bar{\rho}$ - $\bar{\eta}$  plane in Section 7, where we discuss the important impact of  $B_s^0$ - $\bar{B}_s^0$  mixing in more detail (see Fig. 22), and in Section 11, where we consider models with minimal flavour violation [12, 13], a simple class of extensions of the Standard Model. In this framework, various interesting bounds on the unitarity triangle,  $\sin 2\beta$  and  $K \rightarrow \pi\nu\bar{\nu}$  decays can be derived [46, 47].

### 3 Non-leptonic $B$ Decays

#### 3.1 Preliminaries

We may divide weak decays of  $B$ -mesons into leptonic, semi-leptonic and non-leptonic transitions. The first ones, the leptonic modes  $B^- \rightarrow \ell \bar{\nu}_\ell$ , allow – at least in principle – a determination of the  $B$ -meson decay constant  $f_B$ , which is defined by

$$\langle 0 | \bar{u} \gamma_5 \gamma_\mu b | B^-(p) \rangle = i f_B p_\mu. \quad (3.1)$$

However, the corresponding rates suffer from a helicity suppression proportional to  $(m_\ell/M_B)^2$ , and are hence very small. For  $\ell = e$  and  $\mu$ , we have branching ratios at the  $10^{-10}$  and  $10^{-7}$  levels, respectively. Consequently, these decays are very hard to measure. In the case of  $\ell = \tau$ , the helicity suppression is not effective, but the experimental reconstruction of the  $\tau$ -leptons is unfortunately very challenging [48].

Using heavy-quark arguments, exclusive and inclusive semi-leptonic decays caused by  $b \rightarrow c \ell^- \bar{\nu}_\ell$  and  $b \rightarrow u \ell^- \bar{\nu}_\ell$  quark-level transitions allow extractions of the CKM matrix elements  $|V_{cb}|$  and  $|V_{ub}|$ , respectively, as we have seen in Subsection 2.6.

With respect to testing the Standard-Model description of CP violation, the major rôle is played by non-leptonic  $B$  decays. At the quark level, they are mediated by the following processes:

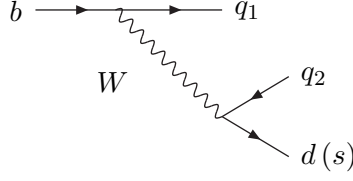
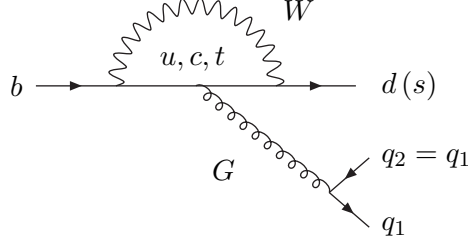
$$b \rightarrow q_1 \bar{q}_2 d(s), \quad (3.2)$$

where  $q_1, q_2 \in \{u, d, c, s\}$  are quark-flavour labels. In this section, we discuss the basic features of the theoretical framework to deal with such non-leptonic transitions.

#### 3.2 Classification

There are two kinds of topologies contributing to non-leptonic  $B$  decays: “tree-diagram-like” and “penguin” topologies. The latter consist of gluonic (QCD) and electroweak (EW) penguins, which originate from strong and electroweak interactions, respectively. In Figs. 5–7, the corresponding leading-order Feynman diagrams are shown. Depending on their flavour content, we may classify  $b \rightarrow q_1 \bar{q}_2 d(s)$  transitions as follows:

- $q_1 \neq q_2 \in \{u, c\}$ : only tree diagrams contribute.
- $q_1 = q_2 \in \{u, c\}$ : tree and penguin diagrams contribute.
- $q_1 = q_2 \in \{d, s\}$ : only penguin diagrams contribute.

Figure 5: Tree diagrams ( $q_1, q_2 \in \{u, c\}$ ).Figure 6: QCD penguin diagrams ( $q_1 = q_2 \in \{u, d, c, s\}$ ).

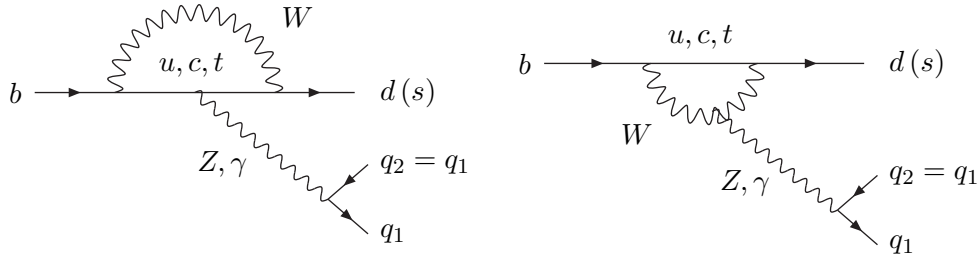
### 3.3 Low-energy Effective Hamiltonians

#### 3.3.1 General Remarks

In order to analyse non-leptonic  $B$  decays theoretically, we employ low-energy effective Hamiltonians, which are calculated by making use of the operator product expansion [49]. This formalism yields transition matrix elements of the following structure:

$$\langle f | \mathcal{H}_{\text{eff}} | i \rangle = \frac{G_F}{\sqrt{2}} \lambda_{\text{CKM}} \sum_k C_k(\mu) \langle f | Q_k(\mu) | i \rangle \equiv \frac{G_F}{\sqrt{2}} \lambda_{\text{CKM}} [\vec{C}^T(\mu) \cdot \langle \vec{Q}(\mu) \rangle]. \quad (3.3)$$

The operator product expansion allows us to disentangle the short-distance contributions to this transition amplitude from the long-distance ones, which are described by perturbative Wilson coefficient functions  $C_k(\mu)$  and non-perturbative hadronic matrix elements  $\langle f | Q_k(\mu) | i \rangle$ , respectively. As usual,  $G_F$  is the Fermi constant,  $\lambda_{\text{CKM}}$  a CKM factor, and  $\mu$  an appropriate renormalization scale. This scale separates, roughly speaking, the short-distance contributions from the long-distance pieces. The  $Q_k$  are local operators, which are generated by electroweak and strong interactions and govern “effectively” the

Figure 7: EW penguin diagrams ( $q_1 = q_2 \in \{u, d, c, s\}$ ).

decay in question. The Wilson coefficients  $C_k(\mu)$  can be considered as scale-dependent couplings related to the vertices described by the  $Q_k$ .

In general, the Wilson coefficients, which describe essentially the whole short-distance dynamics of the transition amplitude (3.3), include contributions from virtual  $W$ - and  $Z$ -bosons, as well as from virtual top quarks. Mathematically, these contributions are related to appropriate ‘‘Inami–Lim functions’’ [50]. If extensions of the Standard Model are considered, also new particles, such as charged Higgs or supersymmetric particles, may contribute to the  $C_k(\mu)$ . The resulting dependence on the masses of these particles can be calculated by evaluating penguin and box diagrams with full  $W$ ,  $Z$ , top-quark and possible new-particle exchanges [51]. The  $\mu$  dependence of the Wilson coefficients is governed by the properly included short-distance QCD corrections. This  $\mu$  dependence has to cancel that of the non-perturbative hadronic matrix elements  $\langle f|Q_k(\mu)|i\rangle$ , since the physical transition amplitude (3.3) cannot depend on the choice of the renormalization scale. In this cancellation, usually several terms on the right-hand side of (3.3) are involved. The  $C_k(\mu)$  depend, in general, also on the employed renormalization scheme. This dependence has again to be cancelled by the one of the hadronic matrix elements.

### 3.3.2 Tree Decays

Let us consider the decay  $\overline{B}_d^0 \rightarrow D^+ K^-$  as an example. At the quark level, it originates from  $b \rightarrow \overline{c} \overline{u} s$  transitions, as can be seen in Fig. 8. Consequently, according to the classification introduced in Subsection 3.2, it is a pure ‘‘tree’’ decay, receiving no penguin contributions. In order to derive the relevant low-energy effective Hamiltonian, we have to consider the quark-level process in Fig. 8, yielding the following transition amplitude:

$$-\frac{g_2^2}{8} V_{us}^* V_{cb} [\overline{s} \gamma^\nu (1 - \gamma_5) u] \left[ \frac{g_{\nu\mu}}{k^2 - M_W^2} \right] [\overline{c} \gamma^\mu (1 - \gamma_5) b]. \quad (3.4)$$

Because of  $k^2 \approx m_b^2 \ll M_W^2$ , we may write

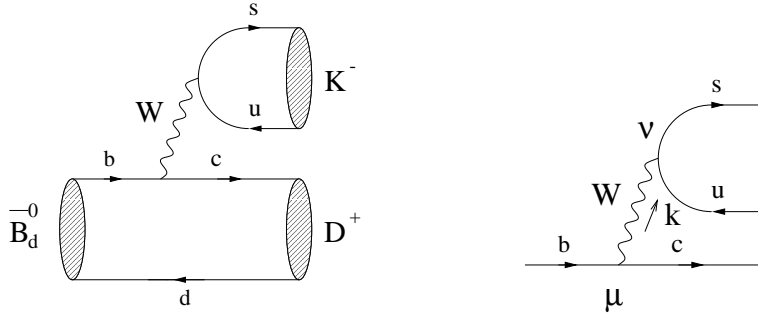
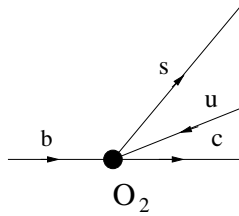
$$\frac{g_{\nu\mu}}{k^2 - M_W^2} \longrightarrow -\frac{g_{\nu\mu}}{M_W^2} \equiv -\left( \frac{8G_F}{\sqrt{2}g_2^2} \right) g_{\nu\mu}, \quad (3.5)$$

i.e. we may ‘‘integrate out’’ the  $W$ -boson in (3.4), and arrive at

$$\begin{aligned} \mathcal{H}_{\text{eff}} &= \frac{G_F}{\sqrt{2}} V_{us}^* V_{cb} [\overline{s}_\alpha \gamma_\mu (1 - \gamma_5) u_\alpha] [\overline{c}_\beta \gamma^\mu (1 - \gamma_5) b_\beta] \\ &\equiv \frac{G_F}{\sqrt{2}} V_{us}^* V_{cb} (\overline{s}_\alpha u_\alpha)_{V-A} (\overline{c}_\beta b_\beta)_{V-A} \equiv \frac{G_F}{\sqrt{2}} V_{us}^* V_{cb} O_2, \end{aligned} \quad (3.6)$$

where  $\alpha$  and  $\beta$  denote  $SU(3)_C$  colour indices. Effectively, the vertex shown in Fig. 8 is now described by the ‘‘current–current’’ operator  $O_2$ , as illustrated in Fig. 9.



Figure 8: Feynman diagram contributing at leading order to  $\overline{B}_d^0 \rightarrow D^+ K^-$ .Figure 9: The vertex described by the current–current operator  $O_2$ .

If we take into account QCD effects, we have to distinguish between factorizable and non-factorizable QCD vertex corrections. In the former case, the gluons are exchanged separately *within* the  $\bar{s}u$  and  $\bar{c}b$  quark currents, whereas the gluons are *interchanged* between these currents in the non-factorizable case. The factorizable QCD corrections just renormalize the  $O_2$  operator. However, the non-factorizable QCD corrections induce another “current–current” operator through “operator mixing”. It is given by

$$O_1 = [\bar{s}_\alpha \gamma_\mu (1 - \gamma_5) u_\beta] [\bar{c}_\beta \gamma^\mu (1 - \gamma_5) b_\alpha], \quad (3.7)$$

i.e. it differs from  $O_2$  through its colour structure. Consequently, if we take into account QCD corrections, the low-energy effective Hamiltonian takes the following form:

$$\mathcal{H}_{\text{eff}} = \frac{G_F}{\sqrt{2}} V_{us}^* V_{cb} [C_1(\mu) O_1 + C_2(\mu) O_2], \quad (3.8)$$

where  $C_1(\mu) \neq 0$  and  $C_2(\mu) \neq 1$  are due to QCD renormalization effects. This Hamiltonian applies to all decay processes, which are mediated by  $b \rightarrow \bar{c}us$  transitions. The amplitudes of different channels belonging to this decay class arise from different hadronic matrix elements of  $O_1$  and  $O_2$ . An approach to deal with these quantities, referred to as “factorization”, will be discussed in more detail in Subsection 3.6.

Let us now have a closer look at the evaluation of the Wilson coefficients [52]. To this end, we first have to calculate the QCD corrections to the vertices shown in Figs. 8

and 9, yielding the QCD-corrected transition amplitude

$$A_{\text{QCD}} = \vec{A}^T(\mu) \cdot \langle \vec{O} \rangle_0, \quad (3.9)$$

and the QCD-corrected matrix elements

$$\langle \vec{O}(\mu) \rangle = \hat{M}(\mu) \cdot \langle \vec{O} \rangle_0, \quad (3.10)$$

respectively. Here the column vector  $\langle \vec{O} \rangle_0$  contains the tree-level matrix elements of the operators  $O_1$  and  $O_2$ . The Wilson coefficients are now obtained by expressing the QCD-corrected transition amplitude (3.9) in terms of the QCD-corrected matrix elements (3.10) as in (3.3):

$$A_{\text{QCD}} = \vec{C}^T(\mu) \cdot \langle \vec{O}(\mu) \rangle, \quad (3.11)$$

yielding

$$\vec{C}(\mu) = \vec{A}^T(\mu) \cdot \hat{M}^{-1}(\mu). \quad (3.12)$$

This procedure is called ‘‘matching’’ of the full theory onto an effective theory, which is described by the low-energy effective Hamiltonian  $\mathcal{H}_{\text{eff}}$ . At the one-loop level, the results for the  $C_k(\mu)$  obtained this way are given by

$$C_1(\mu) = -3 \left( \frac{\alpha_s}{4\pi} \right) \ln \left( \frac{M_W^2}{\mu^2} \right), \quad C_2(\mu) = 1 + \frac{3}{N_C} \left( \frac{\alpha_s}{4\pi} \right) \ln \left( \frac{M_W^2}{\mu^2} \right), \quad (3.13)$$

where  $N_C$  denotes the number of quark colours, i.e.  $N_C = 3$  for the QCD gauge group  $SU(3)_C$ .

The characteristic feature of the expressions given in (3.13) are the terms proportional to  $\alpha_s \ln(M_W^2/\mu^2)$ . Although the renormalization scale  $\mu$  can, in principle, be chosen arbitrarily, it is natural to use  $\mu = \mathcal{O}(m_b)$  in analyses of  $B$  decays. For such scales, we have to deal with large logarithms in (3.13). Sloppily speaking, these large logarithms compensate the smallness of the running QCD coupling  $\alpha_s(\mu)$ . In order to obtain a reliable result, these terms have to be resummed to all orders in  $\alpha_s$ , which can be accomplished with the help of renormalization-group techniques. Here one exploits that the transition amplitude (3.3) cannot depend on the chosen renormalization scale  $\mu$ . The general expression for the  $C_k(\mu)$  can be written as

$$\vec{C}(\mu) = \hat{U}(\mu, M_W) \cdot \vec{C}(M_W), \quad (3.14)$$

where  $\vec{C}(M_W)$  denotes the initial conditions, depending on the short-distance physics at high-energy scales. The evolution matrix is given by

$$\hat{U}(\mu, M_W) = T_g \left\{ \exp \left[ \int_{g_s(M_W)}^{g_s(\mu)} dg' \frac{\hat{\gamma}^T(g')}{\beta(g')} \right] \right\}, \quad (3.15)$$

where  $g_s$  is the QCD coupling, the operator  $T_g$  denotes coupling-constant ordering such that the couplings increase from right to left, the QCD “beta function”  $\beta(g)$  governs the renormalization-group evolution of  $g$ ,

$$\mu \frac{d}{d\mu} g(\mu) = \beta(g(\mu)), \quad (3.16)$$

and  $\hat{\gamma}$  is the “anomalous dimension matrix” of the operators  $\vec{O}$ , entering in

$$\frac{d}{dg} \vec{C}(g) = \frac{\hat{\gamma}^T(g)}{\beta(g)} \cdot \vec{C}(g). \quad (3.17)$$

Using these renormalization-group techniques, it is possible to sum up the following terms of the Wilson coefficients in a systematic way:

$$\alpha_s^n \left[ \ln \left( \frac{\mu}{M_W} \right) \right]^n \text{ (LO),} \quad \alpha_s^n \left[ \ln \left( \frac{\mu}{M_W} \right) \right]^{n-1} \text{ (NLO),} \quad \dots, \quad (3.18)$$

where the abbreviations LO and NLO refer to the “leading logarithmic” and “next-to-leading logarithmic” approximations, respectively. For many applications, the LO corrections are not sufficient. Important examples are the meaningful use of the QCD scale parameter  $\Lambda_{\overline{\text{MS}}}$  [53] extracted from various high-energy processes, and the penguin processes discussed below, where the matching procedure required to calculate the top-quark mass dependence of the Wilson coefficients can only be performed properly by going beyond the LO approximation. In this case, also dependences of the Wilson coefficients on the employed renormalization schemes show up, which have to be cancelled through the hadronic matrix elements of the corresponding operators. Moreover, scale dependences can usually be reduced by going beyond LO.

Let us, in order to see the structure of the NLO Wilson coefficients, give the result for the current–current operators. Here it is convenient to introduce operators  $O_{\pm}$  with coefficients  $C_{\pm}(\mu)$ , which do not mix under renormalization and are defined by

$$O_{\pm} \equiv \frac{1}{2} (O_2 \pm O_1) \quad \text{with} \quad C_{\pm}(\mu) = C_2(\mu) \pm C_1(\mu). \quad (3.19)$$

The NLO renormalization-group evolution from  $M_W$  to  $\mu = \mathcal{O}(m_b)$  is described by

$$C_{\pm}(\mu) = U_{\pm}(\mu, M_W) C_{\pm}(M_W), \quad (3.20)$$

with

$$U_{\pm}(\mu, M_W) = \left[ 1 + \frac{\alpha_s(\mu)}{4\pi} J_{\pm} \right] \left[ \frac{\alpha_s(M_W)}{\alpha_s(\mu)} \right]^{d_{\pm}} \left[ 1 - \frac{\alpha_s(M_W)}{4\pi} J_{\pm} \right] \quad (3.21)$$

and

$$C_{\pm}(M_W) = 1 + \frac{\alpha_s(M_W)}{4\pi} B_{\pm}. \quad (3.22)$$

Here

$$J_{\pm} = \frac{d_{\pm}}{\beta_0} \beta_1 - \frac{\gamma_{\pm}^{(1)}}{2\beta_0}, \quad d_{\pm} = \frac{\gamma_{\pm}^{(0)}}{2\beta_0}, \quad B_{\pm} = \frac{N_C \mp 1}{2N_C} [\pm 11 + \kappa_{\pm}], \quad (3.23)$$

with

$$\beta_0 = \frac{11N_C - 2f}{3}, \quad \beta_1 = \frac{34}{3}N_C^2 - \frac{10}{3}N_C f - 2 \left[ \frac{N_C^2 - 1}{2N_C} \right] f \quad (3.24)$$

and

$$\gamma_{\pm}^{(0)} = \pm 12 \left[ \frac{N_C \mp 1}{2N_C} \right], \quad \gamma_{\pm}^{(1)} = \frac{N_C \mp 1}{2N_C} \left[ -21 \pm \frac{57}{N_C} \mp \frac{19}{3}N_C \pm \frac{4}{3}f - 2\beta_0 \kappa_{\pm} \right]. \quad (3.25)$$

The parameter  $f$  denotes the number of active quark flavours (5 in our example, as the top quark is integrated out), and  $\kappa_{\pm}$  distinguishes between different renormalization schemes [54]. The  $\beta$  and  $\gamma$  coefficients in (3.23)–(3.25) arise from the expansions

$$\beta(g_s) = -\beta_0 \frac{g_s^3}{16\pi^2} - \beta_1 \frac{g_s^5}{(16\pi^2)^2} + \dots, \quad \gamma_{\pm}(\alpha_s) = \gamma_{\pm}^{(0)} \left( \frac{\alpha_s}{4\pi} \right) + \gamma_{\pm}^{(1)} \left( \frac{\alpha_s}{4\pi} \right)^2 + \dots, \quad (3.26)$$

where the former governs the NLO effective QCD coupling

$$\frac{\alpha_s(\mu)}{4\pi} = \frac{1}{\beta_0 \ln(\mu^2/\Lambda_{\overline{\text{MS}}}^2)} - \frac{\beta_1}{\beta_0^3} \left[ \frac{\ln \ln(\mu^2/\Lambda_{\overline{\text{MS}}}^2)}{\ln^2(\mu^2/\Lambda_{\overline{\text{MS}}}^2)} \right]. \quad (3.27)$$

If we set  $J_{\pm}$  and  $B_{\pm}$  in (3.21) and (3.22) equal to zero, we obtain the LO result.

This example shows that things are getting rather complicated and technical at the NLO level. However, for the phenomenological considerations of this review, we have just to be familiar with the general structure of the appropriate low-energy effective Hamiltonians. For detailed discussions of the renormalization-group techniques sketched above, we refer the interested reader to the excellent presentations given in [55, 56].

### 3.3.3 Decays with Tree and Penguin Contributions

In the exploration of CP violation in the  $B$  system, non-leptonic decays receiving both tree and penguin contributions, i.e.  $|\Delta B| = 1$ ,  $\Delta C = \Delta U = 0$  modes (see Subsection 3.2), play a key rôle. This feature is due to the fact that CP asymmetries originate from certain interference effects, which are provided by such channels. Because of the penguin topologies, the operator basis is now much larger than in (3.8), where we considered a pure “tree” decay. We have to deal with

$$\mathcal{H}_{\text{eff}} = \frac{G_F}{\sqrt{2}} \left[ \sum_{j=u,c} V_{jr}^* V_{jb} \left\{ \sum_{k=1}^2 C_k(\mu) Q_k^{jr} + \sum_{k=3}^{10} C_k(\mu) Q_k^r \right\} \right], \quad (3.28)$$

where the four-quark operators  $Q_k^{jr}$  ( $j \in \{u, c\}$ ,  $r \in \{d, s\}$ ) can be divided as follows:

- Current–current operators:

$$\begin{aligned} Q_1^{jr} &= (\bar{r}_\alpha j_\beta)_{V-A} (\bar{j}_\beta b_\alpha)_{V-A} \\ Q_2^{jr} &= (\bar{r}_\alpha j_\alpha)_{V-A} (\bar{j}_\beta b_\beta)_{V-A}. \end{aligned} \quad (3.29)$$

- QCD penguin operators:

$$\begin{aligned} Q_3^r &= (\bar{r}_\alpha b_\alpha)_{V-A} \sum_{q'} (\bar{q}'_\beta q'_\beta)_{V-A} \\ Q_4^r &= (\bar{r}_\alpha b_\beta)_{V-A} \sum_{q'} (\bar{q}'_\beta q'_\alpha)_{V-A} \\ Q_5^r &= (\bar{r}_\alpha b_\alpha)_{V-A} \sum_{q'} (\bar{q}'_\beta q'_\beta)_{V+A} \\ Q_6^r &= (\bar{r}_\alpha b_\beta)_{V-A} \sum_{q'} (\bar{q}'_\beta q'_\alpha)_{V+A}. \end{aligned} \quad (3.30)$$

- EW penguin operators ( $e_{q'}$ : electrical quark charges):

$$\begin{aligned} Q_7^r &= \frac{3}{2} (\bar{r}_\alpha b_\alpha)_{V-A} \sum_{q'} e_{q'} (\bar{q}'_\beta q'_\beta)_{V+A} \\ Q_8^r &= \frac{3}{2} (\bar{r}_\alpha b_\beta)_{V-A} \sum_{q'} e_{q'} (\bar{q}'_\beta q'_\alpha)_{V+A} \\ Q_9^r &= \frac{3}{2} (\bar{r}_\alpha b_\alpha)_{V-A} \sum_{q'} e_{q'} (\bar{q}'_\beta q'_\beta)_{V-A} \\ Q_{10}^r &= \frac{3}{2} (\bar{r}_\alpha b_\beta)_{V-A} \sum_{q'} e_{q'} (\bar{q}'_\beta q'_\alpha)_{V-A}. \end{aligned} \quad (3.31)$$

The current–current operators, which are related to the tree processes shown in Fig. 5, are analogous to the operators  $O_1$  and  $O_2$  we encountered in (3.6) and (3.7); they have just a different flavour content. The QCD and EW penguin operators are associated with the QCD and EW penguin processes shown in Figs. 6 and 7, respectively. In the latter case, also certain box diagrams contribute, which are not shown explicitly in Fig. 7. Note that the unitarity of the CKM matrix, implying

$$V_{tr}^* V_{tb} = -V_{ur}^* V_{ub} - V_{cr}^* V_{cb}, \quad (3.32)$$

has been used in (3.28) to eliminate the CKM factor  $V_{tr}^* V_{tb}$ , which is related to penguin topologies with internal top-quark exchanges.

The Wilson coefficient functions, including both LO and NLO QCD corrections and LO corrections in the QED coupling  $\alpha$ , were calculated in [57, 58]. In Table 2, we have collected the values for these coefficients for up-dated input parameters, as obtained in [56], where also a very detailed discussion of the technicalities of the corresponding calculations can be found. The next-to-leading order results are given for two renormalization schemes, the naïve dimensional regularization scheme (NDR) and the 't Hooft–Veltman scheme (HV), corresponding to anticommuting and non-anticommuting  $\gamma_5$  in  $\mathcal{D} \neq 4$  dimensions, respectively [59]. As usual,  $\overline{m}_b(m_b)$  denotes the running  $b$ -quark mass in the  $\overline{\text{MS}}$  scheme [53], and  $\alpha = 1/129$  is the QED coupling.

The results listed in Table 2 correspond to the Standard Model. In scenarios for new physics, we usually have to deal with new operators, i.e. the operator basis (3.29)–(3.31) is enlarged. The  $\Delta F = 1$  case, including also the  $B$ -meson decays with tree

Scheme	$\Lambda_{\overline{\text{MS}}}^{(5)} = 160 \text{ MeV}$			$\Lambda_{\overline{\text{MS}}}^{(5)} = 225 \text{ MeV}$			$\Lambda_{\overline{\text{MS}}}^{(5)} = 290 \text{ MeV}$		
	LO	NDR	HV	LO	NDR	HV	LO	NDR	HV
$C_1$	-0.283	-0.171	-0.209	-0.308	-0.185	-0.228	-0.331	-0.198	-0.245
$C_2$	1.131	1.075	1.095	1.144	1.082	1.105	1.156	1.089	1.114
$C_3$	0.013	0.013	0.012	0.014	0.014	0.013	0.016	0.016	0.014
$C_4$	-0.028	-0.033	-0.027	-0.030	-0.035	-0.029	-0.032	-0.038	-0.032
$C_5$	0.008	0.008	0.008	0.009	0.009	0.009	0.009	0.009	0.010
$C_6$	-0.035	-0.037	-0.030	-0.038	-0.041	-0.033	-0.041	-0.045	-0.036
$C_7/\alpha$	0.043	-0.003	0.006	0.045	-0.002	0.005	0.047	-0.002	0.005
$C_8/\alpha$	0.043	0.049	0.055	0.048	0.054	0.060	0.053	0.059	0.065
$C_9/\alpha$	-1.268	-1.283	-1.273	-1.280	-1.292	-1.283	-1.290	-1.300	-1.293
$C_{10}/\alpha$	0.302	0.243	0.245	0.328	0.263	0.266	0.352	0.281	0.284

Table 2: The  $|\Delta B| = 1$ ,  $\Delta C = \Delta U = 0$  Wilson coefficients at  $\mu = \overline{m}_b(m_b) = 4.40 \text{ GeV}$  for  $m_t = 170 \text{ GeV}$  as obtained in [56].

and penguin contributions discussed here, was considered in [60], where the two-loop anomalous dimension matrices for the dim-6 four-quark operators were calculated. The corresponding results for the  $\Delta F = 2$  case can be found in [60, 61].

Let us now return to the Standard Model. Roughly speaking, the origin of the penguin operators in (3.28) is due to the penguin topologies in Figs. 6 and 7 with internal top-quark exchanges. In the matching procedure, the top quark is integrated out – together with the  $W$ - and  $Z$ -bosons – at a scale  $\mu = \mathcal{O}(M_W)$ . Consequently, these particles do not show up explicitly in the low-energy effective Hamiltonian (3.28). However, their presence is included in the initial values of the renormalization group evolution (3.14), leading in particular to a top-quark mass dependence of the penguin coefficients. As can be seen in Figs. 6 and 7, there are also penguin topologies with internal up- and charm-quark exchanges. Within the language of effective field theory, these contributions show up as penguin matrix elements of the current–current operators  $Q_{1,2}^j$  with internal  $j$ -quark exchanges ( $j \in \{u, c\}$ ), as illustrated in Fig. 10. Their proper treatment requires us to go beyond the LO approximation, representing another example for the importance of NLO calculations [62, 63]. Following these lines, we arrive at the renormalization-scheme independent expression

$$\begin{aligned}
\langle \vec{Q}^T(\mu) \cdot \vec{C}(\mu) \rangle^{\text{pen}} &= \sum_{k=3}^{10} \langle Q_k \rangle_0 \overline{C}_k(\mu) + \frac{\alpha_s(\mu)}{8\pi} \left[ \frac{10}{9} - G(m_j, k, \mu) \right] \\
&\quad \times \left\{ \left( -\frac{1}{3} \langle Q_3 \rangle_0 + \langle Q_4 \rangle_0 - \frac{1}{3} \langle Q_5 \rangle_0 + \langle Q_6 \rangle_0 \right) \overline{C}_2(\mu) \right.
\end{aligned}$$

$$+ \frac{8}{9} \frac{\alpha}{\alpha_s(\mu)} (\langle Q_7 \rangle_0 + \langle Q_9 \rangle_0) \left( 3\overline{C}_1(\mu) + \overline{C}_2(\mu) \right) \Big\}, \quad (3.33)$$

where

$$G(m, k, \mu) = -4 \int_0^1 dx x(1-x) \ln \left[ \frac{m^2 - x(1-x)k^2}{\mu^2} \right] \quad (3.34)$$

describes the loop process shown in Fig. 10, with  $k$  denoting the four-momentum of the gluons and photons. The  $\overline{C}_k(\mu)$  are the renormalization-scheme independent Wilson coefficients introduced in [57]. Expression (3.33) is at the basis of the implementation of the ‘‘Bander–Silverman–Soni (BSS) mechanism’’ [64] in the operator language. It allows us to estimate CP-conserving strong phases, which are an essential ingredient for ‘‘direct’’ CP violation, through the absorptive part of the function  $G(m_j, k, \mu)$ . Several applications of the BSS mechanism can be found in the literature (see, for instance, [62]–[70]). Let us discuss the impact of penguin topologies with internal charm- and up-quark exchanges in more detail in the following subsection.

### 3.4 Penguins with Internal Charm- and Up-Quark Exchanges

Looking at Figs. 6 and 7, we observe that the amplitude for a generic  $b \rightarrow r$  penguin process can be written as follows ( $r \in \{d, s\}$ ):

$$A_{\text{pen}}^{(r)} = V_{cr}^* V_{cb} P_c^{(r)} + V_{ur}^* V_{ub} P_u^{(r)} + V_{tr}^* V_{tb} P_t^{(r)}, \quad (3.35)$$

where the  $P_j^{(r)}$  denote the strong amplitudes of penguin topologies with internal  $j$ -quark exchanges. To be more specific,  $P_t^{(r)}$  describes the hadronic matrix elements of the penguin operators (3.30) and (3.31), whereas  $P_c^{(r)}$  and  $P_u^{(r)}$  are related to the matrix elements shown in Fig. 10, which are associated with (3.33). Using the unitarity relation (3.32) to eliminate  $V_{ur}^* V_{ub}$ , we obtain

$$A_{\text{pen}}^{(r)} = V_{tr}^* V_{tb} \left[ 1 + \left( \frac{V_{cr}^* V_{cb}}{V_{tr}^* V_{tb}} \right) \Delta P_r \right] [P_t^{(r)} - P_u^{(r)}], \quad (3.36)$$

where

$$\Delta P_r \equiv \frac{P_c^{(r)} - P_u^{(r)}}{P_t^{(r)} - P_u^{(r)}}. \quad (3.37)$$

Moreover, the generalized Wolfenstein parametrization (2.17) with (2.46) yields

$$\frac{V_{cd}^* V_{cb}}{V_{td}^* V_{tb}} = -\frac{e^{-i\beta}}{R_t} [1 + \mathcal{O}(\lambda^4)], \quad \frac{V_{cs}^* V_{cb}}{V_{ts}^* V_{tb}} = -[1 + \mathcal{O}(\lambda^2)]. \quad (3.38)$$

In the limit of degenerate up- and charm-quark masses,  $\Delta P_r$  would vanish because of the ‘‘Glashow–Iliopoulos–Maiani (GIM) mechanism’’ [71]. However, since  $m_u \approx 5$  MeV,

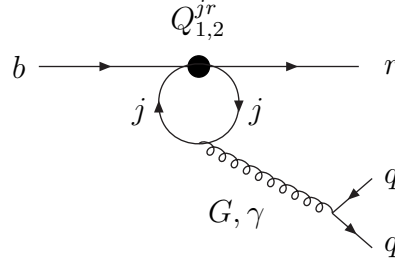


Figure 10: The one-loop QCD and QED time-like penguin matrix elements of the current–current operators  $Q_{1,2}^{jr}$  ( $j \in \{u, c\}$ ,  $r \in \{d, s\}$ ,  $q \in \{u, d, c, s\}$ ).

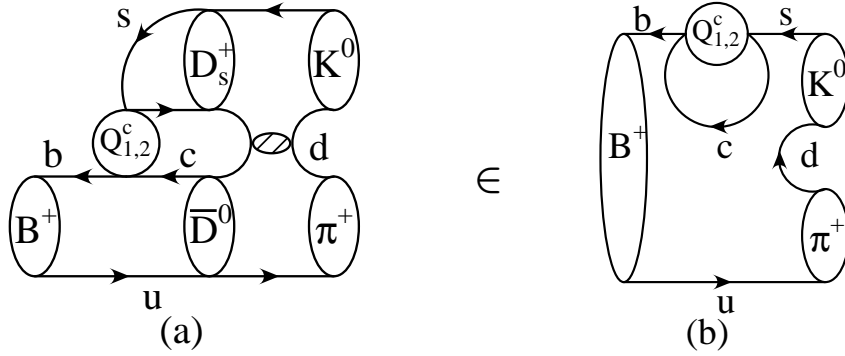


Figure 11: Illustration of a rescattering process of the kind  $B^+ \rightarrow \{\overline{D}^0 D_s^+\} \rightarrow \pi^+ K^0$  (a), which is contained in penguin topologies with internal charm-quark exchanges (b).

whereas  $m_c \approx 1.3 \text{ GeV}$ , this GIM cancellation is incomplete, and  $\Delta P_r$  may well be sizeable, thereby affecting (3.36) significantly. Estimates using the BSS mechanism sketched above yield that  $|\Delta P_r|$  may be as large as  $\mathcal{O}(0.5)$ , with a large CP-conserving strong phase [72]. Consequently, the assumption made in many analyses that QCD penguin processes are dominated by internal top-quark exchanges is not justified, and penguin topologies with internal charm and up quarks have also an important phenomenological impact [72]. An interesting example is the decay  $B_d \rightarrow K^0 \overline{K}^0$ , where the Standard Model would predict *vanishing* CP violation, if top-quark penguins played the dominant rôle. However, this feature is spoiled by a sizeable value of  $\Delta P_d$  [73]. Using additional information provided by  $B_s \rightarrow K^0 \overline{K}^0$ , or considering the  $B_{d,s} \rightarrow K^{*0} \overline{K}^{*0}$  system, weak phases can still be extracted with the help of  $U$ -spin flavour-symmetry arguments [74], as we will see in Subsection 10.2. The importance of “charming” penguins, i.e. penguin topologies with internal charm-quark exchanges, was also emphasized in [75]–[77].

The amplitudes  $P_u^{(r)}$  and  $P_c^{(r)}$  may also receive large contributions from rescattering



processes [78], which can be considered as long-distance penguin topologies with internal up and charm quarks [79]. An important example is the decay  $B^+ \rightarrow \pi^+ K^0$ , which receives rescattering contributions of the following kind:

$$B^+ \rightarrow \{\overline{D^0} D_s^+, \overline{D^0} D_s^{*+}, \overline{D^{*0}} D_s^{*+}, \dots\} \rightarrow \pi^+ K^0 \quad (3.39)$$

$$B^+ \rightarrow \{\pi^0 K^+, \pi^0 K^{*+}, \rho^0 K^{*+}, \dots\} \rightarrow \pi^+ K^0. \quad (3.40)$$

Here the dots include also intermediate multibody states. In the first class of rescattering processes, (3.39), we have to deal with decays that are caused by the  $Q_{1,2}^c$  current–current operators through insertions into tree-diagram-like topologies, and may rescatter into the final state  $\pi^+ K^0$ . These final-state interaction effects are related to penguin topologies with internal charm-quark exchanges, as can be seen in Fig. 11. In the case of (3.40), we have to deal both with analogous penguin topologies, where all charm quarks are replaced by up quarks, and with annihilation topologies. These issues received a lot of attention in the context of extractions of  $\gamma$  from  $B \rightarrow \pi K$  decays (see Section 9), and require also careful attention for several other modes.

### 3.5 Electroweak Penguin Effects

Since the ratio  $\alpha/\alpha_s = \mathcal{O}(10^{-2})$  of the QED and QCD couplings is very small, we would naïvely expect that EW penguins should play a minor rôle in comparison with QCD penguins. This would actually be the case if the top quark was not heavy. However, the Wilson coefficient of the EW penguin operator  $Q_9^r$  increases strongly with the top-quark mass  $m_t$ . As can be seen in Table 2, calculated for  $m_t = 170 \text{ GeV}$ ,  $C_9$  becomes comparable in magnitude with Wilson coefficients of QCD penguin operators.

Because of this feature, we obtain interesting EW penguin effects in several non-leptonic  $B$  decays [63] (for a review, see [80]). A prominent example is  $B^- \rightarrow \phi K^-$ , which is governed by QCD penguins [65]. However, EW penguins may contribute to this channel in “colour-allowed” form, thereby reducing its branching ratio by  $\mathcal{O}(30\%)$  [63, 81]. There are even decays, which are *dominated* by EW penguins, for example  $B^- \rightarrow \phi \pi^-$  [82] and  $B_s^0 \rightarrow \phi \pi^0$  [83]. Unfortunately, the corresponding branching ratios of  $\mathcal{O}(10^{-8})$  and  $\mathcal{O}(10^{-7})$ , respectively, are very small. On the other hand, the  $B^- \rightarrow \phi K^-$  mode has already been observed by the  $B$ -factories, with branching ratios at the  $10^{-5}$  level. We shall come back to this channel in Subsection 6.2.

EW penguins have also an important impact on the phenomenology of  $B \rightarrow \pi K$  decays [84, 85]. As we will see in Section 9, these modes provide several strategies to extract the CKM angle  $\gamma$ . Alternatively, if  $\gamma$  is used as an input, EW penguin amplitudes can be determined from  $B \rightarrow \pi K$  branching ratios [86, 87], thereby allowing an interesting comparison with the Standard-Model predictions. In [88], in addition to strategies for extracting the CKM angle  $\gamma$  and obtaining experimental insights into the

world of EW penguins, also a transparent expression for the ratio of EW penguin to tree amplitudes was derived.

### 3.6 Factorization of Hadronic Matrix Elements

In order to discuss “factorization”, let us consider again the decay  $\overline{B}_d^0 \rightarrow D^+ K^-$ , which we encountered already in the discussion of the low-energy effective Hamiltonian (3.8). The problem in the evaluation of the  $\overline{B}_d^0 \rightarrow D^+ K^-$  transition amplitude is the calculation of the hadronic matrix elements of the  $O_{1,2}$  operators between the  $\langle K^- D^+ |$  final and  $|\overline{B}_d^0\rangle$  initial states. Making use of the well-known  $SU(N_C)$  colour-algebra relation

$$T_{\alpha\beta}^a T_{\gamma\delta}^a = \frac{1}{2} \left( \delta_{\alpha\delta} \delta_{\beta\gamma} - \frac{1}{N_C} \delta_{\alpha\beta} \delta_{\gamma\delta} \right) \quad (3.41)$$

to re-write the operator  $O_1$ , we obtain

$$\begin{aligned} \langle K^- D^+ | \mathcal{H}_{\text{eff}} | \overline{B}_d^0 \rangle &= \frac{G_F}{\sqrt{2}} V_{us}^* V_{cb} \left[ a_1 \langle K^- D^+ | (\overline{s}_\alpha u_\alpha)_{V-A} (\overline{c}_\beta b_\beta)_{V-A} | \overline{B}_d^0 \rangle \right. \\ &\quad \left. + 2 C_1 \langle K^- D^+ | (\overline{s}_\alpha T_{\alpha\beta}^a u_\beta)_{V-A} (\overline{c}_\gamma T_{\gamma\delta}^a b_\delta)_{V-A} | \overline{B}_d^0 \rangle \right], \end{aligned} \quad (3.42)$$

with

$$a_1 = \frac{C_1}{N_C} + C_2. \quad (3.43)$$

It is now straightforward to “factorize” the hadronic matrix elements:

$$\begin{aligned} &\langle K^- D^+ | (\overline{s}_\alpha u_\alpha)_{V-A} (\overline{c}_\beta b_\beta)_{V-A} | \overline{B}_d^0 \rangle \Big|_{\text{fact}} \\ &= \langle K^- | [\overline{s}_\alpha \gamma_\mu (1 - \gamma_5) u_\alpha] | 0 \rangle \langle D^+ | [\overline{c}_\beta \gamma^\mu (1 - \gamma_5) b_\beta] | \overline{B}_d^0 \rangle \\ &\propto f_K [\text{decay constant}] \times F_{BD}(M_K^2; 0^+) [\text{form factor}], \end{aligned} \quad (3.44)$$

$$\langle K^- D^+ | (\overline{s}_\alpha T_{\alpha\beta}^a u_\beta)_{V-A} (\overline{c}_\gamma T_{\gamma\delta}^a b_\delta)_{V-A} | \overline{B}_d^0 \rangle \Big|_{\text{fact}} = 0. \quad (3.45)$$

The quantity introduced in (3.43) is a phenomenological “colour factor”, governing “colour-allowed” decays [89, 90]. The  $\overline{B}_d^0 \rightarrow D^+ K^-$  mode belongs to this category, since the colour indices of the  $K^-$ -meson and the  $\overline{B}_d^0$ - $D^+$  system in Fig. 8 run independently from each other. In the case of “colour-suppressed” transitions, for instance  $\overline{B}_d^0 \rightarrow D^0 \pi^0$ , this is not the case, and we have to deal with the combination

$$a_2 = C_1 + \frac{C_2}{N_C}. \quad (3.46)$$

The coefficients  $a_1$  and  $a_2$  were analysed beyond the leading logarithmic approximation in different renormalization schemes in [54]. Whereas  $a_1 = 1.01 \pm 0.02$  is very stable

under changes of  $\Lambda_{\overline{\text{MS}}}$  and the renormalization scale and scheme,  $a_2 = \mathcal{O}(0.2)$  is affected sizeably by such variations.

The phenomenological concept of the “factorization” of hadronic matrix elements in weak non-leptonic decays has a long history (see, for example, [89]–[95]). One possibility to justify it is provided by the large  $N_C$  limit [96], where the transition amplitudes factorize at leading order in a  $1/N_C$ -expansion, which can also be combined with the framework of “Heavy-Meson Chiral Perturbation Theory” [97]. Recently, an interesting approach was proposed in [98]–[100], representing an important step towards a rigorous theoretical description of a large class of non-leptonic two-body  $B$  decays. Within this framework, the physical idea [92] that factorization should hold for hadrons containing a heavy quark  $Q$  with  $m_Q \gg \Lambda_{\text{QCD}}$  is confirmed, and a formalism to calculate the relevant amplitudes at the leading order of a  $\Lambda_{\text{QCD}}/m_Q$ -expansion is provided. Let us consider a decay  $\overline{B} \rightarrow M_1 M_2$ , where  $M_1$  picks up the spectator quark. If  $M_1$  is either a heavy ( $D$ ) or a light ( $\pi$ ,  $K$ ) meson, and  $M_2$  a light ( $\pi$ ,  $K$ ) meson, it can be shown that the corresponding transition amplitude takes the following generic form [98]:

$$A(\overline{B} \rightarrow M_1 M_2) = [\text{naïve factorization}] \times [1 + \text{calculable } \mathcal{O}(\alpha_s) + \mathcal{O}(\Lambda_{\text{QCD}}/m_b)]. \quad (3.47)$$

While the  $\mathcal{O}(\alpha_s)$  terms, containing also radiative non-factorizable corrections to “naïve” factorization, can be calculated in a systematic way, the main limitation is due to the  $\mathcal{O}(\Lambda_{\text{QCD}}/m_b)$  terms. A very detailed discussion of  $B$  decays into heavy–light final states within this “QCD factorization” approach, including also the  $\overline{B}_d^0 \rightarrow D^+ K^-$  mode considered above, was given in [99], whereas the implications for  $B \rightarrow \pi K, \pi\pi$  modes were studied in [100]. Another QCD approach to deal with non-leptonic  $B$  decays into charmless final states – the perturbative hard-scattering (or “PQCD”) approach – was developed independently in [101]–[103], and differs from the “QCD factorization” formalism in some technical aspects. As far as phenomenological applications are concerned, the crucial question is obviously the importance of the  $\mathcal{O}(\Lambda_{\text{QCD}}/m_b)$  terms, which are hard to estimate. We shall come back to these issues in more detail in Section 9.

## 4 A Brief Look at the Kaon System

In 1964, CP violation was discovered in the famous experiment by Christenson *et al.* [1], who have observed  $K_L \rightarrow \pi^+ \pi^-$  decays. If the CP symmetry was conserved by weak interactions, as was believed until the experimental discovery of CP violation, the mass eigenstates  $K_S$  and  $K_L$  of the Hamiltonian describing  $K^0$ – $\overline{K}^0$  mixing were eigenstates of the CP operator with eigenvalues  $+1$  and  $-1$ , respectively. Consequently, since  $\pi^+ \pi^-$  is a CP-even final state, the detection of  $K_L \rightarrow \pi^+ \pi^-$  decays signals the non-invariance of weak interactions under CP transformations, i.e. CP violation.

Since we are mainly concerned with  $B$  decays in this review, the discussion of CP violation in the kaon system will be rather brief, and we refer the reader for more detailed presentations to [7, 8, 104]. The major aspects of kaon physics we have to deal with are the CP-violating parameter  $\varepsilon$ , which plays an important rôle to constrain the unitarity triangle, as we have already seen in Subsection 2.6, and the rare kaon decays  $K^+ \rightarrow \pi^+ \nu \bar{\nu}$  and  $K_L \rightarrow \pi^0 \nu \bar{\nu}$ , providing interesting relations to the  $B$ -meson system, as we will discuss in Section 11.

## 4.1 CP-violating Observables

In the neutral kaon system, CP violation is described by two complex quantities, called  $\varepsilon$  and  $\varepsilon'$ , which are defined by the following ratios of decay amplitudes:

$$\frac{A(K_L \rightarrow \pi^+ \pi^-)}{A(K_S \rightarrow \pi^+ \pi^-)} \approx \varepsilon + \varepsilon', \quad \frac{A(K_L \rightarrow \pi^0 \pi^0)}{A(K_S \rightarrow \pi^0 \pi^0)} \approx \varepsilon - 2\varepsilon'. \quad (4.1)$$

These parameters are related to “indirect” and “direct” CP violation, as illustrated in Fig. 12, where  $K_1$  and  $K_2$  denote the CP eigenstates of the neutral kaon system with CP eigenvalues  $+1$  and  $-1$ , respectively. Here indirect CP violation is due to the fact that the mass eigenstate  $K_L$  of the neutral kaon system is *not* a CP eigenstate because of the small admixture of the CP-even  $K_1$  state, which may decay through a CP-conserving transition into a  $\pi\pi$  final state. On the other hand, direct CP violation originates from *direct* transitions of the CP-odd  $K_2$  state into the CP-even  $\pi\pi$  final state.

After the discovery of indirect CP violation in  $K_L \rightarrow \pi^+ \pi^-$ , it was also observed in  $K_L \rightarrow \pi^0 \pi^0$ ,  $\pi \ell \bar{\nu}_\ell$ ,  $\pi^+ \pi^- \gamma$  modes, and recently in  $K_L \rightarrow \pi^+ \pi^- e^+ e^-$  transitions. All these effects can be described by

$$\varepsilon = (2.280 \pm 0.013) \times e^{i\frac{\pi}{4}} \times 10^{-3}. \quad (4.2)$$

As we have noted in Subsection 2.6, this observable fixes a hyperbola in the  $\bar{\rho}-\bar{\eta}$  plane, which is given as follows [8]:

$$\bar{\eta} \left[ (1 - \bar{\rho}) A^2 \eta_2 S_0(x_t) + P_c(\varepsilon) \right] A^2 \hat{B}_K = 0.204, \quad (4.3)$$

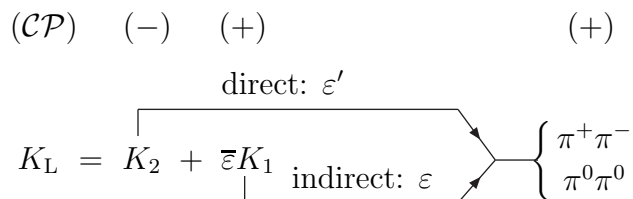


Figure 12: Indirect and direct CP violation in  $K_L \rightarrow \pi\pi$  decays.

and plays an important rôle to constrain the unitarity triangle. In this expression,  $\eta_2 = 0.57$  is a perturbative QCD factor [105],  $S_0(x_t) \approx 2.38$  with  $x_t \equiv m_t^2/M_W^2$  is the Inami–Lim function [50] resulting from box diagrams with  $(t, W^\pm)$  exchanges (see Fig. 13 for the analogous diagrams contributing to  $B_q^0-\overline{B}_q^0$  mixing), and  $P_c(\varepsilon) = 0.30 \pm 0.05$  [106] summarizes the contributions not proportional to  $V_{ts}^*V_{td}$ . The renormalization-group invariant quantity

$$\hat{B}_K \equiv B_K(\mu) \left[ \alpha_s^{(3)}(\mu) \right]^{-2/9} \left[ 1 + \frac{\alpha_s^{(3)}(\mu)}{4\pi} J_3 \right] \quad (4.4)$$

parametrizes the relevant hadronic matrix element through

$$\langle \overline{K^0} | (\overline{s}d)_{V-A} (\overline{s}d)_{V-A} | K^0 \rangle \equiv \frac{8}{3} B_K(\mu) f_K^2 M_K^2, \quad (4.5)$$

where  $\alpha_s^{(3)}(\mu)$  is the QCD coupling for three active quark flavours,  $J_3 = 1.895$  in the NDR scheme [105],  $f_K = 160 \text{ MeV}$  is the kaon decay constant, and  $M_K$  the kaon mass. A reasonable range for  $\hat{B}_K$  is [8]

$$\hat{B}_K = 0.85 \pm 0.15, \quad (4.6)$$

which agrees well with recent lattice results (for reviews, see [38, 107]), is slightly above the large- $N_C$  estimates [108], and a bit below the chiral quark-model estimates [109]. The numerical value in (4.3) and the value for  $P_c(\varepsilon)$  differ slightly from those given in [8] due to  $\lambda = 0.222$  used here instead of  $\lambda = 0.22$  used in that paper [47]. This increase of  $\lambda$  is made in order to be closer to the experimental value of  $|V_{ud}|$  [38, 45].

Direct CP violation in  $K \rightarrow \pi\pi$  transitions is measured by the quantity  $\text{Re}(\varepsilon'/\varepsilon)$ , which is governed by the competition between QCD and EW penguins. For large top-quark masses, a cancellation between these contributions arises, suppressing  $\text{Re}(\varepsilon'/\varepsilon)$  strongly [110]. In 1999, new measurements of this observable have demonstrated that it is different from zero, thereby establishing direct CP violation and excluding “superweak” models [111]. The present results read as follows:

$$\text{Re}(\varepsilon'/\varepsilon) = \begin{cases} (20.7 \pm 2.8) \times 10^{-4} \text{ (KTeV Collaboration [112])}, \\ (15.3 \pm 2.6) \times 10^{-4} \text{ (NA48 Collaboration [113])}. \end{cases} \quad (4.7)$$

Taking into account also the previous measurements yields a world average of

$$\text{Re}(\varepsilon'/\varepsilon) = (17.2 \pm 1.8) \times 10^{-4}. \quad (4.8)$$

Although the short-distance contributions to  $\text{Re}(\varepsilon'/\varepsilon)$  are now fully under control [57, 58], the theoretical predictions are unfortunately affected by large uncertainties arising from hadronic matrix elements. In units of  $10^{-4}$ , the various estimates for  $\text{Re}(\varepsilon'/\varepsilon)$  that can be found in the literature range from 5 to 40, demonstrating the unsatisfactory

present theoretical status of this observable (for reviews, see [8, 114]). Consequently, it does not allow a stringent test of the CP-violating sector of the Standard Model, unless better techniques to deal with the hadronic matrix elements of the relevant operators are available. A nice representation of the experimental results on  $\text{Re}(\varepsilon'/\varepsilon)$  through contours in a plane of hadronic parameters, which may be useful in this respect, was recently proposed in [115].

## 4.2 The Rare Decays $K^+ \rightarrow \pi^+ \nu \bar{\nu}$ and $K_L \rightarrow \pi^0 \nu \bar{\nu}$

In order to test the Standard-Model description of CP violation, the decays  $K^+ \rightarrow \pi^+ \nu \bar{\nu}$  and  $K_L \rightarrow \pi^0 \nu \bar{\nu}$  are considerably more promising than  $\text{Re}(\varepsilon'/\varepsilon)$ . Within the Standard Model, these loop-induced modes originate from  $Z$ -penguins and box diagrams, and are governed by a single short-distance function  $X_0(x_t) \approx 1.5$ . The  $K \rightarrow \pi \nu \bar{\nu}$  modes are particularly interesting since they provide remarkable relations to the  $B$  system and are very clean from a theoretical point of view. The latter feature arises from the fact that the required hadronic matrix elements are just quark-current matrix elements between pion and kaon states, which can be determined from very accessible semi-leptonic  $K$  decays. Moreover, it was shown that other long-distance contributions are negligible [116], as well as contributions from higher dimensional operators [117, 118]. Consequently, the major theoretical uncertainties affecting analyses of  $K \rightarrow \pi \nu \bar{\nu}$  modes originate from the scale ambiguities associated with perturbative QCD calculations. The inclusion of NLO QCD corrections has reduced these uncertainties considerably [119, 120], thereby making  $K \rightarrow \pi \nu \bar{\nu}$  modes an important probe of the Standard Model.

The derivation of the  $K \rightarrow \pi \nu \bar{\nu}$  branching ratios has recently been reviewed in [8]. Within the Standard Model, the predictions are given as follows:

$$\text{BR}(K^+ \rightarrow \pi^+ \nu \bar{\nu}) = (7.5 \pm 2.9) \times 10^{-11}, \quad \text{BR}(K_L \rightarrow \pi^0 \nu \bar{\nu}) = (2.6 \pm 1.2) \times 10^{-11}. \quad (4.9)$$

The former channel has already been observed at Brookhaven [121], with

$$\text{BR}(K^+ \rightarrow \pi^+ \nu \bar{\nu}) = (1.5_{-1.2}^{+3.4}) \times 10^{-10}. \quad (4.10)$$

For a review of the experimental prospects concerning these modes, see [10].

Interestingly, the  $K \rightarrow \pi \nu \bar{\nu}$  branching ratios allow a determination of  $\sin 2\beta$  [122]. To this end, it is useful to introduce the following “reduced” branching ratios:

$$B_1 \equiv \frac{1}{\kappa_+} \text{BR}(K^+ \rightarrow \pi^+ \nu \bar{\nu}), \quad B_2 \equiv \frac{1}{\kappa_L} \text{BR}(K_L \rightarrow \pi^0 \nu \bar{\nu}), \quad (4.11)$$

where

$$\kappa_+ = r_{K^+} \left[ \frac{3 \alpha^2 \text{BR}(K^+ \rightarrow \pi^0 e^+ \nu_e)}{2 \pi^2 \sin^4 \Theta_W} \right] \lambda^8 = 4.42 \times 10^{-11}, \quad (4.12)$$

and

$$\kappa_L = \left[ \frac{r_{K_L} \tau(K_L)}{r_{K^+} \tau(K^+)} \right] \kappa_+ = 1.93 \times 10^{-10}. \quad (4.13)$$

Here  $r_{K^+} = 0.901$  and  $r_{K_L} = 0.944$  describe isospin-breaking corrections, which arise in relating  $K^+ \rightarrow \pi^+\nu\bar{\nu}$  and  $K_L \rightarrow \pi^0\nu\bar{\nu}$  to  $K^+ \rightarrow \pi^0 e^+ \nu_e$ , respectively. In the Standard Model, we have to an excellent approximation

$$\sin 2\beta = \frac{2r_s}{1+r_s^2} \quad (4.14)$$

with

$$r_s = \sqrt{\sigma} \left[ \frac{\sqrt{\sigma(B_1 - B_2)} - P_c(\nu\bar{\nu})}{\sqrt{B_2}} \right], \quad (4.15)$$

where the quantity  $P_c(\nu\bar{\nu}) = 0.40 \pm 0.06$  describes the internal charm-quark contribution to  $K^+ \rightarrow \pi^+\nu\bar{\nu}$  [120], and

$$\sigma = \frac{1}{(1 - \lambda^2/2)^2}. \quad (4.16)$$

In writing (4.14), we have assumed that  $\sin 2\beta > 0$ , as expected in the Standard Model. Note that the numerical values in (4.12) and (4.13), as well as the value for  $P_c(\nu\bar{\nu})$ , differ slightly from those given in [120, 122] due to  $\lambda = 0.222$  used here instead of  $\lambda = 0.22$  used in these papers [47].

The strength of expression (4.14) is its theoretical cleanness, allowing a precise determination of  $\sin 2\beta$  free of hadronic uncertainties, and independent of other parameters, such as  $|V_{cb}|$ ,  $|V_{ub}/V_{cb}|$  and  $m_t$ . Moreover, it provides a remarkable bridge to CP violation in the  $B$  system, since  $\sin 2\beta$  can also be determined in a clean way through CP-violating effects in  $B_d \rightarrow J/\psi K_S$  decays, as we will see in Subsection 6.1. The comparison of these two determinations of  $\sin 2\beta$  with each other is particularly well suited for tests of CP violation in the Standard Model, and offers a powerful tool to probe the physics beyond it [122, 123]. We shall return to this exciting issue in more detail in Section 11, where we discuss various aspects of the unitarity triangle,  $\sin 2\beta$  and  $K \rightarrow \pi\nu\bar{\nu}$  decays in models with minimal flavour violation [47]. There we will also derive a generalization of (4.14).

In order to obtain the whole picture of CP violation, it is essential to study this phenomenon outside the kaon system. In this respect, the  $B$  system – the central topic of this review – is most promising. Let us turn to decays of neutral  $B$ -mesons first.

## 5 Time Evolution of Neutral $B$ Decays

A characteristic feature of the neutral  $B_q$ -meson system is  $B_q^0 - \overline{B}_q^0$  mixing ( $q \in \{d, s\}$ ). Within the Standard Model, this phenomenon is induced at lowest order through the box diagrams shown in Fig. 13. The Wigner–Weisskopf formalism [124] yields the following effective Schrödinger equation:

$$i \frac{d}{dt} \begin{pmatrix} a(t) \\ b(t) \end{pmatrix} = \left[ \begin{pmatrix} M_0^{(q)} & M_{12}^{(q)} \\ M_{12}^{(q)*} & M_0^{(q)} \end{pmatrix} - \frac{i}{2} \begin{pmatrix} \Gamma_0^{(q)} & \Gamma_{12}^{(q)} \\ \Gamma_{12}^{(q)*} & \Gamma_0^{(q)} \end{pmatrix} \right] \cdot \begin{pmatrix} a(t) \\ b(t) \end{pmatrix}, \quad (5.1)$$

which describes the time evolution of the state vector

$$|\psi_q(t)\rangle = a(t) |B_q^0\rangle + b(t) |\overline{B}_q^0\rangle. \quad (5.2)$$

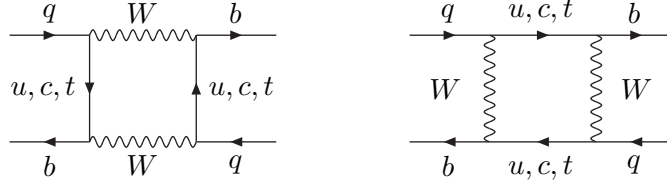


Figure 13: Box diagrams contributing to  $B_q^0 - \overline{B}_q^0$  mixing ( $q \in \{d, s\}$ ).

### 5.1 Solution of the Schrödinger Equation

It is a straightforward exercise to calculate the eigenstates  $|B_\pm^{(q)}\rangle$  and eigenvalues  $\lambda_\pm^{(q)}$  of the Hamiltonian given in (5.1):

$$|B_\pm^{(q)}\rangle = \frac{1}{\sqrt{1 + |\alpha_q|^2}} \left( |B_q^0\rangle \pm \alpha_q |\overline{B}_q^0\rangle \right) \quad (5.3)$$

$$\lambda_\pm^{(q)} = \left( M_0^{(q)} - \frac{i}{2} \Gamma_0^{(q)} \right) \pm \left( M_{12}^{(q)} - \frac{i}{2} \Gamma_{12}^{(q)} \right) \alpha_q, \quad (5.4)$$

where

$$\alpha_q e^{+i(\Theta_{\Gamma_{12}}^{(q)} + n'\pi)} = \sqrt{\frac{4 |M_{12}^{(q)}|^2 e^{-i2\delta\Theta_{M/\Gamma}^{(q)}} + |\Gamma_{12}^{(q)}|^2}{4 |M_{12}^{(q)}|^2 + |\Gamma_{12}^{(q)}|^2 - 4 |M_{12}^{(q)}| |\Gamma_{12}^{(q)}| \sin \delta\Theta_{M/\Gamma}^{(q)}}}. \quad (5.5)$$

Here  $M_{12}^{(q)} \equiv e^{i\Theta_{M_{12}}^{(q)}} |M_{12}^{(q)}|$ ,  $\Gamma_{12}^{(q)} \equiv e^{i\Theta_{\Gamma_{12}}^{(q)}} |\Gamma_{12}^{(q)}|$  and  $\delta\Theta_{M/\Gamma}^{(q)} \equiv \Theta_{M_{12}}^{(q)} - \Theta_{\Gamma_{12}}^{(q)}$ . The  $n' \in \{0, 1\}$  parametrizes the sign of the square root appearing in (5.5).



Calculating the dispersive parts of the box diagrams, which are dominated to an excellent approximation by the internal top-quark exchanges, gives [125]

$$M_{12}^{(q)} = \frac{G_F^2 M_W^2}{12\pi^2} \eta_B M_{B_q} \hat{B}_{B_q} f_{B_q}^2 (V_{tq}^* V_{tb})^2 S_0(x_t) e^{i(\pi - \phi_{\text{CP}}(B_q))}. \quad (5.6)$$

Here  $\eta_B = 0.55$  is a perturbative QCD factor [105, 126], which is common to  $M_{12}^{(d)}$  and  $M_{12}^{(s)}$ , and  $M_{B_q}$  denotes the  $B_q$ -meson mass. The non-perturbative parameter  $\hat{B}_{B_q}$  is the counterpart of  $\hat{B}_K$  introduced in (4.4), parametrizing  $\langle \overline{B}_q^0 | (\bar{b}q)_{\text{V-A}} (\bar{b}q)_{\text{V-A}} | B_q^0 \rangle$ , and  $f_{B_q}$  is the  $B_q$  decay constant. There is a vast literature on the calculations of these parameters, using lattice [38, 127] and QCD sum-rule techniques [128]; both approaches give compatible results. A reasonable range for the combination relevant for (5.6) is [8]

$$\sqrt{\hat{B}_{B_d}} f_{B_d} = (230 \pm 40) \text{ MeV}. \quad (5.7)$$

Finally, the Inami–Lim function  $S_0(x_t) \approx 2.38$  appeared already in Subsection 4.1, and the convention-dependent phase  $\phi_{\text{CP}}(B_q)$  is defined through

$$(\mathcal{CP}) | B_q^0 \rangle = e^{i\phi_{\text{CP}}(B_q)} | \overline{B}_q^0 \rangle. \quad (5.8)$$

Evaluating the absorptive parts of the box diagrams yields

$$\frac{\Gamma_{12}^{(q)}}{M_{12}^{(q)}} \approx -\frac{3\pi}{2S_0(x_t)} \frac{m_b^2}{M_W^2} = \mathcal{O}(m_b^2/m_t^2) \ll 1, \quad (5.9)$$

where we have taken into account that  $S_0(x_t) \propto x_t = m_t^2/M_W^2$ . If we expand (5.5) in powers of this small quantity and neglect second-order terms, we arrive at

$$\alpha_q = \left[ 1 + \frac{1}{2} \left| \frac{\Gamma_{12}^{(q)}}{M_{12}^{(q)}} \right| \sin \delta\Theta_{M/\Gamma}^{(q)} \right] e^{-i(\Theta_{M_{12}}^{(q)} + n'\pi)}. \quad (5.10)$$

The deviation of  $|\alpha_q|$  from 1 describes CP violation in  $B_q^0 - \overline{B}_q^0$  oscillations, and can be probed through “wrong-charge” lepton asymmetries:

$$\mathcal{A}_{\text{SL}}^{(q)} \equiv \frac{\Gamma(B_q^0(t) \rightarrow \ell^- \bar{\nu} X) - \Gamma(\overline{B}_q^0(t) \rightarrow \ell^+ \nu X)}{\Gamma(B_q^0(t) \rightarrow \ell^- \bar{\nu} X) + \Gamma(\overline{B}_q^0(t) \rightarrow \ell^+ \nu X)} = \frac{|\alpha_q|^4 - 1}{|\alpha_q|^4 + 1} \approx \left| \frac{\Gamma_{12}^{(q)}}{M_{12}^{(q)}} \right| \sin \delta\Theta_{M/\Gamma}^{(q)}. \quad (5.11)$$

Note that the time dependences cancel in (5.11). Because of  $|\Gamma_{12}^{(q)}|/|M_{12}^{(q)}| \propto m_b^2/m_t^2$  and  $\sin \delta\Theta_{M/\Gamma}^{(q)} \propto m_c^2/m_b^2$ , the asymmetry  $\mathcal{A}_{\text{SL}}^{(q)}$  is suppressed by a factor  $m_c^2/m_t^2 = \mathcal{O}(10^{-4})$ , and is hence very small in the Standard Model. Consequently, it represents an interesting probe to search for new physics. A recent analysis of the CLEO collaboration [129] yields

$$\mathcal{A}_{\text{SL}}^{(d)}/4 = -0.0035 \pm 0.0103 \pm 0.0015. \quad (5.12)$$

## 5.2 Mixing Parameters and Decay Rates

The time evolution of initially, i.e. at time  $t = 0$ , pure  $B_q^0$ - and  $\overline{B}_q^0$ -meson states is given as follows:

$$|B_q^0(t)\rangle = f_+^{(q)}(t) |B_q^0\rangle + \alpha_q f_-^{(q)}(t) |\overline{B}_q^0\rangle \quad (5.13)$$

$$|\overline{B}_q^0(t)\rangle = \frac{1}{\alpha_q} f_-^{(q)}(t) |B_q^0\rangle + f_+^{(q)}(t) |\overline{B}_q^0\rangle, \quad (5.14)$$

where

$$f_{\pm}^{(q)}(t) = \frac{1}{2} \left[ e^{-i\lambda_+^{(q)}t} \pm e^{-i\lambda_-^{(q)}t} \right]. \quad (5.15)$$

These time-dependent state vectors allow the calculation of the corresponding transition rates. To this end, it is useful to introduce

$$|g_{\pm}^{(q)}(t)|^2 = \frac{1}{4} \left[ e^{-\Gamma_L^{(q)}t} + e^{-\Gamma_H^{(q)}t} \pm 2 e^{-\Gamma_q t} \cos(\Delta M_q t) \right] \quad (5.16)$$

$$g_-^{(q)}(t) g_+^{(q)}(t)^* = \frac{1}{4} \left[ e^{-\Gamma_L^{(q)}t} - e^{-\Gamma_H^{(q)}t} + 2i e^{-\Gamma_q t} \sin(\Delta M_q t) \right], \quad (5.17)$$

and

$$\xi_f^{(q)} = e^{-i\Theta_{M_{12}}^{(q)}} \frac{A(\overline{B}_q^0 \rightarrow f)}{A(B_q^0 \rightarrow f)}, \quad \xi_{\overline{f}}^{(q)} = e^{-i\Theta_{M_{12}}^{(q)}} \frac{A(\overline{B}_q^0 \rightarrow \overline{f})}{A(B_q^0 \rightarrow \overline{f})}, \quad (5.18)$$

where

$$\Theta_{M_{12}}^{(q)} = \pi + 2 \arg(V_{tq}^* V_{tb}) - \phi_{\text{CP}}(B_q) \quad (5.19)$$

can be read off from (5.6). Whereas  $\Theta_{M_{12}}^{(q)}$  depends on the chosen CKM and CP phase conventions,  $\xi_f^{(q)}$  and  $\xi_{\overline{f}}^{(q)}$  are *convention-independent* observables.

In (5.19), it has been taken into account that  $S_0(x_t) > 0$ , and it has been assumed implicitly that the bag parameter  $\hat{B}_{B_d}$  is positive. As emphasized in [130], for  $\hat{B}_{B_d} < 0$ ,  $\Theta_{M_{12}}^{(q)}$  given in (5.19) would be shifted by  $\pi$ . However, this case appears to be very unlikely. Indeed, all existing non-perturbative methods give  $\hat{B}_{B_d} > 0$ , which we shall also assume in this review. A similar comment applies to  $\hat{B}_K$ . On the other hand, in the case of models with minimal flavour violation, the Inami–Lim function  $S_0(x_t)$  is replaced by a new parameter  $F_{tt}$ , which needs not be positive. In this case, the shift of (5.19) by  $\pi$  has to be taken into account [47], and leads to subtleties, as discussed in Section 11.

The  $g_{\pm}^{(q)}(t)$  are related to the  $f_{\pm}^{(q)}(t)$ . However, whereas the latter functions depend on  $n'$ , the  $g_{\pm}^{(q)}(t)$  do not depend on this parameter. The  $n'$ -dependence is cancelled by introducing the *positive* mass difference

$$\Delta M_q \equiv M_H^{(q)} - M_L^{(q)} = 2 |M_{12}^{(q)}| > 0 \quad (5.20)$$

of the mass eigenstates  $|B_q^H\rangle$  (“heavy”) and  $|B_q^L\rangle$  (“light”). The quantities  $\Gamma_H^{(q)}$  and  $\Gamma_L^{(q)}$  denote the corresponding decay widths. Their difference can be expressed as

$$\Delta\Gamma_q \equiv \Gamma_H^{(q)} - \Gamma_L^{(q)} = \frac{4 \operatorname{Re} [M_{12}^{(q)} \Gamma_{12}^{(q)*}]}{\Delta M_q}, \quad (5.21)$$

whereas their average is given by

$$\Gamma_q \equiv \frac{\Gamma_H^{(q)} + \Gamma_L^{(q)}}{2} = \Gamma_0^{(q)}. \quad (5.22)$$

There is the following interesting relation:

$$\frac{\Delta\Gamma_q}{\Gamma_q} \approx -\frac{3\pi}{2S_0(x_t)} \frac{m_b^2}{M_W^2} x_q = \mathcal{O}(10^{-2}) \times x_q, \quad (5.23)$$

where

$$x_q \equiv \frac{\Delta M_q}{\Gamma_q} = \begin{cases} 0.75 \pm 0.02 & (q = d) \\ \mathcal{O}(20) & (q = s) \end{cases} \quad (5.24)$$

denotes the  $B_q^0 - \overline{B}_q^0$  “mixing parameter”. Consequently, there may be a sizeable width difference in the  $B_s$  system, whereas  $\Delta\Gamma_d$  is expected to be negligibly small. We shall come back to  $\Delta\Gamma_s$  in Section 7.

Combining the formulae listed above, we arrive at the following transition rates for decays of initially, i.e. at  $t = 0$ , present  $B_q^0$ - or  $\overline{B}_q^0$ -mesons:

$$\Gamma(B_q^{\overline{(-)}}(t) \rightarrow f) = \left[ |g_{\mp}^{(q)}(t)|^2 + |\xi_f^{(q)}|^2 |g_{\pm}^{(q)}(t)|^2 - 2 \operatorname{Re} \{ \xi_f^{(q)} g_{\pm}^{(q)}(t) g_{\mp}^{(q)}(t)^* \} \right] \tilde{\Gamma}_f, \quad (5.25)$$

where the time-independent rate  $\tilde{\Gamma}_f$  corresponds to the “unevolved” decay amplitude  $A(B_q^0 \rightarrow f)$ , which can be calculated by performing the usual phase-space integrations. The rates into the CP-conjugate final state  $\overline{f}$  can be obtained straightforwardly from (5.25) through the substitutions

$$\tilde{\Gamma}_f \rightarrow \tilde{\Gamma}_{\overline{f}}, \quad \xi_f^{(q)} \rightarrow \xi_{\overline{f}}^{(q)}. \quad (5.26)$$

### 5.3 Determination of $R_t$ from $\Delta M_d$

As we have noted in our discussion of the constraints on the apex of the unitarity triangle in the  $\overline{\rho} - \overline{\eta}$  plane (see Subsection 2.6), the mass difference of the eigenstates of the  $B_d$  system allows us to determine  $R_t$ . This feature is nicely described by [8, 13, 46, 47]

$$R_t = 1.10 \times \frac{R_0}{A} \frac{1}{\sqrt{|S_0(x_t)|}} \quad \text{with} \quad R_0 \equiv \sqrt{\frac{\Delta M_d}{0.50/\text{ps}}} \left[ \frac{230 \text{ MeV}}{\sqrt{\hat{B}_d f_{B_d}}} \right] \sqrt{\frac{0.55}{\eta_B}}, \quad (5.27)$$

where we have kept the Inami–Lim function  $S_0(x_t) \approx 2.38$  explicitly, which will be useful for the discussion of models with minimal flavour violation in Section 11. The experimental range for  $\Delta M_d$  is given by [131]

$$\Delta M_d = (0.487 \pm 0.009) \text{ ps}^{-1}. \quad (5.28)$$

Alternatively,  $R_t$  may be fixed through the ratio  $\Delta M_d/\Delta M_s$  with the help of  $SU(3)$  flavour-symmetry arguments. Concerning theoretical uncertainties, this approach, which will be discussed together with the  $B_s$  system in Section 7, is much cleaner.

## 5.4 CP-violating Asymmetries

A particularly simple and interesting situation arises if we restrict ourselves to decays of neutral  $B_q$ -mesons into CP self-conjugate final states  $|f\rangle$ , satisfying the relation

$$(\mathcal{CP})|f\rangle = \pm |f\rangle. \quad (5.29)$$

Consequently, we have  $\xi_f^{(q)} = \xi_{\bar{f}}^{(q)}$  in this case (see (5.18)). Using (5.25), the corresponding time-dependent CP asymmetry can be expressed as follows:

$$\begin{aligned} a_{\text{CP}}(t) &\equiv \frac{\Gamma(B_q^0(t) \rightarrow f) - \Gamma(\overline{B}_q^0(t) \rightarrow f)}{\Gamma(B_q^0(t) \rightarrow f) + \Gamma(\overline{B}_q^0(t) \rightarrow f)} \\ &= \left[ \frac{\mathcal{A}_{\text{CP}}^{\text{dir}}(B_q \rightarrow f) \cos(\Delta M_q t) + \mathcal{A}_{\text{CP}}^{\text{mix}}(B_q \rightarrow f) \sin(\Delta M_q t)}{\cosh(\Delta\Gamma_q t/2) - \mathcal{A}_{\Delta\Gamma}(B_q \rightarrow f) \sinh(\Delta\Gamma_q t/2)} \right]. \end{aligned} \quad (5.30)$$

In this expression, we have separated the “direct” from the “mixing-induced” CP-violating contributions, which are described by

$$\mathcal{A}_{\text{CP}}^{\text{dir}}(B_q \rightarrow f) \equiv \frac{1 - |\xi_f^{(q)}|^2}{1 + |\xi_f^{(q)}|^2} \quad \text{and} \quad \mathcal{A}_{\text{CP}}^{\text{mix}}(B_q \rightarrow f) \equiv \frac{2 \text{Im} \xi_f^{(q)}}{1 + |\xi_f^{(q)}|^2}, \quad (5.31)$$

respectively. The terminology “direct CP violation” refers to CP-violating effects, which arise directly at the decay-amplitude level and are due to interference between different CKM amplitudes; it is the same kind of CP violation, which is probed in the neutral kaon system by  $\text{Re}(\varepsilon'/\varepsilon)$ . On the other hand, “mixing-induced CP violation” originates from interference effects between  $B_q^0$ – $\overline{B}_q^0$  mixing and decay processes. The width difference  $\Delta\Gamma_q$ , which may be sizeable in the  $B_s$  system, provides another observable

$$\mathcal{A}_{\Delta\Gamma}(B_q \rightarrow f) \equiv \frac{2 \text{Re} \xi_f^{(q)}}{1 + |\xi_f^{(q)}|^2}, \quad (5.32)$$

which is, however, not independent from  $\mathcal{A}_{\text{CP}}^{\text{dir}}(B_q \rightarrow f)$  and  $\mathcal{A}_{\text{CP}}^{\text{mix}}(B_q \rightarrow f)$ , satisfying the following relation:

$$\left[\mathcal{A}_{\text{CP}}^{\text{dir}}(B_q \rightarrow f)\right]^2 + \left[\mathcal{A}_{\text{CP}}^{\text{mix}}(B_q \rightarrow f)\right]^2 + \left[\mathcal{A}_{\Delta\Gamma}(B_q \rightarrow f)\right]^2 = 1. \quad (5.33)$$

In order to calculate the observable  $\xi_f^{(q)}$ , which contains essentially all the information needed to evaluate the CP asymmetry (5.30), we employ the low-energy effective Hamiltonian (3.28), yielding the transition amplitude

$$\begin{aligned} A(\overline{B}_q^0 \rightarrow f) &= \langle f | \mathcal{H}_{\text{eff}}(\Delta B = -1) | \overline{B}_q^0 \rangle = \\ & \left\langle f \left| \frac{G_{\text{F}}}{\sqrt{2}} \left[ \sum_{j=u,c} V_{jr}^* V_{jb} \left\{ \sum_{k=1}^2 C_k(\mu) Q_k^{jr}(\mu) + \sum_{k=3}^{10} C_k(\mu) Q_k^r(\mu) \right\} \right] \right| \overline{B}_q^0 \right\rangle, \end{aligned} \quad (5.34)$$

where  $r \in \{d, s\}$  distinguishes between  $b \rightarrow d$  and  $b \rightarrow s$  transitions. On the other hand, we have also

$$\begin{aligned} A(B_q^0 \rightarrow f) &= \langle f | \mathcal{H}_{\text{eff}}(\Delta B = -1)^\dagger | B_q^0 \rangle = \\ & \left\langle f \left| \frac{G_{\text{F}}}{\sqrt{2}} \left[ \sum_{j=u,c} V_{jr} V_{jb}^* \left\{ \sum_{k=1}^2 C_k(\mu) Q_k^{jr\dagger}(\mu) + \sum_{k=3}^{10} C_k(\mu) Q_k^{r\dagger}(\mu) \right\} \right] \right| B_q^0 \right\rangle. \end{aligned} \quad (5.35)$$

If we perform appropriate CP transformations in this expression, i.e. insert the operator  $(\mathcal{CP})^\dagger(\mathcal{CP}) = \hat{1}$  both after  $\langle f |$  and in front of  $|B_q^0\rangle$ , we obtain

$$\begin{aligned} A(B_q^0 \rightarrow f) &= \pm e^{i\phi_{\text{CP}}(B_q)} \times \\ & \left\langle f \left| \frac{G_{\text{F}}}{\sqrt{2}} \left[ \sum_{j=u,c} V_{jr} V_{jb}^* \left\{ \sum_{k=1}^2 C_k(\mu) Q_k^{jr}(\mu) + \sum_{k=3}^{10} C_k(\mu) Q_k^r(\mu) \right\} \right] \right| \overline{B}_q^0 \right\rangle, \end{aligned} \quad (5.36)$$

where we have applied the relation

$$(\mathcal{CP}) (Q_k^{jr})^\dagger (\mathcal{CP})^\dagger = Q_k^{jr}, \quad (5.37)$$

and have furthermore taken into account (5.8). Using now (5.18) and (5.19), we finally arrive at

$$\xi_f^{(q)} = \mp e^{-i\phi_q} \left[ \frac{\sum_{j=u,c} V_{jr}^* V_{jb} \langle f | Q^{jr} | \overline{B}_q^0 \rangle}{\sum_{j=u,c} V_{jr} V_{jb}^* \langle f | Q^{jr} | \overline{B}_q^0 \rangle} \right], \quad (5.38)$$

where

$$Q^{jr} \equiv \sum_{k=1}^2 C_k(\mu) Q_k^{jr} + \sum_{k=3}^{10} C_k(\mu) Q_k^r, \quad (5.39)$$

and where

$$\phi_q \equiv 2 \arg(V_{tq}^* V_{tb}) = \begin{cases} +2\beta & (q = d) \\ -2\delta\gamma & (q = s) \end{cases} \quad (5.40)$$

is related to the weak  $B_q^0 - \overline{B}_q^0$  mixing phase. For the interpretation of  $\beta$  and  $\delta\gamma$  in terms of the unitarity triangles of the CKM matrix, see Fig. 3. Note that the phase-convention-dependent quantity  $\phi_{\text{CP}}(B_q)$  cancels in (5.38).

In general, the observable  $\xi_f^{(q)}$  suffers from large hadronic uncertainties, which are introduced by the hadronic matrix elements in (5.38). However, if the decay  $B_q \rightarrow f$  is dominated by a single CKM amplitude, i.e.

$$A(B_q^0 \rightarrow f) = e^{-i\phi_f/2} \left( e^{i\delta_f} |M_f| \right), \quad (5.41)$$

the strong matrix element  $e^{i\delta_f} |M_f|$  with the CP-conserving strong phase  $\delta_f$  cancels, and  $\xi_f^{(q)}$  takes the simple form

$$\xi_f^{(q)} = \mp \exp[-i(\phi_q - \phi_f)]. \quad (5.42)$$

If the  $V_{jr}^* V_{jb}$  amplitude plays the dominant rôle in  $\overline{B}_q^0 \rightarrow f$ , we have

$$\phi_f = 2 \arg(V_{jr}^* V_{jb}) = \begin{cases} -2\gamma & (j = u) \\ 0 & (j = c). \end{cases} \quad (5.43)$$

In (5.40) and (5.43), we have employed (2.46), corresponding to the phase convention chosen in the standard and the generalized Wolfenstein parametrizations of the CKM matrix. However, the results for the observable  $\xi_f^{(q)}$  arising from (5.42) do of course not depend on the choice of the phase convention of the CKM matrix.

Since  $B_q^0 - \overline{B}_q^0$  mixing plays an important rôle for new physics to manifest itself in mixing-induced CP asymmetries of neutral  $B_q$  decays, let us leave the framework of the Standard Model for a moment in the next Subsection, following closely [132].

## 5.5 Impact of Physics Beyond the Standard Model

The generic way of introducing physics beyond the Standard Model into analyses of non-leptonic  $B$  decays is to use the language of effective field theory and to write down all possible dim-6 operators. Of course, this has been known already for a long time and lists of the dim-6 operators involving all the Standard-Model particles have been published in the literature [133]. After having introduced these additional operators, we have to construct the generalization of the relevant Standard-Model effective Hamiltonian at the scale of the  $b$  quark, where we encounter again dim-6 operators, with Wilson coefficients containing now a Standard-Model contribution, and a possible piece of new physics.

The problem with this generic point of view is that the operator basis is enlarged to such an extent that this general approach becomes almost useless for phenomenological

applications. However, we are dealing with non-leptonic decays, in which we are, because of our ignorance of the hadronic matrix elements, sensitive neither to the helicity structure of the operators nor to their colour structure. The only information that is relevant in this case is the flavour structure, and hence we introduce the notation

$$[(\bar{q}_3 q_2)(\bar{q}_1 Q)] = \sum [\text{Wilson coeff.}] \times [\text{dim-6 operator mediating } Q \rightarrow q_1 \bar{q}_2 q_3]. \quad (5.44)$$

This sum is renormalization-group invariant, and involves, at the scale of the  $b$  quark, Standard-Model as well as possible non-Standard-Model contributions. In particular, it allows us to estimate the relative size of a possible new-physics contribution.

This language can also be applied to the  $\Delta B = \pm 2$  operators mediating  $B_d^0 - \bar{B}_d^0$  mixing, yielding

$$\mathcal{H}_{\text{eff}}^{(d)}(\Delta B = +2) = G_d [(\bar{b}d)(\bar{b}d)] \quad (5.45)$$

as the relevant flavour structure. Within the Standard Model, (5.45) originates from the box diagrams shown in Fig. 13 for  $q = d$ , which are strongly suppressed by the CKM factor  $(V_{td}V_{tb}^*)^2$ , as well as by a loop factor

$$\frac{g_2^2}{64\pi^2} = \frac{G_F M_W^2}{\sqrt{128}\pi^2} \approx 1 \times 10^{-3}, \quad (5.46)$$

making the Standard-Model contribution very small, of the order of

$$G_{\text{SM}}^{(d)} = \frac{G_F}{\sqrt{2}} \left( \frac{G_F M_W^2}{\sqrt{128}\pi^2} \right) (V_{td}V_{tb}^*)^2. \quad (5.47)$$

Here we did not include the Inami–Lim function  $S_0(x_t)$  and the perturbative QCD corrections for simplicity (see Subsection 5.1), as we are now only interested in order of magnitude estimates. Because of the strongly suppressed Standard-Model piece, a new-physics contribution may well be of similar size. If  $\Lambda$  denotes the characteristic scale of physics beyond the Standard Model, we have

$$G_{\text{NP}}^{(d)} = \frac{G_F}{\sqrt{2}} \left( \frac{G_F M_W^2}{\sqrt{128}\pi^2} \right) \frac{M_W^2}{\Lambda^2} e^{-i2\psi_d}, \quad (5.48)$$

where  $\psi_d$  is a possible weak phase, which is induced by the new-physics contribution. Finally, we arrive at

$$G_d = \frac{G_F}{\sqrt{2}} \left( \frac{G_F M_W^2}{\sqrt{128}\pi^2} \right) \left[ (V_{td}V_{tb}^*)^2 + \frac{M_W^2}{\Lambda^2} e^{-i2\psi_d} \right] \equiv |R_d| e^{-i\phi_d^{\text{NP}}}, \quad (5.49)$$

where the weak phase  $\phi_d^{\text{NP}}$  is the generalization of (5.40), entering the mixing-induced CP asymmetries. Using (2.46), we obtain

$$\tan \phi_d^{\text{NP}} = \frac{\sin 2\beta + \varrho_d^2 \sin 2\psi_d}{\cos 2\beta + \varrho_d^2 \cos 2\psi_d} \quad (5.50)$$

with

$$\varrho_d = \left( \frac{1}{\lambda^3 AR_t} \right) \left( \frac{M_W}{\Lambda} \right). \quad (5.51)$$

Since  $\varrho_d$  can be of order one even for large  $\Lambda$ , there can be a large phase shift in the mixing phase. If we assume, for example,  $AR_t = 1$ , this term equals 1 for a new-physics scale of  $\Lambda \sim 8$  TeV. Such contributions affect of course not only the CP-violating phase  $\phi_d^{\text{NP}}$ , but also the “strength”  $|R_d|$  of  $B_d^0 - \overline{B}_d^0$  mixing, which would manifest itself as an inconsistency in the usual “standard analysis” of the unitarity triangle discussed in Subsection 2.6. Similar considerations can of course also be made for  $B_s^0 - \overline{B}_s^0$  mixing, which will be addressed in Subsection 7.4.

The formalism developed above has important applications and allows us to discuss key modes for the  $B$ -factories, which will be our next topic.

## 6 Important Benchmark Modes for the $B$ -Factories

### 6.1 The $B \rightarrow J/\psi K$ System

The most important application of the formalism discussed in Subsection 5.4 is the extraction of  $\beta$  from CP-violating effects in the “gold-plated” mode  $B_d \rightarrow J/\psi K_S$  [134].

#### 6.1.1 Extracting $\beta$ from $B_d \rightarrow J/\psi K_S$

The decay  $B_d^0 \rightarrow J/\psi K_S$  is a transition into a CP eigenstate with eigenvalue  $-1$  (note that the  $J/\psi K_S$  system is created in a  $P$ -wave state), and originates from  $\bar{b} \rightarrow \bar{c}c\bar{s}$  quark-level processes. As can be seen in Fig. 14, we have to deal both with tree-diagram-like and with penguin topologies. The corresponding amplitude can be written as [135]

$$A(B_d^0 \rightarrow J/\psi K_S) = \lambda_c^{(s)} (A_{\text{CC}}^{c'} + A_{\text{pen}}^{c'}) + \lambda_u^{(s)} A_{\text{pen}}^{u'} + \lambda_t^{(s)} A_{\text{pen}}^{t'}, \quad (6.1)$$

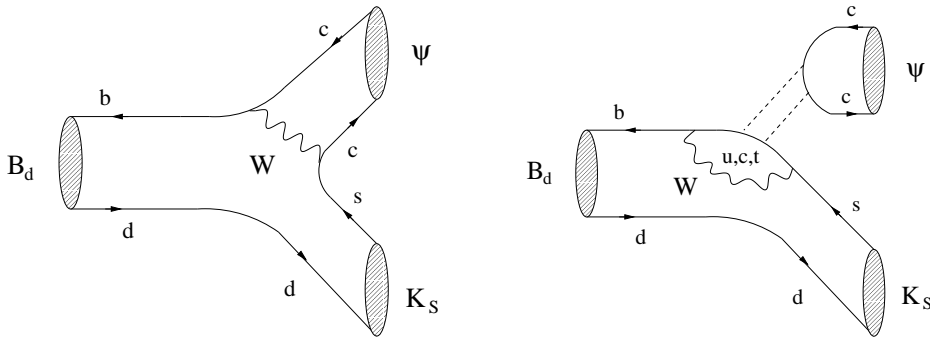


Figure 14: Feynman diagrams contributing to  $B_d^0 \rightarrow J/\psi K_S$ . The dashed lines in the penguin topology represent a colour-singlet exchange.



where  $A_{\text{CC}}^{c'}$  denotes the current–current (CC) contributions, i.e. the “tree” processes shown in Fig. 14, and the strong amplitudes  $A_{\text{pen}}^{q'}$  describe the contributions from penguin topologies with internal  $q$  quarks ( $q \in \{u, c, t\}$ ). These penguin amplitudes take into account both QCD and EW penguin contributions. The primes in (6.1) remind us that we are dealing with a  $\bar{b} \rightarrow \bar{s}$  transition, and the

$$\lambda_q^{(s)} \equiv V_{qs} V_{qb}^* \quad (6.2)$$

are CKM factors. If we employ the unitarity of the CKM matrix to eliminate  $\lambda_t^{(s)}$  (see (3.32)), and make use of the generalized Wolfenstein parametrization (2.17), we obtain

$$A(B_d^0 \rightarrow J/\psi K_S) = \left(1 - \frac{\lambda^2}{2}\right) \mathcal{A}' \left[1 + \left(\frac{\lambda^2}{1 - \lambda^2}\right) a' e^{i\theta'} e^{i\gamma}\right], \quad (6.3)$$

where

$$\mathcal{A}' \equiv \lambda^2 A \left(A_{\text{CC}}^{c'} + A_{\text{pen}}^{ct'}\right) \quad (6.4)$$

with  $A_{\text{pen}}^{ct'} \equiv A_{\text{pen}}^{c'} - A_{\text{pen}}^{t'}$ , and

$$a' e^{i\theta'} \equiv R_b \left(\frac{A_{\text{pen}}^{ut'}}{A_{\text{CC}}^{c'} + A_{\text{pen}}^{ct'}}\right). \quad (6.5)$$

The quantity  $A_{\text{pen}}^{ut'}$  is defined in analogy to  $A_{\text{pen}}^{ct'}$ , and  $A$  and  $R_b$  are the usual CKM factors, with present experimental ranges given in (2.49) and (2.51), respectively.

Because of various reasons, it is very difficult to calculate the “penguin” parameter  $a' e^{i\theta'}$ , introducing  $e^{i\gamma}$  into the  $B_d^0 \rightarrow J/\psi K_S$  amplitude, reliably: the QCD penguins contributing to  $B_d^0 \rightarrow J/\psi K_S$  require a colour-singlet exchange, as indicated in Fig. 14 through the dashed lines, and are “Zweig-suppressed”. Such a comment does not apply to the EW penguins, which contribute in colour-allowed form. On the other hand, the current–current amplitude  $A_{\text{CC}}^{c'}$  is due to colour-suppressed topologies, so that the ratio  $A_{\text{pen}}^{ut'}/(A_{\text{CC}}^{c'} + A_{\text{pen}}^{ct'})$ , which governs  $a' e^{i\theta'}$ , may well be sizeable; a plausible estimate is  $a' = \mathcal{O}(0.2)$ . Fortunately, this parameter – and therefore also  $e^{i\gamma}$  – enters in (6.3) in a doubly Cabibbo-suppressed way. Consequently, we have to a very good approximation  $\phi_{\psi K_S} = 0$ , and obtain with the help of (5.31) and (5.42)

$$a_{\psi K_S} \equiv -\mathcal{A}_{\text{CP}}^{\text{mix}}(B_d \rightarrow J/\psi K_S) = -\sin[-(\phi_d - 0)] = \sin 2\beta. \quad (6.6)$$

Hence  $B_d \rightarrow J/\psi K_S$  is referred to as the “gold-plated” mode to determine  $\beta$  [134].

At this point, we have to discuss a subtlety, which arises in  $B_q \rightarrow f$  decays into a final CP eigenstate  $|f\rangle$  involving a  $K_S$ -meson, such as  $B_{d(s)} \rightarrow J/\psi K_S$  or  $B_d \rightarrow \phi K_S$ . In this case, we have also to take into account the weak  $K^0 - \bar{K}^0$  mixing phase  $\phi_K = 2 \arg(V_{us}^* V_{ud})$ , modifying the convention-independent combination of phases in (5.42) as follows:

$$\phi_q + \phi_K - \phi_f. \quad (6.7)$$

However, for the generalized Wolfenstein parametrization (2.17) applied in (5.40) and (5.43),  $\phi_K$  is negligibly small and does not show up explicitly in the mixing-induced CP asymmetries. Owing to the small value of the CP-violating parameter  $\varepsilon$  of the neutral kaon system,  $\phi_K$  can only affect the mixing-induced CP asymmetries in very contrived models of new physics [130, 136].

Concerning the measurement of  $\sin 2\beta$  through (6.6), there were already important first steps by the OPAL, CDF and ALEPH collaborations:

$$\sin 2\beta = \begin{cases} 3.2_{-2.0}^{+1.8} \pm 0.5 & \text{(OPAL [137])} \\ 0.79_{-0.44}^{+0.41} & \text{(CDF [138])} \\ 0.84_{-1.04}^{+0.82} \pm 0.16 & \text{(ALEPH [139]).} \end{cases} \quad (6.8)$$

In the summer of 2001, the asymmetric  $e^+e^-$   $B$ -factories could establish CP violation in the  $B$  system, with the following results for  $\sin 2\beta$ :

$$\sin 2\beta = \begin{cases} 0.59 \pm 0.14 \pm 0.05 & \text{(BaBar [2])} \\ 0.99 \pm 0.14 \pm 0.06 & \text{(Belle [3]).} \end{cases} \quad (6.9)$$

Taking also into account the previous CDF and ALEPH results gives an average of

$$\sin 2\beta = 0.79 \pm 0.10. \quad (6.10)$$

In comparison with  $\sin 2\beta = 0.34 \pm 0.20 \pm 0.05$  [140] and  $0.58_{-0.34-0.10}^{+0.32+0.09}$  [141] reported by the BaBar and Belle collaborations in the spring of 2001, respectively, the central values have now moved up considerably. The first results for  $\sin 2\beta$  announced by these experiments in the summer of 2000,  $0.12 \pm 0.37 \pm 0.09$  [142] and  $0.45_{-0.44-0.09}^{+0.43+0.07}$  [143], gave even smaller central values. Despite the large experimental uncertainties, these numbers led already to some excitement in the  $B$ -physics community [46, 47, 144, 145, 146, 147], as they would have been in disagreement with the “standard analysis” of the unitarity triangle discussed in Subsection 2.6, yielding

$$0.5 \lesssim \sin 2\beta \lesssim 0.9. \quad (6.11)$$

In view of the recent Belle result [3], the upper bounds given in (2.48) and (2.52) may become important for the search for new physics.

Since the BaBar and Belle numbers in (6.9) are not fully consistent with each other, the measurement of  $\sin 2\beta$  will continue to be a very exciting topic. Moreover, it should be noted that the  $B$ -factory results given in (6.9) actually correspond to an average over various channels, including  $B_d \rightarrow J/\psi K_S$ ,  $\psi(2S)K_S$ ,  $\chi_{c1}K_S$ ,  $J/\psi K_L$  and  $J/\psi K^*$  modes. If just  $B_d \rightarrow J/\psi K_S [\rightarrow \pi^+\pi^-]$  decays are employed, BaBar and Belle obtain  $\sin 2\beta = 0.45 \pm 0.18$  [2] and  $0.81 \pm 0.20$  [3], respectively. On the other hand, the BaBar and Belle data for  $B_d \rightarrow J/\psi K_L$  modes give  $\sin 2\beta = 0.70 \pm 0.34$  [2] and  $1.31 \pm 0.23$  [3], respectively. We shall come back to these issues in 6.1.6 and Section 11.

After a couple of years of collecting data, an uncertainty of  $\Delta \sin 2\beta|_{\text{exp}} = 0.05$  seems to be achievable at the  $B$ -factories. In the LHC era, this experimental uncertainty should be reduced further by one order of magnitude [148]. In view of such a tremendous accuracy, it is crucial to obtain deeper insights into the theoretical uncertainties affecting (6.6). A possibility to control them is provided by  $B_s \rightarrow J/\psi K_S$  modes [135] (see Subsection 10.1). Moreover, also direct CP violation allows us to probe the corresponding penguin effects [80]. In order to fully exploit the physics potential of  $B_d \rightarrow J/\psi K_S$  decays, their charged counterparts  $B^\pm \rightarrow J/\psi K^\pm$  have to be considered as well [132].

### 6.1.2 Isospin Relations between $B_d \rightarrow J/\psi K_S$ and $B^\pm \rightarrow J/\psi K^\pm$

The most general discussion of the  $B \rightarrow J/\psi K$  system can be performed in terms of an isospin decomposition [132]. Here the corresponding initial and final states are grouped in the following isodoublets:

$$\begin{bmatrix} |1/2; +1/2\rangle \\ |1/2; -1/2\rangle \end{bmatrix} : \quad \underbrace{\begin{bmatrix} |B^+\rangle \\ |B_d^0\rangle \end{bmatrix}, \begin{bmatrix} |\overline{B}_d^0\rangle \\ -|B^-\rangle \end{bmatrix}}_{\text{CP}}, \quad \underbrace{\begin{bmatrix} |J/\psi K^+\rangle \\ |J/\psi K^0\rangle \end{bmatrix}, \begin{bmatrix} |J/\psi \overline{K}^0\rangle \\ -|J/\psi K^-\rangle \end{bmatrix}}_{\text{CP}}, \quad (6.12)$$

which are related by CP conjugation. The decays  $B^+ \rightarrow J/\psi K^+$  and  $B_d^0 \rightarrow J/\psi K^0$  are described by an effective low-energy Hamiltonian of the following structure:

$$\mathcal{H}_{\text{eff}} = \frac{G_F}{\sqrt{2}} \left[ V_{cs} V_{cb}^* \left( \mathcal{Q}_{\text{CC}}^c - \mathcal{Q}_{\text{QCD}}^{\text{pen}} - \mathcal{Q}_{\text{EW}}^{\text{pen}} \right) + V_{us} V_{ub}^* \left( \mathcal{Q}_{\text{CC}}^u - \mathcal{Q}_{\text{QCD}}^{\text{pen}} - \mathcal{Q}_{\text{EW}}^{\text{pen}} \right) \right], \quad (6.13)$$

where the  $\mathcal{Q}$  denote linear combinations of Wilson coefficients and four-quark operators, consisting of CC, QCD penguin and EW penguin operators, as listed in (3.29)–(3.31). For the following considerations, the flavour structure of these operators is crucial:

$$\mathcal{Q}_{\text{CC}}^c \sim (\overline{c}c)(\overline{b}s), \quad \mathcal{Q}_{\text{CC}}^u \sim (\overline{u}u)(\overline{b}s), \quad (6.14)$$

$$\mathcal{Q}_{\text{QCD}}^{\text{pen}} \sim [(\overline{c}c) + \{(\overline{u}u) + (\overline{d}d)\} + (\overline{s}s)] (\overline{b}s), \quad (6.15)$$

$$\mathcal{Q}_{\text{EW}}^{\text{pen}} \sim \frac{1}{3} [2(\overline{c}c) + \{2(\overline{u}u) - (\overline{d}d)\} - (\overline{s}s)] (\overline{b}s). \quad (6.16)$$

Since

$$(\overline{u}u) = \frac{1}{2} \underbrace{(\overline{u}u + \overline{d}d)}_{I=0} + \frac{1}{2} \underbrace{(\overline{u}u - \overline{d}d)}_{I=1}, \quad 2(\overline{u}u) - (\overline{d}d) = \frac{1}{2} \underbrace{(\overline{u}u + \overline{d}d)}_{I=0} + \frac{3}{2} \underbrace{(\overline{u}u - \overline{d}d)}_{I=1}, \quad (6.17)$$

we conclude that (6.13) is a combination of isospin  $I = 0$  and  $I = 1$  pieces:

$$\mathcal{H}_{\text{eff}} = \mathcal{H}_{\text{eff}}^{I=0} + \mathcal{H}_{\text{eff}}^{I=1}, \quad (6.18)$$

where  $\mathcal{H}_{\text{eff}}^{I=0}$  receives contributions from all of the operators in (6.14)–(6.16), whereas  $\mathcal{H}_{\text{eff}}^{I=1}$  is only due to  $\mathcal{Q}_{\text{CC}}^u$  and  $\mathcal{Q}_{\text{EW}}^{\text{pen}}$ . Using the isospin symmetry, we obtain

$$\langle J/\psi K^+ | \mathcal{H}_{\text{eff}}^{I=0} | B^+ \rangle = + \langle J/\psi K^0 | \mathcal{H}_{\text{eff}}^{I=0} | B_d^0 \rangle \quad (6.19)$$

$$\langle J/\psi K^+ | \mathcal{H}_{\text{eff}}^{I=1} | B^+ \rangle = - \langle J/\psi K^0 | \mathcal{H}_{\text{eff}}^{I=1} | B_d^0 \rangle, \quad (6.20)$$

and arrive at<sup>1</sup>

$$A(B^+ \rightarrow J/\psi K^+) = \frac{G_{\text{F}}}{\sqrt{2}} \left[ \lambda_c^{(s)} \{A_c^{(0)} - A_c^{(1)}\} + \lambda_u^{(s)} \{A_u^{(0)} - A_u^{(1)}\} \right] \quad (6.21)$$

$$A(B_d^0 \rightarrow J/\psi K^0) = \frac{G_{\text{F}}}{\sqrt{2}} \left[ \lambda_c^{(s)} \{A_c^{(0)} + A_c^{(1)}\} + \lambda_u^{(s)} \{A_u^{(0)} + A_u^{(1)}\} \right], \quad (6.22)$$

where

$$A_c^{(0)} = A_{\text{CC}}^c - A_{\text{QCD}}^{\text{pen}} - A_{\text{EW}}^{(0)}, \quad A_c^{(1)} = -A_{\text{EW}}^{(1)} \quad (6.23)$$

$$A_u^{(0)} = A_{\text{CC}}^{u(0)} - A_{\text{QCD}}^{\text{pen}} - A_{\text{EW}}^{(0)}, \quad A_u^{(1)} = A_{\text{CC}}^{u(1)} - A_{\text{EW}}^{(1)} \quad (6.24)$$

can be expressed in terms of the corresponding hadronic matrix elements  $\langle J/\psi K | \mathcal{Q} | B \rangle$ , i.e. are CP-conserving strong amplitudes. Consequently, we may write

$$A(B^+ \rightarrow J/\psi K^+) = \frac{G_{\text{F}}}{\sqrt{2}} \tilde{\lambda}^2 A \left[ A_c^{(0)} - A_c^{(1)} \right] \left[ 1 + \left( \frac{\lambda^2}{1 - \lambda^2} \right) R_b \left\{ \frac{A_u^{(0)} - A_u^{(1)}}{A_c^{(0)} - A_c^{(1)}} \right\} e^{i\gamma} \right] \quad (6.25)$$

$$A(B_d^0 \rightarrow J/\psi K^0) = \frac{G_{\text{F}}}{\sqrt{2}} \tilde{\lambda}^2 A \left[ A_c^{(0)} + A_c^{(1)} \right] \left[ 1 + \left( \frac{\lambda^2}{1 - \lambda^2} \right) R_b \left\{ \frac{A_u^{(0)} + A_u^{(1)}}{A_c^{(0)} + A_c^{(1)}} \right\} e^{i\gamma} \right], \quad (6.26)$$

with

$$\tilde{\lambda}^2 \equiv \left( 1 - \frac{\lambda^2}{2} \right) \lambda^2. \quad (6.27)$$

The amplitude of the neutral mode takes the same form as (6.3), making, however, its isospin decomposition explicit. As we have already noted above, an important observation is that  $e^{i\gamma}$  enters in (6.25) and (6.26) in a doubly Cabibbo-suppressed way. Moreover, the  $A_u^{(0,1)}$  amplitudes are governed by penguin-like topologies and annihilation diagrams (see Subsection 3.4), and are hence expected to be suppressed with respect to  $A_c^{(0)}$ , which originates also from tree-diagram-like topologies. In order to keep track of this feature, we introduce a “generic” expansion parameter  $\bar{\lambda} = \mathcal{O}(0.2)$  [86, 149], which is of the same order as the Wolfenstein parameter  $\lambda$ :

$$\left| A_u^{(0,1)} / A_c^{(0)} \right| = \mathcal{O}(\bar{\lambda}). \quad (6.28)$$

<sup>1</sup>For simplicity, the primes of the amplitudes introduced in 6.1.1 are suppressed in the following.

Consequently, the  $e^{i\gamma}$  terms in (6.25) and (6.26) are actually suppressed by  $\mathcal{O}(\bar{\lambda}^3)$ . Since the  $A_c^{(1)}$  amplitude is due to dynamically suppressed matrix elements of EW penguin operators (see (6.23)), we expect

$$\left| A_c^{(1)}/A_c^{(0)} \right| = \underbrace{\mathcal{O}(\bar{\lambda}^2)}_{\text{EW penguins}} \times \underbrace{\mathcal{O}(\bar{\lambda})}_{\text{Dynamics}} = \mathcal{O}(\bar{\lambda}^3), \quad (6.29)$$

and obtain the following expression:

$$A(B^+ \rightarrow J/\psi K^+) = A_{\text{SM}}^{(0)} \left[ 1 + \mathcal{O}(\bar{\lambda}^3) \right] = A(B_d^0 \rightarrow J/\psi K^0), \quad (6.30)$$

with

$$A_{\text{SM}}^{(0)} \equiv \frac{G_{\text{F}}}{\sqrt{2}} \tilde{\lambda}^2 A A_c^{(0)}. \quad (6.31)$$

Let us note that the plausible hierarchy of strong amplitudes given in (6.28) and (6.29) may be spoiled by very large rescattering processes [78, 79]. In the worst case, (6.30) may receive corrections at the  $\bar{\lambda}^2$  level. However, we do not consider this a very likely scenario and note that also the ‘‘QCD factorization’’ approach developed in [98]–[100] is not in favour of such large rescattering effects.

### 6.1.3 New Physics in the $B \rightarrow J/\psi K$ Decay Amplitudes

An important way for new physics to manifest itself in  $B_d \rightarrow J/\psi K_{\text{S}}$  decays is through  $B_d^0 - \bar{B}_d^0$  mixing. As discussed in Subsection 5.5, the mixing-induced CP asymmetry (6.6) may be affected significantly this way. An alternative mechanism for physics beyond the Standard Model to affect the  $B \rightarrow \psi K$  system is provided by new-physics contributions to the decay amplitudes [132, 150]. The corresponding  $\Delta B = \pm 1$  operators can be treated on the same footing as  $B_d^0 - \bar{B}_d^0$  mixing in Subsection 5.5. In the presence of new physics, the corresponding low-energy effective Hamiltonian can still be composed into  $I = 0$  and  $I = 1$  pieces, as in (6.18). New physics may affect the Wilson coefficients, and may introduce new dim-6 operators, modifying (6.30) as follows [132]:

$$A(B^+ \rightarrow J/\psi K^+) = A_{\text{SM}}^{(0)} \left[ 1 + \sum_k r_0^{(k)} e^{i\delta_0^{(k)}} e^{i\varphi_0^{(k)}} - \sum_j r_1^{(j)} e^{i\delta_1^{(j)}} e^{i\varphi_1^{(j)}} \right] \quad (6.32)$$

$$A(B_d^0 \rightarrow J/\psi K^0) = A_{\text{SM}}^{(0)} \left[ 1 + \sum_k r_0^{(k)} e^{i\delta_0^{(k)}} e^{i\varphi_0^{(k)}} + \sum_j r_1^{(j)} e^{i\delta_1^{(j)}} e^{i\varphi_1^{(j)}} \right]. \quad (6.33)$$

Here  $r_0^{(k)}$  and  $r_1^{(j)}$  correspond to the  $I = 0$  and  $I = 1$  pieces, respectively,  $\delta_0^{(k)}$  and  $\delta_1^{(j)}$  are CP-conserving strong phases, and  $\varphi_0^{(k)}$  and  $\varphi_1^{(j)}$  the corresponding CP-violating weak phases. The labels  $k$  and  $j$  distinguish between different new-physics contributions to the  $I = 0$  and  $I = 1$  sectors.

For the following discussion, we have to make assumptions about the size of a possible new-physics piece. We shall assume that the new-physics contributions to the  $I = 0$  sector are smaller compared to the leading Standard-Model amplitude (6.31) by a factor of order  $\bar{\lambda}$ , i.e.

$$r_0^{(k)} = \mathcal{O}(\bar{\lambda}). \quad (6.34)$$

Here we have implicitly assumed that there is no flavour suppression present. In the case where the new-physics effects are even smaller, it is difficult to disentangle them from the Standard-Model contribution. This will be addressed – together with several other scenarios – below. Parametrizing the new-physics amplitudes as in Subsection 5.5 by a scale  $\Lambda$ , we have

$$\frac{G_F}{\sqrt{2}} \frac{M_W^2}{\Lambda^2} \sim \bar{\lambda} \left[ \frac{G_F}{\sqrt{2}} \lambda^2 A \right], \quad (6.35)$$

corresponding to  $\Lambda \sim 1 \text{ TeV}$ . Consequently, as in the example given after (5.51), also here we have a generic new-physics scale in the TeV regime.

As far as possible new-physics contributions to the  $I = 1$  sector are concerned, we assume a similar “generic strength” of the corresponding operators. However, in comparison with the  $I = 0$  pieces, the matrix elements of the  $I = 1$  operators, having the general flavour structure

$$\mathcal{Q}_{I=1} \sim (\bar{u}u - \bar{d}d)(\bar{b}s), \quad (6.36)$$

are expected to suffer from a dynamical suppression. As in (6.28) and (6.29), we shall assume that this brings another factor of  $\bar{\lambda}$  into the game, yielding

$$r_1^{(j)} = \mathcal{O}(\bar{\lambda}^2). \quad (6.37)$$

Employing this kind of counting, the new-physics contributions to the  $I = 1$  sector would be enhanced by a factor of  $\mathcal{O}(\bar{\lambda})$  with respect to the  $I = 1$  Standard-Model pieces. This may actually be the case if new physics shows up, for example, in EW penguin processes.

Consequently, we obtain

$$A(B \rightarrow J/\psi K) = A_{\text{SM}}^{(0)} \left[ 1 + \underbrace{\mathcal{O}(\bar{\lambda})}_{\text{NP}_{I=0}} + \underbrace{\mathcal{O}(\bar{\lambda}^2)}_{\text{NP}_{I=1}} + \underbrace{\mathcal{O}(\bar{\lambda}^3)}_{\text{SM}} \right]. \quad (6.38)$$

In the presence of large rescattering effects, the assumed dynamical suppression through a factor of  $\mathcal{O}(\bar{\lambda})$  would no longer be effective, thereby modifying (6.38) as follows:

$$A(B \rightarrow J/\psi K)|_{\text{res.}} = A_{\text{SM}}^{(0)}|_{\text{res.}} \times \left[ 1 + \underbrace{\mathcal{O}(\bar{\lambda})}_{\text{NP}_{I=0}} + \underbrace{\mathcal{O}(\bar{\lambda})}_{\text{NP}_{I=1}} + \underbrace{\mathcal{O}(\bar{\lambda}^2)}_{\text{SM}} \right]. \quad (6.39)$$

However, as we have noted above, we do not consider this as a very likely scenario, and shall use (6.38) in the following discussion, neglecting the Standard-Model pieces of  $\mathcal{O}(\bar{\lambda}^3)$ , which are not under theoretical control.

Concerning the analysis of CP violation, it is obvious that possible weak phases appearing in the new-physics contributions play the key rôle. As was the case for the  $\Delta B = \pm 2$  operators in Subsection 5.5, also the  $\Delta B = \pm 1$  operators could carry such new weak phases, which would then affect the CP-violating  $B \rightarrow J/\psi K$  observables.

### 6.1.4 Observables for a General Analysis of New Physics

The decays  $B^+ \rightarrow J/\psi K^+$ ,  $B_d^0 \rightarrow J/\psi K^0$  and their charge conjugates provide a set of four decay amplitudes  $A_i$ . Measuring the corresponding rates, we may determine the  $|A_i|^2$ . Since we are not interested in the overall normalization of the decay amplitudes, we may construct the following three independent observables with the help of the  $|A_i|^2$ :

$$\mathcal{A}_{\text{CP}}^{(+)} \equiv \frac{|A(B^+ \rightarrow J/\psi K^+)|^2 - |A(B^- \rightarrow J/\psi K^-)|^2}{|A(B^+ \rightarrow J/\psi K^+)|^2 + |A(B^- \rightarrow J/\psi K^-)|^2} \quad (6.40)$$

$$\mathcal{A}_{\text{CP}}^{\text{dir}} \equiv \frac{|A(B_d^0 \rightarrow J/\psi K^0)|^2 - |A(\overline{B}_d^0 \rightarrow J/\psi \overline{K}^0)|^2}{|A(B_d^0 \rightarrow J/\psi K^0)|^2 + |A(\overline{B}_d^0 \rightarrow J/\psi \overline{K}^0)|^2} \quad (6.41)$$

$$B \equiv \frac{\langle |A(B_d \rightarrow J/\psi K)|^2 \rangle - \langle |A(B^\pm \rightarrow J/\psi K^\pm)|^2 \rangle}{\langle |A(B_d \rightarrow J/\psi K)|^2 \rangle + \langle |A(B^\pm \rightarrow J/\psi K^\pm)|^2 \rangle}, \quad (6.42)$$

where the ‘‘CP-averaged’’ amplitudes are generally defined as follows:

$$\langle |A(B \rightarrow f)|^2 \rangle \equiv \frac{1}{2} [ |A(B \rightarrow f)|^2 + |A(\overline{B} \rightarrow \overline{f})|^2 ], \quad (6.43)$$

and  $\mathcal{A}_{\text{CP}}^{\text{dir}}$  agrees with the corresponding observable introduced in (5.30). Mixing-induced CP violation provides another observable  $\mathcal{A}_{\text{CP}}^{\text{mix}}(B_d \rightarrow J/\psi K_S)$ , which is governed by

$$\xi_{\psi K_S}^{(d)} = e^{-i\phi} \left[ \frac{1 + \sum_k r_0^{(k)} e^{i\delta_0^{(k)}} e^{-i\varphi_0^{(k)}} + \sum_j r_1^{(j)} e^{i\delta_1^{(j)}} e^{-i\varphi_1^{(j)}}}{1 + \sum_k r_0^{(k)} e^{i\delta_0^{(k)}} e^{+i\varphi_0^{(k)}} + \sum_j r_1^{(j)} e^{i\delta_1^{(j)}} e^{+i\varphi_1^{(j)}}} \right], \quad (6.44)$$

as can be seen in (5.31). In order to derive (6.44), we have used the parametrization (6.33) to express the corresponding decay amplitudes. The phase  $\phi$  corresponds to  $\phi_d^{\text{NP}} + \phi_K$ , where  $\phi_d^{\text{NP}}$  was introduced in (5.50), and  $\phi_K$  plays usually a negligible rôle.

In order to search for new-physics effects in the  $B \rightarrow J/\psi K$  system, it is useful to introduce the following combinations of the observables (6.40) and (6.41):

$$S \equiv \frac{1}{2} [\mathcal{A}_{\text{CP}}^{\text{dir}} + \mathcal{A}_{\text{CP}}^{(+)}], \quad D \equiv \frac{1}{2} [\mathcal{A}_{\text{CP}}^{\text{dir}} - \mathcal{A}_{\text{CP}}^{(+)}]. \quad (6.45)$$

Using (6.32) and (6.33), and assuming the hierarchy in (6.38), we obtain

$$S = -2 \left[ \sum_k r_0^{(k)} \sin \delta_0^{(k)} \sin \varphi_0^{(k)} \right] \left[ 1 - 2 \sum_l r_0^{(l)} \cos \delta_0^{(l)} \cos \varphi_0^{(l)} \right] = \mathcal{O}(\overline{\lambda}) + \mathcal{O}(\overline{\lambda}^2) \quad (6.46)$$

$$D = -2 \sum_j r_1^{(j)} \sin \delta_1^{(j)} \sin \varphi_1^{(j)} = \mathcal{O}(\bar{\lambda}^2) \quad (6.47)$$

$$B = +2 \sum_j r_1^{(j)} \cos \delta_1^{(j)} \cos \varphi_1^{(j)} = \mathcal{O}(\bar{\lambda}^2), \quad (6.48)$$

where terms of  $\mathcal{O}(\bar{\lambda}^3)$ , including also a Standard-Model contribution, which is not under theoretical control, have been neglected. Note that if the dynamical suppression of the  $I = 1$  contributions would be larger,  $B$  and  $D$  would be further suppressed relative to  $S$ .

The expression for the mixing-induced CP asymmetry is rather complicated and not very instructive. Let us give it for the special case where the new-physics contributions to the  $I = 0$  and  $I = 1$  sectors involve either the same weak or strong phases:

$$\begin{aligned} a_{\psi K_S} &= \sin \phi + 2 r_0 \cos \delta_0 \sin \varphi_0 \cos \phi + 2 r_1 \cos \delta_1 \sin \varphi_1 \cos \phi \\ &- r_0^2 [(1 - \cos 2\varphi_0) \sin \phi + \cos 2\delta_0 \sin 2\varphi_0 \cos \phi] = \sin \phi + \mathcal{O}(\bar{\lambda}) + \mathcal{O}(\bar{\lambda}^2). \end{aligned} \quad (6.49)$$

Expressions (6.46)–(6.48) also simplify in this case:

$$S = -2 r_0 \sin \delta_0 \sin \varphi_0 + r_0^2 \sin 2\delta_0 \sin 2\varphi_0 \quad (6.50)$$

$$D = -2 r_1 \sin \delta_1 \sin \varphi_1 \quad (6.51)$$

$$B = 2 r_1 \cos \delta_1 \cos \varphi_1. \quad (6.52)$$

### 6.1.5 Possible Scenarios

As far as CP violation in  $B^\pm \rightarrow J/\psi K^\pm$  decays is concerned, dramatic effects are already excluded by

$$\mathcal{A}_{\text{CP}}^{(+)} = \begin{cases} (-1.8 \pm 4.3 \pm 0.4)\% \text{ (CLEO [151])} \\ (-0.4 \pm 2.9 \pm 0.4)\% \text{ (BaBar [152])}. \end{cases} \quad (6.53)$$

Moreover, a recent BaBar analysis yields  $\lambda_{\psi K_S}^{(d)} = 0.93 \pm 0.09 \pm 0.03$  [2], where

$$\lambda_{\psi K_S}^{(d)} = 1/\xi_{\psi K_S}^{(d)*}. \quad (6.54)$$

This result implies

$$\mathcal{A}_{\text{CP}}^{\text{dir}} = (-7 \pm 10)\%. \quad (6.55)$$

Finally, if we use the most recent BaBar and Belle data for  $B \rightarrow J/\psi K$ , we obtain

$$B = \frac{\text{BR}(B_d \rightarrow J/\psi K) \tau - \text{BR}(B^\pm \rightarrow J/\psi K^\pm)}{\text{BR}(B_d \rightarrow J/\psi K) \tau + \text{BR}(B^\pm \rightarrow J/\psi K^\pm)} = \begin{cases} (-6.2 \pm 3.6)\% \text{ (BaBar [153])} \\ (-10.6 \pm 6.8)\% \text{ (Belle [154])}, \end{cases} \quad (6.56)$$

where the numerical values depend rather sensitively on the lifetime ratio  $\tau \equiv \tau_{B^+}/\tau_{B_d^0}$ , assumed to be  $1.060 \pm 0.029$  [41], which is consistent with [155, 156]. Because of the



large uncertainties, we cannot yet draw conclusions. However, the experimental situation should improve significantly in the future.

As can be seen in (6.46)–(6.48), the observable  $S$  provides a “smoking-gun” signal for new-physics contributions to the  $I = 0$  sector, while  $D$  and  $B$  allow us to probe new physics affecting the  $I = 1$  pieces. Since the hierarchy in (6.38) implies

$$S = \underbrace{\mathcal{O}(\bar{\lambda})}_{\text{NP}_{I=0}} + \underbrace{\mathcal{O}(\bar{\lambda}^3)}_{\text{SM}}, \quad D = \underbrace{\mathcal{O}(\bar{\lambda}^2)}_{\text{NP}_{I=1}} + \underbrace{\mathcal{O}(\bar{\lambda}^3)}_{\text{SM}}, \quad B = \underbrace{\mathcal{O}(\bar{\lambda}^2)}_{\text{NP}_{I=1}} + \underbrace{\mathcal{O}(\bar{\lambda}^3)}_{\text{SM}}, \quad (6.57)$$

we conclude that  $S$  may already be accessible at the first-generation  $B$ -factories (BaBar, Belle, Tevatron-II), whereas the latter observables will probably be left for second-generation  $B$  experiments (BTeV, LHCb). However, should  $B$  and  $D$ , in addition to  $S$ , also be found to be at the 10% level, i.e. should be measured at the first-generation  $B$ -factories, we would not only have signals for physics beyond the Standard Model, but also for large rescattering processes.

A more pessimistic scenario one can imagine is that  $S$  is measured at the  $\bar{\lambda}^2$  level in the LHC era, whereas no indications for non-vanishing values of  $D$  and  $B$  are found. Then we would still have evidence for new physics, which would then correspond to  $r_0^{(k)} = \mathcal{O}(\bar{\lambda}^2)$  and  $r_1^{(j)} = \mathcal{O}(\bar{\lambda}^3)$ , i.e.

$$A(B \rightarrow J/\psi K) = A_{\text{SM}}^{(0)} \left[ 1 + \underbrace{\mathcal{O}(\bar{\lambda}^2)}_{\text{NP}_{I=0}} + \underbrace{\mathcal{O}(\bar{\lambda}^3)}_{\text{NP}_{I=1}} + \underbrace{\mathcal{O}(\bar{\lambda}^3)}_{\text{SM}} \right]. \quad (6.58)$$

However, if all three observables are measured to be of  $\mathcal{O}(\bar{\lambda}^2)$ , new-physics effects cannot be distinguished from Standard-Model contributions, which could also be enhanced to the  $\bar{\lambda}^2$  level by large rescattering effects. This would be the most unfortunate case for the strategy to search for new-physics contributions to the  $B \rightarrow J/\psi K$  decay amplitudes discussed above [132]. However, further information can be obtained with the help of the decay  $B_s \rightarrow J/\psi K_S$ , which can be combined with  $B_d \rightarrow J/\psi K_S$  through the  $U$ -spin symmetry of strong interactions and may shed light on new physics even in this case. Within the Standard Model, it allows us to control the – presumably very small – penguin uncertainties in the determination of  $\beta$  from  $a_{\psi K_S}$ , and to extract, moreover, the CKM angle  $\gamma$  [135]. This mode will be addressed in Subsection 10.1.

As can be seen in (6.49), the mixing-induced CP asymmetry  $a_{\psi K_S}$  is affected both by  $I = 0$  and by  $I = 1$  new-physics contributions, where the dominant  $\mathcal{O}(\bar{\lambda})$  effects are expected to be due to the  $I = 0$  sector. Neglecting terms of  $\mathcal{O}(\bar{\lambda}^2)$ , we may write

$$a_{\psi K_S} = \sin(\phi + \delta\phi_{\text{NP}}^{\text{dir}}) \quad \text{with} \quad \delta\phi_{\text{NP}}^{\text{dir}} = 2 \sum_k r_0^{(k)} \cos \delta_0^{(k)} \sin \varphi_0^{(k)}. \quad (6.59)$$

The phase shift  $\delta\phi_{\text{NP}}^{\text{dir}} = \mathcal{O}(\bar{\lambda})$  may be as large as  $\mathcal{O}(20^\circ)$ . Since the Standard-Model range for  $\phi$  is given by  $30^\circ \lesssim \phi = 2\beta \lesssim 70^\circ$ , the mixing-induced CP asymmetry may

also be affected significantly by new-physics contributions to the  $B_d \rightarrow J/\psi K_S$  decay amplitude, and not only in the “standard” fashion, through  $B_d^0 - \overline{B}_d^0$  mixing, as discussed in Subsection 5.5. This would be another possibility to accommodate “anomalously” small or large values of  $a_{\psi K_S}$ . In order to gain confidence into such a scenario, it is crucial to improve also the measurements of the observables  $S$ ,  $D$  and  $B$  [132].

So far, our considerations were completely general. Let us therefore comment briefly on a special case, where the strong phases  $\delta_0^{(k)}$  and  $\delta_1^{(j)}$  take the trivial values 0 or  $\pi$ , as in factorization. In this case, (6.46)–(6.48) would simplify as follows:

$$S \approx 0, \quad D \approx 0, \quad B \approx 2 \sum_j r_1^{(j)} \sin \varphi_1^{(j)} = \mathcal{O}(\overline{\lambda}^2), \quad (6.60)$$

whereas (6.49) would yield

$$a_{\psi K_S} = \sin \phi + 2 r_0 \sin \varphi_0 \cos \phi + 2 r_1 \sin \varphi_1 \cos \phi - r_0^2 [(1 - \cos 2\varphi_0) \sin \phi + \sin 2\varphi_0 \cos \phi] = \sin \phi + \mathcal{O}(\overline{\lambda}) + \mathcal{O}(\overline{\lambda}^2). \quad (6.61)$$

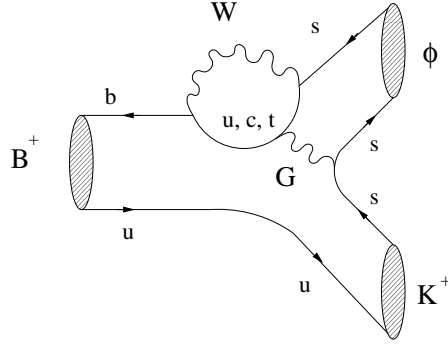
The important point is that  $S$  and  $D$  are governed by sines of the strong phases, whereas the new-physics contributions to  $B$  and  $a_{\psi K_S}$  involve cosines of the corresponding strong phases. Consequently, these terms do *not* vanish for  $\delta \rightarrow 0, \pi$ . The impact of new physics on  $a_{\psi K_S}$  may still be sizeable in this scenario, whereas  $B$  could only be measured in the LHC era [148]. On the other hand, if  $S$  and  $D$  should be observed at the  $\overline{\lambda}$  and  $\overline{\lambda}^2$  levels, respectively, we would not only get a “smoking-gun” signal for new-physics contributions to the  $B \rightarrow J/\psi K$  decay amplitudes, but also for non-factorizable hadronic effects. A measurement of all three observables  $S$ ,  $D$  and  $B$  at the  $\overline{\lambda}$  level would imply, in addition, large rescattering processes, as we have already emphasized above.

### 6.1.6 $B_d \rightarrow J/\psi[\rightarrow \ell^+ \ell^-] K^*[\rightarrow \pi^0 K_S]$ Decays

Let us finally have a look at  $B_d^0 \rightarrow J/\psi K^{*0}$  decays, assuming that direct CP violation vanishes in these channels, as in the Standard Model. If the  $K^{*0}$ -meson is observed to decay to the CP eigenstate  $\pi^0 K_S$ , the time evolution of the angular distribution of the  $B_d^0(t) \rightarrow J/\psi[\rightarrow \ell^+ \ell^-] K^*[\rightarrow \pi^0 K_S]$  decay products also allows us to probe  $\phi$  [157], which is given by  $2\beta$  in the Standard Model. The important feature of the corresponding observables is that they do not only allow us to determine  $\sin \phi$  – in complete analogy to  $a_{\psi K_S}$  – but contain also terms of the following form [158]–[160]:

$$\cos \delta_f \cos \phi. \quad (6.62)$$

Here  $\delta_f$  is a CP-conserving strong phase corresponding to a given final-state configuration of the  $J/\psi K^{*0}$  system. Theoretical tools, such as factorization, may be sufficiently

Figure 15: QCD penguin contributions to  $B^+ \rightarrow \phi K^+$ .

accurate to determine the sign of  $\cos \delta_f$ , thereby allowing the direct extraction of  $\cos \phi$ . The knowledge of this quantity, in combination with  $\sin \phi$ , allows us then to determine  $\phi$  *unambiguously*, resolving a twofold ambiguity, which arises in the extraction of  $\phi$  from the mixing-induced CP asymmetry  $a_{\psi K_S} = \sin \phi$ .

The resolution of this ambiguity is an important issue and has several applications (see, for example, Subsection 6.4 and Section 10); alternative strategies to accomplish this task were proposed in [161]. It may also turn out to be crucial for the search for new physics. In order to illustrate this point, let us assume that  $\sin \phi$  has been measured to be equal to 0.8 (see (6.10)). We would then conclude that  $\phi = 53^\circ$  or  $127^\circ$ , where the former solution would lie perfectly within the range  $30^\circ \lesssim \phi \lesssim 70^\circ$  implied by the “standard analysis” of the unitarity triangle. The two solutions can be distinguished through a measurement of  $\cos \phi$ , which is equal to 0.6 and  $-0.6$  for  $\phi = 53^\circ$  and  $127^\circ$ , respectively. Consequently, a measurement of  $\cos \phi = -0.6$  would imply new physics.

## 6.2 The $B \rightarrow \phi K$ System

An important testing ground for the Standard Model is also provided by  $B \rightarrow \phi K$  decays. As can be seen in Fig. 15, these modes are governed by QCD penguin processes [65], but also EW penguins are sizeable [63, 81], and physics beyond the Standard Model may have an important impact [80, 150, 162, 163]. In the summer of 2000, the observation of the  $B^\pm \rightarrow \phi K^\pm$  channel was announced by the Belle and CLEO collaborations. The experimental situation in the summer of 2001 can be summarized as follows:

$$\text{BR}(B^+ \rightarrow \phi K^+) \times 10^6 = \begin{cases} 11.2_{-2.0}^{+2.2} \pm 1.4 & \text{(Belle [164])} \\ 5.5_{-1.8}^{+2.1} \pm 0.6 & \text{(CLEO [165])} \\ 7.7_{-1.4}^{+1.6} \pm 0.8 & \text{(BaBar [166])}, \end{cases} \quad (6.63)$$

$$\text{BR}(B_d^0 \rightarrow \phi K^0) \times 10^6 = \begin{cases} 8.9_{-2.7}^{+3.4} \pm 1.0 & \text{(Belle [164])} \\ 5.4_{-2.7}^{+3.7} \pm 0.7 & \text{(CLEO [165])} \\ 8.1_{-2.5}^{+3.1} \pm 0.8 & \text{(BaBar [166])}. \end{cases} \quad (6.64)$$

Moreover, a first result for the direct CP asymmetry of the  $B^+ \rightarrow \phi K^+$  transition has already been reported by the BaBar collaboration [152]:

$$\mathcal{A}_{\text{CP}}(B^+ \rightarrow \phi K^+) = (5 \pm 20 \pm 3)\%, \quad (6.65)$$

where  $\mathcal{A}_{\text{CP}}(B^+ \rightarrow \phi K^+)$  is defined in analogy to its  $B^+ \rightarrow J/\psi K^+$  counterpart in (6.40). Recent calculations of  $B \rightarrow \phi K$  modes can be found in [167].

In our discussion of the  $B \rightarrow \phi K$  system, we follow closely [163], and perform an analysis similar to the one for the  $B \rightarrow J/\psi K$  decays given in the previous subsection.

### 6.2.1 Decay Amplitudes in the Standard Model

If we apply the isospin symmetry and follow 6.1.2, we obtain the following model-independent parametrizations of the  $B^+ \rightarrow \phi K^+$ ,  $B_d^0 \rightarrow \phi K^0$  decay amplitudes:

$$A(B^+ \rightarrow \phi K^+) = \frac{G_{\text{F}}}{\sqrt{2}} \tilde{\lambda}^2 A \left[ \mathcal{A}_c^{(0)} - \mathcal{A}_c^{(1)} \right] \left[ 1 + \left( \frac{\lambda^2}{1 - \lambda^2} \right) R_b \left\{ \frac{\mathcal{A}_u^{(0)} - \mathcal{A}_u^{(1)}}{\mathcal{A}_c^{(0)} - \mathcal{A}_c^{(1)}} \right\} e^{i\gamma} \right] \quad (6.66)$$

$$A(B_d^0 \rightarrow \phi K^0) = \frac{G_{\text{F}}}{\sqrt{2}} \tilde{\lambda}^2 A \left[ \mathcal{A}_c^{(0)} + \mathcal{A}_c^{(1)} \right] \left[ 1 + \left( \frac{\lambda^2}{1 - \lambda^2} \right) R_b \left\{ \frac{\mathcal{A}_u^{(0)} + \mathcal{A}_u^{(1)}}{\mathcal{A}_c^{(0)} + \mathcal{A}_c^{(1)}} \right\} e^{i\gamma} \right], \quad (6.67)$$

where  $\mathcal{A}_c^{(0,1)}$  and  $\mathcal{A}_u^{(0,1)}$ , which can be expressed in terms of hadronic matrix elements  $\langle \phi K | \mathcal{Q} | B \rangle$ , correspond to (6.23) and (6.24), respectively.

At first sight, expressions (6.66) and (6.67) are completely analogous to the ones for the  $B^+ \rightarrow J/\psi K^+$  and  $B_d^0 \rightarrow J/\psi K^0$  amplitudes given in (6.25) and (6.26), respectively. However, the dynamics, which is encoded in the strong amplitudes  $\mathcal{A}$ , is very different. In particular, the current–current operators  $\mathcal{Q}_{\text{CC}}^c$  cannot contribute to  $B \rightarrow \phi K$  decays, i.e. to  $\mathcal{A}_{\text{CC}}^c$ , through tree-diagram-like topologies; they may only do so through penguin topologies with internal charm-quark exchanges, which include also

$$B^+ \rightarrow \{D_s^+ \bar{D}^0, \dots\} \rightarrow \phi K^+, \quad B_d^0 \rightarrow \{D_s^+ D^-, \dots\} \rightarrow \phi K^0 \quad (6.68)$$

rescattering processes [79], and may actually play an important rôle (see Subsection 3.4). On the other hand, the  $\mathcal{A}_{\text{CC}}^{u(0,1)}$  amplitudes receive contributions from penguin processes with internal up- and down-quark exchanges, as well as from annihilation topologies.<sup>2</sup> Such penguins may also be important, in particular in the presence of large rescattering processes [78, 79]; a similar comment applies to annihilation topologies. In the  $B \rightarrow \phi K$  system, the relevant rescattering processes are

$$B^+ \rightarrow \{\pi^0 K^+, \dots\} \rightarrow \phi K^+, \quad B_d^0 \rightarrow \{\pi^- K^+, \dots\} \rightarrow \phi K^0, \quad (6.69)$$

---

<sup>2</sup>Note that the isospin projection operators  $\mathcal{Q} \sim (\bar{u}u \pm \bar{d}d)(\bar{b}s)$  involve also  $\bar{d}d$  quark currents.

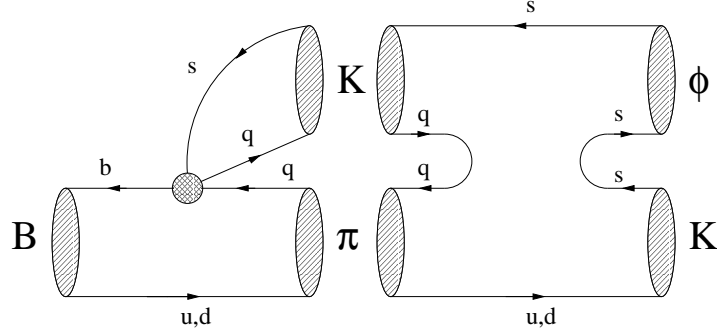


Figure 16: Illustration of rescattering processes contributing to  $B \rightarrow \phi K$  through penguin-like topologies with internal  $q$ -quark exchanges ( $q \in \{u, d\}$ ). The shaded circle represents insertions of the corresponding current–current operators.

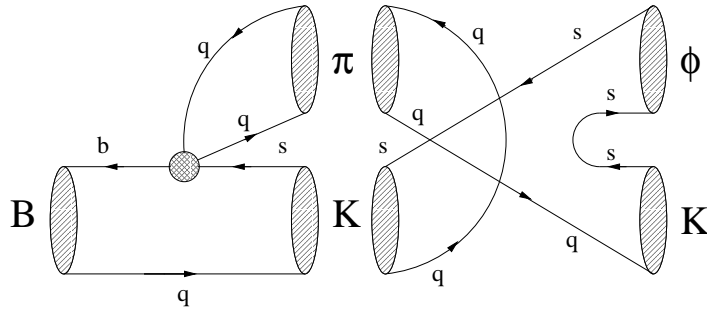


Figure 17: Illustration of rescattering processes contributing to  $B \rightarrow \phi K$  through annihilation topologies. The shaded circle represents insertions of the corresponding current–current operators ( $q \in \{u, d\}$ ).

which are illustrated in Figs. 16 and 17. In contrast to (6.68), large rescattering effects of this kind may affect the search for new physics with  $B \rightarrow \phi K$  decays, since these processes are associated with the weak phase factor  $e^{i\gamma}$ . Moreover, they involve “light” intermediate states, and are hence expected to be enhanced more easily, dynamically, through long-distance effects than (6.68), which involve “heavy” intermediate states.

Let us now have a closer look at the structure of the  $B \rightarrow \phi K$  decay amplitudes, focusing first on the case corresponding to small rescattering effects. From the  $B \rightarrow \phi K$  counterparts of (6.23) and (6.24), we expect

$$\left| \mathcal{A}_u^{(0,1)} / \mathcal{A}_c^{(0)} \right| = \mathcal{O}(1), \quad (6.70)$$

where we have assumed that the CC operators, which contribute only through penguin or annihilation topologies, yield amplitudes of the same order as the QCD penguin

operators. In the case of  $\mathcal{A}_c^{(1)}$ , the situation is different. Here we have to deal with an amplitude that is essentially due to EW penguins. Moreover, the  $B \rightarrow \phi K$  matrix elements of  $I = 1$  operators, having the general flavour structure given in (6.36), are expected to suffer from a dynamical suppression. In order to keep track of these features, we employ, as in Subsection 6.1, again a generic expansion parameter  $\bar{\lambda} = \mathcal{O}(0.2)$ :

$$\left| \mathcal{A}_c^{(1)} / \mathcal{A}_c^{(0)} \right| = \underbrace{\mathcal{O}(\bar{\lambda})}_{\text{EW penguins}} \times \underbrace{\mathcal{O}(\bar{\lambda})}_{\text{Dynamics}} = \mathcal{O}(\bar{\lambda}^2). \quad (6.71)$$

Consequently, we obtain

$$A(B^+ \rightarrow \phi K^+) = \mathcal{A}_{\text{SM}}^{(0)} \left[ 1 + \mathcal{O}(\bar{\lambda}^2) \right] = A(B_d^0 \rightarrow \phi K^0), \quad (6.72)$$

with

$$\mathcal{A}_{\text{SM}}^{(0)} \equiv \frac{G_{\text{F}}}{\sqrt{2}} \lambda^2 A \mathcal{A}_c^{(0)}. \quad (6.73)$$

The terms entering (6.72) at the  $\bar{\lambda}^2$  level contain also pieces that are proportional to the weak phase factor  $e^{i\gamma}$ , thereby leading to direct CP violation in the  $B \rightarrow \phi K$  system.

Let us now consider large rescattering effects of the kind given in (6.69). Although this case does not appear to be a very likely scenario,<sup>3</sup> which is also not favoured by the QCD factorization approach [98]–[100], it deserves careful attention to separate possible new-physics effects from those of the Standard Model. In the worst case, (6.70) would be dynamically enhanced as

$$\left| \mathcal{A}_u^{(0,1)} / \mathcal{A}_c^{(0)} \right| = \mathcal{O}(1/\bar{\lambda}), \quad (6.74)$$

and the dynamical suppression in (6.71) would no longer be effective, i.e.

$$\left| \mathcal{A}_c^{(1)} / \mathcal{A}_c^{(0)} \right| = \mathcal{O}(\bar{\lambda}). \quad (6.75)$$

In such a scenario, (6.72) would receive corrections of  $\mathcal{O}(\bar{\lambda})$ , involving also  $e^{i\gamma}$ . This feature may complicate the search for new physics with the help of CP-violating effects in  $B \rightarrow \phi K$  decays. On the other hand, the rescattering processes described by (6.68) may only affect the amplitude  $\mathcal{A}_{\text{SM}}^{(0)}$  sizeably through its  $\mathcal{A}_{\text{CC}}^c$  piece, and are not related to a CP-violating weak phase factor within the Standard Model.

Before turning to new physics, we would like to emphasize an interesting difference between the  $B \rightarrow \phi K$  and  $B \rightarrow J/\psi K$  systems. In the  $B \rightarrow J/\psi K$  case, the Standard-Model amplitudes corresponding to (6.72) receive corrections at the  $\bar{\lambda}^3$  level (see (6.30)), which may be enhanced to  $\mathcal{O}(\bar{\lambda}^2)$  in the presence of large rescattering effects. Consequently, within the Standard Model, there may be direct CP-violating effects in  $B \rightarrow J/\psi K$  transitions of at most  $\mathcal{O}(\bar{\lambda}^2)$ , whereas such asymmetries may already arise at the  $\bar{\lambda}$  level in the  $B \rightarrow \phi K$  system. On the other hand, as  $B \rightarrow \phi K$  modes are governed by penguin processes, their decay amplitudes are more sensitive to new physics.

<sup>3</sup>Arguments against this possibility, i.e. large rescattering effects, were also given in [168].

### 6.2.2 Effects of Physics Beyond the Standard Model

In order to analyse the impact of possible new-physics contributions to the  $B \rightarrow \phi K$  system, we follow Subsections 5.5 and 6.1.3. In analogy to the  $B \rightarrow J/\psi K$  case, the Standard-Model expression (6.72) is modified as follows:

$$A(B^+ \rightarrow \phi K^+) = \mathcal{A}_{\text{SM}}^{(0)} \left[ 1 + \sum_k v_0^{(k)} e^{i\Delta_0^{(k)}} e^{i\Phi_0^{(k)}} - \sum_j v_1^{(j)} e^{i\Delta_1^{(j)}} e^{i\Phi_1^{(j)}} \right] \quad (6.76)$$

$$A(B_d^0 \rightarrow \phi K^0) = \mathcal{A}_{\text{SM}}^{(0)} \left[ 1 + \sum_k v_0^{(k)} e^{i\Delta_0^{(k)}} e^{i\Phi_0^{(k)}} + \sum_j v_1^{(j)} e^{i\Delta_1^{(j)}} e^{i\Phi_1^{(j)}} \right], \quad (6.77)$$

where  $v_0^{(k)}$  and  $v_1^{(j)}$  correspond to the  $I = 0$  and  $I = 1$  pieces, respectively,  $\Delta_0^{(k)}$  and  $\Delta_1^{(j)}$  are CP-conserving strong phases, and  $\Phi_0^{(k)}$  and  $\Phi_1^{(j)}$  the corresponding CP-violating weak phases.

As we have already noted, within the Standard Model, the  $B \rightarrow \phi K$  system is governed by QCD penguins. Neglecting, for simplicity, EW penguins and the proper renormalization-group evolution, we may write

$$\mathcal{A}_{\text{SM}}^{(0)} \sim \frac{G_{\text{F}}}{\sqrt{2}} \lambda^2 A \left[ \frac{\alpha_s}{4\pi} \mathcal{C} \right] \langle P_{\text{QCD}} \rangle, \quad (6.78)$$

where  $\mathcal{C} = \mathcal{O}(1)$  is a perturbative short-distance coefficient, which is multiplied by the characteristic loop factor  $\alpha_s/(4\pi)$ , and  $P_{\text{QCD}}$  denotes an appropriate linear combination of QCD penguin operators. Since (6.78) is a doubly Cabibbo-suppressed loop amplitude, new physics could well be of the same order of magnitude. If we assume once more that the physics beyond the Standard Model is associated with a scale  $\Lambda$  and impose that it yields contributions to the  $B \rightarrow \phi K$  amplitudes of the same size as the Standard Model, we obtain

$$\frac{G_{\text{F}}}{\sqrt{2}} \frac{M_W^2}{\Lambda^2} \sim \frac{G_{\text{F}}}{\sqrt{2}} \lambda^2 A \left[ \frac{\alpha_s}{4\pi} \mathcal{C} \right], \quad (6.79)$$

corresponding to  $\Lambda \sim 3 \text{ TeV}$ .<sup>4</sup> Consequently, for a generic new-physics scale in the TeV regime, which we also considered in our  $B \rightarrow J/\psi K$  analysis, we may well have

$$v_0^{(k)} = \mathcal{O}(1). \quad (6.80)$$

In deriving (6.79), we have implicitly assumed that the new-physics operators arise at tree level and that there is no flavour suppression. In the case where the new-physics effects are less pronounced, it may be difficult to disentangle them from the Standard-Model contributions. We shall come back to this issue below, discussing various scenarios.

---

<sup>4</sup>In this numerical estimate, we have assumed  $A \times \mathcal{C} \sim 1$  and  $\alpha_s = \alpha_s(m_b) \sim 0.2$ .

Concerning possible new-physics contributions to the  $I = 1$  sector, we assume a “generic strength” of the corresponding operators similar to (6.79). However, since these operators have the general flavour structure given in (6.36), their hadronic  $B \rightarrow \phi K$  matrix elements are expected to suffer from a dynamical suppression. As in (6.71), we assume that this brings a factor of  $\bar{\lambda}$  into the game, yielding

$$v_1^{(j)} = \mathcal{O}(\bar{\lambda}). \quad (6.81)$$

If we impose such a hierarchy of amplitudes, the new-physics contributions to the  $I = 1$  sector would be enhanced by a factor of  $\mathcal{O}(\bar{\lambda})$  with respect to the  $I = 1$  Standard-Model pieces. This may actually be the case if new physics shows up, for example, in EW penguin processes.

Consequently, we finally arrive at

$$A(B \rightarrow \phi K) = \mathcal{A}_{\text{SM}}^{(0)} \left[ 1 + \underbrace{\mathcal{O}(1)}_{\text{NP}_{I=0}} + \underbrace{\mathcal{O}(\bar{\lambda})}_{\text{NP}_{I=1}} + \underbrace{\mathcal{O}(\bar{\lambda}^2)}_{\text{SM}} \right]. \quad (6.82)$$

In deriving this expression, we have assumed that the  $B \rightarrow \phi K$  decays are not affected by rescattering effects. On the other hand, in the presence of large rescattering processes of the kind described by (6.69), the dynamical suppression assumed in (6.81) would no longer be effective, thereby yielding  $v_1^{(j)} = \mathcal{O}(1)$ . Analogously, the  $B \rightarrow \phi K$  matrix elements of  $I = 0$  operators with flavour structure

$$\mathcal{Q}_{I=0}^{\bar{u}u, \bar{d}d} \sim (\bar{u}u + \bar{d}d)(\bar{b}s) \quad (6.83)$$

would no longer be suppressed with respect to those of the dynamically favoured  $I = 0$  operators

$$\mathcal{Q}_{I=0}^{\bar{s}s} \sim (\bar{s}s)(\bar{b}s), \quad (6.84)$$

and would also contribute to  $v_0^{(k)}$  at  $\mathcal{O}(1)$ . A similar comment applies to the matrix elements of the  $I = 0$  operators with the following flavour content:

$$\mathcal{Q}_{I=0}^{\bar{c}c} \sim (\bar{c}c)(\bar{b}s), \quad (6.85)$$

whose dynamical suppression in  $B \rightarrow \phi K$  decays may be reduced through rescattering effects of the kind given in (6.68), which may also affect the  $\mathcal{A}_{\text{SM}}^{(0)}$  amplitude, as we have noted above. Consequently, in the presence of large rescattering effects, the decay amplitude (6.82) is modified as follows:

$$A(B \rightarrow \phi K)|_{\text{res.}} = \mathcal{A}_{\text{SM}}^{(0)}|_{\text{res.}} \times \left[ 1 + \underbrace{\mathcal{O}(1)}_{\text{NP}_{I=0}} + \underbrace{\mathcal{O}(1)}_{\text{NP}_{I=1}} + \underbrace{\mathcal{O}(\bar{\lambda})}_{\text{SM}} \right]. \quad (6.86)$$

Let us emphasize that the rescattering contributions to the prefactor on the right-hand side of this equation are due to (6.68), whereas the hierarchy in square brackets is governed by large rescattering processes of the type described by (6.69).



### 6.2.3 Observables for a General Analysis of New Physics

The observables provided by the  $B \rightarrow \phi K$  system are completely analogous to the set of  $B \rightarrow J/\psi K$  observables introduced in (6.42) and (6.45). The corresponding observables  $\mathcal{S}$ ,  $\mathcal{D}$  and  $\mathcal{B}$  allow us to separate the  $I = 0$  contributions from the  $I = 1$  sector, and play a key rôle in the search for new physics. Moreover, they may provide valuable insights into the  $B \rightarrow \phi K$  hadron dynamics. In the case of the decay  $B_d \rightarrow \phi K_S$ , mixing-induced CP violation yields an additional observable  $\mathcal{A}_{\text{CP}}^{\text{mix}}(B_d \rightarrow \phi K_S)$ . Explicit expressions for these quantities, which are rather complicated, can be found in [163]; let us here just note that they are governed by

$$\mathcal{S} \sim v_0, \quad \mathcal{D} \sim v_1, \quad \mathcal{B} \sim v_1. \quad (6.87)$$

### 6.2.4 Possible Scenarios

An interesting probe to search for new physics is provided by a comparison of the mixing-induced CP asymmetries in  $B_d \rightarrow \phi K_S$  and  $B_d \rightarrow J/\psi K_S$  [80, 150, 162]. Using the hierarchies in (6.38) and (6.82) yields the following relation [163]:

$$\mathcal{A}_{\text{CP}}^{\text{mix}}(B_d \rightarrow \phi K_S) - \mathcal{A}_{\text{CP}}^{\text{mix}}(B_d \rightarrow J/\psi K_S) = \underbrace{\mathcal{O}(1)}_{\text{NP}_{I=0}} + \underbrace{\mathcal{O}(\bar{\lambda})}_{\text{NP}_{I=1}} + \underbrace{\mathcal{O}(\bar{\lambda}^2)}_{\text{SM}}, \quad (6.88)$$

where the  $\sin \phi$  terms, which may also deviate from the Standard-Model expectation, cancel. The contributions entering at the  $\bar{\lambda}$  and  $\bar{\lambda}^2$  levels may also contain new-physics effects from  $B_d \rightarrow J/\psi K_S$ , whereas the  $\mathcal{O}(1)$  term would essentially be due to new physics in the  $B_d \rightarrow \phi K_S$  channel.

As can be seen in (6.87),  $\mathcal{S}$  provides a “smoking-gun” signal for new-physics contributions to the  $I = 0$  amplitude, whereas  $\mathcal{D}$  and  $\mathcal{B}$  probe new-physics effects in the  $I = 1$  sector. If we employ the hierarchy arising in (6.82), we obtain

$$\mathcal{S} = \underbrace{\mathcal{O}(1)}_{\text{NP}_{I=0}} + \underbrace{\mathcal{O}(\bar{\lambda}^2)}_{\text{SM}}, \quad \mathcal{D} = \underbrace{\mathcal{O}(\bar{\lambda})}_{\text{NP}_{I=1}} + \underbrace{\mathcal{O}(\bar{\lambda}^2)}_{\text{SM}}, \quad \mathcal{B} = \underbrace{\mathcal{O}(\bar{\lambda})}_{\text{NP}_{I=1}} + \underbrace{\mathcal{O}(\bar{\lambda}^2)}_{\text{SM}}, \quad (6.89)$$

where the Standard-Model contributions are not under theoretical control. If the dynamical suppression of the  $I = 1$  contributions were larger than  $\mathcal{O}(\bar{\lambda})$ ,  $\mathcal{D}$  and  $\mathcal{B}$  would be further suppressed with respect to  $\mathcal{S}$ . On the other hand, if the rescattering effects described by (6.69) were very large – and not small, as assumed in (6.89) – *all* three observables would be of  $\mathcal{O}(1)$ . In such a situation, we would not only have signals for physics beyond the Standard Model, but also for large rescattering processes.

The discussion given above corresponds to the most optimistic scenario concerning the generic strength of possible new-physics effects in the  $B \rightarrow \phi K$  system. Let us now

consider a more pessimistic case, where the new-physics contributions are smaller by a factor of  $\mathcal{O}(\bar{\lambda})$ :

$$A(B \rightarrow \phi K) = \mathcal{A}_{\text{SM}}^{(0)} \left[ 1 + \underbrace{\mathcal{O}(\bar{\lambda})}_{\text{NP}_{I=0}} + \underbrace{\mathcal{O}(\bar{\lambda}^2)}_{\text{NP}_{I=1}} + \underbrace{\mathcal{O}(\bar{\lambda}^2)}_{\text{SM}} \right]. \quad (6.90)$$

Now the new-physics contributions to the  $I = 1$  sector can no longer be separated from the Standard-Model contributions. However, we would still get an interesting pattern for the  $B \rightarrow \phi K$  observables, providing evidence for new physics: whereas (6.88) and  $\mathcal{S}$  would both be sizeable, i.e. of  $\mathcal{O}(10\%)$  and within reach of the  $B$ -factories,  $\mathcal{D}$  and  $\mathcal{B}$  would be strongly suppressed. However, if these two observables, in addition to (6.88) and  $\mathcal{S}$ , are found to be also at the 10% level, new physics cannot be distinguished from Standard-Model contributions, which could also be enhanced to the  $\bar{\lambda}$  level by large rescattering effects. This would be the most unfortunate case for the search for new-physics contributions to the  $B \rightarrow \phi K$  decay amplitudes [163]. As we have seen in Subsection 6.1, there is an analogous case in the  $B \rightarrow J/\psi K$  system, which does also not appear to be a very likely scenario.

In general,  $B \rightarrow J/\psi K$  and  $B \rightarrow \phi K$  modes offer powerful tools to test the Standard-Model description of CP violation. Hopefully, the experimental data for these decays, which are very accessible at the  $B$ -factories, will shed light on the physics beyond the Standard Model. A decay lying in some sense between these channels is the transition  $B_d \rightarrow \pi^+ \pi^-$ , which is our next topic: whereas  $B \rightarrow J/\psi K$  and  $B \rightarrow \phi K$  are governed by tree-diagram-like and penguin contributions, respectively, both topologies play an important rôle in  $B_d \rightarrow \pi^+ \pi^-$ . This feature leads to serious problems in the extraction of  $\alpha$  from the mixing-induced CP asymmetry of  $B_d \rightarrow \pi^+ \pi^-$ , introducing large hadronic uncertainties into the corresponding Standard-Model expression.

## 6.3 The $B \rightarrow \pi\pi$ System

### 6.3.1 Probing $\alpha$ through $B_d \rightarrow \pi^+ \pi^-$

The transition  $B_d^0 \rightarrow \pi^+ \pi^-$  is a decay into a CP eigenstate with eigenvalue +1, and originates from  $\bar{b} \rightarrow \bar{u}u\bar{d}$  quark-level processes, as can be seen in Fig. 18. Within the Standard Model, the corresponding decay amplitude can be expressed – in analogy to (6.1) – in the following way [169]:

$$A(B_d^0 \rightarrow \pi^+ \pi^-) = \lambda_u^{(d)} (A_{\text{CC}}^u + A_{\text{pen}}^u) + \lambda_c^{(d)} A_{\text{pen}}^c + \lambda_t^{(d)} A_{\text{pen}}^t = \mathcal{C} (e^{i\gamma} - de^{i\theta}), \quad (6.91)$$

where

$$\mathcal{C} \equiv \lambda^3 A R_b (A_{\text{CC}}^u + A_{\text{pen}}^{ut}) \quad \text{with} \quad A_{\text{pen}}^{ut} \equiv A_{\text{pen}}^u - A_{\text{pen}}^t, \quad (6.92)$$

and

$$de^{i\theta} \equiv \frac{1}{R_b} \left( \frac{A_{\text{pen}}^{ct}}{A_{\text{CC}}^u + A_{\text{pen}}^{ut}} \right). \quad (6.93)$$

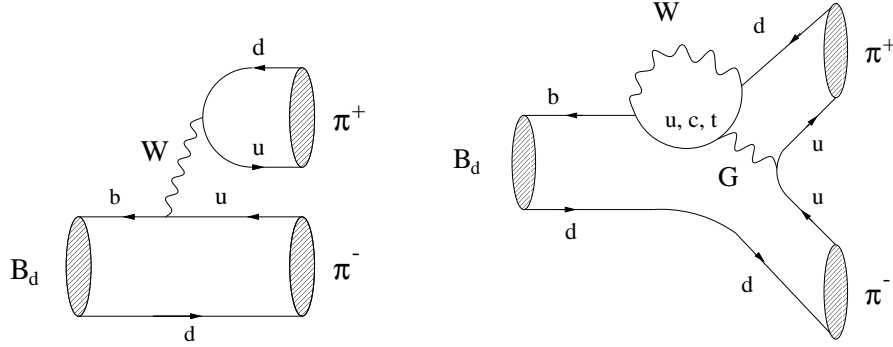


Figure 18: Feynman diagrams contributing to  $B_d^0 \rightarrow \pi^+\pi^-$ .

In contrast to the  $B_d^0 \rightarrow J/\psi K_S$  amplitude (6.3), the “penguin” parameter  $de^{i\theta}$  does *not* enter in (6.91) in a doubly Cabibbo-suppressed way. If we assume, for a moment, that  $d = 0$ , the formalism discussed in Subsection 5.4 yields

$$\mathcal{A}_{\text{CP}}^{\text{mix}}(B_d \rightarrow \pi^+\pi^-) = -\sin[-(2\beta + 2\gamma)] = -\sin 2\alpha, \quad (6.94)$$

which would allow a determination of  $\alpha$ . Unfortunately, it is expected that this relation is strongly affected by penguin effects, which were analysed by many authors over the last couple of years [75, 77, 98, 100, 170, 171].

Large penguin effects in  $B_d \rightarrow \pi^+\pi^-$  are also indicated by the  $B$ -factory data. In the summer of 1999, the observation of this channel was announced by the CLEO collaboration. The present results for its CP-averaged branching ratio read as follows:

$$\text{BR}(B_d \rightarrow \pi^+\pi^-) \times 10^6 = \begin{cases} 4.3_{-1.4}^{+1.6} \pm 0.5 & \text{(CLEO [172])} \\ 4.1 \pm 1.0 \pm 0.7 & \text{(BaBar [173])} \\ 5.6_{-2.0}^{+2.3} \pm 0.4 & \text{(Belle [174]).} \end{cases} \quad (6.95)$$

Using  $SU(3)$  flavour-symmetry arguments and plausible dynamical assumptions, the CP-averaged  $B_d \rightarrow \pi^+\pi^-$  branching ratio can be combined with that of  $B_d \rightarrow \pi^\mp K^\pm$  [171] to derive constraints on the penguin parameter  $d$  [175]. The present  $B$ -factory results imply  $d \gtrsim 0.2$ , as we will discuss in more detail in 10.3.5 (see Fig. 35). Moreover, theoretical considerations are also in favour of sizeable values of  $d$  (see (10.46)). Consequently, we have already strong evidence that the approximation  $d = 0$ , i.e. the neglect of penguins in  $B_d \rightarrow \pi^+\pi^-$ , is not justified.

Concerning the direct and mixing-induced CP-violating observables of  $B_d \rightarrow \pi^+\pi^-$ , first results are already available from the BaBar collaboration [176]:

$$\mathcal{A}_{\text{CP}}^{\text{dir}}(B_d \rightarrow \pi^+\pi^-) = (-25_{-47}^{+45} \pm 14)\%, \quad \mathcal{A}_{\text{CP}}^{\text{mix}}(B_d \rightarrow \pi^+\pi^-) = (-3_{-53}^{+56} \pm 11)\%. \quad (6.96)$$

Needless to note, because of the large experimental uncertainties, no conclusions can be drawn at present, although a direct CP asymmetry at the level of 25% would also imply large penguin effects.

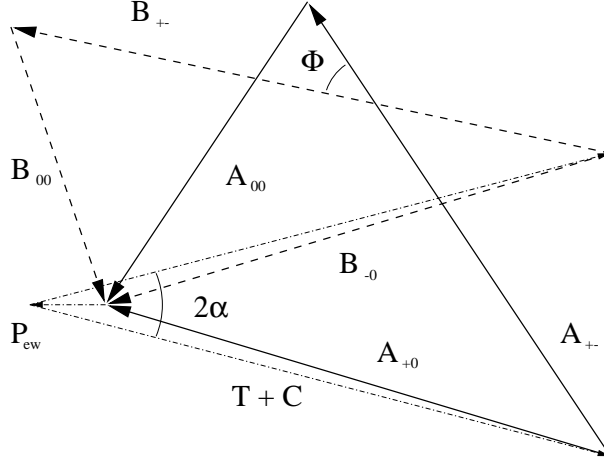


Figure 19: Illustration of the  $B \rightarrow \pi\pi$  isospin triangles. Here the amplitudes  $A$  correspond to (6.99); the amplitudes  $B$  correspond to the ones in (6.100), rotated by  $e^{-2i\beta}$ .

### 6.3.2 Isospin Relations between $B \rightarrow \pi\pi$ Amplitudes

There are various strategies to control the penguin uncertainties affecting the extraction of  $\alpha$  with the help of additional experimental data. The best known approach was proposed by Gronau and London [177], employing isospin relations between the  $B \rightarrow \pi\pi$  decay amplitudes. Since  $B^- \rightarrow \pi^-\pi^0$  is a  $\Delta I = 3/2$  transition, the QCD penguin operators (3.30) with  $r = d$ , which mediate  $\Delta I = 1/2$  transitions, do not contribute. Consequently, if we neglect EW penguins for a moment, this channels receives only contributions from colour-allowed and colour-suppressed tree-diagram-like topologies, which are described by strong amplitudes  $T$  and  $C$ , respectively, and we obtain

$$A(B^\pm \rightarrow \pi^\pm\pi^0) = e^{\pm i\gamma} e^{i\delta T+C} |T + C|, \quad (6.97)$$

yielding

$$\frac{A(B^+ \rightarrow \pi^+\pi^0)}{A(B^- \rightarrow \pi^-\pi^0)} = e^{2i\gamma}. \quad (6.98)$$

Moreover, the isospin symmetry implies the following amplitude relations [177]:

$$\sqrt{2} A(B^+ \rightarrow \pi^+\pi^0) = A(B_d^0 \rightarrow \pi^+\pi^-) + \sqrt{2} A(B_d^0 \rightarrow \pi^0\pi^0) \quad (6.99)$$

$$\sqrt{2} A(B^- \rightarrow \pi^-\pi^0) = A(\overline{B}_d^0 \rightarrow \pi^+\pi^-) + \sqrt{2} A(\overline{B}_d^0 \rightarrow \pi^0\pi^0), \quad (6.100)$$

which can be represented as two triangles in the complex plane. These triangles, i.e. their sides, can be fixed through the six  $B \rightarrow \pi\pi$  branching ratios. In order to determine also their relative orientation, we rotate the CP-conjugate triangle by  $e^{-2i\beta}$ . The resulting situation is illustrated in Fig. 19, where the angle  $\Phi$  can be extracted from mixing-induced

CP violation [86]: applying the formalism discussed in Subsection 5.4, we obtain

$$\xi_{\pi^+\pi^-}^{(d)} = -e^{-i2\beta} \left[ \frac{A(\overline{B}_d^0 \rightarrow \pi^+\pi^-)}{A(B_d \rightarrow \pi^+\pi^-)} \right] = - \left| \frac{B_{+-}}{A_{+-}} \right| e^{i\Phi}, \quad (6.101)$$

which implies

$$\mathcal{A}_{\text{CP}}^{\text{mix}}(B_d \rightarrow \pi^+\pi^-) = - \frac{2|A_{+-}||B_{+-}|}{|A_{+-}|^2 + |B_{+-}|^2} \sin \Phi. \quad (6.102)$$

If we use (6.98), and take into account that the CP-conjugate triangle was rotated by  $e^{-2i\beta}$ , we conclude that the angle between the  $B^+ \rightarrow \pi^+\pi^0$  and  $B^- \rightarrow \pi^-\pi^0$  amplitudes is given by  $2\alpha$ . For simplicity, we have chosen  $\phi_{\text{CP}} = 0$  in the discussion given above. The corresponding determination of  $\alpha$  does, of course, not depend on the choice of this CP phase. It is an easy exercise to convince ourselves from this feature.

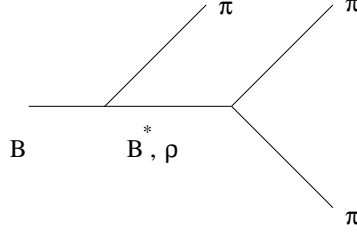
On the other hand, the EW penguin amplitude  $P_{\text{ew}}$ , which we have neglected so far, does affect this extraction of  $\alpha$ , as can be seen in Fig. 19. Although the determination of the sides of the isospin triangles and of their relative orientation remains unchanged, the angle between  $A_{+0}$  and  $B_{-0}$  is shifted from  $\alpha$  by  $\Delta\alpha = \mathcal{O}(|P_{\text{ew}}|/|T + C|)$ , which corresponds to a small correction of at most a few degrees [85, 88]. As was noticed recently [87, 178], also the EW penguin contribution can be taken into account with the help of the  $SU(2)$  isospin symmetry, yielding

$$\left[ \frac{P_{\text{ew}}}{T + C} \right] = -1.3 \times 10^{-2} \times \left| \frac{V_{td}}{V_{ub}} \right| e^{i\alpha}, \quad (6.103)$$

where the numerical factor depends only on Wilson coefficients of EW penguin and CC operators, i.e. does not involve hadronic matrix elements.

Isospin is broken not only by the quark charges, as in the EW penguin operators, but also by the up- and down-quark mass difference, which generates  $\pi^0$ - $\eta$ ,  $\eta'$  mixing and converts the isospin triangle relations (6.99) and (6.100) between the  $B \rightarrow \pi\pi$  amplitudes into quadrilaterals. The impact of these isospin-violating effects on the extraction of  $\alpha$  was analysed in [179], and was found to be significant if  $\sin 2\alpha$  is small.

Unfortunately, the  $B \rightarrow \pi\pi$  triangle approach is very challenging from an experimental point of view, since it requires a measurement of the  $B_d^0 \rightarrow \pi^0\pi^0$  branching ratio and its CP conjugate. Because of the two neutral pions in the final state, this mode is very difficult to reconstruct. Moreover, the corresponding CP-averaged branching ratio is expected to be very small, i.e.  $\text{BR}(B_d \rightarrow \pi^0\pi^0)|_{\text{TH}} \lesssim \mathcal{O}(10^{-6})$ . In a recent analysis, the CLEO collaboration has obtained the upper limit  $\text{BR}(B_d \rightarrow \pi^0\pi^0) < 5.7 \times 10^{-6}$  (90% C.L.) [180]. Such upper bounds may be useful to constrain the QCD penguin uncertainties affecting the determination of  $\alpha$  from  $B_d \rightarrow \pi^+\pi^-$  decays [181]–[183].

Figure 20: Polar diagrams contributing to  $B \rightarrow \pi\pi\pi$ .

### 6.3.3 Extracting $\alpha$ from $B \rightarrow \rho\pi$ Modes

Because of the  $B_d \rightarrow \pi^0\pi^0$  problem of the Gronau–London approach to extract  $\alpha$  from  $B \rightarrow \pi\pi$  isospin relations, alternative strategies are very desirable. An interesting one is provided by  $B \rightarrow \rho\pi$  modes [184]. These decays are more complicated than the  $B \rightarrow \pi\pi$  system, since their final states consist of the three different isospin configurations  $I = 0, 1, 2$  instead of  $I = 0, 2$ . Performing an isospin analysis of the decays  $B^+ \rightarrow \rho^+\pi^0$ ,  $B^+ \rightarrow \rho^0\pi^+$ ,  $B_d^0 \rightarrow \rho^+\pi^-$ ,  $B_d^0 \rightarrow \rho^-\pi^+$ ,  $B_d^0 \rightarrow \rho^0\pi^0$  and of their charge conjugates yields the following two pentagonal relations:

$$\sqrt{2} (A^{+0} + A^{0+}) = A^{+-} + A^{-+} + 2A^{00} \quad (6.104)$$

$$\sqrt{2} (\bar{A}^{+0} + \bar{A}^{0+}) = \bar{A}^{+-} + \bar{A}^{-+} + 2\bar{A}^{00}, \quad (6.105)$$

which correspond to the  $B \rightarrow \pi\pi$  triangle relations (6.99) and (6.100). The ten  $B \rightarrow \rho\pi$  rates allow us to fix the sides of both isospin pentagons. Measuring in addition mixing-induced CP violation in  $B_d \rightarrow \rho^+\pi^-$ ,  $\rho^-\pi^+$ ,  $\rho^0\pi^0$ , it is also possible to determine  $\alpha$ .

In practice, this approach is obviously quite complicated and suffers from multiple discrete ambiguities. In order to avoid them, Quinn and Snyder have considered a maximum-likelihood fit to the parameters of the full Dalitz plot distribution, and found that it is possible to extract  $\alpha$ , as well as other parameters, with  $\mathcal{O}(10^3)$  Monte–Carlo-generated events [185]. Here the basic assumption is that the  $B \rightarrow 3\pi$  events are fully dominated by  $B \rightarrow \rho\pi$ . Taking into account detector efficiencies and background effects, one finds that  $\mathcal{O}(10^4)$   $B \rightarrow \rho\pi$  events are required, corresponding to  $\mathcal{O}(10^9)$   $B\bar{B}$  events, which may be beyond of what can be achieved in first-generation  $B$ -factory experiments. The approach appears even to be challenging for the LHC era.

To attack this problem, strategies to use “early” data on  $B \rightarrow \rho\pi$  modes were recently proposed in [186], employing Dalitz plot analyses of  $B_d \rightarrow \rho\pi \rightarrow \pi^+\pi^-\pi^0$  decays. In that paper, it was pointed out that important parameters – unfortunately not  $\alpha$  – can be determined from untagged and tagged time-integrated measurements, suggesting that the extraction of  $\alpha$  from the time-dependent data sample can be accomplished with a smaller data sample than would be required if all parameters were to be obtained from that time-dependent data sample alone.

Another recent development concerning  $B \rightarrow \rho\pi$  modes are studies of the impact of the “polar diagrams” shown in Fig. 20. As was pointed out in [187], these processes may lead to significant effects in  $B^\mp \rightarrow \pi^\mp \pi^\mp \pi^\pm$  decays, whereas they are expected to be negligible in other charged decays. In the neutral case, only  $B_d \rightarrow \rho^0 \pi^0$  transitions may be affected. Since the processes induced by such polar diagrams represent an irreducible background in the Dalitz plot, charged  $B \rightarrow \rho\pi$  and neutral  $B_d \rightarrow \rho^0 \pi^0$  channels should be discarded from the extraction of  $\alpha$  [187]. Further studies of these issues are desirable.

### 6.3.4 Other Approaches to Extract $\alpha$

Another strategy to extract  $\alpha$  is provided by  $B^\pm \rightarrow \rho^\pm \rho^0(\omega) \rightarrow \rho^\pm \pi^+ \pi^-$  decays, where  $\rho^0(\omega)$  denotes the  $\rho^0$ - $\omega$  interference region [188]. In this case, experimental data on  $e^+e^- \rightarrow \pi^+ \pi^-$  processes can be used to constrain the hadronic uncertainties affecting the corresponding direct CP asymmetry, which is related to  $\sin \alpha$  and may well be as large as  $\mathcal{O}(20\%)$  at the  $\omega$  invariant mass. In this context, it is worth mentioning that also direct CP violation in three-body decays such as  $B^\pm \rightarrow K^\pm \pi^+ \pi^-$ , involving various intermediate resonances, was considered [189]. Here the Dalitz plot distributions may provide information on the CKM angle  $\gamma$  (see also [190]).

A possibility to eliminate the penguin uncertainties in the extraction of  $\alpha$  from mixing-induced CP violation in  $B_d \rightarrow \pi^+ \pi^-$  is also provided by the  $B_d \rightarrow K^0 \bar{K}^0$  channel, which can be related to  $B_d \rightarrow \pi^+ \pi^-$  through the  $SU(3)$  flavour symmetry of strong interactions [191].

Another – rather simple – strategy to determine  $\alpha$  was proposed in [192]. Using the unitarity of the CKM matrix to eliminate  $\lambda_c^{(d)}$ , we may rewrite (6.91) as follows:

$$A(B_d^0 \rightarrow \pi^+ \pi^-) = e^{i\gamma} T + e^{-i\beta} P, \quad (6.106)$$

where

$$T \equiv |\lambda_u^{(d)}| \left( A_{\text{CC}}^u + A_{\text{pen}}^u - A_{\text{pen}}^c \right) \quad \text{and} \quad P \equiv |\lambda_t^{(d)}| \left( A_{\text{pen}}^t - A_{\text{pen}}^c \right). \quad (6.107)$$

For the following considerations, also the CP-conserving strong phase  $\delta \equiv \arg(PT^*)$  plays an important rôle. Since the  $B_d^0$ - $\bar{B}_d^0$  mixing phase is given by  $2\beta$  in the Standard Model, the unitarity relation  $\alpha + \beta + \gamma = 180^\circ$  allows us to express the CP-violating observables  $\mathcal{A}_{\text{CP}}^{\text{dir}}(B_d \rightarrow \pi^+ \pi^-)$  and  $\mathcal{A}_{\text{CP}}^{\text{mix}}(B_d \rightarrow \pi^+ \pi^-)$  as functions of the CKM angle  $\alpha$  and the two hadronic parameters  $|P/T|$  and  $\delta$ . Consequently, we have two observables at our disposal, depending on three “unknowns”. The corresponding expressions simplify considerably, if we keep only the leading-order terms in  $x \equiv |P/T|$ , yielding

$$\mathcal{A}_{\text{CP}}^{\text{dir}}(B_d \rightarrow \pi^+ \pi^-) = 2x \sin \delta \sin \alpha + \mathcal{O}(x^2) \quad (6.108)$$

$$\mathcal{A}_{\text{CP}}^{\text{mix}}(B_d \rightarrow \pi^+ \pi^-) = -\sin 2\alpha - 2x \cos \delta \cos 2\alpha \sin \alpha + \mathcal{O}(x^2). \quad (6.109)$$

If the parameter  $x$  is fixed through an additional input, both  $\alpha$  and the strong phase  $\delta$  can be determined from (6.108) and (6.109). To this end, we may use, for example, the  $SU(3)$  flavour symmetry and certain dynamical assumptions [192]:

$$x \approx \lambda R_t \left( \frac{f_\pi}{f_K} \right) \sqrt{\frac{\text{BR}(B^+ \rightarrow \pi^+ K^0)}{2 \text{BR}(B^+ \rightarrow \pi^+ \pi^0)}}. \quad (6.110)$$

Refinements of this approach were discussed in [182]. It should be emphasized that  $\mathcal{A}_{\text{CP}}^{\text{dir}}(B_d \rightarrow \pi^+ \pi^-)$  and  $\mathcal{A}_{\text{CP}}^{\text{mix}}(B_d \rightarrow \pi^+ \pi^-)$  allow us to fix contours in the  $\alpha$ - $x$  plane in a *theoretically clean* way. Unfortunately, it appears very challenging to determine also  $x$ , which would allow the extraction of  $\alpha$ , in a theoretically reliable manner. In order not to comprise the LHC year-1 statistics,  $x$  would be required with a theoretical uncertainty smaller than 10% [148]. Despite the recent theoretical progress made in [98]–[103], it appears questionable whether such an accuracy can eventually be achieved (see [77] and Subsection 9.4). Moreover, any QCD-based approach to calculate  $x$  requires also the CKM factor  $|V_{td}/V_{ub}|$ . This input can be avoided, if all weak phases are expressed in terms of the generalized Wolfenstein parameters  $\bar{\rho}$  and  $\bar{\eta}$ , allowing us to fix contours in the  $\bar{\rho}$ - $\bar{\eta}$  plane through the  $B_d \rightarrow \pi^+ \pi^-$  observables [182].

Let us finally note that a particularly promising strategy is provided by the decay  $B_s \rightarrow K^+ K^-$ , which is related to  $B_d \rightarrow \pi^+ \pi^-$  by interchanging all down and strange quarks, i.e. through the  $U$ -spin flavour symmetry of strong interactions. A combined analysis of these two channels allows a simultaneous determination of  $\beta$  and  $\gamma$  [169], which has certain theoretical advantages, appears to be promising for Tevatron-II [193], and is ideally suited for the LHC era [148]. This approach will be discussed in Subsection 10.3.

## 6.4 $B_d \rightarrow D^{(*)\pm} \pi^\mp$ Decays

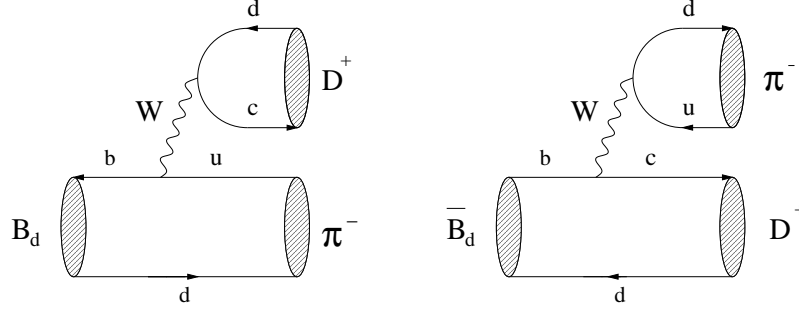
So far, we have put a strong emphasis on neutral  $B$  decays into CP eigenstates. However, in order to extract angles of the unitarity triangle, there are also interesting decays into final states that are *not* eigenstates of the CP operator. An important example is given by  $B_d \rightarrow D^{(*)\pm} \pi^\mp$  decays, which are mediated by  $\bar{b} \rightarrow \bar{u} c \bar{d}$  ( $b \rightarrow c \bar{u} d$ ) quark-level processes and receive hence only contributions from tree-diagram-like topologies. As can be seen in Fig. 21,  $B_d^0$ - and  $\bar{B}_d^0$ -mesons may both decay into  $D^{(*)+} \pi^-$ , thereby leading to interference effects between  $B_d^0$ - $\bar{B}_d^0$  mixing and decay processes. These interference effects allow an interesting – theoretically clean – determination of  $2\beta + \gamma$ .

The relevant transition amplitudes can be expressed as hadronic matrix elements of

$$\mathcal{H}_{\text{eff}}(\bar{B}_d^0 \rightarrow f) = \frac{G_F}{\sqrt{2}} \bar{v} \left[ \bar{\mathcal{O}}_1 C_1(\mu) + \bar{\mathcal{O}}_2 C_2(\mu) \right] \quad (6.111)$$

$$\mathcal{H}_{\text{eff}}(B_d^0 \rightarrow f) = \frac{G_F}{\sqrt{2}} v^* \left[ \mathcal{O}_1^\dagger C_1(\mu) + \mathcal{O}_2^\dagger C_2(\mu) \right], \quad (6.112)$$



Figure 21: Feynman diagrams contributing to  $B_d^0, \bar{B}_d^0 \rightarrow D^{(*)+} \pi^-$  decays.

where  $f$  is a final state with valence-quark content  $c\bar{d}d\bar{u}$ , for example  $D^{*+}\pi^-$ , and  $\bar{\mathcal{O}}_k$  and  $\mathcal{O}_k$  denote current–current operators, which are given by

$$\begin{aligned} \bar{\mathcal{O}}_1 &= (\bar{d}_\alpha u_\beta)_{V-A} (\bar{c}_\beta b_\alpha)_{V-A}, & \bar{\mathcal{O}}_2 &= (\bar{d}_\alpha u_\alpha)_{V-A} (\bar{c}_\beta b_\beta)_{V-A}, \\ \mathcal{O}_1 &= (\bar{d}_\alpha c_\beta)_{V-A} (\bar{u}_\beta b_\alpha)_{V-A}, & \mathcal{O}_2 &= (\bar{d}_\alpha c_\alpha)_{V-A} (\bar{u}_\beta b_\beta)_{V-A}, \end{aligned} \quad (6.113)$$

and are analogous to the ones we encountered in 3.3.2; their NLO Wilson coefficients can be calculated with the help of (3.19)–(3.25). Using (2.17) and (2.46) yields

$$\bar{v} \equiv V_{ud}^* V_{cb} = \left(1 - \frac{\lambda^2}{2}\right) A \lambda^2, \quad v \equiv V_{cd}^* V_{ub} = -A \lambda^4 \left(\frac{R_b}{1 - \lambda^2/2}\right) e^{-i\gamma}. \quad (6.114)$$

On the other hand, taking into account CP relations (5.8) and (5.37), we obtain

$$\begin{aligned} &\langle f | \mathcal{O}_1^\dagger(\mu) C_1(\mu) + \mathcal{O}_2^\dagger(\mu) C_2(\mu) | B_d^0 \rangle \\ &= \langle f | (\mathcal{CP})^\dagger (\mathcal{CP}) \left[ \mathcal{O}_1^\dagger(\mu) C_1(\mu) + \mathcal{O}_2^\dagger(\mu) C_2(\mu) \right] (\mathcal{CP})^\dagger (\mathcal{CP}) | B_d^0 \rangle \\ &= e^{i\phi_{\text{CP}}(B_d)} \langle \bar{f} | \mathcal{O}_1(\mu) C_1(\mu) + \mathcal{O}_2(\mu) C_2(\mu) | \bar{B}_d^0 \rangle. \end{aligned} \quad (6.115)$$

Consequently, the relevant decay amplitudes take the following form:

$$A(\bar{B}_d^0 \rightarrow f) = \langle f | \mathcal{H}_{\text{eff}}(\bar{B}_d^0 \rightarrow f) | \bar{B}_d^0 \rangle = \frac{G_F}{\sqrt{2}} \bar{v} \bar{M}_f \quad (6.116)$$

$$A(B_d^0 \rightarrow f) = \langle f | \mathcal{H}_{\text{eff}}(B_d^0 \rightarrow f) | B_d^0 \rangle = e^{i\phi_{\text{CP}}(B_d)} \frac{G_F}{\sqrt{2}} v^* M_{\bar{f}}, \quad (6.117)$$

with hadronic matrix elements

$$\bar{M}_f \equiv \langle f | \bar{\mathcal{O}}_1(\mu) C_1(\mu) + \bar{\mathcal{O}}_2(\mu) C_2(\mu) | \bar{B}_d^0 \rangle \quad (6.118)$$

$$M_{\bar{f}} \equiv \langle \bar{f} | \mathcal{O}_1(\mu) C_1(\mu) + \mathcal{O}_2(\mu) C_2(\mu) | B_d^0 \rangle. \quad (6.119)$$

We are now in a position to calculate the observable  $\xi_f^{(d)}$ , governing the time evolution of the  $B_d^0(t), \bar{B}_d^0(t) \rightarrow f$  decay processes. Using (5.18) and (5.19), we arrive at

$$\xi_f^{(d)} = e^{-i\theta_{M_{12}}^{(d)}} \frac{A(\bar{B}_d^0 \rightarrow f)}{A(B_d^0 \rightarrow f)} = -e^{-i(\phi_d + \gamma)} \left(\frac{1 - \lambda^2}{\lambda^2 R_b}\right) \frac{\bar{M}_f}{M_{\bar{f}}}. \quad (6.120)$$

Performing an analogous calculation for  $\bar{f} \equiv D^{(*)-}\pi^+$  yields

$$\xi_{\bar{f}}^{(d)} = e^{-i\Theta_{M_{12}}^{(d)}} \frac{A(\overline{B}_d^0 \rightarrow \bar{f})}{A(B_d^0 \rightarrow \bar{f})} = -e^{-i(\phi_d + \gamma)} \left( \frac{\lambda^2 R_b}{1 - \lambda^2} \right) \frac{M_{\bar{f}}}{\overline{M}_f}. \quad (6.121)$$

If the time-dependent rates corresponding to  $B_d^0(t), \overline{B}_d^0(t) \rightarrow f$  and  $B_d^0(t), \overline{B}_d^0(t) \rightarrow \bar{f}$  decay processes are measured, the observables  $\xi_f^{(d)}$  and  $\xi_{\bar{f}}^{(d)}$  can be determined (see (5.25)). Since the hadronic matrix elements  $\overline{M}_f$  and  $M_{\bar{f}}$ , as well as the rather poorly known CKM factor  $R_b$ , cancel in the following combination [80]:

$$\xi_f^{(d)} \times \xi_{\bar{f}}^{(d)} = e^{-2i(\phi_d + \gamma)}, \quad (6.122)$$

we may extract the weak phase  $\phi_d + \gamma$  in a *theoretically clean* way [194]. Moreover, as  $\phi_d$ , i.e.  $2\beta$ , can be determined straightforwardly with the help of the “gold-plated” mode  $B_d \rightarrow J/\psi K_S$  (see also 6.1.6), we may extract  $\gamma$  from (6.122).

Unfortunately, the  $\bar{b} \rightarrow \bar{u}c\bar{d}$  transition in Fig. 21 is doubly Cabibbo-suppressed by  $\lambda^2 R_b \approx 0.02$  with respect to  $b \rightarrow c\bar{u}d$ , so that the interference effects are tiny. However, the approach is nevertheless experimentally interesting, if decays into  $D^{*\pm}\pi^\mp$  states are considered, where the  $D^{*\pm}$ -mesons continue to decay through strong interactions,  $D^{*\pm} \rightarrow D\pi^\pm$ . Here the branching ratios are large, i.e.  $\mathcal{O}(10^{-3})$ , and the  $D^{*\pm}\pi^\mp$  states can be reconstructed with a good efficiency and modest backgrounds. In order to boost statistics, a partial reconstruction technique can be applied. Experimental feasibility studies for BaBar and the LHC were performed in [195] and [148], respectively. The analyses can also be extended to  $B_d \rightarrow D^{*\pm}a_1^\mp$  modes, exhibiting a branching ratio that is about three times larger than that of  $B_d \rightarrow D^{*\pm}\pi^\mp$  [148]; advantages of other resonances were emphasized in [196]. However, the two spin-1 particles arising in  $B_d \rightarrow D^{*\pm}a_1^\mp$  complicate the extraction of  $\phi_d + \gamma$ , requiring an angular analysis (for an analogous problem, see [197]).

## 6.5 Summary

In this section, we have discussed  $B$ -factory benchmark modes. The key features of these transitions are interference effects between  $B_d^0\text{--}\overline{B}_d^0$  mixing and decay processes, providing observables for the extraction of weak phases, where hadronic matrix elements cancel.

The most important channel is the “gold-plated” decay  $B_d \rightarrow J/\psi K_S$ , allowing a determination of  $\sin 2\beta$ . Using this and similar modes, CP violation in the  $B$  system could recently be observed by the BaBar and Belle collaborations. Since their results for  $\sin 2\beta$  are not fully consistent with each other, the measurement of this quantity will continue to be a very exciting topic. Taking into account also previous results from the CDF and ALEPH collaborations, the resulting average is now in good agreement with the range implied by the “standard analysis” of the unitarity triangle. However, as we

have illustrated in the context of  $B_d \rightarrow J/\psi[\rightarrow \ell^+\ell^-]K^*[\rightarrow \pi^0 K_S]$  decays, new physics may even hide in such a situation, making it important to determine also  $\cos 2\beta$ .

The preferred mechanism for physics beyond the Standard Model to manifest itself in these measurements is through contributions to  $B_d^0\text{--}\overline{B}_d^0$  mixing. In order to obtain the whole picture,  $B^\pm \rightarrow J/\psi K^\pm$  modes, which are related to  $B_d \rightarrow J/\psi K_S$  through the isospin symmetry of strong interactions, should be considered as well. Then we may – in addition to the usual mixing-induced CP asymmetry  $a_{\psi K_S}$  – introduce a set of three observables, allowing a general analysis of possible new-physics contributions to the different isospin sectors of the  $B \rightarrow J/\psi K$  system. Imposing a plausible dynamical hierarchy of amplitudes, we have seen that one of these observables may already be accessible at the first-generation  $B$ -factories, whereas the remaining ones will probably be left for the LHC era. However, in the presence of large rescattering effects, all three new-physics observables may be sizeable.

A similar analysis can also be performed for the  $B \rightarrow \phi K$  system, which is very sensitive to new-physics effects at the amplitude level, since these modes originate from  $\overline{b} \rightarrow \overline{s}$  penguin processes. Within the Standard Model, mixing-induced CP violation in  $B_d \rightarrow \phi K_S$  is related to  $\sin 2\beta$ , as in the  $B_d \rightarrow J/\psi K_S$  case. A difference between these measurements would probably be due to new-physics contributions to the  $B \rightarrow \phi K$  decay amplitudes. In order to get the full picture, three additional observables have to be measured, providing not only “smoking-gun” signals for new-physics contributions to the two different  $B \rightarrow \phi K$  isospin channels, but also valuable insights into hadron dynamics. Whereas the  $B \rightarrow \phi K$  system is, in general, a powerful tool to search for indications of new physics, there is also an unfortunate case, where such effects cannot be distinguished from those of the Standard Model.

If penguin effects played a negligible rôle in the decay  $B_d \rightarrow \pi^+\pi^-$ , the angle  $\alpha$  of the unitarity triangle could be determined from the corresponding mixing-induced CP asymmetry. However, both experimental data and theoretical considerations indicate that the penguin effects cannot be neglected. Using isospin relations between  $B \rightarrow \pi\pi$  amplitudes, the corresponding hadronic uncertainties could in principle be eliminated, thereby allowing a determination of  $\alpha$ . Since this approach requires a measurement of  $B_d \rightarrow \pi^0\pi^0$ , it is unfortunately very difficult in practice. An alternative to solve the penguin problem in the extraction of  $\alpha$  is given by  $B \rightarrow \rho\pi$  modes, and a particularly promising way to make use of the CP-violating  $B_d \rightarrow \pi^+\pi^-$  observables is offered by  $B_s \rightarrow K^+K^-$  modes, as we will see in Subsection 10.3.

Finally, we have also considered the pure “tree” decays  $B_d \rightarrow D^{(*)\pm}\pi^\mp$ , providing a theoretically clean determination of the weak phase  $2\beta + \gamma$ . Although the relevant interference effects between  $B_d^0\text{--}\overline{B}_d^0$  mixing and decay processes are doubly Cabibbo-suppressed, this approach is nevertheless experimentally interesting. It has also a counterpart in the  $B_s$  system, which is our next topic.

## 7 A Closer Look at the $B_s$ System

### 7.1 General Remarks and Differences to the $B_d$ System

Unfortunately, at the  $e^+e^-$   $B$ -factories operating at the  $\Upsilon(4S)$  resonance (BaBar, Belle, CLEO), no  $B_s$ -mesons are accessible, since  $\Upsilon(4S)$  states decay only to  $B_{u,d}$ -mesons, but not to  $B_s$ .<sup>5</sup> On the other hand, the physics potential of the  $B_s$  system is very promising for hadron machines (Tevatron, LHC), where plenty of  $B_s$ -mesons are produced [148]. In some sense,  $B_s$  physics is therefore the ‘‘El Dorado’’ for  $B$  experiments at hadron colliders. There are important differences between the  $B_d$  and  $B_s$  systems:

- Within the Standard Model, the  $B_s^0\text{--}\overline{B}_s^0$  mixing phase probes the tiny angle  $\delta\gamma$  in the unitarity triangle shown in Fig. 3 (b), and is hence negligibly small:

$$\phi_s = -2\delta\gamma = -2\lambda^2\eta = \mathcal{O}(-0.03) = \mathcal{O}(-2^\circ), \quad (7.1)$$

whereas  $\phi_d = 2\beta = \mathcal{O}(45^\circ)$ .

- A large mixing parameter  $x_s = \mathcal{O}(20)$  is expected in the Standard Model, whereas  $x_d = 0.75 \pm 0.02$  (see (5.24)). The present lower bound is given as follows [131]:

$$\Delta M_s > 15.0 \text{ ps}^{-1}, \quad x_s > 21.3 \text{ (95\% C.L.)}. \quad (7.2)$$

- There may be a sizeable width difference  $\Delta\Gamma_s/\Gamma_s = \mathcal{O}(-10\%)$  between the mass eigenstates of the  $B_s$  system that is due to CKM-favoured  $b \rightarrow c\bar{c}s$  quark-level transitions into final states common to  $\overline{B}_s^0$  and  $B_s^0$  [125, 199], whereas  $\Delta\Gamma_d$  is negligibly small.<sup>6</sup> The present CDF and LEP average is given as follows [200]:

$$\Delta\Gamma_s/\Gamma_s = -0.16_{-0.13}^{+0.16}, \quad |\Delta\Gamma_s|/\Gamma_s < 0.31 \text{ (95\% C.L.)}. \quad (7.3)$$

Let us next discuss interesting phenomenological implications of the mixing parameters  $\Delta M_s$  and  $\Delta\Gamma_s$  in more detail.

### 7.2 $\Delta M_s$ and Constraints in the $\overline{\rho}\text{--}\overline{\eta}$ Plane

As we have already noted in Subsections 2.6 and 5.3, the mass difference  $\Delta M_d$  plays an important rôle to constrain the apex of the unitarity triangle. In particular, it allows us to fix a circle in the  $\overline{\rho}\text{--}\overline{\eta}$  plane around  $(1, 0)$  with radius  $R_t$  through (5.27). The theoretical cleanliness of this determination of  $R_t$  is limited by the non-perturbative

<sup>5</sup>Operating these machines at the  $\Upsilon(5S)$  resonance would also make  $B_s$ -mesons accessible [198].

<sup>6</sup>Note that  $\Delta\Gamma_s$  is negative in the Standard Model, as can be seen in (5.23).

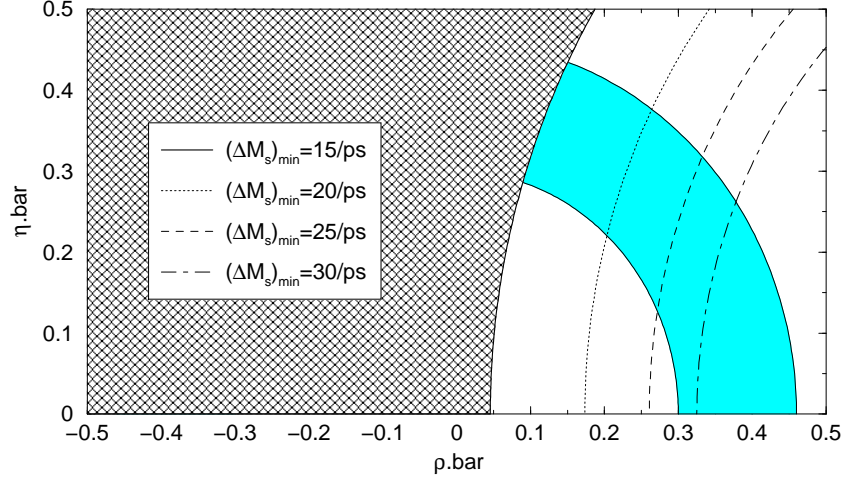


Figure 22: The impact of the upper limit  $(R_t)_{\max}$  on the allowed range in the  $\bar{\rho}-\bar{\eta}$  plane for  $\xi = 1.15$ . The shaded region corresponds to  $R_b = 0.38 \pm 0.08$ .

parameter  $\sqrt{\hat{B}_{B_d}} f_{B_d}$ , with its current range given in (5.7). In view of these uncertainties, it is actually more advantageous to employ

$$\left| \frac{V_{td}}{V_{ts}} \right| = \xi \sqrt{\frac{M_{B_s}}{M_{B_d}}} \sqrt{\frac{\Delta M_d}{\Delta M_s}}. \quad (7.4)$$

Using  $|V_{ts}| = |V_{cb}|$ , which holds up to corrections of  $\mathcal{O}(\lambda^2)$ , we arrive at [8, 13, 46, 47]

$$R_t = 0.83 \times \xi \times \sqrt{\frac{\Delta M_d}{0.50 \text{ ps}^{-1}}} \sqrt{\frac{15.0 \text{ ps}^{-1}}{\Delta M_s}}, \quad (7.5)$$

which is much cleaner than (5.27), since the  $SU(3)$ -breaking parameter

$$\xi \equiv \frac{\sqrt{\hat{B}_{B_s}} f_{B_s}}{\sqrt{\hat{B}_{B_d}} f_{B_d}} = 1.15 \pm 0.06 \quad (7.6)$$

can be obtained with an accuracy that is considerably higher than those of the  $\sqrt{\hat{B}_{B_q}} f_{B_q}$  [38, 127]. Interestingly, the presently available experimental lower bound on  $\Delta M_s$  can be transformed into an upper bound on  $R_t$  [201]. Using  $(\Delta M_d)_{\max} = 0.50 \text{ ps}^{-1}$ , we obtain

$$(R_t)_{\max} = 0.83 \times \xi \times \sqrt{\frac{15.0 \text{ ps}^{-1}}{(\Delta M_s)_{\min}}}. \quad (7.7)$$

In Fig. 22, we show the impact of this relation on the allowed range in the  $\bar{\rho}-\bar{\eta}$  plane. The strong experimental lower bound  $\Delta M_s > 15.0 \text{ ps}^{-1}$  (95% C.L.) excludes already a large part in the  $\bar{\rho}-\bar{\eta}$  plane (crossed region for  $\xi = 1.15$ ), implying in particular  $\gamma < 90^\circ$ .

The present experiments searching for  $B_s^0\text{--}\overline{B}_s^0$  mixing, which give the lower bound (7.2), yield also a local minimum of the log-likelihood function around  $\Delta M_s = 17.7 \text{ ps}^{-1}$ , which is  $2.5\sigma$  away from being zero. The consequences of a possible future measurement of  $\Delta M_s = (17.7 \pm 1.4) \text{ ps}^{-1}$  motivated by this observation were recently studied both within the Standard Model and within supersymmetric models with minimal flavour violation [42]. In this analysis, it was argued that if  $\Delta M_s$  should actually be found in this range, a large class of supersymmetric models would be disfavoured, and of all models considered in [42], the best fit to the data would be obtained for the Standard Model. It is expected that run II of the Tevatron will provide a measurement of  $\Delta M_s$  in the near future.

### 7.3 $\Delta\Gamma_s$ and Untagged Decay Rates

The most appropriate tool to analyse  $\Delta\Gamma_s$  is provided by the heavy-quark expansion, where  $1/m_b$  corrections were determined [202], and next-to-leading order QCD corrections were calculated [203]. In order to predict  $\Delta\Gamma_s$ , certain hadronic matrix elements, parametrized through non-perturbative bag parameters and  $f_{B_s}$ , are required. Recent lattice analyses give

$$-\left(\frac{\Delta\Gamma_s}{\Gamma_s}\right) = \begin{cases} (9.7_{-3.5}^{+1.4} \pm 2.5 \pm 2.0 \pm 1.6)\% & \text{(Hashimoto *et al.* [204])} \\ (4.7 \pm 1.5 \pm 1.6)\% & \text{(Becirevic *et al.* [205]).} \end{cases} \quad (7.8)$$

Although the relevant bag parameters are in rather good agreement in these papers, the results in (7.8) differ since  $\Delta\Gamma_s$  was expressed in [205] using  $\Delta M_d$  as a normalization. The advantage of this approach is that hadronic uncertainties enter only in ratios. On the other hand,  $|V_{ts}/V_{td}|^2$  is required as an input, making the prediction of  $\Delta\Gamma_s$  sensitive to the fits of the unitarity triangle discussed in Subsection 2.6, which depend also on theoretical assumptions and may be affected by new physics. A detailed discussion of the present theoretical status of  $\Delta\Gamma_s$  was recently given in [206], where the result

$$\Delta\Gamma_s/\Gamma_s = -\left(9.3_{-4.6}^{+3.4}\right)\% \quad (7.9)$$

was obtained. The main uncertainties are due to residual scale dependences and  $1/m_b$  corrections. As argued in [206], further improvements appear to be very challenging.

A non-vanishing width difference  $\Delta\Gamma_s$  would allow the extraction of CP-violating weak phases from the following ‘‘untagged’’  $B_s$  rates [197, 207, 208, 209, 210]:

$$\Gamma_s[f(t)] \equiv \Gamma(B_s^0(t) \rightarrow f) + \Gamma(\overline{B}_s^0(t) \rightarrow f). \quad (7.10)$$

If we use (5.25), we obtain

$$\Gamma_s[f(t)] \propto \left[ \left(1 + |\xi_f^{(s)}|^2\right) \left(e^{-\Gamma_L^{(s)}t} + e^{-\Gamma_H^{(s)}t}\right) - 2 \text{Re} \xi_f^{(s)} \left(e^{-\Gamma_L^{(s)}t} - e^{-\Gamma_H^{(s)}t}\right) \right], \quad (7.11)$$

providing the observable  $\mathcal{A}_{\Delta\Gamma}(B_s \rightarrow f)$  introduced in (5.32). Interestingly, the  $\Delta M_s t$  terms appearing in the “tagged” rates  $\Gamma(B_s^0(t) \rightarrow f)$  and  $\Gamma(\overline{B}_s^0(t) \rightarrow f)$  cancel in their “untagged” combination (7.10). Because of the large mixing parameter  $x_s$ , the  $\Delta M_s t$  terms oscillate very rapidly and are hard to resolve. Although it should nevertheless be feasible to keep track of these oscillations, studies of untagged rates are also interesting in terms of efficiency, acceptance and purity. The following channels are particularly promising in the context of extracting weak phases from untagged  $B_s$  data samples:

- $B_s \rightarrow J/\psi\phi$ , allowing us to probe  $\phi_s = -2\delta\gamma$  [208].
- The  $B_s \rightarrow K^{*+}K^{*-}, K^{*0}\overline{K}^{*0}$  system, providing a strategy to extract  $\gamma - 2\delta\gamma$  [208]; bounds implied by  $B_s \rightarrow K^+K^-, K^0\overline{K}^0$  were studied in [209].
- $B_s$  decays caused by  $\bar{b} \rightarrow \bar{u}c\bar{s}$  ( $b \rightarrow c\bar{u}s$ ) quark-level processes [197], for example  $B_s \rightarrow D_s^{*\pm}K^{*\mp}$  or  $B_s \rightarrow D^{*0}\phi$ , allowing also a determination of  $\gamma - 2\delta\gamma$ .

Here  $-2\delta\gamma$  is negligibly small in the Standard Model, as we have noted above. In the case of  $B \rightarrow VV$  decays into two vector mesons, the untagged angular distributions of their decay products have to be considered, which provide many more observables than  $B \rightarrow PP$  modes into two pseudoscalar mesons (for a general discussion of the observables of  $B \rightarrow VV$  decays, see [211]). This feature is exploited in the untagged strategies listed above. Since the  $B_s \rightarrow J/\psi\phi$  mode is of central interest for hadron colliders, we shall come back to this channel in Subsection 7.6.

## 7.4 Impact of New Physics

As we have seen in Subsection 5.5,  $B_d^0\text{--}\overline{B}_d^0$  and  $B_s^0\text{--}\overline{B}_s^0$  mixing may be strongly affected by new physics, since these are highly CKM-suppressed loop-induced fourth order weak interaction processes. In particular – in addition to  $\Delta M_s = 2|M_{12}^{(s)}|$  – also the  $B_s^0\text{--}\overline{B}_s^0$  mixing phase  $\phi_s \sim \arg M_{12}^{(s)}$  may be modified in the presence of new physics as follows:

$$\tan \phi_s^{\text{NP}} \approx \frac{-2\delta\gamma + \varrho_s^2 \sin 2\psi_s}{1 + \varrho_s^2 \cos 2\psi_s} \approx \frac{\varrho_s^2 \sin 2\psi_s}{1 + \varrho_s^2 \cos 2\psi_s}, \quad (7.12)$$

where

$$\varrho_s = \left( \frac{1}{\lambda^2 A} \right) \left( \frac{M_W}{\Lambda} \right). \quad (7.13)$$

For a new-physics scale  $\Lambda$  in the TeV regime,  $\varrho_s$  would be of order one. The impact on  $\Delta M_s$  would affect the determination of  $R_t$  with the help of (7.5), provided new physics enters differently in  $\Delta M_d$ . In contrast to  $B_d^0\text{--}\overline{B}_d^0$  mixing (see (5.50) and (5.51)), the Standard-Model “background”  $\phi_s^{\text{SM}} = -2\delta\gamma = -2\lambda^2\eta$  is negligibly small in (7.12). Consequently, CP-violating effects in  $B_s$  decays represent a very sensitive probe for new

physics [136, 160]. To simplify the following discussion, we shall write from now on generically  $\phi_s$  for the  $B_s^0-\overline{B}_s^0$  mixing phase.

Interestingly, new-physics contributions to  $B_s^0-\overline{B}_s^0$  mixing may also affect the width difference  $\Delta\Gamma_s$  [212]. Using expression (5.21) for  $\Delta\Gamma_s$ , we obtain

$$\Delta\Gamma_s = \Delta\Gamma_s^{\text{SM}} \cos \phi_s, \quad (7.14)$$

which yields a reduction of  $|\Delta\Gamma_s|$  for  $\phi_s \neq 0$  or  $\pi$ . This relation is of course convention-independent, as shown explicitly in [160]. In (7.14), we have employed – as we do throughout this review – the phase convention of the standard and generalized Wolfenstein parametrizations of the CKM matrix, where the phase of  $\Gamma_{12}^{(s)}$  vanishes to an excellent approximation, as  $b \rightarrow c\bar{c}s$  processes play the key rôle for this off-diagonal element of the  $B_s^0-\overline{B}_s^0$  decay matrix.<sup>7</sup> Consequently, we may identify  $\phi_s$  with

$$\arg\left(M_{12}^{(s)}\right) - \arg\left(-\Gamma_{12}^{(s)}\right) = \phi_s - 0, \quad (7.15)$$

which actually enters in (7.14).

In a recent paper [160], various strategies to detect a sizeable phase  $\phi_s$  were proposed, providing “smoking-gun” signals for new-physics contributions to  $B_s^0-\overline{B}_s^0$  mixing. For the untagged case, also a new approach was presented, allowing the determination of  $\phi_s$  from simple measurements of lifetimes and branching ratios. Here no two-exponential fits as in (7.11) are involved, thereby requiring considerably less statistics. Moreover, also methods to determine  $\phi_s$  *unambiguously* were suggested, which play – among other things – an important rôle for the extraction of  $\gamma$  from the strategies discussed in the next subsection. In the corresponding decays, as well as in  $B_s \rightarrow J/\psi\phi$ ,  $B_s^0-\overline{B}_s^0$  mixing represents the preferred mechanism for new physics to manifest itself.

## 7.5 Strategies using Pure Tree Decays of $B_s$ -Mesons

An interesting class of  $B_s$  decays is due to  $\bar{b} \rightarrow \bar{u}c\bar{s}$  ( $b \rightarrow c\bar{u}s$ ) quark-level transitions, providing the  $B_s$  variant of the  $B_d \rightarrow D^{(*)\pm}\pi^\mp$  approach to extract  $\phi_d + \gamma$  discussed in Subsection 6.4. Here we have also to deal with pure “tree” decays, where both  $B_s^0$ - and  $\overline{B}_s^0$ -mesons may decay into the same final state  $f$ . The resulting interference effects between decay and mixing processes allow a *theoretically clean* extraction of  $\phi_s + \gamma$  from

$$\xi_f^{(s)} \times \xi_{\bar{f}}^{(s)} = e^{-2i(\phi_s + \gamma)}. \quad (7.16)$$

An interesting difference to the  $B_d \rightarrow D^{(*)\pm}\pi^\mp$  approach is that both decay paths of  $B_s^0, \overline{B}_s^0 \rightarrow f$  are of the same order in  $\lambda$ , thereby leading to larger interference effects. There are several strategies making use of these features:

---

<sup>7</sup>Since  $\Gamma_{12}^{(s)}$  is governed by CKM-favoured tree-level decays, it is practically insensitive to new physics.



- We may consider the colour-allowed decays  $B_s \rightarrow D_s^\pm K^\mp$  [213], or the colour-suppressed modes  $B_s \rightarrow D^0\phi$  [214]. In these strategies, “tagged” analyses of the corresponding time-dependent rates have to be performed, i.e. the  $\Delta M_s t$  terms have to be resolved. The selection of  $B_s \rightarrow D_s^\pm K^\mp$  transitions is unfortunately experimentally challenging, since  $B_s \rightarrow D_s^\pm \pi^\mp$  events, which come with a 20 times larger branching ratio, have to be rejected [148].
- As we have seen above, in the case of  $B_s \rightarrow D_s^{*\pm} K^{*\mp}$  or  $B_s \rightarrow D^{*0}\phi$ , the observables of the corresponding angular distributions provide sufficient information to extract  $\phi_s + \gamma$  from “untagged” analyses [197], requiring a sizeable  $\Delta\Gamma_s$ . A “tagged” strategy involving  $B_s \rightarrow D_s^{*\pm} K^{*\mp}$  modes was proposed in [215].
- Recently, strategies making use of “CP-tagged”  $B_s$  decays were proposed [216], which require a symmetric  $e^+e^-$  collider operated at the  $\Upsilon(5S)$  resonance. In this approach, initially present CP eigenstates  $B_s^{\text{CP}}$  are employed, which can be tagged through the fact that the  $B_s^0/\overline{B}_s^0$  mixtures have anti-correlated CP eigenvalues at the  $\Upsilon(5S)$  resonance. Here  $B_s \rightarrow D_s^\pm K^\mp, D_s^\pm K^{*\mp}, D_s^{*\pm} K^{*\mp}$  modes may be used.

The extraction of  $\gamma$  from the weak phase  $\phi_s + \gamma$  provided by these approaches requires  $\phi_s$  as an additional input, which is negligibly small in the Standard Model. Whereas it appears to be quite unlikely that the amplitudes of the pure tree decays listed above are affected significantly by new physics, as they involve no flavour-changing neutral-current processes, this is not the case for the  $B_s^0-\overline{B}_s^0$  mixing phase  $\phi_s$ . In order to probe this quantity,  $B_s \rightarrow J/\psi\phi$  transitions offer interesting strategies.

## 7.6 The Golden Mode $B_s \rightarrow J/\psi\phi$

This decay is the  $B_s$  counterpart of  $B_d \rightarrow J/\psi K_S$  and provides interesting strategies to extract  $\Delta M_s$  and  $\Delta\Gamma_s$ , and to probe  $\phi_s$  [158, 160]; experimental feasibility studies for the LHC can be found in [148]. The corresponding Feynman diagrams are analogous to those shown in Fig. 14. Since the final state of  $B_s \rightarrow J/\psi\phi$  is an admixture of different CP eigenstates, we have to use the angular distribution of the  $J/\psi \rightarrow \ell^+\ell^-$  and  $\phi \rightarrow K^+K^-$  decay products to disentangle them [217].

### 7.6.1 Structure of the Angular Distribution

The time-dependent angular distribution of the  $B_s^0 \rightarrow J/\psi[\rightarrow \ell^+\ell^-]\phi[\rightarrow K^+K^-]$  decay products can be written generically as follows [158]:

$$f(\Theta, \Phi, \Psi; t) = \sum_k b^{(k)}(t) g^{(k)}(\Theta, \Phi, \Psi), \quad (7.17)$$

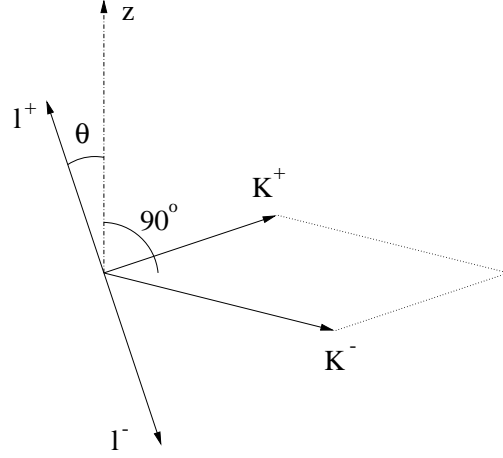


Figure 23: The kinematics of  $B_s^0 \rightarrow J/\psi[\rightarrow \ell^+\ell^-]\phi[\rightarrow K^+K^-]$  in the  $J/\psi$  rest frame.

where we have denoted the angles describing the kinematics of the decay products of  $J/\psi \rightarrow \ell^+\ell^-$  and  $\phi \rightarrow K^+K^-$  by  $\Theta$ ,  $\Phi$  and  $\Psi$ . For instance,  $\Theta$  describes the angle between the direction of the  $\ell^+$  and the  $z$  axis in the  $J/\psi$  rest frame, where the  $z$  axis is defined to be perpendicular to the decay plane of  $\phi \rightarrow K^+K^-$ , as shown in Fig. 23

The functions  $b^{(k)}(t)$  describe the time evolution of the angular distribution (7.17). They can be expressed in terms of real or imaginary parts of the following bilinear combinations of decay amplitudes:

$$A_{\tilde{f}}^*(t)A_f(t) = \langle (J/\psi\phi)_{\tilde{f}} | \mathcal{H}_{\text{eff}} | B_s^0(t) \rangle^* \langle (J/\psi\phi)_f | \mathcal{H}_{\text{eff}} | B_s^0(t) \rangle, \quad (7.18)$$

where  $\mathcal{H}_{\text{eff}}$  is the hermitian conjugate of (3.28) with  $r = s$ , and  $|B_s^0(t)\rangle$  is given by (5.13). The labels  $f$  and  $\tilde{f}$  specify the relative polarization of the  $J/\psi$ - and  $\phi$ -mesons in given final-state configurations  $(J/\psi\phi)_f$  and  $(J/\psi\phi)_{\tilde{f}}$ , respectively. It is convenient to introduce linear polarization amplitudes  $A_0(t)$ ,  $A_{\parallel}(t)$  and  $A_{\perp}(t)$  [218], corresponding to linear polarization states of the vector mesons, which are either longitudinal (0) or transverse to their directions of motion. In the latter case, the polarization states may either be parallel ( $\parallel$ ) or perpendicular ( $\perp$ ) to one another. Whereas  $A_{\perp}(t)$  describes a CP-odd final-state configuration, both  $A_0(t)$  and  $A_{\parallel}(t)$  correspond to CP-even final-state configurations, i.e. to the CP eigenvalues  $-1$  and  $+1$ , respectively. The observables  $b^{(k)}(t)$  are then given by

$$|A_f(t)|^2 \quad \text{with} \quad f \in \{0, \parallel, \perp\}, \quad (7.19)$$

as well as by the interference terms

$$\text{Re}\{A_0^*(t)A_{\parallel}(t)\} \quad \text{and} \quad \text{Im}\{A_f^*(t)A_{\perp}(t)\} \quad \text{with} \quad f \in \{0, \parallel\}. \quad (7.20)$$

### 7.6.2 Structure of the Observables

Applying once more the formalism discussed in Section 5, we find that the time evolution of the  $b^{(k)}(t)$  is governed by

$$\xi_{\psi\phi}^{(s)} \propto e^{-i2\phi_s} \left[ \frac{\lambda_u^{(s)*} \tilde{A}_{\text{pen}}^{ut'} + \lambda_c^{(s)*} (\tilde{A}_{\text{CC}}^{c'} + \tilde{A}_{\text{pen}}^{ct'})}{\lambda_u^{(s)} \tilde{A}_{\text{pen}}^{ut'} + \lambda_c^{(s)} (\tilde{A}_{\text{CC}}^{c'} + \tilde{A}_{\text{pen}}^{ct'})} \right], \quad (7.21)$$

where the amplitudes are analogous to the ones introduced in (6.1); for simplicity, we have suppressed the label  $f$  of the  $(J/\psi\phi)_f$  final-state configuration in this expression. We expect – as in our discussion of the  $B_d \rightarrow J/\psi K_S$  case – that

$$\left| \frac{\lambda_u^{(s)} \tilde{A}_{\text{pen}}^{ut}}{\lambda_c^{(s)} (\tilde{A}_{\text{CC}}^c + \tilde{A}_{\text{pen}}^{ct})} \right| = \mathcal{O}(\bar{\lambda}^3), \quad (7.22)$$

yielding

$$\xi_{\psi\phi}^{(s)} \propto e^{-i\phi_s} [1 - i \sin \gamma \times \mathcal{O}(\bar{\lambda}^3)]. \quad (7.23)$$

Since  $\phi_s = \mathcal{O}(0.03)$  in the Standard Model, there may well be – in contrast to the determination of  $\phi_d$  from  $B_d \rightarrow J/\psi K_S$  – significant hadronic uncertainties in the extraction of  $\phi_s$  from the  $B_s \rightarrow J/\psi[\rightarrow \ell^+\ell^-]\phi[\rightarrow K^+K^-]$  angular distribution. These hadronic uncertainties, which may become an important issue for the LHC, can be controlled with the help of the decay  $B_d \rightarrow J/\psi\rho^0$ , which has also some other interesting features [74].

In the following discussion, we assume

$$\xi_{\psi\phi}^{(s)} \propto e^{-i\phi_s}, \quad (7.24)$$

i.e. that the  $B_s \rightarrow J/\psi\phi$  decay amplitudes do not involve a CP-violating weak phase, which implies vanishing direct CP violation. The general formalism, where this assumption is not made and also penguin effects are taken into account, was presented in [74]. Moreover, we also assume, for simplicity, that new physics does not affect the structure of (7.24), thereby manifesting itself only through a *sizeable* value of  $\phi_s$ . Since the decays  $B_s \rightarrow J/\psi\phi$  and  $B_d \rightarrow J/\psi K_S$  originate from the same quark-level transitions, the general new-physics analysis discussed in Subsection 6.1 allows us to test this assumption already in the  $B \rightarrow J/\psi K$  system.

### 7.6.3 CP Asymmetries and Manifestation of New Physics

An important implication of (7.24) is that  $B_s \rightarrow J/\psi\phi$  exhibits very small CP violation in the Standard Model, making this channel an interesting probe to search for indications of new physics [136, 160]. The quantity  $\sin \phi_s$  governs CP violation in  $B_s \rightarrow J/\psi\phi$ , as can be seen in the following expression:

$$\frac{\Gamma(t) - \bar{\Gamma}(t)}{\Gamma(t) + \bar{\Gamma}(t)} = \left[ \frac{1 - D}{F_+(t) + DF_-(t)} \right] \sin(\Delta M_s t) \sin \phi_s. \quad (7.25)$$

Here  $\Gamma(t)$  and  $\bar{\Gamma}(t)$  denote the time-dependent rates for decays of initially, i.e. at time  $t = 0$ , present  $B_s^0$ - and  $\bar{B}_s^0$ -mesons into  $J/\psi\phi$  final states, respectively,

$$D \equiv \frac{|A_{\perp}(0)|^2}{|A_0(0)|^2 + |A_{\parallel}(0)|^2} = 0.1 \dots 0.5 \quad (7.26)$$

is a hadronic factor, and

$$F_{\pm}(t) \equiv \frac{1}{2} \left[ (1 \pm \cos \phi_s) e^{+\Delta\Gamma_s t/2} + (1 \mp \cos \phi_s) e^{-\Delta\Gamma_s t/2} \right]. \quad (7.27)$$

The range in (7.26) corresponds to factorization [158], and is in good agreement with a recent analysis of the  $B_s \rightarrow J/\psi\phi$  polarization amplitudes  $A_0(0)$ ,  $A_{\parallel}(0)$ ,  $A_{\perp}(0)$  performed by the CDF collaboration [219].

In fact,  $\sin \phi_s$  may be sizeable in extensions of the Standard Model. An example is the symmetrical  $SU_L(2) \times SU_R(2) \times U(1)$  model with spontaneous CP violation (SB-LR) [220]–[222], which was applied to the  $B_s \rightarrow J/\psi\phi$  observables in [223]. In this model,  $\sin \phi_s$  may be as large as  $\mathcal{O}(-40\%)$ . On the other hand, small values of  $a_{\psi K_S}$  are favoured, which are no longer compatible with the recently updated  $B$ -factory results, yielding the average given in (6.10). Another scenario for new physics, where large values of  $\sin \phi_s$  may arise, is provided by models allowing mixing to a new isosinglet down quark, as in  $E_6$  [224]. Let us note that the new-physics contributions to the  $B_s \rightarrow J/\psi\phi$  decay amplitudes are negligible in these and the SB-LR model, as assumed above.

Although the CP asymmetry (7.25) may provide a “smoking-gun” signal for new-physics contributions to  $B_s^0$ - $\bar{B}_s^0$ , mixing, it does not allow a clean determination of  $\sin \phi_s$  because of the hadronic parameter  $D$ . This feature is due to the fact that the  $J/\psi\phi$  final states are admixtures of different CP eigenstates. As we have noted above, in order to solve this problem, an angular analysis of the  $B_s \rightarrow J/\psi[\rightarrow \ell^+\ell^-]\phi[\rightarrow K^+K^-]$  decay products has to be performed. Since the full three-angle distribution is quite complicated,<sup>8</sup> let us consider here the one-angle distribution

$$\frac{d\Gamma(t)}{d\cos\Theta} \propto (|A_0(t)|^2 + |A_{\parallel}(t)|^2) \frac{3}{8} (1 + \cos^2\Theta) + |A_{\perp}(t)|^2 \frac{3}{4} \sin^2\Theta, \quad (7.28)$$

where the kinematics and the definition of the polar angle  $\Theta$  is illustrated in Fig. 23. The one-angle distribution (7.28) allows us now to extract the observables

$$P_+(t) \equiv |A_0(t)|^2 + |A_{\parallel}(t)|^2, \quad P_-(t) \equiv |A_{\perp}(t)|^2, \quad (7.29)$$

as well as their CP conjugates, thereby providing the CP asymmetries

$$\frac{P_{\pm}(t) - \bar{P}_{\pm}(t)}{P_{\pm}(t) + \bar{P}_{\pm}(t)} = \pm \frac{1}{F_{\pm}(t)} \sin(\Delta M_s t) \sin \phi_s. \quad (7.30)$$

<sup>8</sup>It is given in [158], together with appropriate weighting functions to extract the observables.

On the other hand, untagged data samples are sufficient to determine

$$P_{\pm}(t) + \overline{P}_{\pm}(t) \propto \left[ (1 \pm \cos \phi_s) e^{-\Gamma_L^{(s)} t} + (1 \mp \cos \phi_s) e^{-\Gamma_H^{(s)} t} \right]. \quad (7.31)$$

New-physics effects would be indicated by the following features:

- Sizeable values of the CP-violating asymmetries (7.30).
- The untagged observables (7.31) depend on two exponentials.

In contrast to (7.25), these observables do not involve the hadronic parameter  $D$  and allow a clean determination of  $\phi_s$ . A detailed discussion of other strategies to search for new physics with  $B_s$  decays is given in [160], where also the general time-dependent expressions for the observables of the  $B_s \rightarrow J/\psi\phi$  three-angle distribution can be found.

## 7.7 Summary

The  $B_s$ -meson system has several interesting features and offers a nice play ground for  $B$  experiments at hadron machines (Tevatron-II, LHC and BTeV). Already the present experimental lower bound on  $\Delta M_s$  has an important impact on the allowed range for the apex of the unitarity triangle in the  $\overline{\rho}-\overline{\eta}$  plane, implying in particular  $\gamma < 90^\circ$ . It is expected that  $B_s^0-\overline{B}_s^0$  mixing will be observed at the Tevatron in the near future, which would provide much more stringent constraints on the unitarity triangle.

In contrast to the  $B_d$ -meson system, the width difference between the mass eigenstates may be sizeable in the  $B_s$  case, i.e. at the level of 10%. This width difference may allow extractions of CP-violating weak phases from “untagged”  $B_s$  data samples.

Since the  $B_s^0-\overline{B}_s^0$  mixing phase  $\phi_s$  is negligibly small in the Standard Model, CP violation is tiny in  $B_s \rightarrow J/\psi\phi$ , which is the  $B_s$  counterpart of  $B_d \rightarrow J/\psi K_S$ . In addition to strategies to determine the  $B_s^0-\overline{B}_s^0$  mixing parameters, this mode is therefore a very sensitive tool to search for new-physics contributions, allowing in particular an extraction of  $\phi_s$ . Further  $B_s$  benchmark modes are the  $B_s \rightarrow D_s^{(*)\pm} K^{(*)\mp}$  channels, which are pure “tree” decays and offer various strategies to determine the weak phase  $\phi_s + \gamma$ .

In the approaches to explore CP violation we have considered so far, interference effects between  $B_{d,s}^0-\overline{B}_{d,s}^0$  mixing and decay processes played a key rôle to get rid of poorly known hadronic matrix elements, thereby allowing the extraction of CP-violating weak phases. Let us now turn to decays of charged  $B$ -mesons, where amplitude relations have to be used to accomplish this task.

## 8 CP Violation in Charged $B$ Decays

## 8.1 General Remarks

Since there are no mixing effects present in the charged  $B$ -meson system, non-vanishing CP asymmetries of the kind

$$\mathcal{A}_{\text{CP}}(B^+ \rightarrow f) \equiv \frac{\Gamma(B^+ \rightarrow f) - \Gamma(B^- \rightarrow \bar{f})}{\Gamma(B^+ \rightarrow f) + \Gamma(B^- \rightarrow \bar{f})}, \quad (8.1)$$

which correspond to  $\mathcal{A}_{\text{CP}}^{\text{dir}}(B_q \rightarrow f)$  defined in (5.31), would give us immediate and unambiguous evidence for direct CP violation in the  $B$  system. As we have seen in Subsection 4.1, this kind of CP violation has already been established in the neutral kaon system through the measurement of  $\text{Re}(\varepsilon'/\varepsilon) \neq 0$ . Recently, the NA48 collaboration has reported the following CP asymmetry [113]:

$$\frac{\Gamma(K^0 \rightarrow \pi^+\pi^-) - \Gamma(\bar{K}^0 \rightarrow \pi^+\pi^-)}{\Gamma(K^0 \rightarrow \pi^+\pi^-) + \Gamma(\bar{K}^0 \rightarrow \pi^+\pi^-)} = (5.0 \pm 0.9) \times 10^{-6}, \quad (8.2)$$

which is the neutral  $K$ -meson analogue of  $\mathcal{A}_{\text{CP}}^{\text{dir}}(B_q \rightarrow f)$ , and makes direct CP violation in the kaon system more apparent than the observable  $\text{Re}(\varepsilon'/\varepsilon)$ .

Whereas direct CP violation is extremely small in kaon decays, the CP-violating asymmetries (8.1) may be as large as  $\mathcal{O}(30\%)$  in the most fortunate cases, for example in  $B^+ \rightarrow K^+\bar{K}^0$  [73], because of the different CKM structure of the relevant  $B$ -decay amplitudes. These CP asymmetries arise from the interference between amplitudes with different CP-violating weak and CP-conserving strong phases. Due to the unitarity of the CKM matrix, any non-leptonic  $B$ -decay amplitude can be expressed, within the Standard Model, in the following way:

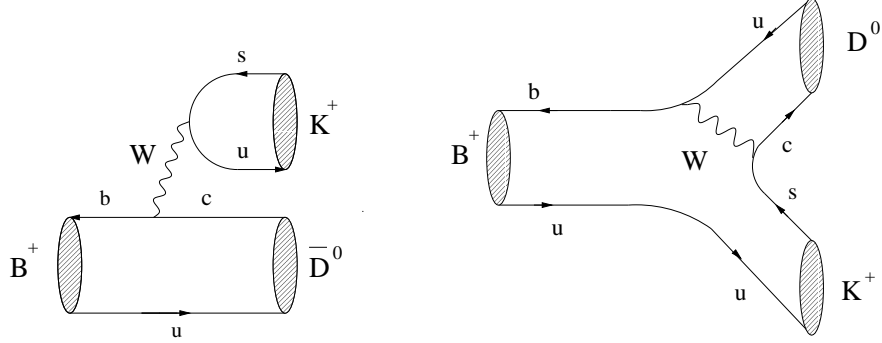
$$A(B^+ \rightarrow f) = |A_1|e^{i\delta_1}e^{+i\varphi_1} + |A_2|e^{i\delta_2}e^{+i\varphi_2} \quad (8.3)$$

$$A(B^- \rightarrow \bar{f}) = |A_1|e^{i\delta_1}e^{-i\varphi_1} + |A_2|e^{i\delta_2}e^{-i\varphi_2}. \quad (8.4)$$

Here the  $\delta_{1,2}$  are CP-conserving strong phases, which are induced by final-state interaction processes, whereas the  $\varphi_{1,2}$  are CP-violating weak phases, which originate from the CKM matrix. Using (8.3) and (8.4), we obtain

$$\mathcal{A}_{\text{CP}}(B^+ \rightarrow f) = \frac{-2|A_1||A_2|\sin(\varphi_1 - \varphi_2)\sin(\delta_1 - \delta_2)}{|A_1|^2 + 2|A_1||A_2|\cos(\varphi_1 - \varphi_2)\cos(\delta_1 - \delta_2) + |A_2|^2}. \quad (8.5)$$

Consequently, a non-vanishing direct CP asymmetry  $\mathcal{A}_{\text{CP}}(B^+ \rightarrow f)$  requires both a non-trivial strong and a non-trivial weak phase difference. In addition to the hadronic amplitudes  $|A_{1,2}|$ , the strong phases  $\delta_{1,2}$  lead to particularly large hadronic uncertainties in (8.5), thereby destroying the clean relation to the CP-violating phase difference  $\varphi_1 - \varphi_2$ , which is usually related to the angle  $\gamma$  of the unitarity triangle.

Figure 24: Feynman diagrams contributing to  $B^+ \rightarrow K^+ \overline{D}^0$  and  $B^+ \rightarrow K^+ D^0$ .

## 8.2 Extracting $\gamma$ from $B^\pm \rightarrow K^\pm D$ Decays

### 8.2.1 Triangle Relations and Experimental Problems

An important tool to eliminate the hadronic uncertainties in charged  $B$  decays is given by amplitude relations. The prototype of this approach, which was proposed by Gronau and Wyler [225], uses  $B^\pm \rightarrow K^\pm D$  decays and allows a *theoretically clean* extraction of the CKM angle  $\gamma$ . The decays  $B^+ \rightarrow K^+ \overline{D}^0$  and  $B^+ \rightarrow K^+ D^0$  are pure “tree” decays, as can be seen in Fig. 24. If we make, in addition, use of the transition  $B^+ \rightarrow D_+^0 K^+$ , where  $D_+^0$  denotes the CP eigenstate of the neutral  $D$ -meson system with eigenvalue +1,

$$|D_+^0\rangle = \frac{1}{\sqrt{2}} (|D^0\rangle + |\overline{D}^0\rangle), \quad (8.6)$$

we obtain

$$\sqrt{2}A(B^+ \rightarrow K^+ D_+^0) = A(B^+ \rightarrow K^+ D^0) + A(B^+ \rightarrow K^+ \overline{D}^0) \quad (8.7)$$

$$\sqrt{2}A(B^- \rightarrow K^- D_+^0) = A(B^- \rightarrow K^- \overline{D}^0) + A(B^- \rightarrow K^- D^0). \quad (8.8)$$

These relations can be represented as two triangles in the complex plane. Since we have only to deal with tree-diagram-like topologies, we obtain moreover

$$A(B^+ \rightarrow K^+ \overline{D}^0) = A(B^- \rightarrow K^- D^0) \quad (8.9)$$

$$A(B^+ \rightarrow K^+ D^0) = A(B^- \rightarrow K^- \overline{D}^0) \times e^{2i\gamma}, \quad (8.10)$$

allowing a clean extraction of  $\gamma$ , as shown in Fig. 25. Unfortunately, these triangles are very squashed, since  $B^+ \rightarrow K^+ D^0$  is colour-suppressed with respect to  $B^+ \rightarrow K^+ \overline{D}^0$ :

$$\tilde{r} \equiv \left| \frac{A(B^+ \rightarrow K^+ D^0)}{A(B^+ \rightarrow K^+ \overline{D}^0)} \right| = \left| \frac{A(B^- \rightarrow K^- \overline{D}^0)}{A(B^- \rightarrow K^- D^0)} \right| \approx \frac{1}{\lambda} \frac{|V_{ub}|}{|V_{cb}|} \times \frac{a_2}{a_1} \approx 0.1, \quad (8.11)$$

where the phenomenological “colour” factors were introduced in Subsection 3.6.

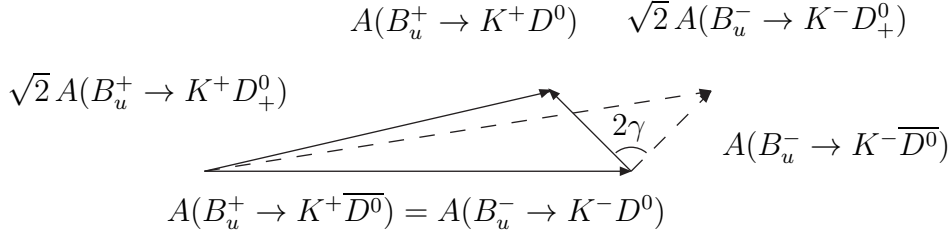


Figure 25: The extraction of  $\gamma$  from  $B_u^\pm \rightarrow K^\pm \{D^0, \overline{D}^0, D^0_+\}$  decays.

In 1998, the CLEO collaboration reported the observation of the colour-allowed decay  $B^+ \rightarrow K^+ \overline{D}^0$  with the following branching ratio [226]:

$$\text{BR}(B^+ \rightarrow K^+ \overline{D}^0) = (0.257 \pm 0.065 \pm 0.032) \times 10^{-3}. \quad (8.12)$$

Meanwhile, this decay has also been seen by Belle [227]. Using (8.11), we expect

$$\text{BR}(B^+ \rightarrow K^+ D^0) \approx 10^{-2} \times \text{BR}(B^+ \rightarrow K^+ \overline{D}^0). \quad (8.13)$$

While  $\text{BR}(B^+ \rightarrow K^+ \overline{D}^0)$  can be determined using conventional methods, the measurement of  $\text{BR}(B^+ \rightarrow K^+ D^0)$  suffers from considerable experimental problems [228]:

- If this colour-suppressed branching ratio is measured through Cabibbo-favoured hadronic decays of the  $D^0$ , e.g. through  $B^+ \rightarrow K^+ D^0 [\rightarrow K^- \pi^+]$ , we obtain large interference effects with the colour-allowed decay chain  $B^+ \rightarrow K^+ \overline{D}^0 [\rightarrow K^- \pi^+]$ , where the  $\overline{D}^0$  decay is doubly Cabibbo-suppressed.
- All possible hadronic tags of the  $D^0$ -meson in  $B^+ \rightarrow K^+ D^0$  will be affected by such interference effects.
- These problems could be circumvented through semi-leptonic tags  $D^0 \rightarrow \ell^+ \nu_\ell X_s$ . However, here we have to deal with large backgrounds due to  $B^+ \rightarrow \ell^+ \nu_\ell X_c$ , which are difficult to control.

Moreover, decays of neutral  $D$ -mesons into CP eigenstates, such as  $D^0_+ \rightarrow \pi^+ \pi^-$  or  $D^0_+ \rightarrow K^+ K^-$ , involve small efficiencies and are experimentally challenging.

### 8.2.2 Alternative Approaches and Constraints on $\gamma$

As we have just seen, the original method proposed by Gronau and Wyler [225] will unfortunately be very difficult in practice. A variant of this approach was proposed by Atwood, Duniety and Soni [228]. In order to overcome the problems listed above, these authors consider the following decay chains:

$$B^+ \rightarrow K^+ \overline{D}^0 [\rightarrow f_i], \quad B^+ \rightarrow K^+ D^0 [\rightarrow f_i], \quad (8.14)$$



where  $f_i$  denotes doubly Cabibbo-suppressed (Cabibbo-favoured) non-CP modes of the  $\overline{D^0}$  ( $D^0$ ), for instance,  $f_i = K^-\pi^+$ ,  $K^-\pi^+\pi^0$ . In order to determine  $\gamma$ , at least two different final states  $f_i$  have to be employed. In this method, one makes use of the large interference effects, which spoil the hadronic tag of the  $D^0$ -meson in the original Gronau–Wyler method. In contrast to the case of  $B^+ \rightarrow K^+ D_\pm^0$  discussed above, here both contributing decay amplitudes should be of comparable size, thereby leading to potentially large CP-violating effects. Furthermore, the difficult to measure branching ratio  $\text{BR}(B^+ \rightarrow K^+ D^0)$  is not required, but can rather be determined as a by-product. Unfortunately, this approach is also challenging, since many channels are involved, with total branching ratios of  $\mathcal{O}(10^{-7})$  or even smaller. An accurate determination of the relevant  $D$ -meson branching ratios  $\text{BR}(D^0 \rightarrow f_i)$  and  $\text{BR}(\overline{D^0} \rightarrow f_i)$  is also essential for this method. For further refinements of this approach, see [229].

The experimental problems related to the measurement of  $\text{BR}(B^+ \rightarrow K^+ D^0)$  were also avoided in [230, 231], where the colour-allowed mode  $B^+ \rightarrow K^+ \overline{D^0}$  and the two CP eigenstates  $|D_\pm^0\rangle$  were considered, providing the observables

$$R_\pm \equiv 2 \left[ \frac{\text{BR}(B^+ \rightarrow K^+ D_\pm^0) + \text{BR}(B^- \rightarrow K^- D_\pm^0)}{\text{BR}(B^+ \rightarrow K^+ \overline{D^0}) + \text{BR}(B^- \rightarrow K^- D^0)} \right] = 1 \pm 2 \tilde{r} \cos \tilde{\delta} \cos \gamma + \tilde{r}^2, \quad (8.15)$$

where  $\tilde{r}$  was introduced in (8.11) and  $\tilde{\delta}$  denotes a strong phase. As in the case of certain CP-averaged  $B \rightarrow \pi K$  branching ratios [232] (see 9.2.2), the ratios in (8.15) imply

$$\sin^2 \gamma \leq \min(R_+, R_-), \quad (8.16)$$

constraining  $\gamma$  in the case of  $\min(R_+, R_-) < 1$ . Moreover, we have

$$R_+ + R_- = 2(1 + \tilde{r}^2), \quad (8.17)$$

allowing in principle the determination of  $\tilde{r}$ , and the CP-violating observables

$$\mathcal{A}_\pm \equiv \frac{\text{BR}(B^+ \rightarrow K^+ D_\pm^0) - \text{BR}(B^- \rightarrow K^- D_\pm^0)}{\text{BR}(B^+ \rightarrow K^+ \overline{D^0}) + \text{BR}(B^- \rightarrow K^- D^0)}, \quad (8.18)$$

which are equal in magnitude and have opposite signs, yielding the combined asymmetry

$$\mathcal{A} \equiv \mathcal{A}_- - \mathcal{A}_+ = 2 \tilde{r} \sin \tilde{\delta} \sin \gamma. \quad (8.19)$$

Consequently, we have three observables at our disposal,  $R_+$ ,  $R_-$  and  $\mathcal{A}$ , allowing the extraction of  $\gamma$ ,  $\tilde{\delta}$  and  $\tilde{r}$ . However, because of  $\tilde{r} \approx 0.1$ , this approach will also be very challenging in practice, in particular the resolution of the  $\tilde{r}^2$  terms in (8.17) and of the CP-violating effects will be very difficult. It is possible to gain the knowledge of  $\gamma$  by using, in addition, isospin-related neutral  $B \rightarrow K^{(*)} D$  decays and neglecting certain

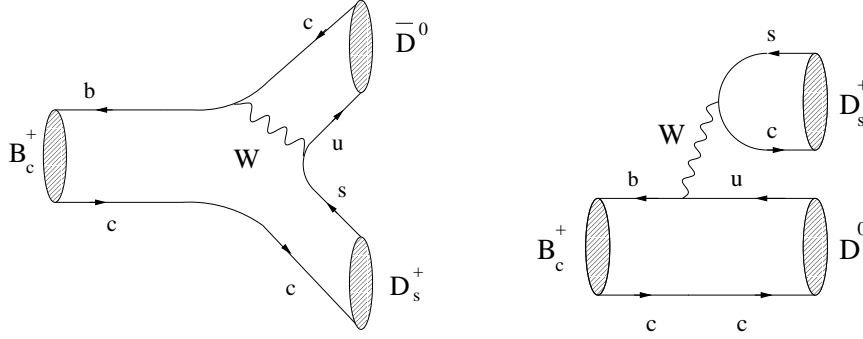


Figure 26: Feynman diagrams contributing to  $B_c^+ \rightarrow D_s^+ \overline{D}^0$  and  $B_c^+ \rightarrow D_s^+ D^0$ .

annihilation topologies [233, 234]. This dynamical assumption can be tested through  $B^+ \rightarrow K^{(*)0} D^+$  modes, requiring branching ratios at the  $10^{-7}$  level or even smaller [233].

Another alternative for the extraction of  $\gamma$  is provided by  $B_d \rightarrow K^{*0} D$  decays [235], where the triangles are more equilateral and the interference effects associated with the hadronic tags of the  $D^0$ -mesons are less pronounced. But all sides are small, i.e. colour-suppressed, so that these decays are also not perfectly suited for the “triangle” approach.

### 8.3 Extracting $\gamma$ from $B_c^\pm \rightarrow D_s^\pm D$ Decays

#### 8.3.1 Ideal Realization of Triangle Relations

The decays  $B_c^\pm \rightarrow D_s^\pm D$  are the  $B_c$ -meson counterparts of the  $B_u^\pm \rightarrow K^\pm D$  modes and allow also an extraction of  $\gamma$  [236], which relies on the amplitude relations

$$\sqrt{2}A(B_c^+ \rightarrow D_s^+ D_+^0) = A(B_c^+ \rightarrow D_s^+ D^0) + A(B_c^+ \rightarrow D_s^+ \overline{D}^0) \quad (8.20)$$

$$\sqrt{2}A(B_c^- \rightarrow D_s^- D_+^0) = A(B_c^- \rightarrow D_s^- \overline{D}^0) + A(B_c^- \rightarrow D_s^- D^0), \quad (8.21)$$

with

$$A(B_c^+ \rightarrow D_s^+ \overline{D}^0) = A(B_c^- \rightarrow D_s^- D^0) \quad (8.22)$$

$$A(B_c^+ \rightarrow D_s^+ D^0) = A(B_c^- \rightarrow D_s^- \overline{D}^0) \times e^{2i\gamma}. \quad (8.23)$$

At first sight, everything is completely analogous to the  $B_u^\pm \rightarrow K^\pm D$  case. However, there is an important difference [237], which becomes obvious by comparing the Feynman diagrams shown in Figs. 24 and 26: in the  $B_c^\pm \rightarrow D_s^\pm D$  system, the amplitude with the rather small CKM matrix element  $V_{ub}$  is not colour suppressed, while the larger element  $V_{cb}$  comes with a colour-suppression factor. Therefore, we obtain

$$\left| \frac{A(B_c^+ \rightarrow D_s^+ D^0)}{A(B_c^+ \rightarrow D_s^+ \overline{D}^0)} \right| = \left| \frac{A(B_c^- \rightarrow D_s^- \overline{D}^0)}{A(B_c^- \rightarrow D_s^- D^0)} \right| \approx \frac{1}{\lambda} \frac{|V_{ub}|}{|V_{cb}|} \times \frac{a_1}{a_2} = \mathcal{O}(1), \quad (8.24)$$

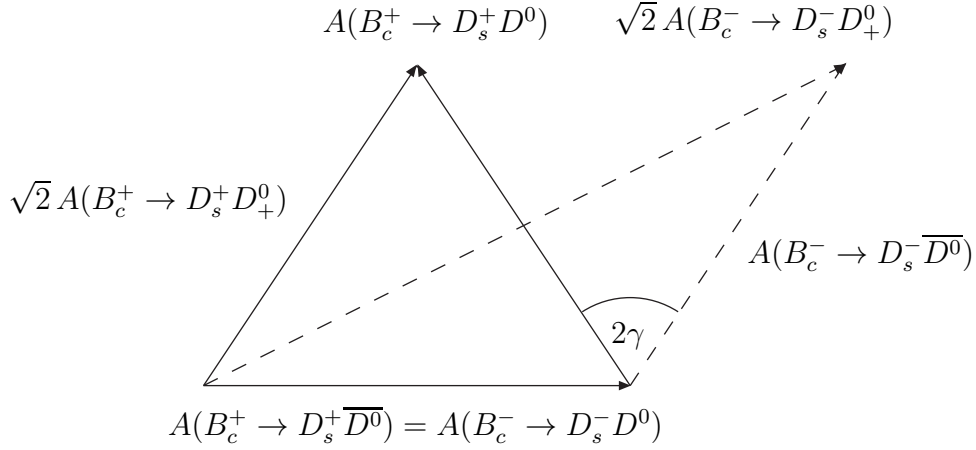


Figure 27: The extraction of  $\gamma$  from  $B_c^\pm \rightarrow D_s^\pm \{D^0, \overline{D^0}, D_+^0\}$  decays.

and conclude that the two amplitudes are similar in size. In contrast to this favourable situation, in the decays  $B_u^\pm \rightarrow K^\pm D$ , the matrix element  $V_{ub}$  comes with the colour-suppression factor, resulting in a very stretched triangle. The extraction of  $\gamma$  from the  $B_c^\pm \rightarrow D_s^\pm D$  triangles is illustrated in Fig. 27, which should be compared with the squashed  $B_u^\pm \rightarrow K^\pm D$  triangles shown in Fig. 25.

### 8.3.2 $U$ -Spin Relations and Experimental Remarks

A situation similar to the  $B_u^\pm \rightarrow K^\pm D$  system arises in  $B_c^\pm \rightarrow D^\pm D$  decays, which are obtained from the  $B_c^\pm \rightarrow D_s^\pm D$  channels by interchanging all down and strange quarks, i.e. through the  $U$ -spin symmetry of strong interactions. These modes satisfy the amplitude relations

$$\sqrt{2}A(B_c^+ \rightarrow D^+ D_+^0) = A(B_c^+ \rightarrow D^+ D^0) + A(B_c^+ \rightarrow D^+ \overline{D^0}) \quad (8.25)$$

$$\sqrt{2}A(B_c^- \rightarrow D^- D_+^0) = A(B_c^- \rightarrow D^- \overline{D^0}) + A(B_c^- \rightarrow D^- D^0), \quad (8.26)$$

as well as

$$A(B_c^+ \rightarrow D^+ \overline{D^0}) = A(B_c^- \rightarrow D^- D^0) \quad (8.27)$$

$$A(B_c^+ \rightarrow D^+ D^0) = e^{i2\gamma} A(B_c^- \rightarrow D^- \overline{D^0}). \quad (8.28)$$

Because of CKM factors different from the  $B_c^\pm \rightarrow D_s^\pm D$  case, we obtain

$$\left| \frac{A(B_c^+ \rightarrow D^+ D^0)}{A(B_c^+ \rightarrow D^+ \overline{D^0})} \right| = \left| \frac{A(B_c^- \rightarrow D^- \overline{D^0})}{A(B_c^- \rightarrow D^- D^0)} \right| \approx \lambda^2 \times \left( \frac{1}{\lambda} \frac{|V_{ub}|}{|V_{cb}|} \times \frac{a_1}{a_2} \right) \lesssim 0.1, \quad (8.29)$$

implying triangles of the same shape as in the  $B_u^\pm \rightarrow K^\pm D$  approach. The decays  $B_d \rightarrow K^{*0} D$  [235], whose amplitudes are all colour suppressed and proportional to  $\lambda^3 R_b$ , have no analogue in the  $B_c$  system.

The  $B_c^\pm \rightarrow D^\pm D$  strategy is obviously affected by interference problems of the same kind as the original Gronau–Wyler approach, i.e. we expect amplitudes of the same order of magnitude for the decay chains  $B_c^+ \rightarrow D^+ D^0 [\rightarrow K^- \pi^+]$  and  $B_c^+ \rightarrow D^+ \overline{D}^0 [\rightarrow K^- \pi^+]$ . In order to extract  $\gamma$ , we could employ the same idea as in [228]. However, in the case of the  $B_c$  system, an alternative is provided by the following  $U$ -spin relations:

$$A(B_c^+ \rightarrow D^+ D^0) = -\lambda/(1 - \lambda^2/2) A(B_c^+ \rightarrow D_s^+ D^0) \quad (8.30)$$

$$A(B_c^+ \rightarrow D^+ \overline{D}^0) = (1 - \lambda^2/2)/\lambda A(B_c^+ \rightarrow D_s^+ \overline{D}^0). \quad (8.31)$$

Since the amplitudes on the right-hand sides of these equations are of the same order of magnitude (see (8.24)), the interference effects due to  $D^0, \overline{D}^0 \rightarrow \pi^\pm K^\mp$  are practically unimportant in their measurement and in the associated  $B_c^\pm \rightarrow D_s^\pm D$  strategy to determine  $\gamma$ . Consequently, this is the preferred  $B_c$  approach to extract  $\gamma$ . Nevertheless, the Cabibbo-enhanced decay  $B_c^+ \rightarrow D^+ \overline{D}^0$  plays an important rôle to increase the statistics for the measurement of the basis of the triangles shown in Fig. 27 with the help of (8.31).

At the LHC, one expects  $\mathcal{O}(10^{10})$  untriggered  $B_c$ -mesons per year of running [238]. Estimates of  $B_c$  branching ratios can already be found in the literature [239], yielding, however, in several cases conflicting results. The following values seem reasonable [237]:

$$\text{BR}(B_c^+ \rightarrow D_s^+ D^0) \approx 10^{-5}, \quad \text{BR}(B_c^+ \rightarrow D_s^+ \overline{D}^0) \approx 10^{-5} - 10^{-6}. \quad (8.32)$$

Moreover, we expect

$$\text{BR}(B_c^+ \rightarrow D^+ \overline{D}^0) \approx 10^{-4} - 10^{-5}, \quad (8.33)$$

allowing the measurement of the  $B_c^+ \rightarrow D_s^+ \overline{D}^0$  branching ratio with the help of (8.31). A very crude feasibility study using (8.32) gives around 20 events per year at the LHC, demonstrating that the  $B_c$  system may well contribute to our understanding of CP violation. More refined experimental feasibility studies of the  $B_c^\pm \rightarrow D_{(s)}^\pm D$  system are strongly encouraged. From a theoretical point of view, it provides an ideal realization of the “triangle” approach to extract  $\gamma$  [237].

## 8.4 Impact of New Physics: $D^0 - \overline{D}^0$ Mixing enters the Stage

Since the charged  $B$  decays considered in the previous two subsections receive only contributions from tree-diagram-like topologies, involving no flavour-changing neutral-current processes, it appears to be quite unlikely that their amplitudes are affected significantly through new-physics contributions. However, we have to keep in mind that  $D^0 - \overline{D}^0$  mixing has been neglected in the corresponding strategies to extract  $\gamma$ . This phenomenon is usually characterized by a CP-violating weak phase  $\theta_D$ , and by

$$x_D \equiv \frac{\Delta M_D}{\Gamma_D}, \quad y_D \equiv \frac{\Delta \Gamma_D}{2\Gamma_D}, \quad (8.34)$$

where  $\Delta M_D$  and  $\Delta\Gamma_D$  denote the mass and width differences of the neutral  $D$ -meson mass eigenstates, respectively, and  $\Gamma_D$  is the average width. These mixing parameters are very small in the Standard Model, typical estimates give values for  $x_D$  and  $y_D$  at the  $10^{-3}$  level. The parameter  $x_D$  is governed by virtual transitions and may hence well be enhanced by one order of magnitude through new physics, whereas this appears to be rather unlikely for  $y_D$ , as this quantity is closely related to  $D$  decay rates, where large new-physics effects are quite unlikely. However,  $y_D$  may be enhanced by certain resonance effects in the Standard Model (for a recent review of these issues, see [19]).

A recent result  $y_D = (3.42 \pm 1.39 \pm 0.74)\%$  from the FOCUS collaboration [240], corresponding to a signal at the  $2\sigma$  level, led already to some excitement [241]. However, this effect has still to be confirmed by other experiments – the results reported in [242, 243] are consistent with zero – and it is crucial to investigate whether such a value could also be accommodated in the Standard Model. Moreover, there is a problem of compatibility between the FOCUS and a recent CLEO result [244], which may point towards a large CP-conserving strong phase difference. The  $B$ -factories will also provide very valuable insights into charm physics [195]; a recent Belle study finds  $y_D = (1.16_{-1.65}^{+1.67})\%$  [245].

Apart from being a powerful tool to search for physics beyond the Standard Model, charm physics is also an important ingredient for  $B^\pm \rightarrow K^\pm D$  strategies to extract  $\gamma$ . The impact of  $D^0-\bar{D}^0$  mixing on these approaches was analysed in [229, 246, 247]. Since we have to deal with interference effects of  $\mathcal{O}(10^{-1})$  in these modes, mixing parameters  $x_D$  and  $y_D$  at the  $10^{-2}$  level may affect the extraction of  $\gamma$  significantly [246, 247]. Strategies to include  $D^0-\bar{D}^0$  mixing in the determination of  $\gamma$  from  $B^\pm \rightarrow K^\pm D$  decays can be found in [229, 247]. Since all amplitudes are of the same order of magnitude in the  $B_c^\pm \rightarrow D_s^\pm D$  approach, the sensitivity to  $D^0-\bar{D}^0$  mixing is considerably smaller in this case, which is another advantage of the  $B_c$  decays.

## 8.5 Summary

Since charged  $B$ -mesons do not exhibit mixing-induced CP violation, we have to search for fortunate decays, where the hadronic uncertainties affecting the extraction of weak phases from direct CP asymmetries can be eliminated through amplitude relations. The prototype of this approach employs  $B_u^\pm \rightarrow K^\pm \{D^0, \bar{D}^0, D_+^0\}$  modes, allowing a clean determination of  $\gamma$  with the help of certain triangle relations, which are due to the CP eigenstate  $D_+^0$  of the neutral  $D$ -meson system. Unfortunately, the corresponding amplitude triangles are very squashed, and further problems related to hadronic tags of the  $D$ -mesons arise; variants of the  $B_u^\pm \rightarrow K^\pm D$  strategy were proposed to deal with these problems. From a theoretical point of view, the triangle approach is realized in an ideal way in the  $B_c^\pm \rightarrow D_s^\pm \{D^0, \bar{D}^0, D_+^0\}$  system, where all amplitudes are of similar size. On the other hand,  $B_c$ -mesons are not as accessible as “ordinary”  $B_u$ - or  $B_d$ -mesons.

Decay Mode	CLEO [172]	BaBar [173]	Belle [174]
$B_d \rightarrow \pi^\mp K^\pm$	$17.2^{+2.5}_{-2.4} \pm 1.2$	$16.7 \pm 1.6 \pm 1.3$	$19.3^{+3.4+1.5}_{-3.2-0.6}$
$B^\pm \rightarrow \pi^0 K^\pm$	$11.6^{+3.0+1.4}_{-2.7-1.3}$	$10.8^{+2.1}_{-1.9} \pm 1.0$	$16.3^{+3.5+1.6}_{-3.3-1.8}$
$B^\pm \rightarrow \pi^\pm K$	$18.2^{+4.6}_{-4.0} \pm 1.6$	$18.2^{+3.3}_{-3.0} \pm 2.0$	$13.7^{+5.7+1.9}_{-4.8-1.8}$
$B_d \rightarrow \pi^0 K$	$14.6^{+5.9+2.4}_{-5.1-3.3}$	$8.2^{+3.1}_{-2.7} \pm 1.2$	$16.0^{+7.2+2.5}_{-5.9-2.7}$
$B_d \rightarrow \pi^+ \pi^-$	$4.3^{+1.6}_{-1.4} \pm 0.5$	$4.1 \pm 1.0 \pm 0.7$	$5.6^{+2.3}_{-2.0} \pm 0.4$
$B^\pm \rightarrow \pi^\pm \pi^0$	$5.6^{+2.6}_{-2.3} \pm 1.7$	$5.1^{+2.0}_{-1.8} \pm 0.8$	$7.8^{+3.8+0.8}_{-3.2-1.2}$
$B_d \rightarrow K^+ K^-$	$< 1.9$ (90% C.L.)	$< 2.5$ (90% C.L.)	$< 2.7$ (90% C.L.)
$B^\pm \rightarrow K^\pm K$	$< 5.1$ (90% C.L.)	$< 2.4$ (90% C.L.)	$< 5.0$ (90% C.L.)

Table 3: CP-averaged  $B \rightarrow \pi K, \pi\pi, KK$  branching ratios in units of  $10^{-6}$ .

The preferred mechanism for new physics to manifest itself in these strategies is  $D^0-\overline{D}^0$  mixing, which may lead to significant effects in the  $B_u^\pm \rightarrow K^\pm D$  approaches. Amplitude relations will also play a key rôle in the following  $B \rightarrow \pi K$  discussion.

## 9 Phenomenology of $B \rightarrow \pi K$ Decays

### 9.1 General Remarks and Experimental Status

The physics potential of  $B \rightarrow \pi K$  modes is very interesting for the  $B$ -factories, as these channels provide promising strategies to probe the angle  $\gamma$  of the unitarity triangle. In contrast to the  $B^\pm \rightarrow K^\pm D$  and  $B_c^\pm \rightarrow D_s^\pm D$  decays discussed in the previous section,  $B \rightarrow \pi K$  transitions are very accessible at these machines, thereby providing experimentally feasible constraints or determinations of  $\gamma$ . On the other hand, the  $B \rightarrow \pi K$  strategies are not theoretically clean, and require flavour-symmetry arguments and certain plausible dynamical assumptions. In 1994, Gronau, Hernández, London and Rosner pointed out in a series of pioneering papers that such a theoretical input allows extractions of weak phases from  $B \rightarrow \pi K, \pi\pi, KK$  modes [248, 249].

The first observation of  $B \rightarrow \pi K$  decays was announced by the CLEO collaboration in 1997 [250], and has triggered a lot of theoretical work. In this context, the bound on  $\gamma$  derived in [232], making use of an approach to determine this angle with the help of the  $B_d^0 \rightarrow \pi^- K^+, B^+ \rightarrow \pi^+ K^0$  system [88], received a lot of attention. Since 1997, the experimental situation has improved considerably due to the efforts by the CLEO, BaBar and Belle collaborations. Now we have not only results available for  $B_d^0 \rightarrow \pi^- K^+$  and  $B^+ \rightarrow \pi^+ K^0$ , but the whole set of  $B \rightarrow \pi K$  decays has been observed. The present status of the measurements of the corresponding CP-averaged branching ratios, which are defined in accordance with (6.43), is summarized in Table 3. Since the  $B \rightarrow \pi K$

Decay Mode	CLEO [251]	BaBar [173]	Belle [252]
$B_d \rightarrow \pi^\mp K^\pm$	$0.04 \pm 0.16$	$0.19 \pm 0.10 \pm 0.03$	$-0.044^{+0.167+0.021}_{-0.186-0.018}$
$B^\pm \rightarrow \pi^0 K^\pm$	$0.29 \pm 0.23$	$0.00 \pm 0.18 \pm 0.04$	$0.059^{+0.196+0.017}_{-0.222-0.055}$
$B^\pm \rightarrow \pi^\pm K$	$-0.18 \pm 0.24$	$0.21 \pm 0.18 \pm 0.03$	$-0.098^{+0.343+0.063}_{-0.430-0.020}$
$B_d \rightarrow \pi^0 K$	n.a.	n.a.	n.a.

Table 4: CP asymmetries  $\mathcal{A}_{\text{CP}}$  as defined in (8.1) for  $B \rightarrow \pi K$  modes.

strategies to probe  $\gamma$  require also some input from the  $B \rightarrow \pi\pi$  system, we have included these modes as well, whereas the decays  $B_d \rightarrow K^+K^-$  and  $B^\pm \rightarrow K^\pm K$  represent sensitive probes for rescattering effects. First analyses of CP-violating asymmetries in  $B \rightarrow \pi K$  modes have also been performed. The corresponding results are listed in Table 4, and do not yet provide signals for direct CP violation.<sup>9</sup> In the future, the experimental situation should continue to improve significantly through the  $B$ -factories.

During the last couple of years, there was of course also theoretical progress. As far as the  $B_d \rightarrow \pi^\mp K^\pm$ ,  $B^\pm \rightarrow \pi^\pm K$  system is concerned, more refined strategies to probe  $\gamma$  were proposed in [253, 254]. Moreover, it was noticed that the charged  $B^\pm \rightarrow \pi^0 K^\pm$ ,  $B^\pm \rightarrow \pi^\pm K$  [255, 256] and neutral  $B_d \rightarrow \pi^\mp K^\pm$ ,  $B_d \rightarrow \pi^0 K$  [87, 257] modes are particularly well suited to extract  $\gamma$ , where in the latter case also mixing-induced CP violation in  $B_d \rightarrow \pi^0 K_S$  can be employed as an additional ingredient. The charged and neutral approaches have certain theoretical advantages and are less sensitive to possible rescattering effects, which can be probed – and even taken into account – through additional data on  $B^\pm \rightarrow K^\pm K$  modes [79, 87, 253, 258, 259, 260, 261].

The philosophy of these strategies is to extract a maximal amount of information, including  $\gamma$  and hadronic parameters, with a “minimal” input from theory, using only flavour-symmetry and plausible dynamical arguments. Concerning the description of the dynamics of  $B \rightarrow \pi K$ ,  $\pi\pi$  decays, important theoretical progress has recently been made through the development of the “QCD factorization” [98]–[100] and the perturbative hard-scattering (or “PQCD”) approaches [101]–[103], allowing the systematic calculation of the relevant hadronic parameters at the leading order of a  $\Lambda_{\text{QCD}}/m_b$ -expansion, and estimates of some of the contributions entering at the next-to-leading order level.

A very detailed analysis was recently performed within the QCD factorization approach in [100], providing valuable insights and allowing a reduction of the  $SU(3)$ -breaking corrections, which affect the strategies to probe  $\gamma$ . Moreover, rescattering processes are found to play a very minor rôle. If one is willing to use a stronger input from QCD factorization, concerning mainly CP-conserving strong phases, more strin-

<sup>9</sup>The CP asymmetry for  $B_d \rightarrow \pi^\mp K^\pm$  obtained by the BaBar Collaboration has recently been updated at the Lepton Photon 01 Conference, with the result  $0.07 \pm 0.08 \pm 0.02$  [176].

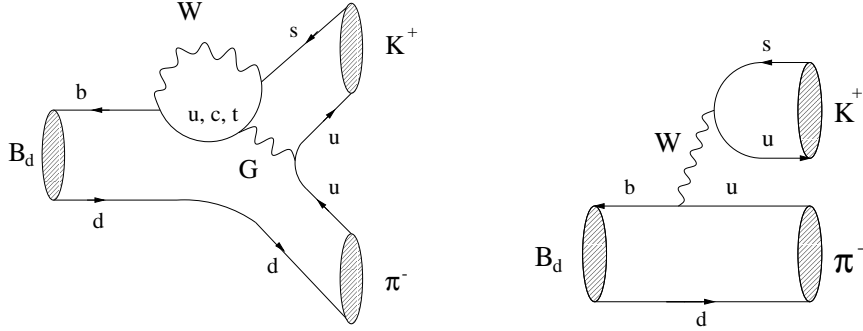


Figure 28: Feynman diagrams contributing to  $B_d^0 \rightarrow \pi^- K^+$ .

gent constraints on  $\gamma$  can be obtained. Exploiting QCD factorization in a maximal way,  $\gamma$  can be determined by fitting simultaneously all calculated CP-averaged  $B \rightarrow \pi K, \pi\pi$  branching ratios to the corresponding experimental results.<sup>10</sup> Here the central question is of course whether power corrections in  $\Lambda_{\text{QCD}}/m_b$  can really be controlled reliably. In a recent paper [77], it was argued that non-perturbative penguin topologies with internal charm- and up-quark exchanges [72, 75] (see Subsection 3.4) may play an important rôle in this context, thereby precluding the extraction of  $\gamma$  from the calculated  $B \rightarrow \pi K, \pi\pi$  branching ratios. Moreover, large CP asymmetries in certain modes are found in this analysis, in contrast to the predictions of QCD factorization.

In this review, we shall focus on the former kind of strategies, using a “minimal” theoretical input. These approaches do not only allow the extraction of  $\gamma$ , but also of strong phases and certain ratios of tree to penguin amplitudes. The hadronic parameters thus determined can then be compared with the theoretical predictions, provided, for example, by the QCD factorization or PQCD approaches.

## 9.2 The $B_d \rightarrow \pi^\mp K^\pm, B^\pm \rightarrow \pi^\pm K$ System

### 9.2.1 Amplitude Structure and Isospin Relations

In order to get more familiar with  $B \rightarrow \pi K$  modes, let us consider the  $B_d \rightarrow \pi^\mp K^\pm, B^\pm \rightarrow \pi^\pm K$  system first [88, 232, 253]. The decay  $B_d^0 \rightarrow \pi^- K^+$  receives contributions both from penguin and from colour-allowed tree-diagram-like topologies, as can be seen in Fig. 28. Within the framework of the Standard Model, we may write

$$A(B_d^0 \rightarrow \pi^- K^+) = -\lambda_u^{(s)} [\tilde{P}_u + \tilde{P}_{\text{ew}}^{(u)\text{C}} + \tilde{T}] - \lambda_c^{(s)} [\tilde{P}_c + \tilde{P}_{\text{ew}}^{(c)\text{C}}] - \lambda_t^{(s)} [\tilde{P}_t + \tilde{P}_{\text{ew}}^{(t)\text{C}}], \quad (9.1)$$

where the overall minus sign is related to the definition of  $SU(3)$  meson states adopted in [248, 249],  $\tilde{P}_q$  and  $\tilde{P}_{\text{ew}}^{(q)\text{C}}$  denote contributions from QCD and EW penguin topologies with

<sup>10</sup>Using “naïve” factorization, such an approach was advocated in [262].



internal  $q$ -quark exchanges ( $q \in \{u, c, t\}$ ), respectively,  $\tilde{\mathcal{T}}$  is due to the colour-allowed  $\bar{b} \rightarrow \bar{u}u\bar{s}$  tree-diagram-like topologies, and the CKM factors  $\lambda_q^{(s)}$  were introduced in (6.2). The label ‘‘C’’ reminds us that only colour-suppressed EW penguin topologies contribute to  $B_d^0 \rightarrow \pi^- K^+$ . Because of the tiny ratio  $|\lambda_u^{(s)}/\lambda_t^{(s)}| \approx 0.02$ , QCD penguins play the dominant rˆole in (9.1), despite their loop suppression. This interesting feature applies to all  $B \rightarrow \pi K$  modes. Consequently, these decays are governed by flavour-changing neutral-current processes and are sensitive probes for new-physics effects [263]–[267].

Performing a similar exercise for the decay  $B^+ \rightarrow \pi^+ K^0$  yields

$$A(B^+ \rightarrow \pi^+ K^0) = \lambda_u^{(s)} [P_u + P_{\text{ew}}^{(u)\text{C}} + \mathcal{A}] + \lambda_c^{(s)} [P_c + P_{\text{ew}}^{(c)\text{C}}] + \lambda_t^{(s)} [P_t + P_{\text{ew}}^{(t)\text{C}}], \quad (9.2)$$

where the notation is as in (9.1), and  $\mathcal{A}$  describes annihilation topologies. If we make use of the unitarity of the CKM matrix to eliminate  $\lambda_t^{(s)}$  and apply the generalized Wolfenstein parametrization (2.17), we obtain

$$A(B^+ \rightarrow \pi^+ K^0) \equiv P_c = - \left(1 - \frac{\lambda^2}{2}\right) \lambda^2 A (1 + \rho_c e^{i\theta_c} e^{i\gamma}) \mathcal{P}_{tc}^c, \quad (9.3)$$

where

$$\mathcal{P}_{tc}^c \equiv |\mathcal{P}_{tc}^c| e^{i\delta_{tc}^c} = P_t - P_c + P_{\text{ew}}^{(t)\text{C}} - P_{\text{ew}}^{(c)\text{C}}, \quad (9.4)$$

and

$$\rho_c e^{i\theta_c} = \left(\frac{\lambda^2}{1 - \lambda^2}\right) R_b \left[1 - \left(\frac{\mathcal{P}_{uc}^c + \mathcal{A}}{\mathcal{P}_{tc}^c}\right)\right]. \quad (9.5)$$

In these expressions,  $\delta_{tc}^c$  and  $\theta_c$  denote CP-conserving strong phases, and  $\mathcal{P}_{uc}^c$  is defined in analogy to (9.4). The quantity  $\rho_c e^{i\theta_c}$ , where the label ‘‘c’’ reminds us that we are dealing with a charged  $B \rightarrow \pi K$  decay, is a measure of the strength of certain rescattering effects, as we will see below. This notation will be useful in Subsection 9.3.

If we apply the  $SU(2)$  isospin symmetry of strong interactions, implying

$$\tilde{P}_c = P_c \quad \text{and} \quad \tilde{P}_t = P_t, \quad (9.6)$$

the QCD penguin topologies with internal top- and charm-quark exchanges contributing to  $B_d^0 \rightarrow \pi^- K^+$  and  $B^+ \rightarrow \pi^+ K^0$  can be related to each other, yielding

$$A(B_d^0 \rightarrow \pi^- K^+) + A(B^+ \rightarrow \pi^+ K^0) = - (T + P_{\text{ew}}^{\text{C}}), \quad (9.7)$$

where

$$P_{\text{ew}}^{\text{C}} = - \left(1 - \frac{\lambda^2}{2}\right) \lambda^2 A \left[ \left\{ \tilde{P}_{\text{ew}}^{(t)\text{C}} - \tilde{P}_{\text{ew}}^{(c)\text{C}} \right\} - \left\{ P_{\text{ew}}^{(t)\text{C}} - P_{\text{ew}}^{(c)\text{C}} \right\} \right] \quad (9.8)$$

is essentially due to EW penguins, and

$$T = \lambda^4 A R_b \left[ \tilde{\mathcal{T}} - \mathcal{A} + \left\{ \tilde{P}_u - P_u \right\} + \left\{ \tilde{P}_{\text{ew}}^{(u)\text{C}} - \tilde{P}_{\text{ew}}^{(t)\text{C}} \right\} - \left\{ P_{\text{ew}}^{(u)\text{C}} - P_{\text{ew}}^{(t)\text{C}} \right\} \right] e^{i\gamma} \quad (9.9)$$

is usually referred to as a “tree” amplitude. However, owing to a subtlety in the implementation of the isospin symmetry,  $T$  does not only receive contributions from colour-allowed tree-diagram-like topologies, but also from penguin and annihilation topologies [79, 253]. Since the amplitudes  $T$  and  $P_{\text{ew}}^{\text{C}}$  have the following phase structure:

$$T \equiv |T|e^{i\delta_T}e^{i\gamma}, \quad P_{\text{ew}}^{\text{C}} \equiv -|P_{\text{ew}}^{\text{C}}|e^{i\delta_{\text{ew}}^{\text{C}}}, \quad (9.10)$$

where  $\delta_T$  and  $\delta_{\text{ew}}^{\text{C}}$  denote CP-conserving strong phases, we obtain

$$A(B_d^0 \rightarrow \pi^- K^+) + A(B^+ \rightarrow \pi^+ K^0) = -\left(e^{i\gamma} - q_{\text{C}}e^{i\omega_{\text{C}}}\right)|T|e^{i\delta_T}, \quad (9.11)$$

with

$$q_{\text{C}} \equiv \left|P_{\text{ew}}^{\text{C}}/T\right| \quad \text{and} \quad \omega_{\text{C}} \equiv \delta_{\text{ew}}^{\text{C}} - \delta_T. \quad (9.12)$$

Relation (9.11) allows us to probe  $\gamma$  through the  $B_d \rightarrow \pi^\mp K^\pm$ ,  $B^\pm \rightarrow \pi^\pm K$  system. As we will see below, the charged  $B^\pm \rightarrow \pi^0 K^\pm$ ,  $B^\pm \rightarrow \pi^\pm K$  and neutral  $B_d \rightarrow \pi^\mp K^\pm$ ,  $B_d \rightarrow \pi^0 K$  modes also satisfy isospin relations of the same structure.

### 9.2.2 A Simple Bound on $\gamma$

Interestingly, already the CP-averaged  $B_d \rightarrow \pi^\mp K^\pm$ ,  $B^\pm \rightarrow \pi^\pm K$  branching ratios may imply interesting constraints on  $\gamma$  [232]. To simplify the discussion, we make the following plausible dynamical assumptions:

- The parameter  $\rho_c e^{i\theta_c} \propto \lambda^2 R_b \approx 0.02$  plays a negligible rôle in (9.3), i.e.

$$A(B^+ \rightarrow \pi^+ K^0) = -|P_c|e^{i\delta_{tc}^{\text{c}}} = A(B^- \rightarrow \pi^- \overline{K^0}). \quad (9.13)$$

- The colour-suppressed EW penguins play also a negligible rôle.

Using isospin relation (9.11), we may then re-write the  $B_d^0 \rightarrow \pi^- K^+$  decay amplitude as follows:

$$A(B_d^0 \rightarrow \pi^- K^+) = |P_c|e^{i\delta_{tc}^{\text{c}}} \left(1 - r e^{i\delta} e^{i\gamma}\right), \quad (9.14)$$

where

$$r \equiv |T/P_c| \quad \text{and} \quad \delta \equiv \delta_T - \delta_{tc}^{\text{c}}. \quad (9.15)$$

Taking into account (9.13), we observe that (9.14) implies amplitude triangles in the complex plane that are analogous to those shown in Fig. 25, allowing an extraction of  $\gamma$  if  $r$  is known [88]. From (9.3), (9.6) and (9.9) we expect

$$r \approx \lambda^2 R_b \left| \tilde{\mathcal{T}} / \tilde{\mathcal{P}}_{tc} \right| = \mathcal{O}(\bar{\lambda}), \quad (9.16)$$

where we have employed once more the generic expansion parameter  $\bar{\lambda}$  introduced in Subsection 6.1. This relation demonstrates nicely the dominance of the QCD penguin topologies in a quantitative way.

Observable	CLEO [172]	BaBar [173]	Belle [174]
$R$	$1.00 \pm 0.30$	$0.97 \pm 0.23$	$1.50 \pm 0.66$
$R_c$	$1.27 \pm 0.47$	$1.19 \pm 0.35$	$2.38 \pm 1.12$
$R_n$	$0.59 \pm 0.27$	$1.02 \pm 0.40$	$0.60 \pm 0.29$

Table 5: Ratios of CP-averaged  $B \rightarrow \pi K$  branching ratios as defined in (9.19), (9.54) and (9.59). For the evaluation of  $R$ , we have used  $\tau_{B^+}/\tau_{B_d^0} = 1.060 \pm 0.029$ .

In order to probe  $\gamma$ , we consider the CP-averaged decay amplitude

$$\langle |A(B_d \rightarrow \pi^\mp K^\pm)|^2 \rangle = |P_c|^2 (1 - 2r \cos \delta \cos \gamma + r^2), \quad (9.17)$$

where the overall normalization can be fixed through

$$\langle |A(B^\pm \rightarrow \pi^\pm K)|^2 \rangle = |P_c|^2. \quad (9.18)$$

Finally, we arrive at the simple expression

$$R \equiv \frac{\text{BR}(B_d^0 \rightarrow \pi^- K^+) + \text{BR}(\overline{B}_d^0 \rightarrow \pi^+ K^-)}{\text{BR}(B^+ \rightarrow \pi^+ K^0) + \text{BR}(B^- \rightarrow \pi^- \overline{K}^0)} \frac{\tau_{B^+}}{\tau_{B_d^0}} = 1 - 2r \cos \delta \cos \gamma + r^2. \quad (9.19)$$

If we take a very conservative point of view, the hadronic quantities  $\delta$  and  $r$  are unknown parameters. Let us, therefore, treat them as free parameters, which yields the following minimal value for  $R$ :

$$R_{\min|\delta,r} = \sin^2 \gamma \leq R, \quad (9.20)$$

implying the allowed range [232]

$$0^\circ \leq \gamma \leq \gamma_0 \quad \vee \quad 180^\circ - \gamma_0 \leq \gamma \leq 180^\circ, \quad (9.21)$$

with

$$\gamma_0 = \arccos(\sqrt{1 - R}). \quad (9.22)$$

This constraint on  $\gamma$  is only effective if  $R$  is found to be smaller than one. In 1997, when CLEO reported the first result on the CP-averaged  $B_d \rightarrow \pi^\mp K^\pm$ ,  $B^\pm \rightarrow \pi^\pm K$  branching ratios, the result was  $R = 0.65 \pm 0.40$ . The central value  $R = 0.65$  would imply  $\gamma_0 = 54^\circ$  [232], thereby excluding a large range in the  $\overline{\rho}-\overline{\eta}$  plane [44]. The present experimental status of  $R$  is summarized in Table 5, where  $R_c$  and  $R_n$  are the counterparts of  $R$  in the charged and neutral  $B \rightarrow \pi K$  systems, respectively, which will be discussed in Subsection 9.3. Unfortunately, the present experimental uncertainties are still too large to draw any conclusions and to decide whether  $R < 1$ . The experimental situation should, however, improve significantly in the next couple of years.

### 9.2.3 Impact of Rescattering Processes

An important limitation of the theoretical accuracy of the  $B_d \rightarrow \pi^\mp K^\pm$ ,  $B^\pm \rightarrow \pi^\pm K$  strategies to probe  $\gamma$  is due to rescattering effects, which may affect the two dynamical assumptions made in 9.2.2. In particular, we expect naively from (9.5) that

$$\rho_c e^{i\theta_c} = \mathcal{O}(\bar{\lambda}^2), \quad (9.23)$$

and conclude that this parameter should play a negligible rôle in  $B^+ \rightarrow \pi^+ K^0$ . Moreover, this channel should hence exhibit tiny CP violation at the few percent level. These expectations, and the smallness of the colour-suppressed EW penguins, may in principle be affected by very large rescattering effects [78, 79].

As we have seen in Subsection 3.4, there are basically two different kinds of rescattering processes, originating from  $\bar{b} \rightarrow \bar{c}c\bar{s}$  and  $\bar{b} \rightarrow \bar{u}u\bar{s}$  quark-level transitions. In the case of the  $B^+ \rightarrow \pi^+ K^0$  mode, we have to deal with  $B^+ \rightarrow \{\bar{D}^0 D_s^+, \dots\} \rightarrow \pi^+ K^0$  and  $B^+ \rightarrow \{\pi^0 K^+, \dots\} \rightarrow \pi^+ K^0$  rescattering processes. Similar contributions arise also in the  $B_d^0 \rightarrow \pi^- K^+$  channel. The former kind of rescattering effects can be considered as penguin topologies with internal charm-quark exchanges (see Fig. 11), and is included in the amplitudes  $\tilde{P}_c$  and  $P_c$  in (9.1) and (9.2), respectively. These processes may contribute significantly to the  $B_d \rightarrow \pi^\mp K^\pm$ ,  $B^\pm \rightarrow \pi^\pm K$  branching ratios. However, as  $P_c$  appears both in the numerator and in the denominator in (9.5), the parameter  $\rho_c e^{i\theta_c}$  is unlikely to be enhanced significantly from the  $\bar{\lambda}^2$  level by this kind of rescattering. On the other hand, the latter kind of rescattering processes is related to penguin topologies with internal up-quark exchanges and annihilation topologies (for analogous processes, see Figs. 16 and 17), affecting  $\tilde{P}_u$ ,  $P_u$  and  $\mathcal{A}$ . Whereas these amplitudes play a minor rôle for the branching ratios, they affect the parameter  $\rho_c e^{i\theta_c}$ . In the presence of dramatic rescattering processes of this kind, i.e. of

$$B^+ \rightarrow \{\pi^0 K^+, \pi^0 K^{*+}, \dots\} \rightarrow \pi^+ K^0, \quad (9.24)$$

the parameter  $\rho_c$  may be enhanced to the  $\bar{\lambda}$  level:

$$\rho_c e^{i\theta_c} \Big|_{\text{res.}} = \mathcal{O}(\bar{\lambda}), \quad (9.25)$$

thereby implying CP-violating asymmetries in  $B^\pm \rightarrow \pi^\pm K$  of  $\mathcal{O}(10\%)$ . In several of the analyses listed in [78], assuming elastic rescattering as a toy model or making use of Regge phenomenology, such an enhancement was actually found.

Fortunately, we may also obtain experimental insights into these issues. In this respect, the decay  $B^+ \rightarrow K^+ \bar{K}^0$ , which is related to  $B^+ \rightarrow \pi^+ K^0$  by interchanging all down and strange quarks, i.e. through the  $U$ -spin flavour symmetry of strong interactions, plays a key rôle [79, 253, 258, 259]. Using a notation similar to that in (9.3) yields

$$A(B^+ \rightarrow K^+ \bar{K}^0) = \lambda^3 A \left[ 1 - \left( \frac{1 - \lambda^2}{\lambda^2} \right) \rho^{(d)} e^{i\theta^{(d)}} e^{i\gamma} \right] \mathcal{P}_{tc}^{(d)}, \quad (9.26)$$

where  $\rho^{(d)} e^{i\theta^{(d)}}$  corresponds to  $\rho_c e^{i\theta_c}$  given in (9.5). Since this parameter enters – in contrast to (9.3) – with  $1/\lambda^2$  in the  $B^+ \rightarrow K^+ \overline{K}^0$  amplitude, the corresponding branching ratio and CP asymmetry represent a very sensitive probe for an enhancement of  $\rho^{(d)}$  through rescattering processes. The  $U$ -spin symmetry of strong interactions implies

$$\rho^{(d)} = \rho_c, \quad \theta^{(d)} = \theta_c, \quad (9.27)$$

allowing us to determine  $\rho_c$  and  $\theta_c$  as functions of  $\gamma$  through the observables of the  $B^\pm \rightarrow \pi^\pm K$ ,  $B^\pm \rightarrow K^\pm K$  system [253, 259]. Moreover, we obtain the following relation between the corresponding CP asymmetries and CP-averaged branching ratios:

$$\frac{\mathcal{A}_{\text{CP}}(B^+ \rightarrow \pi^+ K^0)}{\mathcal{A}_{\text{CP}}(B^+ \rightarrow K^+ \overline{K}^0)} = -R_{SU(3)}^2 \left[ \frac{\text{BR}(B^\pm \rightarrow K^\pm K)}{\text{BR}(B^\pm \rightarrow \pi^\pm K)} \right], \quad (9.28)$$

where  $R_{SU(3)}$  describes  $SU(3)$  breaking, with

$$R_{SU(3)} \Big|_{\text{fact}} = \left[ \frac{M_B^2 - M_\pi^2}{M_B^2 - M_K^2} \right] \left[ \frac{F_{B\pi}(M_K^2; 0^+)}{F_{BK}(M_K^2; 0^+)} \right]. \quad (9.29)$$

Here the form factors  $F_{B\pi}(M_K^2; 0^+)$  and  $F_{BK}(M_K^2; 0^+)$  parametrize the quark–current matrix elements  $\langle \pi | (\overline{b}d)_{V-A} | B \rangle$  and  $\langle K | (\overline{b}s)_{V-A} | B \rangle$ , respectively. Using the model of Bauer, Stech and Wirbel (BSW) [89] yields  $R_{SU(3)} = \mathcal{O}(0.7)$ .

The presently available upper bounds on the CP-averaged  $B^\pm \rightarrow K^\pm K$  branching ratio imply already interesting upper bounds on  $\rho_c$ . To this end, we employ the  $U$ -spin relations in (9.27), and consider the quantity [257]

$$K \equiv \left[ \frac{1}{\epsilon R_{SU(3)}^2} \right] \left[ \frac{\text{BR}(B^\pm \rightarrow \pi^\pm K)}{\text{BR}(B^\pm \rightarrow K^\pm K)} \right] = \frac{1 + 2\rho_c \cos\theta_c \cos\gamma + \rho_c^2}{\epsilon^2 - 2\epsilon\rho_c \cos\theta_c \cos\gamma + \rho_c^2}, \quad (9.30)$$

where  $\epsilon \equiv \lambda^2/(1 - \lambda^2)$ . The expression on the right-hand side implies the following allowed range for  $\rho_c$  (for detailed discussions, see [175, 275] and 10.3.5):

$$\frac{1 - \epsilon\sqrt{K}}{1 + \sqrt{K}} \leq \rho_c \leq \frac{1 + \epsilon\sqrt{K}}{|1 - \sqrt{K}|}. \quad (9.31)$$

The present CLEO data give  $\text{BR}(B^\pm \rightarrow K^\pm K)/\text{BR}(B^\pm \rightarrow \pi^\pm K) < 0.3$  (90% C.L.) [172]. Using (9.31), this upper bound implies  $\rho_c < 0.15$  for  $R_{SU(3)} = 0.7$ , and is not in favour of dramatic rescattering effects, although the bound on  $\rho_c$  is still one order of magnitude above the naïve  $\mathcal{O}(\overline{\lambda}^2)$  expectation.<sup>11</sup> Rescattering effects can also be probed through  $B_d \rightarrow K^+ K^-$  modes [260], which also do not seem to show an anomalous enhancement.

<sup>11</sup>If we assume  $\text{BR}(B^\pm \rightarrow K^\pm K)/\text{BR}(B^\pm \rightarrow \pi^\pm K) < 0.15$ , as indicated by the BaBar bound on  $\text{BR}(B^\pm \rightarrow K^\pm K)$  in Table 3, we obtain  $\rho_c < 0.12$ .

The second dynamical assumption in 9.2.2 was related to the colour-suppressed EW penguins. Using the expressions for the corresponding four-quark operators (see (3.31)), neglecting  $Q_7^s$  and  $Q_8^s$  because of their tiny Wilson coefficients, and performing appropriate Fierz transformations, we may write [87, 253] (see also [88])

$$q_C e^{i\omega_C} = \frac{3}{2\lambda^2 R_b} \left[ \frac{C'_1(\mu)C_{10}(\mu) - C'_2(\mu)C_9(\mu)}{C_2^2(\mu) - C_1^{\prime 2}(\mu)} \right] a_C e^{i\omega_C}, \quad (9.32)$$

where

$$C'_1(\mu) \equiv C_1(\mu) + \frac{3}{2} C_9(\mu), \quad C'_2(\mu) \equiv C_2(\mu) + \frac{3}{2} C_{10}(\mu), \quad (9.33)$$

and

$$a_C e^{i\omega_C} \equiv \frac{a_2^{\text{eff}}}{a_1^{\text{eff}}} = \frac{C'_1(\mu) \zeta(\mu) + C'_2(\mu)}{C'_1(\mu) + C'_2(\mu) \zeta(\mu)} \quad (9.34)$$

with

$$\zeta(\mu) \equiv \frac{\langle K^0 \pi^+ | Q_2^u(\mu) | B^+ \rangle + \langle K^+ \pi^- | Q_2^u(\mu) | B_d^0 \rangle}{\langle K^0 \pi^+ | Q_1^u(\mu) | B^+ \rangle + \langle K^+ \pi^- | Q_1^u(\mu) | B_d^0 \rangle} \quad (9.35)$$

denotes a hadronic parameter, representing a measure of ‘‘colour suppression’’ in the  $B_d \rightarrow \pi^\mp K^\pm$ ,  $B^\pm \rightarrow \pi^\pm K$  system. The combination of Wilson coefficients in (9.32) is essentially renormalization-scale independent and changes only by  $\mathcal{O}(1\%)$  when evolving from  $\mu = M_W$  down to  $\mu = m_b$ . Using the leading-order coefficients in Table 2 for  $\Lambda_{\overline{\text{MS}}}^{(5)} = 225$  MeV yields

$$q_C = 0.71 \times \left[ \frac{0.38}{R_b} \right] \times a_C. \quad (9.36)$$

It is plausible to assume that  $a_C$  is associated with a suppression of  $\mathcal{O}(\bar{\lambda})$ , thereby yielding

$$q_C = \mathcal{O}(\bar{\lambda}). \quad (9.37)$$

Note that this implies  $|P_{\text{ew}}^C/P| = \mathcal{O}(\bar{\lambda}^2)$  because of  $r = \mathcal{O}(\bar{\lambda})$ . Consequently, EW penguins contribute at the same level to the  $B_d \rightarrow \pi^\mp K^\pm$ ,  $B^\pm \rightarrow \pi^\pm K$  amplitudes as the parameter  $\rho_c e^{i\theta_c}$ . In the presence of dramatic rescattering processes of the kind given in (9.24), the dynamical suppression in (9.37) would no longer be effective, i.e.

$$q_C|_{\text{res.}} = \mathcal{O}(1), \quad (9.38)$$

yielding contributions to the decay amplitudes at the  $\bar{\lambda}$  level. The parameter  $r$  would be of  $\mathcal{O}(\bar{\lambda})$  also in the presence of large rescattering effects, although its value may be affected significantly.

Consequently, in the case of large rescattering effects mediated by  $\bar{b} \rightarrow \bar{u}u\bar{s}$  quark-level processes, both assumptions made in 9.2.2 would no longer hold. As we have noted above, the present experimental upper bounds on  $B \rightarrow KK$  modes are not pointing

towards such a picture. Moreover, it is disfavoured theoretically by the QCD factorization approach, where the predictions for the relevant parameters read as follows [100]:<sup>12</sup>

$$\rho_c = \begin{cases} (2.0 \pm 0.1 \pm 0.4) \times 10^{-2} \\ (1.9 \pm 0.1 \pm 0.4) \times 10^{-2}, \end{cases} \quad \theta_c = \begin{cases} (13.6 \pm 4.4)^\circ \\ (16.6 \pm 5.2)^\circ \end{cases} \quad (9.39)$$

$$q_C = \begin{cases} (8.3 \pm 4.5 \mp 1.7) \times 10^{-2} \\ (8.9 \pm 4.9 \mp 1.8) \times 10^{-2}, \end{cases} \quad \omega_C = \begin{cases} (-60.2 \pm 49.5)^\circ \\ (-54.2 \pm 44.2)^\circ. \end{cases} \quad (9.40)$$

In particular, it is found that the bound in (9.20) is violated through these parameters by at most 1.5%, and only in the region  $72^\circ < \gamma < 86^\circ$ . This analysis suggests that these effects can be safely neglected until  $R$  is measured with an accuracy better than 10%.

#### 9.2.4 More Refined Strategies to Probe $\gamma$

In addition to the ratio  $R$  of CP-averaged branching ratios, also the ‘‘pseudo-asymmetry’’

$$A_0 \equiv \left[ \frac{\text{BR}(B_d^0 \rightarrow \pi^- K^+) - \text{BR}(\overline{B}_d^0 \rightarrow \pi^+ K^-)}{\text{BR}(B^+ \rightarrow \pi^+ K^0) + \text{BR}(B^- \rightarrow \pi^- \overline{K}^0)} \right] \frac{\tau_{B^+}}{\tau_{B_d^0}} = \mathcal{A}_{\text{CP}}(B_d^0 \rightarrow \pi^- K^+) R \quad (9.41)$$

plays an important rôle in the probing of  $\gamma$  [254]. In order to derive parametrizations for  $R$  and  $A_0$ , it is useful to introduce the following generalization of  $r$ :

$$r \equiv \frac{|T|}{\sqrt{\langle |A(B^\pm \rightarrow \pi^\pm K)|^2 \rangle}}, \quad (9.42)$$

which reduces to (9.15) for  $\rho_c = 0$ . Using (9.3) and isospin relation (9.7), the observables can be expressed in terms of  $\gamma$  and the hadronic parameters  $r$ ,  $\delta$ ,  $q_C$ ,  $\omega_C$ ,  $\rho_c$ ,  $\theta_c$ . With the help of the corresponding parametrizations, which are given in [253], we may now proceed as in 9.2.2. If we treat both  $\delta$  and  $r$  as unknown quantities, we arrive at [253]

$$R_{\min}|_{\delta,r} = \left[ \frac{1 + 2 q_C \rho_c \cos(\theta_c + \omega_C) + q_C^2 \rho_c^2}{(1 - 2 q_C \cos \omega_C \cos \gamma + q_C^2) (1 + 2 \rho_c \cos \theta_c \cos \gamma + \rho_c^2)} \right] \sin^2 \gamma, \quad (9.43)$$

representing the generalization of (9.20). On the other hand, if we make also use of the asymmetry  $A_0$ , contours in the  $\gamma$ - $r$  plane can be determined, which provide stronger constraints on  $\gamma$ . The sensitivity on  $\rho_c e^{i\theta_c}$  and  $q_C e^{i\omega_C}$  was studied in great detail in [253]. It should be emphasized that the former parameter can be taken into account in (9.43) and the contours in the  $\gamma$ - $r$  plane through the  $B^\pm \rightarrow K^\pm K$  observables. As we have seen above, they can be combined with those of  $B^\pm \rightarrow \pi^\pm K$  through the  $U$ -spin symmetry, thereby allowing us to determine  $\rho_c$  and  $\theta_c$  as functions of  $\gamma$  [253, 259].

<sup>12</sup>The first errors are the sums of all theoretical errors added in quadrature, whereas the second errors are due to  $R_b$ ; the second lines show the results without certain weak annihilation contributions.

If the parameter  $r$ , i.e. the magnitude of the “tree” amplitude  $T$ , can be determined, we are in a position to extract  $\gamma$  and the strong phase  $\delta$ . At this stage, a certain model dependence enters. An approximate way to fix this amplitude is to neglect the colour-suppressed CC operator contributions to  $B^+ \rightarrow \pi^+\pi^0$ , and to use the  $SU(3)$  flavour symmetry to relate the colour-allowed CC amplitude of that decay to  $T$ , yielding [88]

$$r \approx \sqrt{2} \lambda \frac{f_K}{f_\pi} \sqrt{\frac{\text{BR}(B^\pm \rightarrow \pi^\pm \pi^0)}{\text{BR}(B^\pm \rightarrow \pi^\pm K)}}. \quad (9.44)$$

Using this expression, the experimental results in Table 3 imply  $r \approx 0.2$ . Another approach is provided by “naïve” factorization:

$$|T|_{\text{fact}} = \frac{G_F}{\sqrt{2}} \lambda |V_{ub}| a_1 (M_{B_d}^2 - M_\pi^2) f_K F_{B\pi}(M_K^2; 0^+). \quad (9.45)$$

The BSW model [89] and QCD sum rules [268] give  $F_{B\pi}(M_K^2; 0^+) = 0.3$ , leading to

$$|T|_{\text{fact}} = a_1 \times \left[ \frac{|V_{ub}|}{3.2 \times 10^{-3}} \right] \times 7.8 \times 10^{-9} \text{ GeV}. \quad (9.46)$$

As noted in [254], also analyses of semi-leptonic  $B_d^0 \rightarrow \pi^- \ell^+ \nu_\ell$  decays may be very useful to fix  $|T|$  through arguments based on factorization. Using (9.46), we obtain [232]

$$r|_{\text{fact}} = 0.18 \times a_1 \times \left[ \frac{|V_{ub}|}{3.2 \times 10^{-3}} \right] \sqrt{\left[ \frac{1.8 \times 10^{-5}}{\text{BR}(B^\pm \rightarrow \pi^\pm K)} \right] \times \left[ \frac{\tau_{B_u}}{1.6 \text{ ps}} \right]}. \quad (9.47)$$

The most refined theoretical analysis employing QCD factorization gives [100]

$$\bar{r} \equiv u_c r = \begin{cases} (20.6 \pm 3.5 \pm 4.1) \times 10^{-2} \\ (22.0 \pm 3.6 \pm 4.4) \times 10^{-2}, \end{cases} \quad \delta = \begin{cases} (-5.7 \pm 4.4)^\circ \\ (-6.2 \pm 4.6)^\circ, \end{cases} \quad (9.48)$$

where

$$u_c = \sqrt{1 + 2 \rho_c \cos \theta_c \cos \gamma + \rho_c^2}. \quad (9.49)$$

Since  $\rho_c$  is very small in the QCD factorization approach (see (9.39)),  $\bar{r}$  and  $r$  take very similar values, which are also consistent with the other approaches to fix  $r$ . We shall come back to the determination of  $r$  in Subsection 10.4, using  $B_s \rightarrow \pi^\pm K^\mp$  modes.

An advantage of the  $B_d \rightarrow \pi^\mp K^\pm$ ,  $B^\pm \rightarrow \pi^\pm K$  strategies to probe  $\gamma$  is that the corresponding decays do not involve neutral pions and are hence also very accessible at hadron machines, in particular at the LHC. There one expects measurements of  $R$  and  $A_0$  with uncertainties at the 3% level [148]. On the other hand, this approach suffers from the theoretical disadvantage that  $r$  requires some additional input and that the treatment of EW penguins is based on colour-suppression arguments. Moreover,  $r$  may in principle be affected by rescattering processes of the kind given in (9.24), which may also enhance the EW penguin contributions. The charged and neutral  $B \rightarrow \pi K$  systems have interesting theoretical advantages in this respect.



### 9.3 The Charged and Neutral $B \rightarrow \pi K$ Systems

In 1994, Gronau, Rosner and London proposed an  $SU(3)$  strategy to determine  $\gamma$  with the help of the charged decays  $B^\pm \rightarrow \pi^\pm K$ ,  $\pi^0 K^\pm$ ,  $\pi^0 \pi^\pm$  [248]. However, as was pointed out by Deshpande and He [84], this elegant approach is spoiled by EW penguins [85], which play an important rôle because of the large top-quark mass [63]. In 1998, the Gronau–Rosner–London strategy was resurrected by Neubert and Rosner [255], who showed that the EW penguin contributions can be controlled in this case theoretically with the help of the general expressions for the corresponding four-quark operators, appropriate Fierz transformations, and the  $SU(3)$  flavour symmetry of strong interactions (see also [88]). The neutral  $B \rightarrow \pi K$  system is completely analogous in this respect, providing, however, an additional observable, if  $B_d \rightarrow \pi^0 K_S$  modes are considered [87].

#### 9.3.1 Parametrization of Decay Amplitudes and Observables

The starting point of our discussion is the following isospin relation:

$$\begin{aligned} \sqrt{2} A(B^+ \rightarrow \pi^0 K^+) + A(B^+ \rightarrow \pi^+ K^0) &= \sqrt{2} A(B_d^0 \rightarrow \pi^0 K^0) + A(B_d^0 \rightarrow \pi^- K^+) \\ &= -[(T + C) + P_{\text{ew}}] \equiv 3 A_{3/2}, \end{aligned} \quad (9.50)$$

where the combination  $(T + C)$  originates from colour-allowed and colour-suppressed  $\bar{b} \rightarrow \bar{u}u\bar{s}$  tree-diagram-like topologies,  $P_{\text{ew}}$  is due to colour-allowed and colour-suppressed EW penguin contributions, and  $A_{3/2}$  reminds us that there is only an  $I = 3/2$  isospin component in (9.50). In the Standard Model, these amplitudes can be parametrized as

$$T + C \equiv |T + C| e^{i\delta_{T+C}} e^{i\gamma}, \quad P_{\text{ew}} \equiv -|P_{\text{ew}}| e^{i\delta_{\text{ew}}}, \quad (9.51)$$

where  $\delta_{T+C}$  and  $\delta_{\text{ew}}$  denote CP-conserving strong phases. Consequently, we may write

$$\begin{aligned} \sqrt{2} A(B^+ \rightarrow \pi^0 K^+) + A(B^+ \rightarrow \pi^+ K^0) &= \sqrt{2} A(B_d^0 \rightarrow \pi^0 K^0) + A(B_d^0 \rightarrow \pi^- K^+) \\ &= -\left(e^{i\gamma} - qe^{i\omega}\right) |T + C| e^{i\delta_{T+C}}, \end{aligned} \quad (9.52)$$

with

$$q \equiv |P_{\text{ew}}/(T + C)| \quad \text{and} \quad \omega \equiv \delta_{\text{ew}} - \delta_{T+C}. \quad (9.53)$$

Let us focus on the charged  $B \rightarrow \pi K$  system first. Since (9.52) has the same phase structure as the  $B_d^0 \rightarrow \pi^- K^+$ ,  $B^+ \rightarrow \pi^+ K^0$  isospin relation (9.11), we have just to replace  $A(B_d^0 \rightarrow \pi^- K^+)$  by  $\sqrt{2}A(B^+ \rightarrow \pi^0 K^+)$ , where the factor of  $\sqrt{2}$  is related to the wavefunction of the neutral pion. The observables corresponding to  $R$  and  $A_0$ , which were introduced in (9.19) and (9.41), respectively, are hence given as follows:

$$R_c \equiv 2 \left[ \frac{\text{BR}(B^+ \rightarrow \pi^0 K^+) + \text{BR}(B^- \rightarrow \pi^0 K^-)}{\text{BR}(B^+ \rightarrow \pi^+ K^0) + \text{BR}(B^- \rightarrow \pi^- \bar{K}^0)} \right] \quad (9.54)$$

$$A_0^c = 2 \left[ \frac{\text{BR}(B^+ \rightarrow \pi^0 K^+) - \text{BR}(B^- \rightarrow \pi^0 K^-)}{\text{BR}(B^+ \rightarrow \pi^+ K^0) + \text{BR}(B^- \rightarrow \pi^- \bar{K}^0)} \right] = \mathcal{A}_{\text{CP}}(B^+ \rightarrow \pi^0 K^+) R_c. \quad (9.55)$$

Completely general parametrizations for  $R_c$  and  $A_c^0$  can be obtained with the help of the formalism discussed in 9.2.4 by just making the following replacements [87]:<sup>13</sup>

$$r \rightarrow r_c \equiv \frac{|T + C|}{\sqrt{\langle |P_c|^2 \rangle}}, \quad \delta \rightarrow \delta_c \equiv \delta_{T+C} - \delta_{tc}^c, \quad q_C \rightarrow q, \quad \omega_C \rightarrow \omega. \quad (9.56)$$

Since the parameters  $\rho_c$  and  $\theta_c$  are related to the charged mode  $B^+ \rightarrow \pi^+ K^0$ , they do not have to be replaced. These substitutions can of course also be performed in (9.43), yielding then the expression for  $R_{\min}^c|_{\delta_c, r_c}$ .

In the case of the neutral  $B \rightarrow \pi K$  system,  $\sqrt{2}A(B_d^0 \rightarrow \pi^0 K^0)$  takes the rôle of  $A(B^+ \rightarrow \pi^+ K^0)$ . In analogy to (9.3), we may write

$$\sqrt{2}A(B_d^0 \rightarrow \pi^0 K^0) \equiv P_n = - \left(1 - \frac{\lambda^2}{2}\right) \lambda^2 A \left(1 + \rho_n e^{i\theta_n} e^{i\gamma}\right) \mathcal{P}_{tc}^n, \quad (9.57)$$

where

$$\rho_n e^{i\theta_n} = \left(\frac{\lambda^2}{1 - \lambda^2}\right) R_b \left[1 - \left(\frac{\mathcal{P}_{uc}^n - \mathcal{C}}{\mathcal{P}_{tc}^n}\right)\right]. \quad (9.58)$$

Here  $\mathcal{C}$  is due to colour-suppressed tree-diagram-like topologies. The neutral  $B \rightarrow \pi K$  observables corresponding to  $R$  and  $A_0$  are therefore given by

$$R_n \equiv \frac{1}{2} \left[ \frac{\text{BR}(B_d^0 \rightarrow \pi^- K^+) + \text{BR}(\overline{B}_d^0 \rightarrow \pi^+ K^-)}{\text{BR}(B_d^0 \rightarrow \pi^0 K^0) + \text{BR}(\overline{B}_d^0 \rightarrow \pi^0 \overline{K}^0)} \right] \quad (9.59)$$

$$A_0^n = \frac{1}{2} \left[ \frac{\text{BR}(B_d^0 \rightarrow \pi^- K^+) - \text{BR}(\overline{B}_d^0 \rightarrow \pi^+ K^-)}{\text{BR}(B_d^0 \rightarrow \pi^0 K^0) + \text{BR}(\overline{B}_d^0 \rightarrow \pi^0 \overline{K}^0)} \right] = \mathcal{A}_{\text{CP}}(B_d^0 \rightarrow \pi^- K^+) R_n. \quad (9.60)$$

As in the charged  $B \rightarrow \pi K$  case, general parametrizations of these quantities can be obtained straightforwardly from the expressions for the  $B_d \rightarrow \pi^\mp K^\pm$ ,  $B^\pm \rightarrow \pi^\pm K$  observables derived in [253] by performing appropriate substitutions [87]:

$$r \rightarrow r_n \equiv \frac{|T + C|}{\sqrt{\langle |P_n|^2 \rangle}}, \quad \delta \rightarrow \delta_n \equiv \delta_{T+C} - \delta_{tc}^n, \quad q_C \rightarrow q, \quad \omega_C \rightarrow \omega. \quad (9.61)$$

Moreover, the parameters of the  $B^+ \rightarrow \pi^+ K^0$  mode have to be replaced as follows:

$$\rho_c \rightarrow \rho_n, \quad \theta_c \rightarrow \theta_n. \quad (9.62)$$

### 9.3.2 Theoretical Advantages

The theoretical advantages of the charged and neutral  $B \rightarrow \pi K$  systems to probe  $\gamma$  are related to the following two features:

<sup>13</sup>For an alternative parametrization, see [256].

- The amplitude  $T + C$  can be fixed through the  $B^+ \rightarrow \pi^+\pi^0$  decay with the help of the  $SU(3)$  flavour symmetry of strong interactions [248]:

$$T + C = -\sqrt{2} \frac{V_{us}}{V_{ud}} \frac{f_K}{f_\pi} A(B^+ \rightarrow \pi^+\pi^0), \quad (9.63)$$

where the ratio  $f_K/f_\pi = 1.2$  of the kaon and pion decay constants takes into account factorizable  $SU(3)$ -breaking corrections. This relation allows us to determine the parameters  $r_c$  and  $r_n$ .

- Performing similar tricks as in the derivation of (9.32), the EW penguin parameter  $qe^{i\omega}$  can be fixed through the  $SU(3)$  flavour symmetry [255] (see also [87, 88]):

$$qe^{i\omega} = \frac{3}{2\lambda^2 R_b} \left[ \frac{C'_1(\mu)C_{10}(\mu) - C'_2(\mu)C_9(\mu)}{C_2'^2(\mu) - C_1'^2(\mu)} \right] = 0.71 \times \left[ \frac{0.38}{R_b} \right]. \quad (9.64)$$

In contrast to (9.32), this expression does *not* involve a hadronic parameter. Taking into account factorizable  $SU(3)$  breaking, the central value of 0.71 is shifted to 0.68. Expression (9.64) has also a counterpart in the  $B \rightarrow \pi\pi$  system (see (6.103)), which is based on the  $SU(2)$  isospin symmetry and allows us to take into account the EW penguin effects in the  $B \rightarrow \pi\pi$  triangle approach to extract  $\alpha$  [87, 178].

It should be emphasized that (9.63) and (9.64) are consequences of the  $SU(3)$  flavour symmetry. Therefore, these relations cannot be affected by rescattering effects. In the formalism discussed above, such processes may only manifest themselves through anomalously large parameters  $\rho_c e^{i\theta_c}$  and  $\rho_n e^{i\theta_n}$ , which are naïvely expected at the  $\bar{\lambda}^2$  level. Using additional experimental information provided by  $B^\pm \rightarrow K^\pm K$  modes, the parameter  $\rho_c e^{i\theta_c}$  can be taken into account through the  $U$ -spin symmetry, as we have seen in 9.2.3. In the case of the neutral  $B \rightarrow \pi K$  strategy, we have an additional observable  $\mathcal{A}_{\text{CP}}^{\text{mix}}(B_d \rightarrow \pi^0 K_S)$  at our disposal, allowing us to take into account the parameter  $\rho_n e^{i\theta_n}$  in an exact manner, i.e. without making use of flavour-symmetry arguments [87]. A sizeable value of  $\rho_n e^{i\theta_n}$  would be signalled both by a violation of the relation [88]

$$\mathcal{A}_{\text{CP}}^{\text{mix}}(B_d \rightarrow \pi^0 K_S) = \mathcal{A}_{\text{CP}}^{\text{mix}}(B_d \rightarrow J/\psi K_S), \quad (9.65)$$

and by large direct CP violation in the  $B_d \rightarrow \pi^0 K_S$  channel.

### 9.3.3 Strategies to Probe $\gamma$

If the observables  $R_c$ ,  $A_0^c$  and  $R_n$ ,  $A_0^n$  are measured,  $\gamma$  and the strong phases  $\delta_c$  and  $\delta_n$  can be extracted from the charged and neutral  $B \rightarrow \pi K$  decays in a similar manner as discussed in 9.2.4. Looking at Tables 4 and 5, it becomes obvious that this approach cannot yet be performed in practice. In particular, CP violation in  $B^\pm \rightarrow \pi^0 K^\pm$  and

Parameter	CLEO [172]	BaBar [173]	Belle [174]
$r_c$	$0.21 \pm 0.06$	$0.21 \pm 0.05$	$0.30 \pm 0.09$
$r_n$	$0.17 \pm 0.06$	$0.21 \pm 0.06$	$0.19 \pm 0.12$

Table 6: Present experimental results for  $r_c$  and  $r_n$ .

$B_d \rightarrow \pi^\mp K^\pm$  has not yet been observed. However, non-trivial bounds on  $\gamma$  may already be obtained from the ratios  $R_{c,n}$  of the CP-averaged decay rates.

The most simple constraints on  $\gamma$  arise from expression (9.43) for  $R_{\min}|_{\delta,r}$ , if we perform the replacements of variables specified above. In the derivation of this minimal value for  $R$ , both  $\delta$  and  $r$  were treated as free variables. However, in the case of the charged and neutral  $B \rightarrow \pi K$  decays, the parameters  $r_{c,n}$  can be fixed with the help of the  $SU(3)$  flavour symmetry through  $B^\pm \rightarrow \pi^\pm \pi^0$  decays. Using the experimental results listed in Table 3 and adding the uncertainties in quadrature gives the numbers summarized in Table 6. Consequently, it is actually more appropriate to treat only  $\delta_{c,n}$  as an ‘‘unknown’’ hadronic parameter, thereby varying it within the range  $[0, 2\pi]$ . This procedure yields the following extremal, i.e. minimal and maximal, values for  $R_{c,n}$  [87]:

$$R_{c,n}^{\text{ext}}|_{\delta_{c,n}} = 1 \pm 2 \frac{r_{c,n}}{u_{c,n}} \sqrt{h_{c,n}^2 + k_{c,n}^2} + v^2 r_{c,n}^2, \quad (9.66)$$

where

$$h_{c,n} = \cos \gamma + \rho_{c,n} \cos \theta_{c,n} - q [\cos \omega + \rho_{c,n} \cos(\theta_{c,n} - \omega) \cos \gamma] \quad (9.67)$$

$$k_{c,n} = \rho_{c,n} \sin \theta_{c,n} + q [\sin \omega - \rho_{c,n} \sin(\theta_{c,n} - \omega) \cos \gamma] \quad (9.68)$$

$$v = \sqrt{1 - 2q \cos \omega \cos \gamma + q^2}, \quad (9.69)$$

and  $u_c$  was already introduced in (9.49). If  $r$  is fixed through an additional theoretical input and the corresponding straightforward replacements of variables are performed, these general formulae apply of course also to the  $B_d \rightarrow \pi^\mp K^\pm$   $B^\pm \rightarrow \pi^\pm K$  system. The rather complicated expressions simplify considerably, if we assume that  $\rho_c$  and  $\rho_n$  are negligibly small, and take into account that (9.64) implies  $\omega = 0$ .

Let us now illustrate the corresponding bounds on  $\gamma$  in more detail [257]. The present experimental status of  $R_{(c,n)}$  is summarized in Table 5. We observe that both the CLEO and the Belle data point towards  $R_c > 1$  and  $R_n < 1$ , whereas the central values of the BaBar collaboration are close to one, with a small preference of  $R_c > 1$ . In Fig. 29, we show the dependence of the extremal values of  $R_n$  on  $\gamma$ , using the formulae given above. Here the crossed region below the  $R_{\min}$  curve is *excluded*. As in the case of the bound in (9.20), this feature can only be transformed into constraints on  $\gamma$  if  $R_n$  is found to be smaller than one. Interestingly, the present data from the CLEO and Belle collaborations

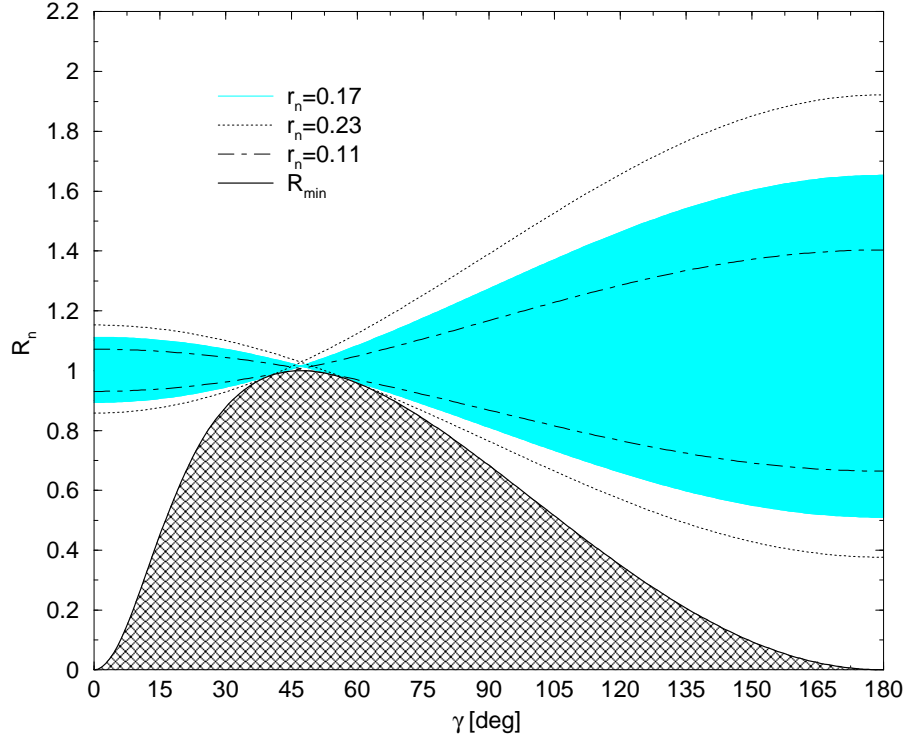


Figure 29: The dependence of the extremal values of  $R_n$  (neutral  $B \rightarrow \pi K$  system) described by (9.43) and (9.66) on the CKM angle  $\gamma$  for  $qe^{i\omega} = 0.68$  and  $\rho_n = 0$ .

may actually indicate that  $R_n < 1$ , although the uncertainties are still too large to draw any definite conclusions on this exciting possibility. Both measurements agree very well, having the same central value  $R_n = 0.6$ . If we consider this number as an example, the  $R_{\min}$  curve in Fig. 29 implies the allowed range  $0^\circ \leq \gamma \leq 19^\circ \vee 97^\circ \leq \gamma \leq 180^\circ$ . If we use additional information on the parameter  $r_n$ , we may put even stronger constraints on  $\gamma$ . For  $r_n = 0.17$ , the *allowed* range (9.66) for  $R_n$  is described by the shaded region in Fig. 29, implying  $134^\circ \leq \gamma \leq 180^\circ$  for  $R_n = 0.6$ .

The curves for the charged  $B \rightarrow \pi K$  system are very similar to the ones shown in Fig. 29. The only difference arises in the contours related to  $R_c^{\text{ext}}|_{\delta_c}$ , since  $r_c$  is expected to be slightly different from  $r_n$ . If  $R_c$  should be found to be larger than one, as favoured by the present  $B$ -factory data, the  $R_{\min}^c|_{\delta_c, r_c}$  curve would not be effective, and the parameter  $r_c$  has to be fixed in order to constrain  $\gamma$ . If we take the central values of the present CLEO data to illustrate this bound,  $r_c = 0.21$  and  $R_c = 1.3$ , we obtain  $84^\circ \leq \gamma \leq 180^\circ$ .

The allowed ranges for  $\gamma$  arising in these examples would be of great phenomenological interest, as they are complementary to the range implied by the usual indirect fits of the unitarity triangle discussed in Subsection 2.6. In particular, as the second quadrant for  $\gamma$  would be favoured, there would be essentially no overlap between these ranges,

which could be interpreted as a manifestation of new physics [257]. Other arguments for  $\cos \gamma < 0$  using  $B \rightarrow PP$ ,  $PV$  and  $VV$  decays were given in [175, 269] (see also 10.3.5). The central values of the Belle collaboration,  $R_c = 2.4$  and  $r_c = 0.3$ , would be an even more striking signal for new physics, as all values of  $\gamma$  would be excluded.<sup>14</sup> However, the large experimental uncertainties do not yet allow us to draw definite conclusions.

Before we can speculate on physics beyond the Standard Model, it is of course crucial to explore the hadronic uncertainties. For the formalism discussed above, this was done in [87]; within a different framework, similar considerations were made in [256]. The theoretical accuracy of the bounds on  $\gamma$  arising from the charged and neutral  $B \rightarrow \pi K$  systems is limited both by non-factorizable  $SU(3)$ -breaking corrections and by rescattering processes. The former may affect the determination of the parameters  $qe^{i\omega}$  and  $r_{c,n}$ , whereas the latter may lead to sizeable values of  $\rho_{c,n}$ .

As we will discuss in the next subsection, the QCD factorization approach provides valuable insights into the  $SU(3)$ -breaking corrections, thereby allowing a reduction of the corresponding uncertainties [100]. Although the parameters  $\rho_{c,n}e^{i\theta_{c,n}}$  are of  $\mathcal{O}(\bar{\lambda}^2)$  in this framework, it should be emphasized that they can be taken into account through additional data, as we have noted above. In order to illustrate their impact on the bounds on  $\gamma$ , let us take  $\rho_n = 0.05$  and  $\theta_n \in \{0^\circ, 180^\circ\}$ . For the example given above, we obtain then the allowed ranges  $0^\circ \leq \gamma \leq (19 \pm 1)^\circ \vee (97 \pm 4)^\circ \leq \gamma \leq 180^\circ$ , and  $(134 \pm 2)^\circ \leq \gamma \leq 180^\circ$ . The feature that the uncertainty due to  $\rho_n$  is larger in the case of  $R_{\min}^n|_{\delta_n, r_n}$  can be understood easily by performing an expansion of (9.43) and (9.66) in powers of  $\rho_n$ , and neglecting second-order terms of  $\mathcal{O}(\rho_n^2)$ ,  $\mathcal{O}(r_n \rho_n)$  and  $\mathcal{O}(r_n^2)$ :

$$R_{\min}^n|_{\delta_n, r_n}^{\text{L.O.}} = \left[ \frac{1 + 2 \rho_n \cos \theta_n (q - \cos \gamma)}{1 - 2 q \cos \gamma + q^2} \right] \sin^2 \gamma \quad (9.70)$$

$$R_n^{\text{ext}}|_{\delta_n}^{\text{L.O.}} = 1 \pm 2 r_n |\cos \gamma - q|. \quad (9.71)$$

Here we have moreover made use of (9.64), which gives  $\omega = 0$ . Interestingly, as was noted for the charged  $B \rightarrow \pi K$  system in [255], there are no terms of  $\mathcal{O}(\rho_n)$  present in (9.71), in contrast to (9.70). Consequently, the bounds on  $\gamma$  related to (9.43) are affected more strongly by  $\rho_n$  than those implied by (9.66).

### 9.3.4 Constraints in the $\bar{\rho}$ - $\bar{\eta}$ Plane

In addition to the theoretical uncertainties due to non-factorizable  $SU(3)$ -breaking corrections and rescattering effects, another uncertainty of the constraints on  $\gamma$  is related to the CKM factor  $R_b$ , which arises in the expression (9.64) for the EW penguin parameter  $qe^{i\omega}$ . Because of this feature, it is actually more appropriate to consider constraints in

<sup>14</sup>For slightly smaller  $R_c$  or larger  $r_c$ , only values of  $\gamma$  close to  $180^\circ$  would be allowed.

the  $\bar{\rho}-\bar{\eta}$  plane instead of the bounds on  $\gamma$  [257, 270]. A similar “trick” was also employed for  $B_d \rightarrow \pi^+\pi^-$  decays in [182], and recently for the  $B \rightarrow \pi K$  system in [100].

The constraints in the  $\bar{\rho}-\bar{\eta}$  plane can be obtained straightforwardly from (9.43) and (9.66). In the former case, we obtain [257]

$$\cos \gamma = R_{c,n} q \pm \sqrt{(1 - R_{c,n})(1 - R_{c,n} q^2)}, \quad (9.72)$$

whereas we have in the latter case

$$\cos \gamma = \frac{1 - R_{c,n} \pm 2 q r_{c,n} + (1 + q^2) r_{c,n}^2}{2 r_{c,n} (q r_{c,n} \pm 1)}. \quad (9.73)$$

In these expressions, we have assumed, for simplicity,  $\rho_{c,n} = 0$  and  $\omega = 0$ . The right-hand sides of these formulae depend implicitly on the CKM factor  $R_b$  through the EW penguin parameter  $q e^{i\omega}$ , which is given by (9.64). In order to get rid of  $R_b$ , we consider contours in the  $\bar{\rho}-\bar{\eta}$  plane. They can be obtained with the help of (9.72) and (9.73) by taking into account (see Fig. 3 (a))

$$\bar{\rho} = R_b \cos \gamma, \quad \bar{\eta} = R_b \sin \gamma, \quad (9.74)$$

and are illustrated in Figs. 30 and 31 for the neutral  $B \rightarrow \pi K$  examples given in 9.3.3. The corresponding allowed ranges in the  $\bar{\rho}-\bar{\eta}$  plane should be compared with the situation in Fig. 22, excluding essentially the whole second quadrant.

### 9.3.5 Bounds on Strong Phases

The general expressions for  $R_{c,n}$  allow us to determine  $\cos \delta_{c,n}$  as functions of  $\gamma$  [257]:

$$\begin{aligned} \cos \delta_{c,n} = & \frac{1}{h_{c,n}^2 + k_{c,n}^2} \left[ \frac{(1 - R_{c,n} + v^2 r_{c,n}^2) u_{c,n} h_{c,n}}{2 r_{c,n}} \right. \\ & \left. \pm k_{c,n} \sqrt{h_{c,n}^2 + k_{c,n}^2 - \left[ \frac{(1 - R_{c,n} + v^2 r_{c,n}^2) u_{c,n}}{2 r_{c,n}} \right]^2} \right]. \end{aligned} \quad (9.75)$$

Taking into account that  $|\cos \delta_{c,n}| \leq 1$ , we obtain again the allowed range for  $\gamma$  related to (9.66). In addition, there arise also constraints on the strong phases  $\delta_{c,n}$ . In the case of  $R_n = 0.6$  and  $r_n = 0.17$ , we obtain  $-1 \leq \cos \delta_n \leq -0.84$ , whereas  $R_c = 1.3$  and  $r_c = 0.21$  would imply  $+0.25 \leq \cos \delta_c \leq +1$ .

As can be seen in (9.56) and (9.61), we have  $\delta_n - \delta_c = \delta_{tc}^c - \delta_{tc}^n$ , where  $\delta_{tc}^c$  and  $\delta_{tc}^n$  are the strong phases of the amplitudes  $\mathcal{P}_{tc}^c$  and  $\mathcal{P}_{tc}^n$ , which describe the differences of the penguin topologies with internal top- and charm-quark exchanges contributing to  $B^+ \rightarrow \pi^+ K^0$  and  $B_d^0 \rightarrow \pi^0 K^0$ , respectively. These topologies consist of QCD and EW penguins, where the latter contribute to  $B^+ \rightarrow \pi^+ K^0$  only in colour-suppressed form. In

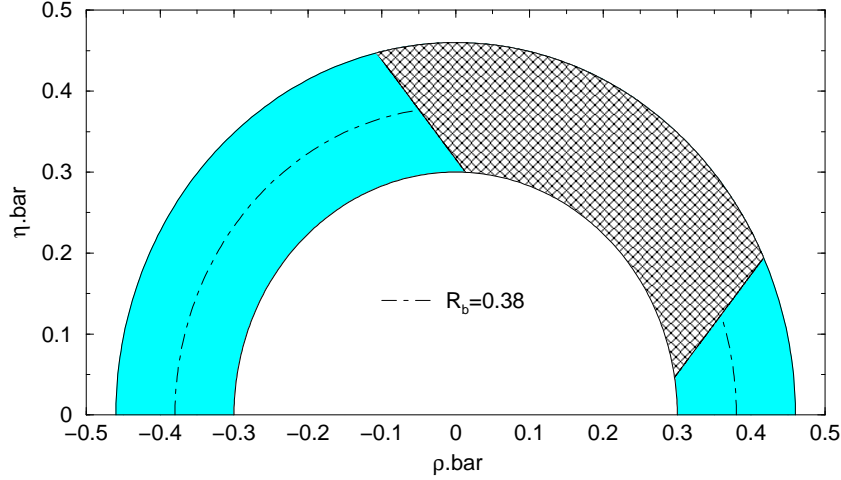


Figure 30: The constraints in the  $\bar{\rho}-\bar{\eta}$  plane implied by (9.43) for  $R_n = 0.6$ ,  $qe^{i\omega} = 0.68 \times [0.38/R_b]$ , and  $\rho_n = 0$ . The shaded region is the allowed range for the apex of the unitarity triangle, whereas the “crossed” region is excluded through  $R_{\min}^n|_{\delta_n, r_n}$ .

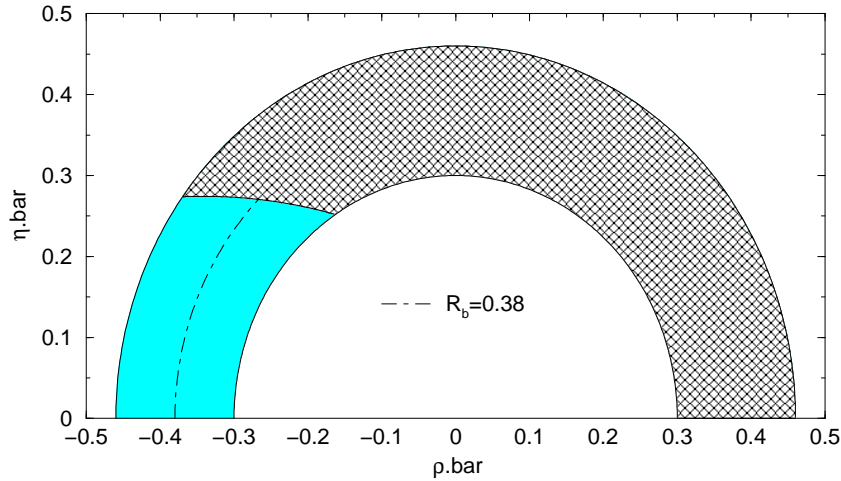


Figure 31: The constraints in the  $\bar{\rho}-\bar{\eta}$  plane implied by (9.66) for  $R_n = 0.6$ ,  $r_n = 0.17$ ,  $qe^{i\omega} = 0.68 \times [0.38/R_b]$ , and  $\rho_n = 0$ . The shaded region is the allowed range for the apex of the unitarity triangle, whereas the “crossed” region is excluded through  $R_n^{\text{ext}}|_{\delta_n}$ .



contrast,  $B_d^0 \rightarrow \pi^0 K^0$  receives contributions both from colour-allowed and from colour-suppressed EW penguins. Nevertheless, they are expected to be at most  $\mathcal{O}(20\%)$  of the QCD penguin contributions. If we neglect the EW penguins and make use of isospin flavour-symmetry arguments, we obtain  $\mathcal{P}_{tc}^n \approx \mathcal{P}_{tc}^c$ , yielding  $\delta_n \approx \delta_c$  and  $\cos \delta_n \approx \cos \delta_c$ . Employing moreover factorization, these cosines are expected to be close to +1.

Consequently, the present CLEO and Belle data point towards a “puzzling” situation, whereas no such discrepancies arise for the results of the BaBar collaboration. It is of course too early to draw any definite conclusions. However, if future data should confirm this “discrepancy”, it may be an indication for new-physics contributions to the EW penguin sector, or a manifestation of large flavour-symmetry-breaking effects [257]. Obviously, further studies are required to distinguish between these possibilities. In this context, it should be kept in mind that there may also be “unconventional” sources for flavour-symmetry-breaking effects. An example is  $\pi^0$ - $\eta, \eta'$  mixing. As was emphasized in [179], the isospin violation arising from such effects could mock new physics in the extraction of the CKM angle  $\alpha$  from  $B \rightarrow \pi\pi$  isospin relations. The impact on the isospin relations involving  $B \rightarrow \pi^0 K$  decays may also be sizeable.

## 9.4 Towards Calculations of $B \rightarrow \pi K, \pi\pi$ Decays

For many years, calculations of  $B \rightarrow \pi K, \pi\pi$  modes employed the Bander–Silverman–Soni mechanism [64] (see 3.3.3), where the strong phases are obtained from absorptive parts of time-like penguin diagrams of the kind shown in Fig. 10. Concerning analyses of exclusive modes (for examples, see [62]–[68]), a problem of this approach is that the transition amplitudes depend, if one applies “naïve” factorization to deal with the hadronic matrix elements, on a variable  $k^2$ , where  $k$  denotes the four-momentum of the gluons and photons appearing in Fig. 10. A conceptual improvement was proposed in [69, 70, 62] by applying the Brodsky–Lepage model [271]. In this approach, the spectator quark is “boosted” through the exchange of an “extra” gluon and the  $k^2$  dependence of the decay rates is removed by folding the perturbatively calculated loop amplitudes with appropriate wavefunctions.

Recently, important theoretical progress could be made through the observation that a rigorous “factorization” formula of the structure given in (3.47) holds also for non-leptonic  $B$ -decays into two light mesons [98]. In the corresponding formalism, the “QCD factorization” approach, soft non-factorizable contributions and final-state interaction effects are suppressed by  $\Lambda_{\text{QCD}}/m_b$ . At the leading order in  $\Lambda_{\text{QCD}}/m_b$ , CP-conserving strong phases arise essentially from perturbatively calculable QCD corrections. Since integrations over the light-cone momentum fractions of the constituent quarks inside the mesons are performed, no dependences of the transition amplitudes on unphysical parameters such as  $k^2$  appear in this approach.

A very comprehensive analysis of  $B \rightarrow \pi K, \pi\pi$  decays within this framework was performed in [100], where also the  $SU(3)$ -breaking corrections affecting the strategies to probe  $\gamma$  discussed in 9.3.3 were explored. Following these lines, it is possible to reduce the corresponding hadronic uncertainties to the level of non-factorizable corrections that violate simultaneously the  $SU(3)$  flavour symmetry and are power suppressed in the heavy-quark limit. Consequently, these corrections are parametrically suppressed by a product of the three small quantities  $1/N_C$ ,  $(m_s - m_d)/\Lambda_{\text{QCD}}$  and  $\Lambda_{\text{QCD}}/m_b$ . The relevant equations, where these corrections enter, are (9.63) and (9.64), which are required to fix  $r_{c,n}$  and  $qe^{i\omega}$ , respectively. Concerning the determination of  $r_c$ , we may write

$$r_c = R_{\text{th}} r_{\text{exp}}^c, \quad (9.76)$$

where

$$r_{\text{exp}}^c = \sqrt{2} \tan \theta_C \frac{f_K}{f_\pi} \sqrt{\frac{\text{BR}(B^\pm \rightarrow \pi^\pm \pi^0)}{\text{BR}(B^\pm \rightarrow \pi^\pm K)}} \quad (9.77)$$

corresponds to the determination of  $T + C$  through (9.63). The analysis of [100] gives

$$R_{\text{th}} = 0.98 \pm 0.05. \quad (9.78)$$

Combining this with the present experimental values for  $r_{\text{exp}}^c$ , averaged over all present  $B$ -factory results, Beneke *et al.* obtain

$$r_c = 0.218 \pm 0.034_{\text{exp}} \pm 0.011_{\text{th}}. \quad (9.79)$$

If both  $SU(3)$ -breaking corrections and small electromagnetic contributions are taken into account, expression (9.64) for the EW penguin parameter  $qe^{i\omega}$  is rescaled by the following factor [100]:

$$R_q = (0.84 \pm 0.10) e^{-i(2.5 \pm 2.8)^\circ}, \quad (9.80)$$

where about half of the deviation from one is due to mostly factorizable  $SU(3)$  breaking. Taking also into account the uncertainty due to the CKM factor  $R_b$ , the final result reads

$$q = (58.8 \pm 6.7 \mp 11.8) \times 10^{-2}, \quad (9.81)$$

where the first error is theoretical and the second error arises from  $R_b$ . The remaining uncertainties of  $R_{\text{th}}$  and  $R_q$  are due to terms of

$$\mathcal{O}\left(\frac{1}{N_C} \times \frac{m_s - m_d}{\Lambda_{\text{QCD}}} \times \frac{\Lambda_{\text{QCD}}}{m_b}\right) = \mathcal{O}\left(\frac{1}{N_C} \times \frac{m_s - m_d}{m_b}\right), \quad (9.82)$$

which are naïvely estimated not to exceed the few percent level. Consequently, it may eventually be possible to determine  $\gamma$  from the  $B \rightarrow \pi K$  strategies reviewed above with a theoretical accuracy of about  $10^\circ$ .

If the parameter  $r_c$  is not determined through (9.76) but calculated directly in the QCD factorization approach, we encounter much larger theoretical uncertainties. The predictions for  $r_c$  and  $\delta_c$  are given as follows [100]:

$$\bar{r}_c \equiv u_c r_c = \begin{cases} (23.9 \pm 4.5 \pm 4.8) \times 10^{-2} \\ (25.7 \pm 4.8 \pm 5.1) \times 10^{-2}, \end{cases} \quad \delta_c = \begin{cases} (-9.6 \pm 3.8)^\circ \\ (-10.2 \pm 4.1)^\circ, \end{cases} \quad (9.83)$$

where the notation is as in (9.39) and (9.40),  $u_c$  was introduced in (9.49), and the CP-conserving strong phase is so small because of

$$\delta_c = \mathcal{O}(\alpha_s(m_b), \Lambda_{\text{QCD}}/m_b). \quad (9.84)$$

Since  $u_c$  is very close to one within QCD factorization,  $\bar{r}_c$  and  $r_c$  take very similar values. It should be noted that the comparison between (9.79) and (9.83) represents a non-trivial test of the QCD factorization approach, which could lead to a reduction of the uncertainties related to the modelling of power corrections to the heavy-quark limit. In this context, potentially large corrections may arise from certain annihilation topologies, as first noted in [102]. Moreover, we have to care about ‘‘chirally enhanced’’ corrections of the following structure:

$$r_\chi^\pi = \frac{2 M_\pi^2}{(m_u + m_d) m_b}, \quad r_\chi^K = \frac{2 M_K^2}{(m_{u,d} + m_s) m_b}, \quad (9.85)$$

which are formally of  $\mathcal{O}(\Lambda_{\text{QCD}}/m_b)$ , but numerically close to unity. Phenomenological analyses of  $B \rightarrow \pi K, \pi\pi$  decays require definite estimates of these corrections. In [100], a certain prescription was used to get some handle on them.

Using an input from QCD factorization that is stronger than (9.78) and (9.80), more stringent constraints on  $\gamma$  and the allowed range in the  $\bar{\rho}-\bar{\eta}$  plane can be obtained. As a first step, we may employ that the CP-conserving strong phase  $\delta_c$  is predicted to be very small due to (9.84), so that  $\cos \delta_c$  governing  $R_c$  is close to one. As a second step, information on  $\gamma$  can be obtained from the predictions for the branching ratios and the observables  $R_{(c,n)}$ . Finally, the information from all CP-averaged  $B \rightarrow \pi K, \pi\pi$  branching ratios can be combined into a single global fit for the generalized Wolfenstein parameters  $\bar{\rho}$  and  $\bar{\eta}$  [100]. For these approaches, it is of course crucial that the contributions entering at the  $\mathcal{O}(\Lambda_{\text{QCD}}/m_b)$  level can be controlled reliably.

In a recent paper [77], it was argued that non-perturbative penguin topologies with internal charm- and up-quark exchanges may play an important rôle in this context. If the analysis of the unitarity triangle performed in [38] is used to determine  $\gamma$ , thereby fixing it to the range in the first quadrant given in (2.54), the  $B \rightarrow \pi K$  branching ratios calculated within QCD factorization [98] are found to be systematically smaller than the measured values, whereas the branching ratio for  $B_d \rightarrow \pi^+ \pi^-$  is about a factor of two larger than the experimental result. On the other hand, if  $\gamma$  is treated as a free parameter,

a fit to the data yields  $\gamma = (163 \pm 12)^\circ$ , which is in strong disagreement to the range given in (2.54) (see also 10.3.5). In the case of  $B_d^0 \rightarrow \pi^- K^+$  and  $B^+ \rightarrow \pi^0 K^+$ , the CP-averaged branching ratios are now enhanced by almost a factor of two, since the interference between penguins and trees is constructive for values of  $\gamma$  in the second quadrant. On the other hand,  $\text{BR}(B_d \rightarrow \pi^+ \pi^-)$  is reduced significantly, as the interference between trees and penguins is now destructive. Since the decays  $B^+ \rightarrow \pi^+ K^0$  and  $B_d^0 \rightarrow \pi^0 K^0$  are essentially independent of the angle  $\gamma$ , their branching ratios – in particular the one of  $B_d^0 \rightarrow \pi^0 K^0$  – are still much smaller than the experimental values.

These features could be interpreted either as a manifestation of new physics, or as an indication of large  $\Lambda_{\text{QCD}}/m_b$  corrections. The authors of [77] focus on the latter possibility and explore the impact of non-perturbative penguin topologies with internal charm- and up-quark exchanges. Actually, as far as the  $B \rightarrow \pi K$  branching ratios are concerned, the most important effects are due to the former “charming” penguins, as we have seen in 9.2.3; they may also affect the strong phases  $\delta_{tc}^{(c,n)}$  significantly, which are a key ingredient for CP violation. In the  $B \rightarrow \pi\pi$  case, also the latter topologies may become important, since they are not Cabibbo-suppressed in  $\bar{b} \rightarrow \bar{d}$  transitions.

If  $\gamma$  is assumed to lie again within the range in (2.54), and the non-perturbative penguin contributions are taken into account by adding appropriate amplitudes, which contain also other  $\mathcal{O}(\Lambda_{\text{QCD}}/m_b)$  terms with the same quantum numbers, for instance the annihilation diagrams considered in [102], the predictions for the branching ratios can be brought closer to the experimental results. Concerning the  $B_d^0 \rightarrow \pi^0 K^0$  mode, the branching ratio is now in perfect agreement with the central value of BaBar, but still much smaller than those of CLEO and Belle. Since the non-perturbative penguin amplitudes cannot (yet) be calculated from first principles, they are determined in this approach through a fit to the data, where  $SU(3)$  flavour-symmetry arguments are used to simplify the analysis. It should be noted that also here no anomalous enhancement of the amplitude corresponding to penguin topologies with internal up-quark exchanges shows up, as would be the case in the presence of dramatic rescattering processes of the kind given in (9.24).

Another interesting feature of this approach is that large direct CP violation arises in the  $B_d^0 \rightarrow \pi^- K^+$ ,  $B^+ \rightarrow \pi^0 K^+$  and  $B_d^0 \rightarrow \pi^+ \pi^-$  channels, which would be in contrast to the picture of QCD factorization. On the other hand, the CP-violating asymmetries in  $B^+ \rightarrow \pi^+ K^0$  and  $B_d^0 \rightarrow \pi^0 K^0$  would be very small, i.e. at the few percent level, as expected “naïvely” from (9.3) and (9.57). It should be noted that the large CP asymmetries of the  $B \rightarrow \pi K$  modes are exactly those that are required for the strategies to extract  $\gamma$  discussed in 9.2.4 and 9.3.3. In the decay  $B_d \rightarrow \pi^+ \pi^-$ , a large sensitivity to  $\Lambda_{\text{QCD}}/m_b$  effects is found, thereby making the extraction of  $\alpha$  from  $\mathcal{A}_{\text{CP}}^{\text{mix}}(B_d \rightarrow \pi^+ \pi^-)$  through a calculation of the hadronic parameters in (6.109) questionable.

Because of the non-perturbative penguin topologies, the sensitivity of the calculated

branching ratios on  $\gamma$  is now lost. In particular, if one tries to fit also  $\gamma$ , one finds that this angle remains essentially undetermined with the present experimental accuracy [77]. An enhancement of the  $B \rightarrow \pi K$  penguin amplitudes through intrinsically non-perturbative charm rescattering was also discussed recently in [272]. The terms entering at  $\mathcal{O}(\Lambda_{\text{QCD}}/m_b)$  in non-leptonic decays will certainly continue to be one of the hot topics in  $B$  physics. Probably it will take some time until this issue will have been settled.

Further progress on the theoretical description of  $B \rightarrow \pi K, \pi\pi$  decays will hopefully be made. For a detailed review of other recent analyses using QCD factorization, we refer the reader to [100], where all technicalities are discussed. Detailed comparisons between QCD factorization and PQCD can be found in [100, 103]. Another approach to calculate the  $B \rightarrow \pi\pi$  hadronic matrix elements using QCD light-cone sum rules was proposed in [273]. As far as the determination of  $\gamma$  is concerned, the strategies considered in 9.3.3 will eventually exhibit the highest theoretical accuracy. Moreover, in addition to  $r_{c,n}$ , they will also provide the strong phases  $\delta_{c,n}$  and the parameters  $\rho_{c,n}e^{i\theta_{c,n}}$ . The insights into hadron dynamics thus obtained will be a very fertile and decisive testing ground for the theoretical approaches to deal with  $B \rightarrow \pi K, \pi\pi$  modes.

## 9.5 Impact of New Physics

In the theoretically clean strategies to measure  $\gamma$  with the help of pure “tree” decays, such as  $B_d \rightarrow D^{*\pm}\pi^\mp$  or  $B_s \rightarrow D_s^\pm K^\mp$ , there are no contributions from flavour-changing neutral-current (FCNC) processes. Consequently, new physics is expected to play a minor rôle in these approaches. On the other hand, penguins are crucial for  $B \rightarrow \pi K$  decays, so that these modes are very sensitive to new physics [263]–[267] (see also the model-independent analysis of the  $B \rightarrow \phi K$  system [163] discussed in 6.2.2).

In order to analyse new-physics effects in the  $B \rightarrow \pi K$  strategies to probe  $\gamma$ , it is useful to distinguish between scenarios of physics beyond the Standard Model, where the isospin symmetry is either preserved or violated [263]. The point is that isospin relations are at the basis of these approaches, as we have seen above. An interesting example for isospin-conserving new physics is given by models with enhanced chromomagnetic dipole operators [274], where  $B^\pm \rightarrow \pi^\pm K$  decays may well exhibit direct CP violation at the level of 10%. On the other hand, the preferred place for isospin-violating scenarios of new physics to manifest themselves is the EW penguin sector, which plays a particularly important rôle in the charged and neutral  $B \rightarrow \pi K$  approaches, employing the isospin relation (9.50), where EW penguins enter also in colour-allowed form. If we consider, for example, models with tree-level FCNC couplings of the  $Z$ -boson, extended gauge models with an extra  $Z'$ -boson, or SUSY models with broken R-parity, EW penguin-like contributions may actually be much larger than those of the Standard-Model EW penguins (for a detailed study, see [265]). Finally, it should not be forgotten that we

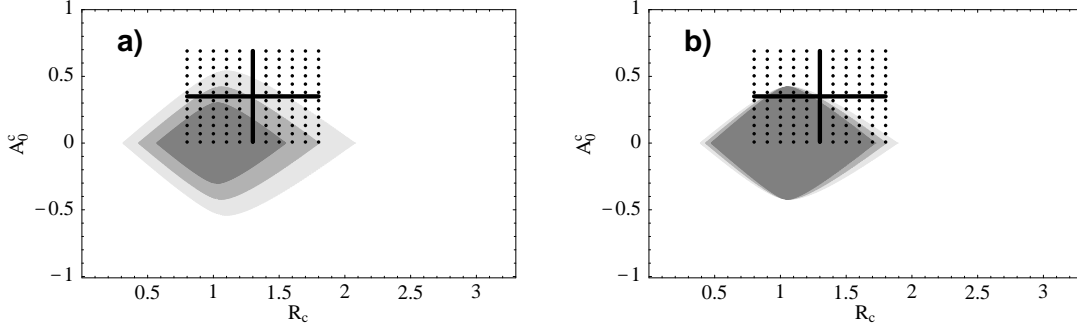


Figure 32: Allowed regions characterizing the  $B^\pm \rightarrow \pi^0 K^\pm, \pi^\pm K$  system in the Standard Model: (a)  $0.15 \leq r_c \leq 0.27, q = 0.63$ ; (b)  $r_c = 0.21, 0.48 \leq q \leq 0.78$  ( $\rho_c = 0$ ).

have used the unitarity of the CKM matrix in the parametrizations of the  $B \rightarrow \pi K$  decay amplitudes. The chances to encounter discrepancies in the  $B \rightarrow \pi K$  strategies are therefore very good. In fact, as we have seen in Subsection 9.3, the present data may already point towards puzzling constraints on  $\gamma$  and strong phases in the charged and neutral  $B \rightarrow \pi K$  decays. Better data are needed to clarify these exciting issues.

We may also arrive at a situation, where *no* solutions for  $\gamma$  and strong phases are found. This would be the most striking signal for new-physics effects in the  $B \rightarrow \pi K$  system. Since the Standard Model predicts strong correlations between the corresponding observables, such a case may be indicated immediately [266]. In Fig. 32, we show the allowed range for the charged  $B \rightarrow \pi K$  system in the  $R_c$ - $A_0^c$  plane. Here the dotted regions correspond to the CLEO results published in [172, 251]. If future measurements should lie significantly outside the allowed ranges shown in this figure, we would have an indication for new physics. On the other hand, if we should find values lying within these regions, this would not automatically imply a “confirmation” of the Standard Model. In this case, we would then be in a position to extract a value for  $\gamma$  by following the strategies described above, which may also lead to discrepancies. Similar allowed regions can of course also be obtained in the observable spaces of the  $B_d \rightarrow \pi^\mp K^\pm, B^\pm \rightarrow \pi^\pm K$  and  $B_d \rightarrow \pi^\mp K^\pm, B_d \rightarrow \pi^0 K$  systems [266]. A set of sum rules relating the CP-averaged branching ratios and CP asymmetries of  $B \rightarrow \pi K$  decays was recently derived in [267], which is useful to analyse the data in view of possible isospin-breaking effects.

## 9.6 Summary

The phenomenology of  $B \rightarrow \pi K$  decays provides interesting strategies to determine  $\gamma$ . To this end, three different combinations of  $B \rightarrow \pi K$  decays may be considered: the  $B_d \rightarrow \pi^\mp K^\pm, B^\pm \rightarrow \pi^\pm K$  system, the charged  $B^\pm \rightarrow \pi^0 K^\pm, B^\pm \rightarrow \pi^\pm K$  system, and the neutral  $B_d \rightarrow \pi^\mp K^\pm, B_d \rightarrow \pi^0 K$  system. In the first case, dynamical assumptions about

rescattering and colour-suppressed EW penguin processes have to be made, in addition to flavour-symmetry arguments. Recent theoretical developments are supporting these plausible assumptions, as well as experimental bounds on  $B \rightarrow KK$  branching ratios. In the case of the charged and neutral  $B \rightarrow \pi K$  strategies, EW penguin topologies, which contribute there also in colour-allowed form, can be taken into account through the  $SU(3)$  flavour symmetry, and the sensitivity to rescattering effects is smaller. Using data on  $B^\pm \rightarrow K^\pm K$  decays, the rescattering processes can in principle be taken into account in the charged  $B \rightarrow \pi K$  strategy, whereas mixing-induced CP violation in  $B_d \rightarrow \pi^0 K_S$  allows us to include these effects exactly in the neutral  $B \rightarrow \pi K$  approach.

Appropriate ratios of CP-averaged  $B \rightarrow \pi K$  decay rates provide valuable constraints both on  $\gamma$  and on CP-conserving strong phases. In order to determine these quantities, also certain CP asymmetries have to be measured. Interestingly, the present data may point towards a “puzzling” situation, although the experimental uncertainties are still too large to draw definite conclusions. Since  $B \rightarrow \pi K$  modes are governed by penguin topologies, they are sensitive probes for new physics. Moreover, the unitarity of the CKM matrix is employed in the strategies to probe  $\gamma$ .

Important theoretical progress concerning the description of the  $B \rightarrow \pi K, \pi\pi$  hadron dynamics has recently been made, providing a framework for systematic calculations in the  $m_b \gg \Lambda_{\text{QCD}}$  limit. Concerning the  $B \rightarrow \pi K$  strategies to probe  $\gamma$ , this interesting development allows a reduction of  $SU(3)$ -breaking corrections, and gives confidence into dynamical assumptions related to rescattering effects. Further theoretical issues concern mainly the importance of  $\Lambda_{\text{QCD}}/m_b$  corrections.

The experimental situation will soon improve significantly. Eventually, it may be possible to extract  $\gamma$  through the  $B \rightarrow \pi K$  strategies with an accuracy of  $\mathcal{O}(10^\circ)$ .

## 10 Phenomenology of $U$ -spin-related $B$ Decays

Let us now focus on strategies to extract the angles of the unitarity triangle – in particular  $\gamma$  – from pairs of  $B$ -meson decays, which are related to each other through the  $U$ -spin flavour symmetry of strong interactions. In analogy to the well-known isospin symmetry,  $U$  spin is also described by an  $SU(2)$  subgroup of the full flavour-symmetry group  $SU(3)_F$ . Whereas isospin relates down and up quarks,  $U$  spin relates down and strange quarks. Consequently,  $U$ -spin-breaking effects are generally expected to be more significant than isospin breaking. On the other hand, an important advantage of the  $U$ -spin symmetry is that it is satisfied – in addition to QCD penguins – also by EW penguin topologies, since the down and strange quarks have the same electrical charges. In this review, we have already encountered  $U$ -spin arguments several times [79, 253, 258, 275, 276], and first approaches to extract CKM phases were pointed out in 1993 [277]. However, the great power of the  $U$ -spin symmetry to determine weak phases and hadronic parameters

was noticed just recently in the strategies proposed in [135, 169, 278], which are our next topic. Since these approaches involve also decays of  $B_s$ -mesons,  $B$  experiments at hadron colliders are required to implement them in practice. At Tevatron-II, we will have first access to the corresponding modes and interesting results are expected [193]. In the era of BTeV and the LHC, the  $U$ -spin strategies can then be fully exploited [148].

## 10.1 The $B_{s(d)} \rightarrow J/\psi K_S$ System

As we have seen in Subsection 6.1, the “gold-plated” mode  $B_d \rightarrow J/\psi K_S$  plays an outstanding rôle in the determination of the  $B_d^0\text{-}\overline{B}_d^0$  mixing phase  $\phi_d$ , i.e. of the CKM angle  $\beta$ . In this subsection, we consider the decay  $B_s \rightarrow J/\psi K_S$  [135], which is related to  $B_d \rightarrow J/\psi K_S$  by interchanging all down and strange quarks (see Fig. 14), and may allow an interesting extraction of  $\gamma$ .

### 10.1.1 Amplitude Structure

In analogy to (6.3), the  $B_s^0 \rightarrow J/\psi K_S$  decay amplitude can be expressed as follows:

$$A(B_s^0 \rightarrow J/\psi K_S) = -\lambda \mathcal{A} (1 - ae^{i\theta} e^{i\gamma}), \quad (10.1)$$

where

$$\mathcal{A} \equiv \lambda^2 A (A_{\text{CC}}^c + A_{\text{pen}}^{ct}) \quad (10.2)$$

and

$$ae^{i\theta} \equiv R_b \left( \frac{A_{\text{pen}}^{ut}}{A_{\text{CC}}^c + A_{\text{pen}}^{ct}} \right) \quad (10.3)$$

correspond to (6.4) and (6.5), respectively. It should be emphasized that the Standard-Model expressions (6.3) and (10.1) rely only on the unitarity of the CKM matrix.

Comparing (10.1) with (6.3), we observe that  $ae^{i\theta}$  enters in the  $B_s^0 \rightarrow J/\psi K_S$  decay amplitude in a Cabibbo-allowed way, whereas  $a'e^{i\theta'}$  is doubly Cabibbo-suppressed in the  $B_d^0 \rightarrow J/\psi K_S$  amplitude. Consequently, there may be sizeable CP violation in  $B_s \rightarrow J/\psi K_S$ , which provides *two* independent observables,  $\mathcal{A}_{\text{CP}}^{\text{dir}}(B_s \rightarrow J/\psi K_S)$  and  $\mathcal{A}_{\text{CP}}^{\text{mix}}(B_s \rightarrow J/\psi K_S)$  or  $\mathcal{A}_{\Delta\Gamma}(B_s \rightarrow J/\psi K_S)$ , depending on the *three* “unknowns”  $a$ ,  $\theta$  and  $\gamma$ , as well as on the  $B_s^0\text{-}\overline{B}_s^0$  mixing phase  $\phi_s$ . Consequently, in order to determine these “unknowns”, we need an additional observable, which is provided by

$$H \equiv \left( \frac{1 - \lambda^2}{\lambda^2} \right) \left| \frac{\mathcal{A}'}{\mathcal{A}} \right|^2 \frac{\langle \Gamma(B_s \rightarrow J/\psi K_S) \rangle}{\langle \Gamma(B_d \rightarrow J/\psi K_S) \rangle}, \quad (10.4)$$

where the CP-averaged decay rates  $\langle \Gamma(B_s \rightarrow J/\psi K_S) \rangle$  and  $\langle \Gamma(B_d \rightarrow J/\psi K_S) \rangle$  can be determined from the “untagged” rates introduced in (7.10) through

$$\langle \Gamma(B_q \rightarrow f) \rangle \equiv \frac{\Gamma_q[f(0)]}{2}. \quad (10.5)$$



### 10.1.2 Extraction of $\gamma$

Since the  $U$ -spin flavour symmetry of strong interactions implies

$$|\mathcal{A}'| = |\mathcal{A}| \quad (10.6)$$

and

$$a' = a, \quad \theta' = \theta, \quad (10.7)$$

we can determine  $a$ ,  $\theta$  and  $\gamma$  as functions of  $\phi_s$  by combining  $H$  with  $\mathcal{A}_{\text{CP}}^{\text{dir}}(B_s \rightarrow J/\psi K_S)$  and  $\mathcal{A}_{\text{CP}}^{\text{mix}}(B_s \rightarrow J/\psi K_S)$  or  $\mathcal{A}_{\Delta\Gamma}(B_s \rightarrow J/\psi K_S)$ . In contrast to isospin relations, EW penguins do not lead to any problems in these  $U$ -spin relations. As we have already noted in Section 7, the  $B_s^0\text{--}\overline{B}_s^0$  mixing phase  $\phi_s$  is negligibly small in the Standard Model, and can be probed nicely through the search for CP violation in  $B_s \rightarrow J/\psi\phi$  modes.

Interestingly, the strategy to extract  $\gamma$  from  $B_{s(d)} \rightarrow J/\psi K_S$  decays does not require a non-trivial CP-conserving strong phase  $\theta$ . However, its experimental feasibility depends strongly on the value of the ‘‘penguin’’ parameter  $a$ , which is very difficult to calculate. In the following, we assume, as in Subsection 6.1, that  $a = \mathcal{O}(\overline{\lambda})$ , which is a plausible estimate. The general formalism to extract  $\gamma$  from the  $B_{s(d)} \rightarrow J/\psi K_S$  system was developed in [135]. Although the corresponding formulae are quite complicated, the basic idea is very simple: if  $\phi_s$  is used as an input,  $\mathcal{A}_{\text{CP}}^{\text{dir}}(B_s \rightarrow J/\psi K_S)$  and  $\mathcal{A}_{\text{CP}}^{\text{mix}}(B_s \rightarrow J/\psi K_S)$  allow us to eliminate the strong phase  $\theta$ , thereby fixing a contour in the  $\gamma$ - $a$  plane in a *theoretically clean* way. Another contour can be fixed with the help of the  $U$ -spin relations (10.6) and (10.7) by combining the observable  $H$  with  $\mathcal{A}_{\text{CP}}^{\text{mix}}(B_s \rightarrow J/\psi K_S)$ . Alternatively, we may combine  $H$  with  $\mathcal{A}_{\Delta\Gamma}(B_s \rightarrow J/\psi K_S)$  to fix a third contour in the  $\gamma$ - $a$  plane. The intersection of these contours gives then  $\gamma$  and  $a$ , so that also the strong phase  $\theta$  can be determined. The general formulae simplify considerably, if we keep only terms linear in  $a$ . Within this approximation, we obtain

$$\tan \gamma \approx \frac{\sin \phi_s + \mathcal{A}_{\text{CP}}^{\text{mix}}(B_s \rightarrow J/\psi K_S)}{(1 - H) \cos \phi_s}. \quad (10.8)$$

Let us illustrate this approach by considering an example. Assuming  $\phi_s = 0$ ,  $\gamma = 60^\circ$ ,  $a = a' = 0.2$  and  $\theta = \theta' = 30^\circ$ , we obtain the following  $B_{s(d)} \rightarrow J/\psi K_S$  observables:  $\mathcal{A}_{\text{CP}}^{\text{dir}}(B_s \rightarrow J/\psi K_S) = 0.20$ ,  $\mathcal{A}_{\text{CP}}^{\text{mix}}(B_s \rightarrow J/\psi K_S) = 0.31$ ,  $\mathcal{A}_{\Delta\Gamma}(B_s \rightarrow J/\psi K_S) = 0.93$  and  $H = 0.86$ . The corresponding contours in the  $\gamma$ - $a$  plane are shown in Fig. 33. Interestingly, in the case of these contours, we would not have to deal with ‘‘physical’’ discrete ambiguities for  $\gamma$ , since values of  $a$  larger than 1 would simply appear unrealistic. If it should be possible to measure  $\mathcal{A}_{\Delta\Gamma}(B_s \rightarrow J/\psi K_S)$  with the help of the width difference  $\Delta\Gamma_s$ , the dotted line could be fixed. In this example, the approximate expression (10.8) yields  $\gamma \approx 65^\circ$ , which deviates from the ‘‘true’’ value of  $\gamma = 60^\circ$  by only 8%. It is also interesting to note that we have  $\mathcal{A}_{\text{CP}}^{\text{dir}}(B_d \rightarrow J/\psi K_S) = -0.89\%$  in our example.

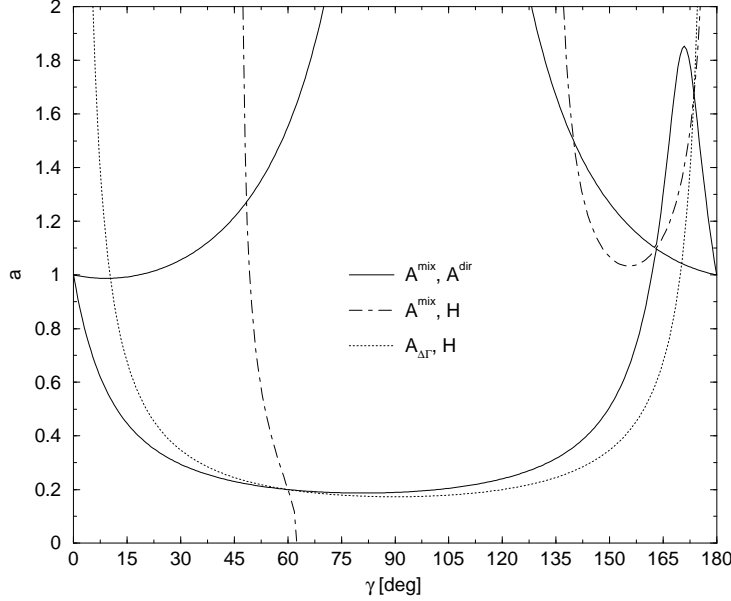


Figure 33: Contours in the  $\gamma$ - $a$  plane fixed through the  $B_{s(d)} \rightarrow J/\psi K_S$  observables for a specific example discussed in the text.

An important by-product of the strategy described above is that the quantities  $a'$  and  $\theta'$  allow us to take into account the penguin contributions in the determination of  $\phi_d$  from  $B_d \rightarrow J/\psi K_S$ , which are expected to enter at the  $\bar{\lambda}^3$  level and are hence presumably very small. However, these uncertainties may become an important issue for the LHC because of the tremendous experimental accuracy for the CP-violating  $B_d \rightarrow J/\psi K_S$  observables that can be achieved there [148].

If we use (10.7), we obtain an interesting relation, which is the counterpart of (9.28):

$$\frac{\mathcal{A}_{\text{CP}}^{\text{dir}}(B_d \rightarrow J/\psi K_S)}{\mathcal{A}_{\text{CP}}^{\text{dir}}(B_s \rightarrow J/\psi K_S)} = - \left| \frac{\mathcal{A}'}{\mathcal{A}} \right|^2 \frac{\langle \Gamma(B_s \rightarrow J/\psi K_S) \rangle}{\langle \Gamma(B_d \rightarrow J/\psi K_S) \rangle}. \quad (10.9)$$

### 10.1.3 Theoretical Uncertainties

Let us finally turn to the theoretical uncertainties. In contrast to the  $B \rightarrow \pi K$  strategies discussed in Section 9, flavour-symmetry arguments are sufficient for the extraction of  $\gamma$ , i.e. we do not have to worry about rescattering effects. The theoretical accuracy is therefore only limited by  $SU(3)$ -breaking effects. Whereas the solid curve in Fig. 33 is *theoretically clean*, the dot-dashed and dotted lines are affected by  $U$ -spin-breaking corrections. Because of the suppression of  $a'e^{i\theta'}$  in (6.3) through  $\lambda^2$ , these contours are essentially unaffected by possible corrections to (10.7), and rely predominantly on the

$U$ -spin relation  $|\mathcal{A}'| = |\mathcal{A}|$ . In the “naïve” factorization approximation, we have

$$\left| \frac{\mathcal{A}'}{\mathcal{A}} \right|_{\text{fact}} = \frac{F_{B_d^0 K^0}(M_{J/\psi}^2; 1^-)}{F_{B_s^0 \overline{K}^0}(M_{J/\psi}^2; 1^-)}, \quad (10.10)$$

where the form factors  $F_{B_d^0 K^0}(M_{J/\psi}^2; 1^-)$  and  $F_{B_s^0 \overline{K}^0}(M_{J/\psi}^2; 1^-)$  parametrize the quark-current matrix elements  $\langle K^0 | (\bar{b}s)_{V-A} | B_d^0 \rangle$  and  $\langle \overline{K}^0 | (\bar{b}d)_{V-A} | B_s^0 \rangle$ , respectively [89]. Quantitative studies of (10.10), which could be performed, for instance, with the help of QCD sum-rule or lattice techniques, are not yet available. In the light-cone sum-rule approach, sizeable  $SU(3)$ -breaking effects were found in the case of the  $B_{d,s} \rightarrow K^*$  form factors [279]. It should be emphasized that also non-factorizable corrections, which are not included in (10.10), may play an important rôle. We are optimistic that we will have a better picture of  $SU(3)$  breaking by the time the  $B_s \rightarrow J/\psi K_S$  measurements can be performed in practice. A feasibility study performed by CMS indicates that  $\gamma$  can be determined at the LHC through the  $B_{s(d)} \rightarrow J/\psi K_S$  approach with an experimental accuracy of  $\sim 9^\circ$  after three years of taking data [148]. A variant of the  $B_{s(d)} \rightarrow J/\psi K_S$  strategy employing  $B_{s(d)} \rightarrow J/\psi \eta$  decays was recently discussed in [280].

## 10.2 The $B_{d(s)} \rightarrow D_{d(s)}^+ D_{d(s)}^-$ and $B_{d(s)} \rightarrow K^0 \overline{K}^0$ Systems

### 10.2.1 Extracting $\gamma$ from $B_{d(s)} \rightarrow D_{d(s)}^+ D_{d(s)}^-$ Decays

Usually, the decay  $B_d \rightarrow D_d^+ D_d^-$  is considered as a tool to probe the  $B_d^0 - \overline{B}_d^0$  mixing phase. In fact, if penguins played a negligible rôle in this mode, we could determine  $\phi_d = 2\beta$  from the corresponding mixing-induced CP asymmetry. However, the penguin topologies, which may in principle also contain important contributions from rescattering processes, may well be sizeable.<sup>15</sup> Interestingly, these penguin topologies allow us to determine  $\gamma$  [135], if the overall normalization of  $B_d \rightarrow D_d^+ D_d^-$  is fixed through the CP-averaged, i.e. “untagged”, rate of its  $U$ -spin partner  $B_s \rightarrow D_s^+ D_s^-$ , and if  $\phi_d$  is determined separately, for instance with the help of the “gold-plated” mode  $B_d \rightarrow J/\psi K_S$ .

The decays  $B_{d(s)}^0 \rightarrow D_{d(s)}^+ D_{d(s)}^-$  are transitions into a CP eigenstate with eigenvalue +1 and originate from  $\bar{b} \rightarrow \bar{c} c \bar{d}$  ( $\bar{s}$ ) quark-level processes. We have to deal both with current-current and with penguin contributions, corresponding to the topologies shown in Fig. 18. In analogy to (6.3) and (10.1), the transition amplitudes can be written as

$$A(B_s^0 \rightarrow D_s^+ D_s^-) = \left(1 - \frac{\lambda^2}{2}\right) \tilde{\mathcal{A}}' \left[1 + \left(\frac{\lambda^2}{1 - \lambda^2}\right) \tilde{a}' e^{i\tilde{\theta}'} e^{i\gamma}\right] \quad (10.11)$$

$$A(B_d^0 \rightarrow D_d^+ D_d^-) = -\lambda \tilde{\mathcal{A}} \left(1 - \tilde{a} e^{i\tilde{\theta}} e^{i\gamma}\right), \quad (10.12)$$

<sup>15</sup>Note that the QCD factorization formula (3.47) does not apply to  $B_{d(s)} \rightarrow D_{d(s)}^+ D_{d(s)}^-$  decays.

where the quantities  $\tilde{\mathcal{A}}$ ,  $\tilde{\mathcal{A}}'$  and  $\tilde{a}e^{i\tilde{\theta}}$ ,  $\tilde{a}'e^{i\tilde{\theta}'}$  take the same form as in the  $B_{s(d)} \rightarrow J/\psi K_S$  case. The dynamics underlying these parameters is, of course, rather different, as can be seen by comparing the relevant Feynman diagrams.

Since the phase structures of the  $B_d^0 \rightarrow D_d^+ D_d^-$  and  $B_s^0 \rightarrow D_s^+ D_s^-$  amplitudes are completely analogous to those of  $B_s^0 \rightarrow J/\psi K_S$  and  $B_d^0 \rightarrow J/\psi K_S$ , respectively, the  $U$ -spin approach discussed in the previous subsection can be applied by just making appropriate replacements of variables. If we neglect tiny phase-space effects, which can be taken into account straightforwardly (see [135]), we have

$$\tilde{H} = \left( \frac{1 - \lambda^2}{\lambda^2} \right) \left| \frac{\tilde{\mathcal{A}}'}{\tilde{\mathcal{A}}} \right|^2 \frac{\langle \Gamma(B_d \rightarrow D_d^+ D_d^-) \rangle}{\langle \Gamma(B_s \rightarrow D_s^+ D_s^-) \rangle}. \quad (10.13)$$

The  $B_{d(s)} \rightarrow D_{d(s)}^+ D_{d(s)}^-$  counterpart of (10.8) takes the following form:

$$\tan \gamma \approx \frac{\sin \phi_d - \mathcal{A}_{\text{CP}}^{\text{mix}}(B_d \rightarrow D_d^+ D_d^-)}{(1 - \tilde{H}) \cos \phi_d}, \quad (10.14)$$

where the different sign of the mixing-induced CP asymmetry is due to the different CP eigenvalues of the  $B_d \rightarrow D_d^+ D_d^-$  and  $B_s \rightarrow J/\psi K_S$  final states. In analogy to the  $B_{s(d)} \rightarrow J/\psi K_S$  system, contours in the  $\gamma$ - $\tilde{a}$  plane can be determined, allowing a transparent determination of  $\gamma$ ,  $\tilde{a}$  and  $\tilde{\theta}$ ; an example is discussed in [135]. Note that there are also strategies to extract  $\cos \phi_d$ , as noted in 6.1.6, complementing  $a_{\psi K_S} = \sin \phi_d$ .

The theoretical accuracy is again only limited by  $U$ -spin-breaking effects, since no dynamical assumptions about rescattering processes are required. The relevant corrections affect the relation  $|\tilde{\mathcal{A}}'| = |\tilde{\mathcal{A}}|$ . In the factorization approximation, we have

$$\left| \frac{\tilde{\mathcal{A}}'}{\tilde{\mathcal{A}}} \right|_{\text{fact}} = \frac{(M_{B_s} - M_{D_s}) \sqrt{M_{B_s} M_{D_s}} (w_s + 1) f_{D_s} \xi_s(w_s)}{(M_{B_d} - M_{D_d}) \sqrt{M_{B_d} M_{D_d}} (w_d + 1) f_{D_d} \xi_d(w_d)}, \quad (10.15)$$

where the restrictions from the Heavy-Quark Effective Theory for the  $B_q \rightarrow D_q$  form factors have been taken into account by introducing appropriate Isgur–Wise functions  $\xi_q(w_q)$  with  $w_q = M_{B_q}/(2M_{D_q})$  [90]. Studies of the light-quark dependence of the Isgur–Wise function were performed within Heavy-Meson Chiral Perturbation Theory, indicating an enhancement of  $\xi_s(w_s)/\xi_d(w_d)$  at the level of 5% [281]. Applying the same formalism to  $f_{D_s}/f_D$  gives values at the 1.2 level [282], which is of the same order of magnitude as the results of recent lattice calculations [127, 283]. Further studies are needed to get a better picture of the  $SU(3)$ -breaking corrections to the ratio  $|\tilde{\mathcal{A}}'|/|\tilde{\mathcal{A}}|$ . Concerning the experimental feasibility, preliminary analyses by LHCb have shown that an experimental precision on  $\gamma$  of a few degrees seems to be achievable [148].

### 10.2.2 Extracting $\gamma$ from $B_{d(s)} \rightarrow K^0\overline{K}^0$ Decays

The formalism developed for the  $B_{d(s)} \rightarrow D_{d(s)}^+ D_{d(s)}^-$  system applies also to the pair of  $U$ -spin-related decays  $B_s^0 \rightarrow K^0\overline{K}^0$  and  $B_d^0 \rightarrow K^0\overline{K}^0$ , originating from  $\bar{b} \rightarrow \bar{s}d\bar{d}$  and  $\bar{b} \rightarrow \bar{d}s\bar{s}$  quark-level transitions, respectively [74]. Although these decays do not receive contributions from current–current operators at the “tree” level, their amplitudes can be written, within the Standard Model, in complete analogy to (10.11) and (10.12). Consequently, as far as the extraction of  $\gamma$  is concerned, the channels  $B_s^0 \rightarrow K^0\overline{K}^0$  and  $B_d^0 \rightarrow K^0\overline{K}^0$  take the rôles of  $B_s^0 \rightarrow D_s^+ D_s^-$  and  $B_d^0 \rightarrow D_d^+ D_d^-$ , respectively. The determination of the corresponding hadronic parameters would be of particular interest to obtain insights into penguin topologies with internal up- and charm-quark exchanges, as becomes obvious from the discussion in Subsection 3.4.

If the decays  $B_s^0 \rightarrow K^{*0}\overline{K}^{*0}$  and  $B_d^0 \rightarrow K^{*0}\overline{K}^{*0}$  are considered, the corresponding angular distributions provide many more observables, so that the  $B_d^0$ – $\overline{B}_d^0$  mixing phase  $\phi_d$  is no longer required as an input for the determination of  $\gamma$ , but can rather be extracted as well [74]. From a practical point of view, these strategies are, however, more complicated than those involving two pseudoscalar mesons in the final states. It should be emphasized that  $B_{d,s} \rightarrow K^{(*)0}\overline{K}^{(*)0}$  decays represent very sensitive probes for new physics, since they are penguin-induced modes (see also 6.2.2).

## 10.3 The $B_d \rightarrow \pi^+\pi^-$ , $B_s \rightarrow K^+K^-$ System

As we have seen in Subsection 6.3, the decay  $B_d \rightarrow \pi^+\pi^-$  is usually considered as a tool to determine  $\alpha = 180^\circ - \beta - \gamma$ . Unfortunately, the extraction of this angle from  $\mathcal{A}_{\text{CP}}^{\text{mix}}(B_d \rightarrow \pi^+\pi^-)$  is affected by large penguin uncertainties, and the strategies to control them through additional data are challenging. Let us now discuss a new approach to extract CKM phases from  $B_d \rightarrow \pi^+\pi^-$  with the help of the decay  $B_s \rightarrow K^+K^-$  [169].

### 10.3.1 Extraction of $\beta$ and $\gamma$

Looking at the Feynman diagrams shown in Fig. 18, we observe that  $B_s \rightarrow K^+K^-$  is obtained from the  $B_d \rightarrow \pi^+\pi^-$  topologies by interchanging all down and strange quarks. The corresponding decay amplitude can be parametrized as follows:

$$A(B_s^0 \rightarrow K^+K^-) = \left( \frac{\lambda}{1 - \lambda^2/2} \right) \mathcal{C}' \left[ e^{i\gamma} + \left( \frac{1 - \lambda^2}{\lambda^2} \right) d' e^{i\theta'} \right], \quad (10.16)$$

where  $\mathcal{C}'$  and  $d' e^{i\theta'}$  take the same form as the parameters  $\mathcal{C}$  and  $d e^{i\theta}$  in the  $B_d \rightarrow \pi^+\pi^-$  amplitude (6.91). Applying the formalism discussed in Subsection 5.4, we arrive at

parametrizations of the following structure:<sup>16</sup>

$$\mathcal{A}_{\text{CP}}^{\text{dir}}(B_d \rightarrow \pi^+\pi^-) = \text{function}(d, \theta, \gamma) \quad (10.17)$$

$$\mathcal{A}_{\text{CP}}^{\text{mix}}(B_d \rightarrow \pi^+\pi^-) = \text{function}(d, \theta, \gamma, \phi_d = 2\beta) \quad (10.18)$$

$$\mathcal{A}_{\text{CP}}^{\text{dir}}(B_s \rightarrow K^+K^-) = \text{function}(d', \theta', \gamma) \quad (10.19)$$

$$\mathcal{A}_{\text{CP}}^{\text{mix}}(B_s \rightarrow K^+K^-) = \text{function}(d', \theta', \gamma, \phi_s \approx 0), \quad (10.20)$$

where the Standard-Model expectation  $\phi_s \approx 0$  can be probed straightforwardly through  $B_s \rightarrow J/\psi\phi$ . Consequently, we have four CP-violating observables at our disposal, depending on six “unknowns”. However, since  $B_d \rightarrow \pi^+\pi^-$  and  $B_s \rightarrow K^+K^-$  are related to each other by interchanging all down and strange quarks, the  $U$ -spin symmetry implies

$$d'e^{i\theta'} = de^{i\theta}. \quad (10.21)$$

Using this relation, the *four* observables (10.17)–(10.20) can be expressed in terms of the *four* quantities  $d$ ,  $\theta$ ,  $\phi_d = 2\beta$  and  $\gamma$ , which can hence be determined.

In comparison with the  $U$ -spin strategies discussed in Subsections 10.1 and 10.2, an important advantage of the  $B_d \rightarrow \pi^+\pi^-$ ,  $B_s \rightarrow K^+K^-$  approach is that the  $U$ -spin symmetry is only applied in the form of (10.21), where  $de^{i\theta}$  and  $d'e^{i\theta'}$  are actually given by ratios of amplitudes (see (6.93)). In particular, no overall normalization of decay amplitudes has to be fixed through  $U$ -spin arguments, where  $U$ -spin-breaking effects are expected to be much larger. We shall come back to this issue below. Moreover, we again do not have to make any dynamical assumptions about rescattering processes, which is an important conceptual advantage in comparison with the  $B \rightarrow \pi K$  strategies to determine  $\gamma$  reviewed in Section 9.

### 10.3.2 Minimal Use of the $U$ -Spin Symmetry

The  $U$ -spin-symmetry arguments can be minimized, if we employ  $\phi_d = 2\beta$  as an input, which can be determined straightforwardly through  $B_d \rightarrow J/\psi K_S$  (see also 6.1.6). The CP-violating observables  $\mathcal{A}_{\text{CP}}^{\text{dir}}(B_d \rightarrow \pi^+\pi^-)$  and  $\mathcal{A}_{\text{CP}}^{\text{mix}}(B_d \rightarrow \pi^+\pi^-)$  allow us then to eliminate the strong phase  $\theta$  and to determine  $d$  as a function of  $\gamma$ . Analogously, we may use  $\mathcal{A}_{\text{CP}}^{\text{dir}}(B_s \rightarrow K^+K^-)$  and  $\mathcal{A}_{\text{CP}}^{\text{mix}}(B_s \rightarrow K^+K^-)$  to eliminate  $\theta'$ , and to determine  $d'$  as a function of  $\gamma$ . The corresponding contours in the  $\gamma$ – $d$  and  $\gamma$ – $d'$  planes can be fixed in a *theoretically clean* way. Using now the  $U$ -spin relation  $d' = d$ , these contours allow the determination both of the CKM angle  $\gamma$  and of the hadronic quantities  $d$ ,  $\theta$ ,  $\theta'$  [169]. It should be emphasized that no  $U$ -spin relation involving the strong phases  $\theta$  and  $\theta'$  has to be employed in this approach. Alternatively, we could also eliminate  $d$  and  $d'$ , and

<sup>16</sup>For the explicit expressions, see [169].

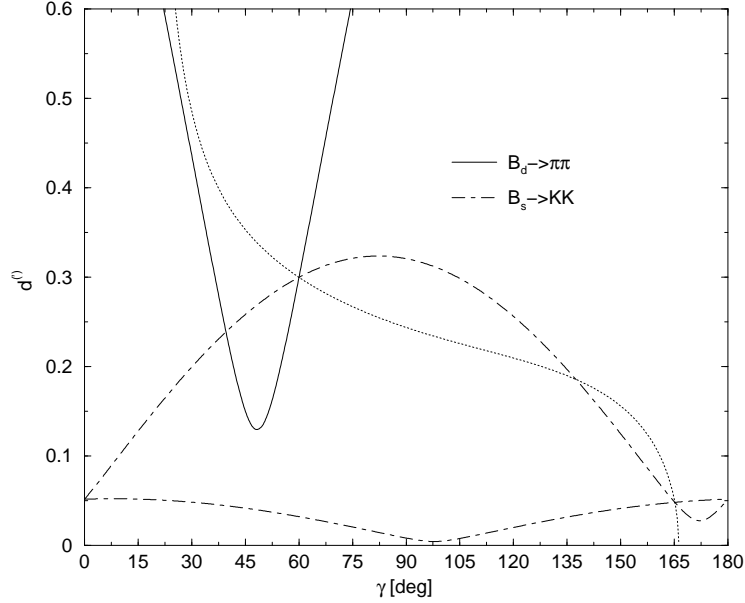


Figure 34: The contours in the  $\gamma$ - $d'$  planes fixed through the CP-violating  $B_d \rightarrow \pi^+\pi^-$  and  $B_s \rightarrow K^+K^-$  observables for a specific example discussed in the text.

could determine  $\gamma$  (as well as  $d$  and  $d'$ ) with the help of theoretically clean contours in the  $\gamma$ - $\theta$  and  $\gamma$ - $\theta'$  planes through  $\theta = \theta'$ . In the following, we shall, however, focus on the former possibility.

Let us illustrate this approach with a simple example. Assuming  $d = d' = 0.3$ ,  $\theta = \theta' = 210^\circ$ ,  $\phi_s = 0$ ,  $\phi_d = 44^\circ$  and  $\gamma = 60^\circ$ , which is in accordance with theoretical estimates and the fits of the unitarity triangle, we obtain the following observables:  $\mathcal{A}_{\text{CP}}^{\text{dir}}(B_d \rightarrow \pi^+\pi^-) = +19\%$ ,  $\mathcal{A}_{\text{CP}}^{\text{mix}}(B_d \rightarrow \pi^+\pi^-) = +62\%$ ,  $\mathcal{A}_{\text{CP}}^{\text{dir}}(B_s \rightarrow K^+K^-) = -17\%$  and  $\mathcal{A}_{\text{CP}}^{\text{mix}}(B_s \rightarrow K^+K^-) = -27\%$ . In Fig. 34, the corresponding contours in the  $\gamma$ - $d$  and  $\gamma$ - $d'$  planes are represented by the solid and dot-dashed lines, respectively. Their intersection yields a twofold solution for  $(\gamma, d)$ , given by  $(39^\circ, 0.24)$  and our input value of  $(60^\circ, 0.30)$ . It should be noted that the  $B_s \rightarrow K^+K^-$  contour would imply in this example *model-independently* that  $d' < 0.32$ . The dotted line is related to the quantity

$$\mathcal{K} \equiv -\frac{1}{\epsilon} \left( \frac{d \sin \theta}{d' \sin \theta'} \right) \left[ \frac{\mathcal{A}_{\text{CP}}^{\text{dir}}(B_s \rightarrow K^+K^-)}{\mathcal{A}_{\text{CP}}^{\text{dir}}(B_d \rightarrow \pi^+\pi^-)} \right] = \frac{1 - 2d \cos \theta \cos \gamma + d^2}{\epsilon^2 + 2\epsilon d' \cos \theta' \cos \gamma + d'^2} \quad (10.22)$$

with

$$\epsilon \equiv \frac{\lambda^2}{1 - \lambda^2}, \quad (10.23)$$

which can be combined with  $\mathcal{A}_{\text{CP}}^{\text{mix}}(B_s \rightarrow K^+K^-)$  through the  $U$ -spin relation (10.21) to fix another contour in the  $\gamma$ - $d$  plane. We shall come back to  $\mathcal{K}$  in 10.3.5. Combining all contours in Fig. 34 with one another, we obtain a single solution for  $\gamma$ , which is given

by the “true” value of  $60^\circ$ . As a “by-product”, also the hadronic parameters  $d$  and  $\theta$ ,  $\theta'$  can be determined, which would allow an interesting comparison with theoretical predictions, thereby providing valuable insights into hadronic physics.

From an experimental point of view, this approach is very promising for CDF-II ( $\Delta\gamma|_{\text{exp}} = \mathcal{O}(10^\circ)$ ) [193], and ideally suited for the LHC experiments, in particular LHCb ( $\Delta\gamma|_{\text{exp}} = \mathcal{O}(1^\circ)$ ) [148]; similar comments apply to BTeV. Moreover, it has interesting features concerning the theoretical cleanliness, which is our next topic.

### 10.3.3 Theoretical Uncertainties

The theoretical accuracy of the determination of  $\gamma$  and the hadronic parameters  $d$ ,  $\theta$ ,  $\theta'$  discussed in 10.3.2 is *only* limited by  $U$ -spin-breaking corrections to  $d' = d$ . In particular, it is not affected by final-state interaction or rescattering effects. For  $d' \neq d$ , there would be a relative shift of the solid and dot-dashed curves in Fig. 34. However, in this example, the extracted value of  $\gamma$  would be very stable under such effects.

Let us, in order to put the  $U$ -spin-breaking corrections to (10.21) on a more quantitative basis, apply the picture of the Bander–Silverman–Soni (BSS) mechanism [64] (see 3.3.3) to calculate the quantity  $de^{i\theta}$  defined in (6.93). Following the formalism developed in [62, 63] and using expression (3.33), we obtain

$$de^{i\theta} = \frac{1}{R_b} \left[ \frac{\mathcal{A}_t + \mathcal{A}_c}{\mathcal{A}_{\text{CC}} + \mathcal{A}_t + \mathcal{A}_u} \right], \quad (10.24)$$

where

$$\mathcal{A}_{\text{CC}} = \frac{1}{3} \overline{\mathcal{C}}_1 + \overline{\mathcal{C}}_2 \quad (10.25)$$

$$\mathcal{A}_t = \frac{1}{3} \left[ \overline{\mathcal{C}}_3 + \overline{\mathcal{C}}_9 + \chi (\overline{\mathcal{C}}_5 + \overline{\mathcal{C}}_7) \right] + \overline{\mathcal{C}}_4 + \overline{\mathcal{C}}_{10} + \chi (\overline{\mathcal{C}}_6 + \overline{\mathcal{C}}_8) \quad (10.26)$$

$$\mathcal{A}_j = \frac{\alpha_s}{9\pi} \left[ \frac{10}{9} - G(m_j, k, m_b) \right] \left[ \overline{\mathcal{C}}_2 + \frac{1}{3} \frac{\alpha}{\alpha_s} (3\overline{\mathcal{C}}_1 + \overline{\mathcal{C}}_2) \right] (1 + \chi), \quad (10.27)$$

with  $j \in \{u, c\}$ . Kinematical considerations at the perturbative quark level imply the following “physical” range for  $k^2$  [69]:

$$\frac{1}{4} \lesssim \frac{k^2}{m_b^2} \lesssim \frac{1}{2}, \quad (10.28)$$

and

$$\chi = \frac{2M_\pi^2}{(m_u + m_d)(m_b - m_u)} \quad (10.29)$$

is due to the use of the equations of motion for the quark fields. Since the “penguin” parameter  $de^{i\theta}$  is actually a ratio of certain amplitudes, the decay constants and form



factors arising typically in factorization (for an example, see (9.45)) cancel in (10.24). It should be noted that this expression gives values for  $d$  and  $\theta$  of the same order of magnitude as those employed in the example leading to the contours shown in Fig. 34. The expression for the  $B_s \rightarrow K^+K^-$  parameter  $d'e^{i\theta'}$  takes the same form as (10.24), where  $\chi$  is replaced in (10.26) and (10.27) by

$$\chi' = \frac{2M_K^2}{(m_u + m_s)(m_b - m_u)}. \quad (10.30)$$

Consequently, in our approach to evaluate  $de^{i\theta}$  and  $d'e^{i\theta'}$ ,  $U$ -spin-breaking corrections enter only through the parameters  $\chi$  and  $\chi'$ . However, up to small electromagnetic corrections, the chiral structure of strong interactions implies

$$\frac{M_\pi^2}{m_u + m_d} = \frac{M_K^2}{m_u + m_s}, \quad (10.31)$$

leading, among other things, to the Gell-Mann–Okubo relation (see, for example, [284]). In our case, this expression has the interesting implication

$$\chi = \chi', \quad (10.32)$$

so that the  $U$ -spin relation (10.21) is not affected by  $U$ -spin-breaking corrections within our formalism. Although (10.24) is a simplified expression, as becomes evident from the unphysical  $k^2$  dependence, it strengthens our confidence into (10.21). Further theoretical studies of the  $U$ -spin-breaking effects in the  $B_d \rightarrow \pi^+\pi^-$ ,  $B_s \rightarrow K^+K^-$  system, using, for example, QCD factorization [100], would be desirable.

Apart from these theoretical considerations, we may also obtain experimental insights into  $U$ -spin breaking. A first consistency check is provided by  $\theta = \theta'$ . Moreover, we may determine the overall normalizations  $|\mathcal{C}|$  and  $|\mathcal{C}'|$  of the  $B_d^0 \rightarrow \pi^+\pi^-$  and  $B_s^0 \rightarrow K^+K^-$  decay amplitudes (see (6.91) and (10.16)) with the help of the corresponding CP-averaged branching ratios. Comparing them with the “factorized” result

$$\left| \frac{\mathcal{C}'}{\mathcal{C}} \right|_{\text{fact}} = \left[ \frac{M_{B_s}^2 - M_K^2}{M_{B_d}^2 - M_\pi^2} \right] \left[ \frac{f_K}{f_\pi} \right] \left[ \frac{F_{B_s K}(M_K^2; 0^+)}{F_{B_d \pi}(M_\pi^2; 0^+)} \right], \quad (10.33)$$

we have another interesting probe for  $U$ -spin-breaking effects. Moreover, the quantity  $\mathcal{K}$  introduced in (10.22) can also be expressed as

$$\mathcal{K} = \frac{1}{\epsilon} \left| \frac{\mathcal{C}'}{\mathcal{C}} \right|^2 \left[ \frac{\text{BR}(B_d \rightarrow \pi^+\pi^-)}{\text{BR}(B_s \rightarrow K^+K^-)} \right] \frac{\tau_{B_s}}{\tau_{B_d}}, \quad (10.34)$$

so that the  $U$ -spin relation (10.21) implies

$$\frac{\mathcal{A}_{\text{CP}}^{\text{dir}}(B_s \rightarrow K^+K^-)}{\mathcal{A}_{\text{CP}}^{\text{dir}}(B_d \rightarrow \pi^+\pi^-)} = - \left| \frac{\mathcal{C}'}{\mathcal{C}} \right|^2 \left[ \frac{\text{BR}(B_d \rightarrow \pi^+\pi^-)}{\text{BR}(B_s \rightarrow K^+K^-)} \right] \frac{\tau_{B_s}}{\tau_{B_d}}. \quad (10.35)$$

In order to obtain further insights, the  $B_d \rightarrow \rho^+ \rho^-$ ,  $B_s \rightarrow K^{*+} K^{*-}$  system would be of particular interest, allowing us to determine  $\gamma$  together with the mixing phases  $\phi_d$  and  $\phi_s$ , and tests of several  $U$ -spin relations [74]. Here the observables of the corresponding angular distributions have to be measured.

### 10.3.4 Searching for New Physics

Since penguin processes play a key rôle in the decays  $B_s \rightarrow K^+ K^-$  and  $B_d \rightarrow \pi^+ \pi^-$ , they – and the strategy to determine  $\gamma$ , where moreover the unitarity of the CKM matrix is employed – may well be affected by new physics. Interestingly, the Standard Model implies a rather restricted region in the space of the CP-violating observables of the  $B_s \rightarrow K^+ K^-$ ,  $B_d \rightarrow \pi^+ \pi^-$  system, as noted in [266]. A future measurement of observables lying significantly outside of this allowed region would be an immediate indication for new physics. On the other hand, if the observables should lie within the region predicted by the Standard Model, we can extract a value for  $\gamma$  by following the strategy discussed above. This value for  $\gamma$  may well be in conflict with those provided by other approaches, which would then also indicate the presence of new physics.

### 10.3.5 Replacing $B_s \rightarrow K^+ K^-$ through $B_d \rightarrow \pi^\mp K^\pm$

Although the  $B_d \rightarrow \pi^+ \pi^-$ ,  $B_s \rightarrow K^+ K^-$  approach is very promising for hadron machines, it cannot be implemented at the asymmetric  $e^+ e^-$   $B$ -factories operating at the  $\Upsilon(4S)$  resonance (BaBar and Belle), since  $B_s$ -mesons are there not accessible. However, there is a variant of this strategy, employing  $B_d^0 \rightarrow \pi^- K^+$  instead of  $B_s^0 \rightarrow K^+ K^-$  [175]. Since these modes differ only in their spectator quarks, we expect

$$\mathcal{A}_{\text{CP}}^{\text{dir}}(B_s \rightarrow K^+ K^-) \approx \mathcal{A}_{\text{CP}}^{\text{dir}}(B_d \rightarrow \pi^\mp K^\pm) \quad (10.36)$$

$$\text{BR}(B_s \rightarrow K^+ K^-) \approx \text{BR}(B_d \rightarrow \pi^\mp K^\pm) \frac{\tau_{B_s}}{\tau_{B_d}}, \quad (10.37)$$

and obtain from (10.34)

$$\mathcal{K} \approx \frac{1}{\epsilon} \left( \frac{f_K}{f_\pi} \right)^2 \left[ \frac{\text{BR}(B_d \rightarrow \pi^+ \pi^-)}{\text{BR}(B_d \rightarrow \pi^\mp K^\pm)} \right] = \begin{cases} 7.3 \pm 2.9 \text{ (CLEO [172])} \\ 7.2 \pm 2.3 \text{ (BaBar [173])} \\ 8.5 \pm 3.7 \text{ (Belle [174])}. \end{cases} \quad (10.38)$$

The advantage of (10.38) is that it allows the determination of  $\mathcal{K}$  without a measurement of the decay  $B_s \rightarrow K^+ K^-$ . On the other hand, this relation relies not only on  $SU(3)$  flavour-symmetry arguments, but also on a certain dynamical assumption. The point is that  $B_s \rightarrow K^+ K^-$  receives also contributions from “exchange” and “penguin annihilation” topologies, which are absent in  $B_d \rightarrow \pi^\mp K^\pm$ . It is usually assumed that these contributions play a minor rôle [85]. However, they may in principle be enhanced through

large rescattering effects [78]. Although these topologies do *not* lead to any problems in the strategies discussed below if  $\mathcal{K}$  is fixed through a measurement of  $B_s \rightarrow K^+K^-$  – even if they should turn out to be sizeable – they may affect (10.36)–(10.38). Their importance can be probed, in addition to (10.36) and (10.37), with the help of the decay  $B_s \rightarrow \pi^+\pi^-$ . The naïve expectation for the corresponding branching ratio is  $\mathcal{O}(10^{-8})$ ; a significant enhancement would signal that the “exchange” and “penguin annihilation” topologies cannot be neglected.

The  $B$ -factory results in (10.38) may be used to obtain a rather restricted range for the hadronic parameter  $d$ , as well as upper bounds on  $|\mathcal{A}_{\text{CP}}^{\text{dir}}(B_d \rightarrow \pi^+\pi^-)|$  and  $|\mathcal{A}_{\text{CP}}^{\text{dir}}(B_d \rightarrow \pi^\mp K^\pm)|$ . In order to derive these constraints, we make use of the right-hand side of (10.22), and assume that (10.21) holds also for the  $B_d \rightarrow \pi^\mp K^\pm$ ,  $B_d \rightarrow \pi^+\pi^-$  system. The quantity  $\mathcal{K}$  allows us then to determine

$$C \equiv \cos \theta \cos \gamma \quad (10.39)$$

as a function of  $d$  [175]:

$$C = \frac{a - d^2}{2bd}, \quad (10.40)$$

where

$$a = \frac{1 - \epsilon^2 \mathcal{K}}{\mathcal{K} - 1} \quad \text{and} \quad b = \frac{1 + \epsilon \mathcal{K}}{\mathcal{K} - 1}. \quad (10.41)$$

Since  $C$  is the product of two cosines, it has to lie between  $-1$  and  $+1$ , thereby implying an allowed range for  $d$ . Taking into account (10.40) and (10.41), we obtain (for  $\mathcal{K} < 1/\epsilon^2$ )

$$\frac{1 - \epsilon \sqrt{\mathcal{K}}}{1 + \sqrt{\mathcal{K}}} \leq d \leq \frac{1 + \epsilon \sqrt{\mathcal{K}}}{|1 - \sqrt{\mathcal{K}}|}. \quad (10.42)$$

Note that this range takes the same form as (9.31). In the special case of  $\mathcal{K} = 1$ , there is only a lower bound on  $d$ , given by  $d_{\text{min}} = (1 - \epsilon)/2$ ; for  $\mathcal{K} < 1$ ,  $C$  takes a minimal value that implies the following allowed range for  $\gamma$ :

$$|\cos \gamma| \geq C_{\text{min}} = \frac{\sqrt{(1 - \epsilon^2 \mathcal{K})(1 - \mathcal{K})}}{1 + \epsilon \mathcal{K}} \approx \sqrt{1 - \mathcal{K}}. \quad (10.43)$$

From a conceptual point of view, this bound on  $\gamma$  is completely analogous to the one derived in [232] (see 9.2.2). Unfortunately, it is only of academic interest in the present case, as (10.38) indicates  $\mathcal{K} > 1$ , which we shall assume in the following discussion. So far, we have treated  $\theta$  and  $\gamma$  as “unknown”, i.e. free parameters. However, for a given value of  $\gamma$ , we have

$$-|\cos \gamma| \leq C \leq +|\cos \gamma|, \quad (10.44)$$

and obtain constraints on  $d$  that are stronger than (10.42):

$$d_{\text{min}}^{\text{max}} = \pm b|\cos \gamma| + \sqrt{a + b^2 \cos^2 \gamma}. \quad (10.45)$$

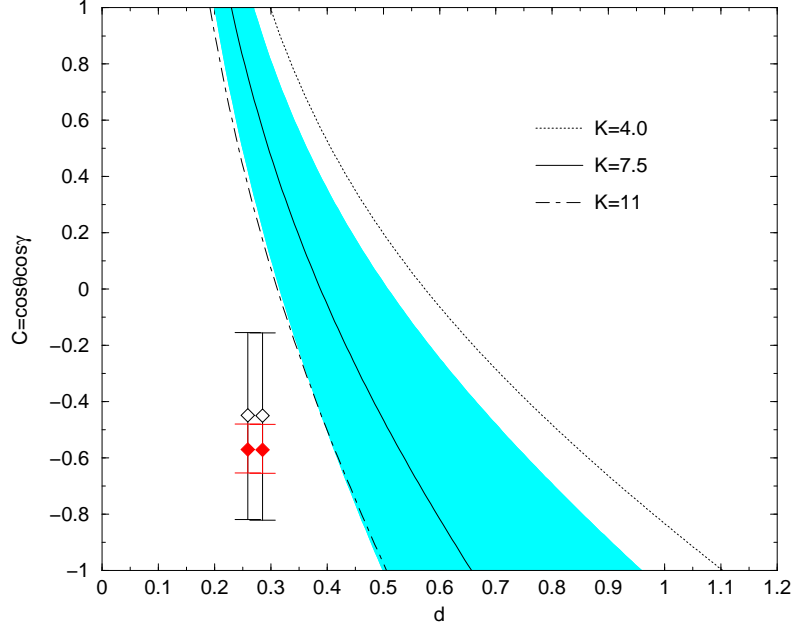


Figure 35:  $C = \cos \theta \cos \gamma$  as a function of  $d$  for various values of  $\mathcal{K}$ . The “diamonds” with error bars represent the QCD factorization results [100] for the ranges for  $\gamma$  obtained in [38] (narrow range) and [42] (wide range). The shaded region corresponds to a variation of  $\xi_d$  within the interval  $[0.8, 1.2]$  for  $\mathcal{K} = 7.5$ .

In Fig. 35, we show the dependence of  $C$  on  $d$  for values of  $\mathcal{K}$  corresponding to (10.38). The “diamonds” represent the predictions of the QCD factorization approach [100]:

$$d = \begin{cases} (28.5 \pm 5.1 \mp 5.7) \times 10^{-2} \\ (25.9 \pm 4.3 \mp 5.2) \times 10^{-2}, \end{cases} \quad \theta - 180^\circ = \begin{cases} (8.2 \pm 3.8)^\circ \\ (9.0 \pm 4.1)^\circ, \end{cases} \quad (10.46)$$

where the notation is as in (9.39) and (9.40). The “error bars” in Fig. 35 correspond to the ranges for  $\gamma$  obtained in [38] and [42] (see (2.54) and Table 1), while the filled and opaque diamonds are evaluated with the central values of (10.46) for the preferred values of  $\gamma = 54.8^\circ$  and  $63^\circ$ , respectively. The shaded region illustrates the variation of

$$\xi_d \equiv d'/d \quad (10.47)$$

between 0.8 and 1.2 for  $\mathcal{K} = 7.5$ , where the regions on the left- and right-hand sides of the solid line correspond to  $\xi_d > 1$  and  $\xi_d < 1$ , respectively. As noted in [175], the impact of a sizeable phase  $\Delta\theta$  in  $\theta' = \theta + \Delta\theta$ , representing the second kind of possible corrections to (10.21), is very small.

Looking at Fig. 35, we observe that the experimental values of  $\mathcal{K}$  imply a rather restricted range for  $d$ . In particular, we get the lower bound of  $d \gtrsim 0.2$ . Moreover, the

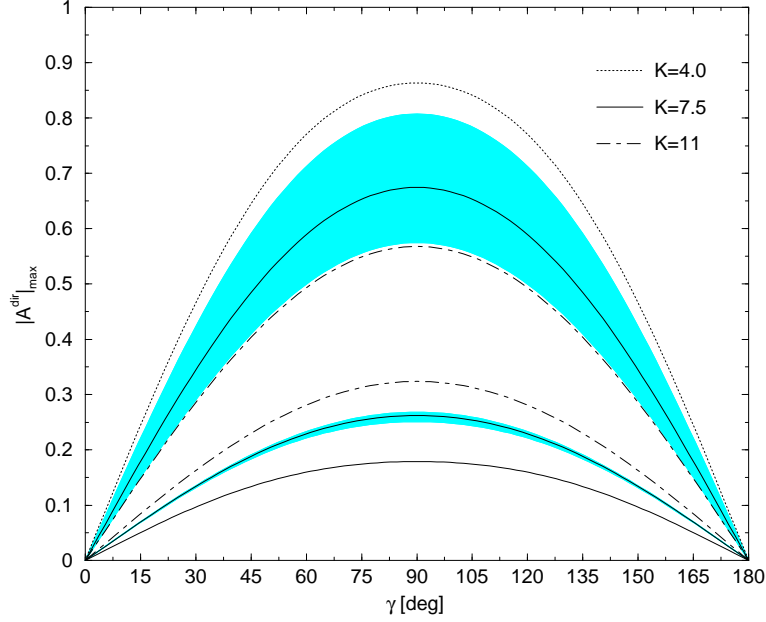


Figure 36: The maximal direct CP asymmetries for  $B_d \rightarrow \pi^+\pi^-$  (upper curves) and  $B_s \rightarrow K^+K^- \approx B_d \rightarrow \pi^\mp K^\pm$  (lower curves) as functions of  $\gamma$  for various values of  $\mathcal{K}$ . The shaded regions correspond to a variation of  $\xi_d$  within  $[0.8, 1.2]$  for  $\mathcal{K} = 7.5$ .

curves are not in favour of an interpretation of the “QCD factorization” results (10.46) within the Standard Model, although the experimental uncertainties are too large to draw definite conclusions. This discrepancy could be resolved for values of  $\gamma$  being significantly larger than  $90^\circ$  [175]. On the other hand, it may also be a manifestation of large  $\Lambda_{\text{QCD}}/m_b$  corrections [77], as we have discussed in Subsection 9.4. In any case, the data tell us that we have definitely to care about penguin effects in  $B_d \rightarrow \pi^+\pi^-$ .

The quantity  $\mathcal{K}$  allows us also to derive constraints on direct CP asymmetries. The corresponding formulae, which can be found in [175], simplify considerably for  $\gamma = 90^\circ$ :

$$\left| \mathcal{A}_{\text{CP}}^{\text{dir}}(B_d \rightarrow \pi^+\pi^-) \right|_{\gamma=90^\circ}^{\text{max}} = 2 \sqrt{\frac{(1 - \epsilon^2 \mathcal{K})(\xi_d^2 \mathcal{K} - 1)}{(\xi_d^2 - \epsilon^2)^2 \mathcal{K}^2}} \approx \frac{2}{\xi_d \sqrt{\mathcal{K}}} \quad (10.48)$$

$$\left| \mathcal{A}_{\text{CP}}^{\text{dir}}(B_s \rightarrow K^+K^-) \right|_{\gamma=90^\circ}^{\text{max}} = 2 \epsilon \xi_d \sqrt{\frac{(1 - \epsilon^2 \mathcal{K})(\xi_d^2 \mathcal{K} - 1)}{(\xi_d^2 - \epsilon^2)^2}} \approx 2 \epsilon \sqrt{\mathcal{K}}. \quad (10.49)$$

Interestingly, the latter expression is essentially *unaffected* by any correction to (10.21) for  $\mathcal{K} = \mathcal{O}(10)$ ; its theoretical accuracy is practically only limited by (10.33), which enters in the determination of  $\mathcal{K}$  through (10.34).

In Fig. 36, we show the dependence of the maximally allowed direct CP asymmetries for  $B_d \rightarrow \pi^+\pi^-$  and  $B_s \rightarrow K^+K^- \approx B_d \rightarrow \pi^\mp K^\pm$  on  $\gamma$  for various values of  $\mathcal{K}$ . The

shaded regions correspond to a variation of the parameter  $\xi_d$  within the interval  $[0.8, 1.2]$  for  $\mathcal{K} = 7.5$ . The values for  $\mathcal{K}$  given in (10.38) disfavour very large direct CP violation in  $B_d \rightarrow \pi^\mp K^\pm$ , which is also consistent with the experimental results summarized in Table 4, and the most recent BaBar update given by  $\mathcal{A}_{\text{CP}}(B_d^0 \rightarrow \pi^- K^+) = (7 \pm 8 \pm 2)\%$  [176]. On the other hand, there is a lot of space left for large direct CP violation in  $B_d \rightarrow \pi^+ \pi^-$  (see also [77]), which is in accordance with (6.96).

As can be seen in Fig. 36, a measurement of non-vanishing CP asymmetries  $|\mathcal{A}_{\text{CP}}^{\text{dir}}|_{\text{exp}}$  would allow us to exclude immediately a certain range of  $\gamma$  around  $0^\circ$  and  $180^\circ$ , since the values corresponding to  $|\mathcal{A}_{\text{CP}}^{\text{dir}}|_{\text{exp}} > |\mathcal{A}_{\text{CP}}^{\text{dir}}|_{\text{max}}$  would be excluded. However, in order to probe this angle, the mixing-induced CP asymmetry  $\mathcal{A}_{\text{CP}}^{\text{mix}}(B_d \rightarrow \pi^+ \pi^-)$  is actually more powerful. If we assume that  $\phi_d$  has been measured through  $B_d \rightarrow J/\psi K_S$  and use  $\cos \theta = C/\cos \gamma$  to eliminate the strong phase  $\theta$ , we obtain  $\mathcal{A}_{\text{CP}}^{\text{mix}}(B_d \rightarrow \pi^+ \pi^-)$  as a monotonic function of  $d^2$ , taking its extremal values for  $d = d_{\text{min}}^{\text{max}}$  given in (10.45). For a fixed value of  $\gamma$ , the allowed range for  $\mathcal{A}_{\text{CP}}^{\text{mix}}(B_d \rightarrow \pi^+ \pi^-)$  is usually very large. However, a measured value of this observable may, on the other hand, imply a rather restricted range for  $\gamma$ , as illustrated in more detail in [175]. Finally, if in addition to  $\mathcal{K}$  and  $\mathcal{A}_{\text{CP}}^{\text{mix}}(B_d \rightarrow \pi^+ \pi^-)$  also direct CP violation in  $B_d \rightarrow \pi^+ \pi^-$  or  $B_d \rightarrow \pi^\mp K^\pm$  is observed, both the angle  $\gamma$  and the hadronic parameters  $d$  and  $\theta$  can be determined.

At CLEO, BaBar and Belle, significantly improved measurements of the  $B_d \rightarrow \pi^+ \pi^-$  and  $B_d \rightarrow \pi^\mp K^\pm$  branching ratios will be obtained, and direct CP violation in these channels will hopefully be observed. The latter two experiments should also determine the mixing-induced CP asymmetry of the  $B_d \rightarrow \pi^+ \pi^-$  mode. On the other hand – in addition to similar measurements – run II of the Tevatron will also provide first access to the  $B_s \rightarrow K^+ K^-$  channel. In the LHC era, the very rich physics potential of these decays can then be fully exploited.

## 10.4 The $B_{(s)} \rightarrow \pi K$ System

Another interesting pair of decays, which are related to each other by interchanging all down and strange quarks, is the  $B_d^0 \rightarrow \pi^- K^+$ ,  $B_s^0 \rightarrow \pi^+ K^-$  system [278]. Starting from the general Standard-Model parametrizations for the corresponding decay amplitudes and eliminating the CKM factors  $\lambda_t^{(s)}$  and  $\lambda_t^{(d)}$  through the unitarity relation (3.32), it is an easy exercise to show that we may – in the strict  $U$ -spin limit – write

$$A(B_d^0 \rightarrow \pi^- K^+) = -P \left(1 - r e^{i\delta} e^{i\gamma}\right) \quad (10.50)$$

$$A(B_s^0 \rightarrow \pi^+ K^-) = P \sqrt{\epsilon} \left(1 + \frac{1}{\epsilon} r e^{i\delta} e^{i\gamma}\right), \quad (10.51)$$

where  $P$  denotes a CP-conserving complex amplitude,  $\epsilon$  was introduced in (10.23),  $r$  is a real parameter and  $\delta$  a CP-conserving strong phase. At first sight, it appears as if  $\gamma$ ,

$r$  and  $\delta$  could be determined from the ratio of the CP-averaged rates and the two CP asymmetries provided by these modes.<sup>17</sup> However, because of the relation

$$\begin{aligned} |A(B_d^0 \rightarrow \pi^- K^+)|^2 - |A(\overline{B}_d^0 \rightarrow \pi^+ K^-)|^2 &= 4r \sin \delta \sin \gamma \\ &= - \left[ |A(B_s^0 \rightarrow \pi^+ K^-)|^2 - |A(\overline{B}_s^0 \rightarrow \pi^- K^+)|^2 \right], \end{aligned} \quad (10.52)$$

we have actually only two independent observables, so that the three parameters  $\gamma$ ,  $r$  and  $\delta$  cannot be determined. To this end, the overall normalization  $P$  has to be fixed, requiring a further input. Making the same dynamical assumptions as in 9.2.2, i.e. assuming that the phase factor  $e^{i\gamma}$  plays a negligible rôle in  $B^+ \rightarrow \pi^+ K^0$  and that colour-suppressed EW penguins can be neglected as well, the isospin symmetry implies

$$P = A(B^+ \rightarrow \pi^+ K^0). \quad (10.53)$$

In order to extract  $\gamma$  and the hadronic parameters, it is useful to introduce observables  $R_s$  and  $A_s$  by replacing  $B_d \rightarrow \pi^\mp K^\pm$  through  $B_s \rightarrow \pi^\pm K^\mp$  in (9.19) and (9.41), respectively. Using (10.50), (10.51) and (10.53), we then obtain

$$R_s = \epsilon + 2r \cos \delta \cos \gamma + \frac{r^2}{\epsilon} \quad (10.54)$$

$$A_s = -2r \sin \delta \sin \gamma = -A_0. \quad (10.55)$$

Together with the parametrization for  $R$  given in (9.19), these observables allow the determination of all relevant parameters. The extraction of  $\gamma$  and  $\delta$  is analogous to the  $B_d \rightarrow \pi^\mp K^\pm$ ,  $B^\pm \rightarrow \pi^\pm K$  approach [88, 253, 254] discussed in 9.2.4. However, now the advantage is that the  $U$ -spin counterparts  $B_s \rightarrow \pi^\pm K^\mp$  of  $B_d \rightarrow \pi^\mp K^\pm$  allow us to determine also the parameter  $r$  without using arguments related to factorization [278]:

$$r = \sqrt{\epsilon \left[ \frac{R + R_s - 1 - \epsilon}{1 + \epsilon} \right]}. \quad (10.56)$$

On the other hand, as emphasized above, we still have to make dynamical assumptions concerning rescattering and colour-suppressed EW penguin effects. A variant of this approach using the CKM angle  $\beta$  as an additional input was proposed in [285].

In addition to the dynamical assumptions, the theoretical accuracy is further limited by  $SU(3)$ -breaking effects. A consistency check is provided by the relation  $A_s = -A_0$ , which is due to (10.52). In the factorization approximation, the relevant  $SU(3)$ -breaking effects are governed by the following ratio of decay constants and form factors:

$$\frac{f_\pi}{f_K} \left[ \frac{F_{B_s K}(M_\pi^2; 0^+)}{F_{B\pi}(M_K^2; 0^+)} \right], \quad (10.57)$$

<sup>17</sup>Note that these observables are independent of  $P$ .

which is estimated to be a few percent smaller than one [278].

In comparison with the  $B_s \rightarrow \pi^+\pi^-$ ,  $B_s \rightarrow K^+K^-$  approach discussed above, the  $B_{(s)} \rightarrow \pi K$  strategy has the following points in its favour:

- It does not require time-dependent analyses.
- It is independent of the  $B_s^0\text{--}\overline{B}_s^0$  mixing phase  $\phi_s$ .

However, it should be no problem for future “hadronic”  $B$  experiments to measure time-dependent  $B_s$  decay rates, and  $\phi_s$  can be taken into account straightforwardly through  $B_s \rightarrow J/\psi\phi$ . The  $B_s \rightarrow \pi^+\pi^-$ ,  $B_s \rightarrow K^+K^-$  strategy [169] has the following advantages:

- It is a pure  $U$ -spin strategy, i.e. it does not involve any dynamical assumptions about rescattering or EW penguin effects.
- The relevant  $U$ -spin relation involves only ratios of certain strong amplitudes that are not affected by  $U$ -spin-breaking corrections within the BSS mechanism.
- It allows the determination of  $\phi_d = 2\beta$  and  $\gamma$ . Using  $\phi_d$  from  $B_d \rightarrow J/\psi K_S$ , the  $U$ -spin input for the extraction of  $\gamma$  can be minimized, providing also  $\theta$  and  $\theta'$ .

## 10.5 Other $U$ -Spin Approaches

As we have already noted several times in this review, the observables of the angular distributions of  $B \rightarrow V_1V_2$  modes, where  $V_1$  and  $V_2$  continue to decay through strong interactions, offer interesting insights into CP violation and the hadronization dynamics of non-leptonic  $B$  decays.

The general formalism to extract CKM phases and hadronic parameters from the time-dependent angular distributions of neutral  $B_q \rightarrow V_1V_2$  decays, taking also into account penguin contributions, was developed in [74]. If we fix the  $B_q^0\text{--}\overline{B}_q^0$  mixing phase  $\phi_q$  separately, it is possible to determine a CP-violating weak phase  $\omega$ , which is usually given by the angles of the unitarity triangle, and interesting hadronic quantities in a *theoretically clean* way as a function of a *single* hadronic parameter. If we determine this parameter, for instance, by comparing  $B_q \rightarrow V_1V_2$  with an  $SU(3)$ -related mode, all remaining parameters, including  $\omega$ , can be extracted. If we are willing to make more extensive use of flavour-symmetry arguments, it is possible to determine  $\phi_q$  as well. This approach can be applied, for example, to the  $U$ -spin pairs  $B_d \rightarrow \rho^+\rho^-$ ,  $B_s \rightarrow K^{*+}K^{*-}$  or  $B_d \rightarrow K^{*0}\overline{K}^{*0}$ ,  $B_s \rightarrow K^{*0}\overline{K}^{*0}$ , providing many more cross-checks of interesting  $U$ -spin relations than their counterparts involving only pseudoscalar mesons in the final state. The formalism presented in [74] is very general and can be applied to many other decays.



In our discussion of  $U$ -spin strategies, we have always encountered certain relations between CP asymmetries and CP-averaged branching ratios of  $U$ -spin related decays (see (9.28), (10.9) and (10.35)). They are equivalent to

$$|A(B \rightarrow f)|^2 - |A(\bar{B} \rightarrow \bar{f})|^2 = - \left[ |A(UB \rightarrow Uf)|^2 - |A(U\bar{B} \rightarrow U\bar{f})|^2 \right], \quad (10.58)$$

where  $U$  denotes a  $U$ -spin transformation. This relation was derived, within a general framework, in [286], where also further strategies to explore  $U$ -spin-breaking effects were proposed.

Applications of (10.58) to the  $U$ -spin-related rare decays  $B^\pm \rightarrow K^{*\pm}\gamma$  and  $B^\pm \rightarrow \rho^\pm\gamma$  were recently discussed in [287]. Introducing

$$\Delta\text{BR}(B \rightarrow K^*\gamma) \equiv \text{BR}(B^+ \rightarrow K^{*+}\gamma) - \text{BR}(B^- \rightarrow K^{*-}\gamma) \quad (10.59)$$

$$\Delta\text{BR}(B \rightarrow \rho\gamma) \equiv \text{BR}(B^+ \rightarrow \rho^+\gamma) - \text{BR}(B^- \rightarrow \rho^-\gamma), \quad (10.60)$$

this relation implies

$$\Delta\text{BR}(B \rightarrow K^*\gamma) + \Delta\text{BR}(B \rightarrow \rho\gamma) = 0. \quad (10.61)$$

The corresponding  $U$ -spin-breaking corrections were investigated in [288], using a framework that is similar to the QCD factorization approach for two-body non-leptonic  $B$  decays. These authors find

$$\Delta\text{BR}(B \rightarrow K^*\gamma) = -7 \times 10^{-7}, \quad \Delta\text{BR}(B \rightarrow \rho\gamma) = +4 \times 10^{-7}, \quad (10.62)$$

so that the sum of these quantities leaves an  $U$ -spin-breaking remainder of  $-3 \times 10^{-7}$ . Actually, this result is not too surprising, if we remember that we also found – employing, however, “naïve” factorization – large  $U$ -spin-breaking corrections to analogous relations between non-leptonic  $B$  decays, as can be seen, for example, in (9.28). Let us finally note that the  $U$ -spin symmetry has also interesting applications in the  $D$  system [289].

## 10.6 Summary

There are several pairs of  $U$ -spin-related  $B$  decays, which allow determinations of weak phases and hadronic parameters. In the case of the  $B_{s(d)} \rightarrow J/\psi K_S$ ,  $B_{d(s)} \rightarrow D_{d(s)}^+ D_{d(s)}^-$  and  $B_{d(s)} \rightarrow K^0 \bar{K}^0$  systems,  $\gamma$  can be extracted in a transparent manner, where  $\phi_d = 2\beta$  is required as an additional input from  $B_d \rightarrow J/\psi K_S$  in the case of the latter two  $U$ -spin pairs. It should be emphasized that no dynamical assumptions about rescattering or EW penguin effects are required to this end, which is an important conceptual advantage in comparison with the  $B \rightarrow \pi K$  strategies to determine  $\gamma$ . Consequently, the theoretical accuracy is only limited by  $U$ -spin-breaking corrections, where those affecting relations between the overall normalizations of decay amplitudes are the most serious ones.

A particularly interesting strategy is provided by the  $B_d \rightarrow \pi^+\pi^-$ ,  $B_s \rightarrow K^+K^-$  system, allowing the determination both of  $\beta$  and  $\gamma$  and of hadronic parameters as functions of the  $B_s^0-\overline{B}_s^0$  mixing phase  $\phi_s$ , which is negligibly small in the Standard Model, and can be probed straightforwardly through  $B_s \rightarrow J/\psi\phi$ . In comparison with the  $U$ -spin strategies listed in the previous paragraph, here the advantage is that the  $U$ -spin symmetry has to be applied only to certain ratios of strong amplitudes, where  $U$ -spin-breaking effects due to form factors and decay constants cancel. Moreover, there are no  $U$ -spin-breaking corrections within the BSS mechanism. Employing  $\phi_d = 2\beta$  as an input, the use of the  $U$ -spin symmetry can be minimized. From a theoretical point of view, this is the cleanest presently known  $U$ -spin approach to determine  $\gamma$ . Moreover, it is very promising for run II of the Tevatron and ideally suited for the LHC era. Eventually, it may allow us to extract  $\gamma$  with an uncertainty of only a few degrees. The hadronic parameters, which can be determined as a “by-product”, are very interesting for comparisons with theoretical calculations. Needless to note, new physics may well lead to discrepancies with other strategies.

Approximately, we may replace  $B_s \rightarrow K^+K^-$ , which cannot be studied at the  $e^+e^-$   $B$ -factories operating at  $\Upsilon(4S)$ , through  $B_d \rightarrow \pi^\mp K^\pm$ . The corresponding experimental results imply already valuable constraints on hadronic parameters – in particular large penguin effects in  $B_d \rightarrow \pi^+\pi^-$  – and upper bounds on direct CP asymmetries. In the case of  $B_d \rightarrow \pi^+\pi^-$ , a lot of space is left for large direct CP violation.

Further  $U$ -spin strategies were proposed. For example,  $B_s \rightarrow \pi^\pm K^\mp$  modes can be combined nicely with the  $B_d \rightarrow \pi^\mp K^\pm$ ,  $B^\pm \rightarrow \pi^\pm K$  system to determine  $\gamma$ . Moreover, angular distributions of certain  $B \rightarrow V_1 V_2$  decays offer important tools to explore CP violation and  $U$ -spin breaking, and various relations between observables can be derived, including also those of the rare decays  $B^\pm \rightarrow K^{*\pm}\gamma$  and  $B^\pm \rightarrow \rho^\pm\gamma$ . It will be exciting to fill these strategies with experimental data!

## 11 Models with Minimal Flavour Violation

### 11.1 General Remarks

So far, we have always discussed new-physics effects in a model-independent manner. Let us now focus on the simplest class of extensions of the Standard Model, which is given by models with “minimal flavour violation” (MFV). In such scenarios for new physics, which are very predictive, as we will see below, the contributions of any new operators beyond those present in the Standard Model are negligible, and all flavour-changing transitions are still governed by the CKM matrix, with no new complex phases beyond the CKM phase [12, 13]. If one assumes, in addition, that all new-physics contributions that are not proportional to  $V_{td(s)}$  play a negligible rôle [13], all Standard-Model expressions for

decay amplitudes, as well as for particle–antiparticle mixing, can be generalized to the MFV models through a straightforward replacement of the initial Wilson coefficients for the renormalization-group evolution from  $\mu = \mathcal{O}(M_W)$  down to appropriate “low-energy” scales  $\mu$ . Within the Standard Model, these coefficients are governed by  $m_t$ -dependent Inami–Lim functions [50], describing penguin and box diagrams with full  $W$ ,  $Z$  and top-quark exchanges [51] (see Subsection 3.3). In the MFV models, the Inami–Lim functions are replaced by new functions  $F_i$ , which acquire now additional dependences on new-physics parameters. If we consider, for instance, expressions (4.3) and (5.6), which are related to  $\varepsilon$  and the off-diagonal element of the  $B_q^0\text{--}\overline{B}_q^0$  mass matrix, respectively, we have just to replace the Inami–Lim function  $S_0(x_t)$  resulting from box diagrams with  $(t, W^\pm)$  exchanges through an appropriate new function, which we denote by  $F_{tt}$  [13, 42]:

$$S_0(x_t) \rightarrow F_{tt}. \quad (11.1)$$

In the case of the rare kaon decays  $K \rightarrow \pi\nu\overline{\nu}$ , we have to deal with a generalized Inami–Lim function  $X$ , replacing the Standard-Model function  $X_0(x_t)$ .

Examples for MFV models of the kind specified above are the Two-Higgs-Doublet Model II (THDM) [290], and the constrained MSSM, if  $\tan\overline{\beta} = v_2/v_1$  is not too large. In the analyses of MFV models performed in [8, 13, 46, 145], it was assumed implicitly that the new functions  $F_i$ , summarizing the Standard-Model and new-physics contributions to  $\varepsilon$ ,  $\Delta M_{d,s}$  and  $K \rightarrow \pi\nu\overline{\nu}$  decays, have the *same* sign as the standard Inami–Lim functions. This assumption is certainly correct in the THDM and the MSSM. On the other hand, as pointed out in [47], it cannot be excluded that there exist MFV models in which the relevant functions  $F_i$  have a sign *opposite* to the corresponding Standard-Model Inami–Lim functions. In fact, in the case of the decay  $B \rightarrow X_s\gamma$ , such a situation is even possible in the MSSM, if particular values of the supersymmetric parameters are chosen. Beyond MFV, scenarios in which the new-physics contributions to neutral meson mixing and rare kaon decays are larger than the Standard-Model contributions and have opposite signs were considered in [291]. Due to the presence of new complex phases and new sources for flavour violation in these general scenarios, their predictive power is, however, much smaller than that of the MFV models considered here. In SUSY scenarios, a vast range of possibilities opens up once the restrictive requirement of MFV is abandoned. Since a detailed discussion of this active research field is beyond the scope of this review, we refer the interested reader to the papers given in [292] and references therein.

The following interesting features of MFV models were recently pointed out:

- There exists a universal unitarity triangle (UUT) [13], which is common to all these models and the Standard Model, and can be constructed by using measurable quantities that depend on the CKM parameters, but are not affected by the new-physics parameters. Simply speaking, these quantities do not depend on the  $F_i$ .

- The interplay between  $\Delta M_d$  and  $\varepsilon$  implies bounds on  $\sin 2\beta$  [46, 47], depending only on  $|V_{cb}|$  and  $|V_{ub}/V_{cb}|$ , as well as on the non-perturbative parameters  $\hat{B}_K$ ,  $\sqrt{\hat{B}_{B_d} f_{B_d}}$  and  $\xi$ , which enter the standard analysis of the unitarity triangle.
- For given  $\text{BR}(K^+ \rightarrow \pi^+ \nu \bar{\nu})$  and  $a_{\psi K_S}$ , only two values for  $\text{BR}(K_L \rightarrow \pi^0 \nu \bar{\nu})$ , corresponding to the two signs of  $X$ , are possible for the full class of MFV models [47]. Moreover, there are absolute lower and upper bounds on  $\text{BR}(K_L \rightarrow \pi^0 \nu \bar{\nu})$  as functions of  $\text{BR}(K^+ \rightarrow \pi^+ \nu \bar{\nu})$ .

The last point, where  $a_{\psi K_S}$  denotes, as usual, the mixing-induced CP asymmetry of the “gold-plated” decay  $B_d \rightarrow J/\psi K_S$  (see (6.6)), provides a remarkable connection between the  $B$ - and  $K$ -meson systems. It should be noted that direct CP violation in  $B_d \rightarrow J/\psi K_S$  is negligibly small in MFV models, as in the Standard Model. Let us now discuss the three points listed above in more detail.

## 11.2 The Universal Unitarity Triangle

Since  $\lambda$  and  $|V_{cb}| = A\lambda^2$  are determined from tree-level  $K$ - and  $B$ -meson decays, these parameters are not affected by new-physics effects in MFV models. A similar comment applies to the determination of  $R_b \propto |V_{ub}/V_{cb}|$ . On the other hand, at first sight, it appears as if the extraction of  $\bar{\rho}$  and  $\bar{\eta}$  was more complicated in MFV models because of additional new-physics parameters. However, as was pointed out in [13], the “true” values of these parameters can still be determined in a transparent way with the help of quantities, which are not affected by the new-physics contributions within MFV models. In particular, a “universal unitarity triangle” (UUT) can be constructed for the Standard Model and the whole class of MFV models. Other “reference” unitarity triangles to search for new physics were proposed in [293].

If we take into account the substitution given in (11.1) and note that the same function  $F_{tt}$  enters in (5.6) for the  $B_d$ - and  $B_s$ -meson systems, we observe that (7.5) allows us to fix  $R_t = |V_{td}/(\lambda V_{cb})|$  also in the case of MFV models. On the other hand, the determination of  $R_t$  through (5.27) depends on  $|F_{tt}|$ , and hence cannot be used for the construction of the UUT.

Whereas  $\Delta M_d/\Delta M_s$  should be available first, there are also other possibilities to determine  $R_t$  in the case of MFV models through  $|V_{td}/V_{ts}|$ , which is – up to corrections of  $\mathcal{O}(\lambda^2)$  – equal to  $|V_{td}/V_{cb}|$  [13]:

$$\frac{\text{BR}(B \rightarrow X_d \nu \bar{\nu})}{\text{BR}(B \rightarrow X_s \nu \bar{\nu})} = \left| \frac{V_{td}}{V_{ts}} \right|^2 \quad (11.2)$$

$$\frac{\text{BR}(B_d \rightarrow \mu^+ \mu^-)}{\text{BR}(B_s \rightarrow \mu^+ \mu^-)} = \frac{\tau_{B_d} M_{B_d}}{\tau_{B_s} M_{B_s}} \left( \frac{f_{B_d}}{f_{B_s}} \right)^2 \left| \frac{V_{td}}{V_{ts}} \right|^2. \quad (11.3)$$

The cleanest relation is (11.2), which is essentially free of hadronic uncertainties (for detailed discussions, see [7, 8]). In (11.3), the theoretical accuracy is limited by  $SU(3)$ -breaking effects in the  $B_d$ - and  $B_s$ -meson decay constants, whereas (7.5) involves, in addition, the ratio  $\sqrt{\hat{B}_{B_s}}/\sqrt{\hat{B}_{B_d}}$ . These  $SU(3)$ -breaking parameters can be determined eventually from lattice calculations with high precision.

As can be seen in Fig. 3 (a), if we measure – in addition to  $R_t$  – the angle  $\beta$ , we may fix the apex of the UUT, yielding  $\bar{\rho}$  and  $\bar{\eta}$ . Since no new phases appear in MFV models, one may think that the determination of  $\beta$  from  $a_{\psi K_S}$  is also not affected by new physics in such scenarios. However, due to a subtlety, this is actually not the case [47]. The point is that we have assumed in the formalism developed in Section 5 that  $S_0(x_t) > 0$ , as emphasized in the paragraph after (5.19). However, since  $S_0(x_t)$  is now replaced by the new parameter  $F_{tt}$ , which needs no longer be positive, the following phase  $\phi_d$  is actually probed through mixing-induced CP violation in  $B_d \rightarrow J/\psi K_S$ :

$$\phi_d = 2\beta + \arg(F_{tt}). \quad (11.4)$$

Consequently, expression (6.6) is generalized as follows:

$$a_{\psi K_S} = \text{sgn}(F_{tt}) \sin 2\beta. \quad (11.5)$$

On the other hand, if we make the replacement (11.1) in (4.3) and (5.27), and do not assume that  $F_{tt} > 0$ , as in the Standard Model, we obtain

$$\sin 2\beta = \text{sgn}(F_{tt}) \frac{1.65}{R_0^2 \eta_2} \left[ \frac{0.204}{A^2 B_K} - \bar{\eta} P_c(\varepsilon) \right], \quad (11.6)$$

where the first term in the parenthesis is typically by a factor 2–3 larger than the second term. Consequently, the sign of  $F_{tt}$  determines the sign of  $\sin 2\beta$ . Moreover, as (4.3) implies  $\bar{\eta} < 0$  for  $F_{tt} < 0$ , also the sign of the second term in the parenthesis is changed. This means that, for a given set of input parameters, not only the sign of  $\sin 2\beta$ , but also its magnitude is affected by a reversal of the sign of  $F_{tt}$ . However, if we use (11.6) to predict  $a_{\psi K_S}$ , we observe that the sign of the resulting CP asymmetry is unaffected:

$$a_{\psi K_S} = \frac{1.65}{R_0^2 \eta_2} \left[ \frac{0.204}{A^2 B_K} - \bar{\eta} P_c(\varepsilon) \right], \quad (11.7)$$

i.e. it is *positive*, which is consistent with the experimental results discussed in 6.1.1.

In [13, 294], a construction of the UUT by means of  $a_{\psi K_S}$  and  $R_t$  determined through  $\Delta M_d/\Delta M_s$  was presented. Generally, for given values of  $(a_{\psi K_S}, R_t)$ , there are eight solutions for  $(\bar{\rho}, \bar{\eta})$ . However, only two solutions – corresponding to the two possible signs of  $F_{tt}$  – are consistent with the upper bound on  $|\beta|$  related to (2.52). For the derivation of the explicit expressions for  $\bar{\rho}$  and  $\bar{\eta}$ , it is useful to consider the following quantity [47]:

$$\text{sgn}(F_{tt}) \text{ctg} \beta = \frac{1 - \bar{\rho}}{|\bar{\eta}|} \equiv f(\beta), \quad (11.8)$$

as (2.45) implies

$$R_t^2 = (1 - \bar{\rho})^2 + \bar{\eta}^2 = [f(\beta)^2 + 1] \bar{\eta}^2. \quad (11.9)$$

Consequently, admitting also negative  $F_{tt}$ , we obtain

$$\bar{\eta} = \text{sgn}(F_{tt}) \left[ \frac{R_t}{\sqrt{f(\beta)^2 + 1}} \right], \quad \bar{\rho} = 1 - f(\beta) |\bar{\eta}|. \quad (11.10)$$

If we take into account the constraint  $\bar{\rho} \leq R_b < 1$ , we conclude that  $f(\beta)$  is always positive. Moreover, because of (11.5), we may write

$$f(\beta) = \frac{1 \pm \sqrt{1 - a_{\psi K_S}^2}}{a_{\psi K_S}} = \text{sgn}(F_{tt}) \left[ \frac{1 \pm |\cos 2\beta|}{\sin 2\beta} \right]. \quad (11.11)$$

Since the upper bound  $|\beta| \lesssim 28^\circ$  corresponding to (2.52) implies  $|\text{ctg}\beta| = f(\beta) \gtrsim 1.9$ , the “–” solution in (11.11) is ruled out, so that the measurement of  $a_{\psi K_S}$  determines  $f(\beta)$  *unambiguously* through

$$f(\beta) = \frac{1 + \sqrt{1 - a_{\psi K_S}^2}}{a_{\psi K_S}}. \quad (11.12)$$

Finally, with the help of (11.10), we arrive at

$$\bar{\eta} = \text{sgn}(F_{tt}) R_t \sqrt{\frac{1 - \sqrt{1 - a_{\psi K_S}^2}}{2}}, \quad \bar{\rho} = 1 - \left[ \frac{1 + \sqrt{1 - a_{\psi K_S}^2}}{a_{\psi K_S}} \right] |\bar{\eta}|. \quad (11.13)$$

Neglecting terms of  $\mathcal{O}(a_{\psi K_S}^4)$ , these expressions simplify to

$$\bar{\eta} = \text{sgn}(F_{tt}) R_t \left[ 1 + \frac{a_{\psi K_S}^2}{8} \right] \frac{a_{\psi K_S}}{2}, \quad \bar{\rho} = 1 - R_t \left[ 1 - \frac{a_{\psi K_S}^2}{8} \right]. \quad (11.14)$$

The function  $f(\beta)$  plays also a key rôle for the analysis of the  $K \rightarrow \pi \nu \bar{\nu}$  system, which will be the topic of Subsection 11.4.

The expressions given in (11.13) are the “master formulae” for the determination of the apex of the UUT. They also allow us – in combination with  $\lambda$  and  $A$  – to calculate  $\varepsilon$ ,  $\Delta M_d$  and  $\Delta M_s$ , as well as the branching ratios for the rare decays in (11.2) and (11.3). Since these quantities depend on the values of the corresponding generalized Inami–Lim functions  $F_i$ , characterizing the various MFV models, a comparison with the data may exclude the Standard Model, and may allow us to differentiate between various MFV scenarios. In particular, it may well be that the observed pattern of observables can only be described by one specific MFV model.

Since  $R_t$  cannot yet be determined through (7.5), the UUT cannot yet be constructed in practice. However, valuable information can nevertheless be obtained from interesting bounds on  $\sin 2\beta$  [46, 47], which hold in the MFV models specified above.

Quantity	Central	Error
$\lambda$	0.222	
$ V_{cb} $	0.041	$\pm 0.002$
$ V_{ub}/V_{cb} $	0.085	$\pm 0.018$
$ V_{ub} $	0.00349	$\pm 0.00076$
$\hat{B}_K$	0.85	$\pm 0.15$
$\sqrt{\hat{B}_{B_d}} f_{B_d}$	230 MeV	$\pm 40$ MeV
$m_t$	166 GeV	$\pm 5$ GeV
$(\Delta M)_d$	$0.487 \text{ ps}^{-1}$	$\pm 0.014 \text{ ps}^{-1}$
$(\Delta M)_s$	$> 15.0 \text{ ps}^{-1}$	
$\xi$	1.15	$\pm 0.06$

Table 7: The ranges of the input parameters for the bounds on  $\sin 2\beta$ .

### 11.3 Bounds on $\sin 2\beta$

The starting point for the derivation of the bounds on  $\sin 2\beta$  is (11.6), where the dependence on new-physics enters implicitly through  $\bar{\eta}$ . Let us first assume that  $\text{sgn}(F_{tt}) = +1$ . Varying over all positive values of  $F_{tt}$  that are consistent with the experimental values for  $\Delta M_{d,s}$ ,  $|V_{ub}/V_{cb}|$  and  $|V_{cb}|$ , and scanning all the relevant input parameters in the ranges given in Table 7 yields the following lower bound on  $\sin 2\beta$  [46]:

$$(\sin 2\beta)_{\min} = 0.42, \quad (11.15)$$

which corresponds to  $\beta \geq 12^\circ$ . This bound could be considerably improved when the values of  $V_{cb}$ ,  $|V_{ub}/V_{cb}|$ ,  $\hat{B}_K$ ,  $\sqrt{\hat{B}_{B_d}} f_{B_d}$ ,  $\xi$  and – in particular of  $\Delta M_s$  – will be known better [8, 46]. A handy approximate formula for  $\sin 2\beta$  as a function of these parameters has recently been given in [145]. Using less conservative ranges of parameters, these authors find  $(\sin 2\beta)_{\min} = 0.52$ .

Let us now consider the case  $\text{sgn}(F_{tt}) = -1$ . Repeating the analysis that lead to (11.15) for  $F_{tt} < 0$  yields the following bound [47]:

$$(-\sin 2\beta)_{\min} = 0.69. \quad (11.16)$$

This result is rather sensitive to the minimal value of  $\sqrt{\hat{B}_{B_d}} f_{B_d}$ . Taking  $(\sqrt{\hat{B}_{B_d}} f_{B_d})_{\min} = 170$  MeV instead of 190 MeV used in (11.16) gives the bound of 0.51. For the same choice, the bound in (11.15) is decreased to 0.35. For  $(\sqrt{\hat{B}_{B_d}} f_{B_d})_{\min} \geq 195$  MeV there are no solutions for  $\sin 2\beta$  for the ranges of parameters given in Table 7; only for  $\hat{B}_K \geq 0.96$ ,  $|V_{cb}| \geq 0.0414$  and  $|V_{ub}/V_{cb}| \geq 0.094$  solutions for  $\sin 2\beta$  exist. Finally, if we assume a smaller uncertainty for  $\Delta M_d$  of  $\pm 0.009 \text{ ps}^{-1}$ , corresponding to (5.28), the numerical value in (11.16) is shifted to 0.71, whereas (11.15) is unaffected.

Since the sign of  $a_{\psi K_S}$  does – in contrast to  $\sin 2\beta$  – not depend on  $\text{sgn}(F_{tt})$ , it is actually more appropriate to consider bounds on this CP-violating observable [47]:

$$(a_{\psi K_S})_{\min} = \begin{cases} 0.42 & (F_{tt} > 0) \\ 0.69 & (F_{tt} < 0). \end{cases} \quad (11.17)$$

The feature that the constraint is substantially stronger for negative  $F_{tt}$  is not surprising, since in this case the contributions to  $\varepsilon$  proportional to  $V_{ts}^* V_{td}$  interfere destructively with the charm contribution. Consequently,  $a_{\psi K_S} = |\sin 2\beta|$  has to be larger to fit  $\varepsilon$ . For  $0.42 < a_{\psi K_S} < 0.69$ , the MFV models with  $F_{tt} < 0$  would be excluded; for  $a_{\psi K_S} < 0.42$ , even all MFV models would be ruled out, thereby implying that new CP-violating phases and/or new operators are required. In anticipation of such a scenario, which was favoured by the “old”  $B$ -factory data, an extension of the MFV supersymmetric models, which could comfortably accommodate lower values of  $a_{\psi K_S}$ , was discussed in [146], introducing an additional flavour-changing structure beyond the CKM matrix. Generalizations of MFV models were also considered in [147], allowing significant contributions of non-standard  $\Delta F = 2$  operators to the low-energy effective Hamiltonian. Their contributions to  $\Delta M_d/\Delta M_s$  would in principle allow  $\gamma$  to be larger than  $90^\circ$  (see Subsection 7.2). For a selection of more general discussions of SUSY models, the reader is referred to [292].

In the spirit of (11.17), the two cases  $F_{tt} > 0$  and  $F_{tt} < 0$  can be distinguished through the measurement of  $a_{\psi K_S}$ . As pointed out in [47], there are also strategies to determine the sign of  $F_{tt}$  directly, allowing interesting consistency checks. For  $a_{\psi K_S} = 0.79 \pm 0.10$ , corresponding to the average given in (6.10), not even the case of MFV models with negative  $F_{tt}$  could be excluded. In view of the most recent Belle result [3] (see (6.9)), the upper bounds given in (2.48) and (2.52), which are implied by  $R_b$  and hold also in MFV models, may play an important rôle to probe these scenarios for new physics in the future. Let us now turn to more refined strategies, using in addition rare kaon decays.

## 11.4 $K \rightarrow \pi\nu\bar{\nu}$ Decays and Connections with $B$ Physics

In MFV models, the short-distance contributions to  $K^+ \rightarrow \pi^+\nu\bar{\nu}$  and  $K_L \rightarrow \pi^0\nu\bar{\nu}$  proportional to  $V_{ts}^* V_{td}$  are described by a function  $X$ , resulting from  $Z^0$ -penguin and box diagrams. As pointed out in [122], if  $\sin 2\beta$  is expressed in terms of the branching ratios for these rare kaon decays, the function  $X$  drops out. Being determined from two branching ratios, there is a four-fold ambiguity in the determination of  $\sin 2\beta$  that is reduced to a two-fold ambiguity for  $\bar{\rho} < 1$ , as required by the size of  $R_b$ . The left over solutions correspond to two signs of  $\sin 2\beta$  that can be adjusted to agree with the analysis of  $\varepsilon$ . In the Standard Model, the THDM and the MSSM, the functions  $F_{tt}$  and  $X$  are both positive, resulting in  $\sin 2\beta$  given by (4.14). However, in general, this needs not be the case, thereby complicating the  $K \rightarrow \pi\nu\bar{\nu}$  analysis; it was recently extended to MFV models with arbitrary signs of  $F_{tt}$  and  $X$  in [47].



### 11.4.1 The Decay $K^+ \rightarrow \pi^+\nu\bar{\nu}$

Within MFV models, the reduced  $K^+ \rightarrow \pi^+\nu\bar{\nu}$  branching ratio  $B_1$  introduced in (4.11) can be expressed as follows:

$$B_1 = \left[ \frac{\text{Im}\lambda_t}{\lambda^5} |X| \right]^2 + \left[ \frac{\text{Re}\lambda_c}{\lambda} \text{sgn}(X) P_c(\nu\bar{\nu}) + \frac{\text{Re}\lambda_t}{\lambda^5} |X| \right]^2, \quad (11.18)$$

where  $\lambda_c \equiv V_{cs}^* V_{cd} = -\lambda(1 - \lambda^2/2)$ , and  $\lambda_t \equiv V_{ts}^* V_{td}$  with

$$\text{Im}\lambda_t = \eta A^2 \lambda^5, \quad \text{Re}\lambda_t = - \left( 1 - \frac{\lambda^2}{2} \right) A^2 \lambda^5 (1 - \bar{\rho}). \quad (11.19)$$

It is now an easy exercise to show that the measured  $K^+ \rightarrow \pi^+\nu\bar{\nu}$  branching ratio determines an ellipse in the  $\bar{\rho}-\bar{\eta}$  plane,

$$\left( \frac{\bar{\rho} - \rho_0}{\bar{\rho}_1} \right)^2 + \left( \frac{\bar{\eta}}{\bar{\eta}_1} \right)^2 = 1, \quad (11.20)$$

centered at  $(\rho_0, 0)$  with

$$\rho_0 = 1 + \text{sgn}(X) \frac{P_c(\nu\bar{\nu})}{A^2 |X|}, \quad (11.21)$$

and having the squared axes

$$\bar{\rho}_1^2 = r_0^2, \quad \bar{\eta}_1^2 = \left( \frac{r_0}{\sigma} \right)^2 \quad \text{with} \quad r_0^2 = \frac{\sigma B_1}{A^4 |X|^2}. \quad (11.22)$$

Note that  $\sigma$  was already defined in (4.16). The ellipse (11.20) intersects with the circle described by (2.44), thereby allowing us to extract  $\bar{\rho}$  and  $\bar{\eta}$ :

$$\bar{\rho} = \frac{1}{1 - \sigma^2} \left[ \rho_0 \mp \sqrt{\sigma^2 \rho_0^2 + (1 - \sigma^2)(r_0^2 - \sigma^2 R_b^2)} \right], \quad \bar{\eta} = \text{sgn}(F_{tt}) \sqrt{R_b^2 - \bar{\rho}^2}. \quad (11.23)$$

The deviation of  $\rho_0$  from unity measures the relative importance of the internal charm contribution. For  $X > 0$ , we have, as usual,  $\rho_0 > 1$  so that the “+” solution in (11.23) is excluded because of  $\bar{\rho} < 1$ . On the other hand, for  $X < 0$ , the center of the ellipse is shifted to  $\rho_0 < 1$ , and for  $|X| \leq P_c(\nu\bar{\nu})/A^2$  can even be at  $\rho_0 \leq 0$ .

### 11.4.2 Unitarity Triangle from $K_L \rightarrow \pi^0\nu\bar{\nu}$ and $K^+ \rightarrow \pi^+\nu\bar{\nu}$

The reduced  $K_L \rightarrow \pi^0\nu\bar{\nu}$  branching ratio  $B_2$  specified in (4.11) is given by

$$B_2 = \left[ \frac{\text{Im}\lambda_t}{\lambda^5} |X| \right]^2. \quad (11.24)$$

$\text{BR}(K^+ \rightarrow \pi^+ \nu \bar{\nu}) [10^{-11}]$	$a_{\psi K_S} = 0.42$	$a_{\psi K_S} = 0.69$	$a_{\psi K_S} = 0.82$
5.0	0.45 (2.0)	1.4 (5.8)	2.2 (8.6)
10.0	1.2 (3.5)	3.8 (10.0)	5.9 (15.0)
15.0	2.1 (4.8)	6.3 (14.0)	9.9 (21.1)
20.0	3.0 (6.2)	9.0 (17.9)	14.1 (27.0)
25.0	3.9 (7.5)	11.8 (21.7)	18.4 (32.8)
30.0	4.9 (8.7)	14.6 (25.4)	22.7 (38.6)

Table 8:  $\text{BR}(K_L \rightarrow \pi^0 \nu \bar{\nu})$  in units of  $10^{-11}$  in MFV models with  $\text{sgn}(X) = +1$  ( $-1$ ) for specific values of  $a_{\psi K_S}$  and  $\text{BR}(K^+ \rightarrow \pi^+ \nu \bar{\nu})$ . We set  $P_c(\nu \bar{\nu}) = 0.40$ .

Following [122], but admitting both signs of  $X$  and  $F_{tt}$ , we obtain

$$\bar{\rho} = 1 + \left[ \frac{\pm \sqrt{\sigma(B_1 - B_2)} + \text{sgn}(X) P_c(\nu \bar{\nu})}{A^2 |X|} \right], \quad \bar{\eta} = \text{sgn}(F_{tt}) \frac{\sqrt{B_2}}{\sqrt{\sigma} A^2 |X|}. \quad (11.25)$$

The dependence on  $|X|$  cancels in the following quantity [47]:

$$r_s \equiv \frac{1 - \bar{\rho}}{\bar{\eta}} = \text{ctg} \beta = \text{sgn}(F_{tt}) \sqrt{\sigma} \left[ \frac{\mp \sqrt{\sigma(B_1 - B_2)} - \text{sgn}(X) P_c(\nu \bar{\nu})}{\sqrt{B_2}} \right], \quad (11.26)$$

allowing the determination of  $\sin 2\beta$  through (4.14). Note that (11.26) reduces to (4.15) in the case of positive values of  $F_{tt}$  and  $X$ . Because of  $a_{\psi K_S} = \text{sgn}(F_{tt}) \sin 2\beta$ , it is actually more appropriate to consider this CP-violating observable, where the  $\text{sgn}(F_{tt})$  factor is cancelled through the one of  $\sin 2\beta$ .

#### 11.4.3 $\text{BR}(K_L \rightarrow \pi^0 \nu \bar{\nu})$ from $a_{\psi K_S}$ and $\text{BR}(K^+ \rightarrow \pi^+ \nu \bar{\nu})$

Since  $a_{\psi K_S}$  and  $\text{BR}(K^+ \rightarrow \pi^+ \nu \bar{\nu})$  will be known rather accurately prior to the measurement of  $\text{BR}(K_L \rightarrow \pi^0 \nu \bar{\nu})$ , it is of particular interest to calculate  $\text{BR}(K_L \rightarrow \pi^0 \nu \bar{\nu})$  as a function of  $a_{\psi K_S}$  and  $\text{BR}(K^+ \rightarrow \pi^+ \nu \bar{\nu})$ . Employing the quantity  $f(\beta)$  introduced in (11.8), we obtain [47]

$$B_1 = B_2 + \left[ \frac{f(\beta) \sqrt{B_2} + \text{sgn}(X) \sqrt{\sigma} P_c(\nu \bar{\nu})}{\sigma} \right]^2. \quad (11.27)$$

In comparison with (11.26), the advantage of (11.27) is the absence of the sign ambiguities due to  $\text{sgn}(F_{tt})$  and the  $\mp$  in front of  $\sqrt{\sigma(B_1 - B_2)}$ . As we have seen in (11.12), the measurement of  $a_{\psi K_S}$  determines  $f(\beta)$  unambiguously. This finding, in combination with (11.27), implies the following interesting feature of the MFV models [47]:

- For given  $a_{\psi K_S}$  and  $\text{BR}(K^+ \rightarrow \pi^+\nu\bar{\nu})$ , only two values of  $\text{BR}(K_L \rightarrow \pi^0\nu\bar{\nu})$ , which correspond to the two possible signs of  $X$ , are allowed for the full class of MFV models, independently of any new parameters present in these models.

Consequently, measuring  $\text{BR}(K_L \rightarrow \pi^0\nu\bar{\nu})$  will either select one of these two possible values, or will rule out all MFV models.

In Table 8, we give  $\text{BR}(K_L \rightarrow \pi^0\nu\bar{\nu})$  in MFV models with  $\text{sgn}(X) = +1$  ( $-1$ ) for specific values of  $a_{\psi K_S}$  and  $\text{BR}(K^+ \rightarrow \pi^+\nu\bar{\nu})$ . Note that the second column gives the absolute lower bound on  $\text{BR}(K_L \rightarrow \pi^0\nu\bar{\nu})$  in the MFV models as a function of  $\text{BR}(K^+ \rightarrow \pi^+\nu\bar{\nu})$ . This bound follows simply from the lower bound in (11.15). On the other hand, the last column gives the corresponding absolute upper bound. This bound is the consequence of (2.52). The third column gives the lower bound on  $\text{BR}(K_L \rightarrow \pi^0\nu\bar{\nu})$  corresponding to the bound in (11.16) that applies for negative  $F_{tt}$ .

The remarkable correlation between the branching ratios of the rare  $K \rightarrow \pi\nu\bar{\nu}$  decays and mixing-induced CP violation in  $B_d \rightarrow J/\psi K_S$  within MFV models becomes more transparent in Figs. 37 and 38. In Fig. 37, we show  $\text{BR}(K_L \rightarrow \pi^0\nu\bar{\nu})$  as a function of  $\text{BR}(K^+ \rightarrow \pi^+\nu\bar{\nu})$  for various values of  $a_{\psi K_S}$  in the case of  $\text{sgn}(X) = +1$ . The corresponding plot for  $\text{sgn}(X) = -1$  is given in Fig. 38. It should be emphasized that these curves are universal for all MFV models. Looking at Table 8 and Figs. 37 and 38, we observe that the measurement of  $\text{BR}(K_L \rightarrow \pi^0\nu\bar{\nu})$ ,  $\text{BR}(K^+ \rightarrow \pi^+\nu\bar{\nu})$  and  $a_{\psi K_S}$  will easily allow us to check whether a MFV model is actually realized and – if so – to distinguish between the two signs of  $X$ . The uncertainty due to  $P_c(\nu\bar{\nu})$  is non-negligible, but should be decreased through improved knowledge of the charm-quark mass.

It is interesting to note that the upper bound on  $\text{BR}(K_L \rightarrow \pi^0\nu\bar{\nu})$  in the last column of Table 8 is substantially stronger than the model-independent bound following from isospin symmetry [295]:

$$\text{BR}(K_L \rightarrow \pi^0\nu\bar{\nu}) < 4.4 \times \text{BR}(K^+ \rightarrow \pi^+\nu\bar{\nu}). \quad (11.28)$$

Indeed, taking the experimental bound  $\text{BR}(K^+ \rightarrow \pi^+\nu\bar{\nu}) \leq 5.9 \times 10^{-10}$  (90% C.L.) from AGS E787 [121] yields [47]

$$\text{BR}(K_L \rightarrow \pi^0\nu\bar{\nu})_{\text{MFV}} \leq \begin{cases} 4.9 \times 10^{-10} & \text{sgn}(X) = +1 \\ 7.1 \times 10^{-10} & \text{sgn}(X) = -1. \end{cases} \quad (11.29)$$

This should be compared with  $\text{BR}(K_L \rightarrow \pi^0\nu\bar{\nu}) < 26 \times 10^{-10}$  (90% C.L.) following from (11.28), and with the present upper bound from the KTeV experiment [296], which is given by  $\text{BR}(K_L \rightarrow \pi^0\nu\bar{\nu}) < 5.9 \times 10^{-7}$ .

The decay  $K^+ \rightarrow \pi^+\nu\bar{\nu}$  has already been observed at Brookhaven, with the branching ratio given in (4.10). In the Standard Model, one expects the  $K \rightarrow \pi\nu\bar{\nu}$  branching ratios listed in (4.9). As can be seen in Table 8 and Figs. 37 and 38, the bounds in (11.29)

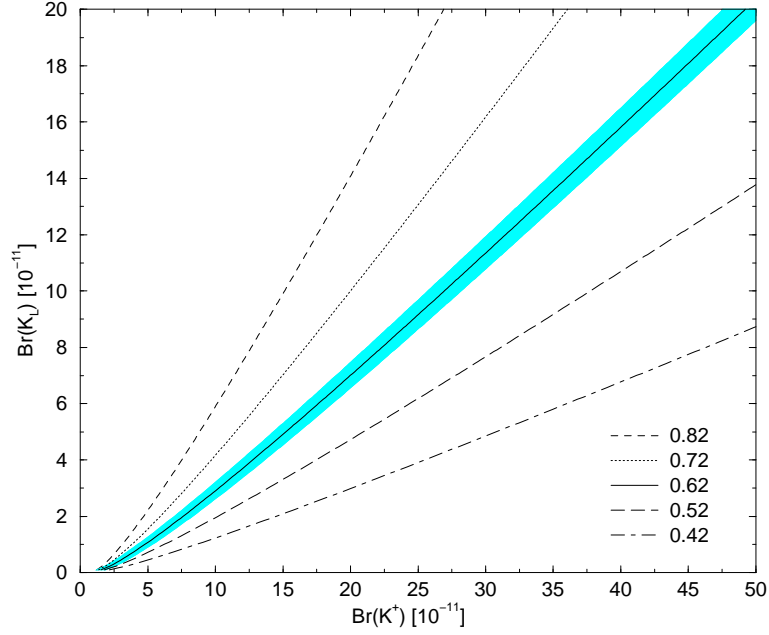


Figure 37:  $\text{BR}(K_L \rightarrow \pi^0 \nu \bar{\nu})$  as a function of  $\text{BR}(K^+ \rightarrow \pi^+ \nu \bar{\nu})$  for several values of the mixing-induced CP asymmetry  $a_{\psi K_S}$  of  $B_d \rightarrow J/\psi K_S$  in the case of  $\text{sgn}(X) = +1$ . The band illustrates the uncertainty due to  $P_c(\nu \bar{\nu}) = 0.40 \pm 0.06$  for  $a_{\psi K_S} = 0.62$ .

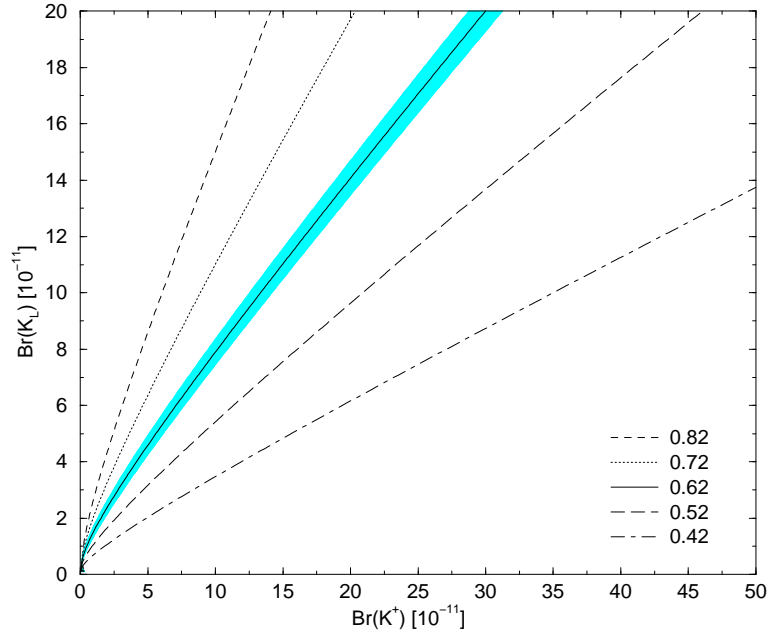


Figure 38:  $\text{BR}(K_L \rightarrow \pi^0 \nu \bar{\nu})$  as a function of  $\text{BR}(K^+ \rightarrow \pi^+ \nu \bar{\nu})$  for several values of the mixing-induced CP asymmetry  $a_{\psi K_S}$  of  $B_d \rightarrow J/\psi K_S$  in the case of  $\text{sgn}(X) = -1$ . The band illustrates the uncertainty due to  $P_c(\nu \bar{\nu}) = 0.40 \pm 0.06$  for  $a_{\psi K_S} = 0.62$ .

can be improved considerably through better measurements of  $\text{BR}(K^+ \rightarrow \pi^+\nu\bar{\nu})$  and  $a_{\psi K_S}$ . A new experiment at Brookhaven, AGS E949, is expected to reach a sensitivity for  $K^+ \rightarrow \pi^+\nu\bar{\nu}$  of  $10^{-11}/\text{event}$ . In the more distant future, the CKM experiment at Fermilab aims at a sensitivity of  $10^{-12}/\text{event}$ , which would correspond to a measurement of  $\text{BR}(K^+ \rightarrow \pi^+\nu\bar{\nu})$  at the level of 10%. The exploration of  $K_L \rightarrow \pi^0\nu\bar{\nu}$  is even more challenging. However, dedicated experiments at Brookhaven, Fermilab and KEK aim nevertheless at measurements of  $\text{BR}(K_L \rightarrow \pi^0\nu\bar{\nu})$  at the level of 10%, which may be available around 2005. For a much more detailed discussion of the experimental prospects for  $K \rightarrow \pi\nu\bar{\nu}$  analyses, we refer the reader to [10].

#### 11.4.4 Upper Bound on $\text{BR}(K_L \rightarrow \pi^0\nu\bar{\nu})$ from $\text{BR}(B \rightarrow X_s\nu\bar{\nu})$

Within MFV models, the branching ratio for the inclusive rare decay  $B \rightarrow X_s\nu\bar{\nu}$  can be written as follows [8]:

$$\text{BR}(B \rightarrow X_s\nu\bar{\nu}) = 1.57 \times 10^{-5} \left[ \frac{\text{BR}(B \rightarrow X_c e \bar{\nu}_e)}{0.104} \right] \left| \frac{V_{ts}}{V_{cb}} \right|^2 \left[ \frac{0.54}{f(z)} \right] X^2, \quad (11.30)$$

where  $f(z) = 0.54 \pm 0.04$  is the phase-space factor for  $B \rightarrow X_c e \bar{\nu}_e$  with  $z = m_c^2/m_b^2$ , and  $\text{BR}(B \rightarrow X_c e \bar{\nu}_e) = 0.104 \pm 0.004$ . Formulae (11.24) and (11.30) imply an interesting relation between the decays  $K_L \rightarrow \pi^0\nu\bar{\nu}$  and  $B \rightarrow X_s\nu\bar{\nu}$ , which is given as follows:

$$\text{BR}(K_L \rightarrow \pi^0\nu\bar{\nu}) = 42.3 \times (\text{Im}\lambda_t)^2 \left[ \frac{0.104}{\text{BR}(B \rightarrow X_c e \bar{\nu}_e)} \right] \left| \frac{V_{cb}}{V_{ts}} \right|^2 \left[ \frac{f(z)}{0.54} \right] \text{BR}(B \rightarrow X_s\nu\bar{\nu}). \quad (11.31)$$

This expression holds for all MFV models and represents another connection between  $K$ - and  $B$ -meson decays, in addition to those discussed above and in [120, 122, 123, 145, 297].

In order to obtain another upper bound on  $\text{BR}(K_L \rightarrow \pi^0\nu\bar{\nu})$ , we take into account the following experimental constraint [298]:

$$\text{BR}(B \rightarrow X_s\nu\bar{\nu}) < 6.4 \times 10^{-4} \quad (90\% \text{ C.L.}), \quad (11.32)$$

as well as the bounds on  $|\text{Im}\lambda_t|$ , which were derived in [47] for MFV models:<sup>18</sup>

$$|\text{Im}\lambda_t|_{\text{max}} = \begin{cases} 1.74 \times 10^{-4} & (F_{tt} > 0) \\ 1.70 \times 10^{-4} & (F_{tt} < 0), \end{cases} \quad |\text{Im}\lambda_t|_{\text{min}} = \begin{cases} 0.55 \times 10^{-4} & (F_{tt} > 0) \\ 1.13 \times 10^{-4} & (F_{tt} < 0). \end{cases} \quad (11.33)$$

Setting, in addition to (11.32),  $\text{Im}\lambda_t = 1.74 \times 10^{-4}$ ,  $|V_{ts}| = |V_{cb}|$ ,  $f(z) = 0.58$  and  $\text{BR}(B \rightarrow X_c e \bar{\nu}_e) = 0.10$ , (11.31) implies the upper bound [47]

$$\text{BR}(K_L \rightarrow \pi^0\nu\bar{\nu}) < 9.2 \times 10^{-10} \quad (90\% \text{ C.L.}), \quad (11.34)$$

which is not much weaker than the bound in (11.29). Since the experimental bound in (11.32) should be improved through the  $B$ -factories, also (11.34) should be improved in the next couple of years.

<sup>18</sup>Note the relation  $J_{\text{CP}} = \lambda(1 - \lambda^2/2) |\text{Im}\lambda_t|$  between the Jarlskog Parameter  $J_{\text{CP}}$  and  $\text{Im}\lambda_t$ .

### 11.4.5 Towards a Determination of $X$

The strategy discussed in 11.4.3, which is based on Figs. 37 and 38 and involves only  $a_{\psi K_S}$ ,  $\text{BR}(K^+ \rightarrow \pi^+ \nu \bar{\nu})$  and  $\text{BR}(K_L \rightarrow \pi^0 \nu \bar{\nu})$ , allows an elegant check whether a MFV model is actually realized in nature and – if so – to determine the sign of  $X$ . In order to determine also  $|X|$ , which would be a very important information, providing valuable constraints on the MFV models,  $\Delta M_d/\Delta M_s$  is needed as an additional input, as illustrated in more detail in [47]. Within the Standard Model, we have  $X \approx 1.5$ . Constraints on this parameter were recently derived in [47, 145], yielding  $|X| < 6.8$ .

## 11.5 Summary

The simplest class of extensions of the Standard Model is given by new-physics scenarios with minimal flavour violation. For such models, a universal unitarity triangle can be constructed through quantities, which are not affected by the new-physics parameters, for instance through the ratio  $\Delta M_d/\Delta M_s$  and the mixing-induced CP asymmetry  $a_{\psi K_S}$  of  $B_d \rightarrow J/\psi K_S$ . Although no new complex phases are present in such MFV models, we may encounter discrepancies between the UUT and the contours in the  $\bar{\rho}-\bar{\eta}$  plane implied by  $\Delta M_d$  and  $\varepsilon$ , thereby indicating physics beyond the Standard Model.

At present, the UUT cannot yet be constructed in practice. However, interesting bounds on  $a_{\psi K_S}$  can be derived, allowing already a comparison with the  $B$ -factory results. Within MFV models, both  $\varepsilon$  and  $B_{d,s}^0 - \overline{B_{d,s}^0}$  mixing are governed by a single generalized Inami–Lim function  $F_{tt}$ . If  $a_{\psi K_S}$  is found to be smaller than 0.69, all models with  $F_{tt} < 0$  would be excluded. In the case of  $a_{\psi K_S} < 0.42$ , also the MFV models with  $F_{tt} > 0$  would be ruled out, which would imply new CP-violating weak phases and/or new operators. The most recent  $B$ -factory data are no longer in favour of small values of  $a_{\psi K_S}$ , and the present world average does not even allow us to exclude MFV models with negative  $F_{tt}$ . In fact, in view of the most recent Belle result, the upper bound  $(a_{\psi K_S})_{\text{max}} = 0.82$  that is due to  $R_b^{\text{max}} = 0.46$  may play an important rôle in the future.

Further insights are provided by remarkable connections between  $B$  physics and the rare kaon decays  $K^+ \rightarrow \pi^+ \nu \bar{\nu}$  and  $K_L \rightarrow \pi^0 \nu \bar{\nu}$ , which are characterized in MFV models through a generalized Inami–Lim function  $X$ . In particular,  $\text{BR}(K_L \rightarrow \pi^0 \nu \bar{\nu})$  can be predicted, for given  $a_{\psi K_S}$ , as a function of  $\text{BR}(K^+ \rightarrow \pi^+ \nu \bar{\nu})$ . These correlations depend only on the sign of  $X$ , i.e. for given  $\text{BR}(K^+ \rightarrow \pi^+ \nu \bar{\nu})$  and  $a_{\psi K_S}$ , only two values for  $\text{BR}(K_L \rightarrow \pi^0 \nu \bar{\nu})$ , corresponding to the two signs of  $X$ , are possible in the full class of MFV models, thereby offering a simple check whether such a model is actually realized in nature. In this context, it should be noted that  $\text{BR}(K^+ \rightarrow \pi^+ \nu \bar{\nu})$  and  $a_{\psi K_S}$  will be known rather accurately prior to the measurement of  $\text{BR}(K_L \rightarrow \pi^0 \nu \bar{\nu})$ . In addition, there are various bounds on  $\text{BR}(K_L \rightarrow \pi^0 \nu \bar{\nu})$ , where also the inclusive rare decay  $B \rightarrow X_s \nu \bar{\nu}$  would be very useful.

## 12 Further Interesting Aspects of $B$ Physics

In addition to the decays to explore CP violation considered in this review, there are also other interesting aspects of  $B$  physics, which we could not cover here. They are mainly related to rare decays of the following kind:  $B \rightarrow K^*\gamma$  and  $B \rightarrow \rho\gamma$ , which appeared briefly in Subsection 10.5,  $B \rightarrow K^*\mu^+\mu^-$  and  $B_{s,d} \rightarrow \mu^+\mu^-$ . The corresponding inclusive decays, for example  $B \rightarrow X_s\gamma$ , are also of particular interest, suffering from smaller theoretical uncertainties. Within the Standard Model, these transitions occur only at the one-loop level, exhibit small branching ratios at the  $10^{-4}$ – $10^{-10}$  level, do not – apart from  $B \rightarrow \rho\gamma$  – show sizeable CP-violating effects, and depend on  $|V_{ts}|$  or  $|V_{td}|$ . A measurement of these CKM factors through such decays would be complementary to the one from  $B_{s,d}^0\text{--}\overline{B}_{s,d}^0$  mixing. Since rare  $B$  decays are absent at the tree level in the Standard Model, they represent interesting probes to search for new physics. Concerning the status of  $B \rightarrow X_s\gamma$ , the present situation is as follows [299]:

$$\text{BR}(B \rightarrow X_s\gamma)_{\text{exp}} = (3.11 \pm 0.39) \times 10^{-4} \quad (12.1)$$

$$\text{BR}(B \rightarrow X_s\gamma)_{\text{th}} = (3.73 \pm 0.30) \times 10^{-4}, \quad (12.2)$$

corresponding to a difference between experiment and theory at the  $1.4\sigma$  level. It will be interesting to see whether a serious discrepancy will arise in the future, which could complement the one between a recent measurement of the anomalous magnetic moment of the myon and the Standard-Model expectation at the  $2.6\sigma$  level [300].

For detailed discussions of the many interesting aspects of rare  $B$  decays, and the hard theoretical work that went into these transitions, the reader is referred to the overview articles listed in [8, 299, 301].

## 13 Conclusions and Outlook

I hope that this review could convince the reader that the phenomenology of CP violation in the  $B$  system is a very interesting topic, and provides a fertile testing ground for the Standard-Model description of CP violation. In this respect, non-leptonic  $B$  decays play a key rôle, allowing various direct measurements of the angles of the unitarity triangle of the CKM matrix. Here the goal is to overconstrain this triangle as much as possible, not only through determinations of its angles, but also through measurements of its sides. Concerning the latter aspect, the observation of  $B_s^0\text{--}\overline{B}_s^0$  mixing, which is expected at run II of the Tevatron, will be an important ingredient. There is a strong hope that discrepancies will show up in this rich research programme, which may eventually open a window to the physics beyond the Standard Model.

Let us summarize in the following the most promising channels:

- The “gold-plated” mode  $B_d \rightarrow J/\psi K_S$  allows us to determine  $\sin 2\beta$  through its mixing-induced CP asymmetry  $a_{\psi K_S}$ . Making use of this and similar channels, the BaBar and Belle collaborations could recently observe CP violation in the  $B$  system, thereby establishing this phenomenon for the first time outside the kaon system. Since the corresponding results for  $\sin 2\beta$  are not fully consistent with each other, the measurement of this quantity will continue to be a very exciting topic. Taking into account also previous results from the CDF and ALEPH collaborations, the resulting average for  $\sin 2\beta$  is now in good agreement with the range implied by the “standard analysis” of the unitarity triangle. However, new physics may even hide in such a situation, since only  $\sin 2\beta$  and not  $\beta$  itself is measured. An important further step would be a determination of  $\cos 2\beta$ . In this context, a time-dependent analysis of the  $B_d \rightarrow J/\psi[\rightarrow \ell^+\ell^-]K^*[\rightarrow \pi^0 K_S]$  angular distribution would be useful. The preferred mechanism for new physics to affect these measurements is through contributions to  $B_d^0-\overline{B}_d^0$  mixing.
- In the Standard Model, the penguin mode  $B_d \rightarrow \phi K_S$  allows also a determination of  $\sin 2\beta$  through its mixing-induced CP asymmetry. A comparison with  $a_{\psi K_S}$  may indicate new-physics contributions to decay amplitudes. Since the  $B_d \rightarrow \phi K_S$  decay is due to  $\overline{b} \rightarrow \overline{s}$  flavour-changing neutral-current processes, it is very sensitive to such effects. In order to get the full picture,  $B^\pm \rightarrow \phi K^\pm$  and  $B^\pm \rightarrow J/\psi K^\pm$  modes should be analysed as well.
- The CP-violating observables of  $B_d \rightarrow \pi^+\pi^-$  should be measured, although an interpretation in terms of  $\alpha$  is problematic because of penguin topologies, requiring further inputs (see below). In addition to certain  $B \rightarrow \pi K$  modes,  $B_d \rightarrow \pi^+\pi^-$  may establish direct CP violation in the  $B$  system. The measurement of  $B^\pm \rightarrow \pi^\pm\pi^0$  should be refined, and efforts be made to constrain  $B_d \rightarrow \pi^0\pi^0$ .
- The physics potential of  $B \rightarrow \pi K$  decays is very promising for the  $B$ -factories to determine  $\gamma$ . Since these modes are governed by penguin topologies, they are sensitive probes for new physics. Consequently, discrepancies of the extracted values of  $\gamma$  with other approaches may well show up. In order to probe the importance of rescattering effects,  $B^\pm \rightarrow K^\pm K$  modes should be measured as well.

All these decays are accessible at the  $e^+e^-$   $B$ -factories operating at the  $\Upsilon(4S)$  resonance. Further exciting perspectives open up at hadron colliders, where also decays of  $B_s$ -mesons can be studied, involving the following major aspects:

- The present lower bound on  $\Delta M_s$  has already an important impact on the allowed range in the  $\overline{\rho}-\overline{\eta}$  plane, implying  $\gamma < 90^\circ$ . Much more stringent constraints can be obtained through a measurement of  $\Delta M_s$ , allowing in particular the construction of the “universal unitarity triangle” for MFV models.



- The “gold-plated” mode for  $B$ -physics studies at hadron machines is  $B_s \rightarrow J/\psi\phi$ , which is the  $B_s$ -meson counterpart of  $B_d \rightarrow J/\psi K_S$ . Its angular distribution allows us to determine the  $B_s^0\text{--}\overline{B}_s^0$  mixing parameters  $\Delta M_s$  and  $\Delta\Gamma_s$ , and to probe the tiny mixing phase  $\phi_s$ , which is related to another unitarity triangle. Since CP violation is very small in  $B_s \rightarrow J/\psi\phi$  within the Standard Model, it is an important tool to search for new physics.
- The decay  $B_s \rightarrow K^+K^-$  is related to  $B_d \rightarrow \pi^+\pi^-$  through the  $U$ -spin symmetry of strong interactions and allows an interesting determination of  $\beta$  and  $\gamma$  that is – apart from other advantages – not affected by penguin or rescattering processes. Further strategies to extract  $\gamma$  are provided by other  $U$ -spin related modes.

It is expected that already run II of the Tevatron will make important contributions to these topics. In the LHC era, the physics potential of the  $B_s$  system can then be fully exploited. As we have seen in this review, there are also many other interesting strategies to explore CP violation, involving, for example,  $B \rightarrow \rho\pi$ ,  $B_d \rightarrow D^{*\pm}\pi^\mp$ ,  $B_u^\pm \rightarrow K^\pm D$ ,  $B_c^\pm \rightarrow D_s^\pm D$  or  $B_s \rightarrow D_s^\pm K^\mp$  decays. However, in the practical implementation of these approaches, we have to deal with more or less serious challenges.

Although there is usually a strong emphasis on the extraction of weak phases from studies of CP violation, it should not be forgotten that the corresponding strategies provide, in several cases, also valuable insights into hadron dynamics. For example, also CP-conserving strong phases or certain penguin parameters can be determined, allowing a comparison with theoretical predictions. Concerning the theoretical description of non-leptonic  $B$  decays, interesting progress has recently been made for a large class of decays in the heavy-quark limit, including  $B \rightarrow \pi K, \pi\pi$  modes. As important applications,  $SU(3)$ -breaking effects in the  $B \rightarrow \pi K$  strategies to probe  $\gamma$  can be controlled more reliably, and rescattering processes are found to play a minor rôle. Further progress, concerning mainly the importance of  $\Lambda_{\text{QCD}}/m_b$  corrections, will hopefully be made.

In the Standard Model and its extensions with minimal flavour violation, there are interesting connections between  $B$  physics and the rare kaon decays  $K^+ \rightarrow \pi^+\nu\bar{\nu}$  and  $K_L \rightarrow \pi^0\nu\bar{\nu}$ . In such models, these decays and  $(\varepsilon, \Delta M_{d,s})$  are characterized by two generalized Inami–Lim functions  $X$  and  $F_{tt}$ , respectively. For given values of  $a_{\psi K_S}$  and  $\text{BR}(K^+ \rightarrow \pi^+\nu\bar{\nu})$ ,  $\text{BR}(K_L \rightarrow \pi^0\nu\bar{\nu})$  can be predicted, where only two values are allowed for the whole class of MFV models, corresponding to the two possible signs of  $X$ . Following these lines, MFV scenarios can be confirmed or excluded in an elegant manner. There are dedicated experiments at Brookhaven, Fermilab and KEK to explore  $K \rightarrow \pi\nu\bar{\nu}$  decays, aiming at measurements of their branching ratios at the 10% level.

Interestingly, already the CP asymmetry  $a_{\psi K_S}$  may provide insights into MFV models, since bounds on this observable can be derived. If  $a_{\psi K_S}$  is found to be smaller than 0.69, the MFV models with  $F_{tt} < 0$  would be excluded, whereas for  $a_{\psi K_S} < 0.42$  also those

with  $F_{tt} > 0$ , i.e. all MFV models would be ruled out. In this exciting case, new CP-violating phases and/or new operators would be required. Due to reduced uncertainties of the relevant input parameters, these bounds can be improved in the future. The most recent  $B$ -factory data are no longer in favour of small values of  $a_{\psi K_S}$ , and the present world average does not even allow us to exclude MFV models with negative  $F_{tt}$ . Consequently, an important rôle may be played in the future by the upper bound on  $a_{\psi K_S}$  that is implied by the CKM factor  $R_b$ , yielding  $(a_{\psi K_S})_{\max} = 0.82$  for  $R_b^{\max} = 0.46$ .

In view of the rich experimental programmes of this decade and the strong interaction between theory and experiment, I have no doubt that an exciting future is ahead of us!

### *Acknowledgements*

First of all, I would like to thank Patricia Ball, Andrzej Buras, Amol Dighe, Isard Dunietz, Thomas Mannel, Joaquim Matias, Ulrich Nierste and Daniel Wyler for the collaborations on several of the topics covered in this review. I am also grateful to Ahmed Ali, Peter Buchholz, Wilfried Buchmüller, Andreas Ringwald, Fridger Schrempp, Alan Schwartz, Guy Wilkinson and Frank Würthwein for interesting discussions.

## References

- [1] J.H. Christenson, J.W. Cronin, V.L. Fitch and R. Turlay, *Phys. Rev. Lett.* **13** (1964) 138.
- [2] BaBar Collaboration (B. Aubert *et al.*), *Phys. Rev. Lett.* **87** (2001) 091801.
- [3] Belle Collaboration (K. Abe *et al.*), *Phys. Rev. Lett.* **87** (2001) 091802.
- [4] G. Branco, L. Lavoura and J. Silva, *CP Violation* (Oxford Science Publications, Clarendon Press, Oxford, 1999);  
I.I. Bigi and A.I. Sanda, *CP Violation* (Cambridge Monographs on Particle Physics, Nuclear Physics and Cosmology, Cambridge University Press, Cambridge, 2000).
- [5] J.L. Rosner, lectures given at TASI 2000, June 4–30, 2000, Boulder, Colorado, EFI-2000-47 [hep-ph/0011355];  
R. Fleischer, lectures given at NATO ASI 2000, June 26 – July 7, 2000, Cascais, Portugal, DESY 00-170 [hep-ph/0011323];  
Y. Nir, lectures given at 27th SLAC Summer Institute on Particle Physics, July 7–16, 1999, Stanford, California, IASSNS-HEP-99-96 [hep-ph/9911321].
- [6] M. Gronau, talk given at BCP4, February 19–23, 2001, Ise-Shima, Japan [hep-ph/0104050];  
Proceedings of the UK Phenomenology Workshop on Heavy Flavour and CP Violation, Durham, England, September 17–22, 2000, T. Hurth *et al.*, *J. Phys.* **G27** (2001) 1277;  
D. Wyler, talk given at RADCOR 2000, September 11–15, 2000, Carmel, California, ZU-01-01 [hep-ph/0101259];  
J. Ellis, *Nucl. Phys. Proc. Suppl.* **99** (2001) 331;  
P. Ball, talk given at 4th Rencontres du Vietnam, July 19–25, 2000, Hanoi, Vietnam, CERN-TH-2000-299 [hep-ph/0010024].
- [7] A.J. Buras and R. Fleischer, in *Heavy Flavours II*, eds. A.J. Buras and M. Lindner, World Scientific, Singapore (1998) p. 65 [hep-ph/9704376].
- [8] A.J. Buras, lectures given at the Erice International School of Subnuclear Physics: Theory and Experiment Heading for New Physics, August 27 – September 5, 2000, Erice, Italy, TUM-HEP-402/01 [hep-ph/0101336].
- [9] *The BaBar Physics Book*, eds. P. Harrison and H.R. Quinn, SLAC report 504 (1998);  
Workshop on *B* Physics at the Tevatron Run II and Beyond, see

- <http://www-theory.fnal.gov/people/ligeti/Brun2/>;  
Report of the  $b$ -decay Working Group of the Workshop *Standard Model Physics (and More) at the LHC*, P. Ball *et al.*, CERN-TH/2000-101 [hep-ph/0003238].
- [10] L. Littenberg, BNL-67772 [hep-ex/0010048].
- [11] For reviews, see Y. Grossman, Y. Nir and R. Rattazzi, in *Heavy Flavours II*, eds. A.J. Buras and M. Lindner, World Scientific, Singapore (1998) p. 755 [hep-ph/9701231];  
A. Masiero and O. Vives, *Ann. Rev. Nucl. Part. Sci.* **51** (2001) 161;  
M. Gronau and D. London *Phys. Rev.* **D55** (1997) 2845;  
Y. Nir and H.R. Quinn, *Annu. Rev. Nucl. Part. Sci.* **42** (1992) 211;  
R. Fleischer, in the proceedings of the 7th International Symposium on Heavy Flavor Physics, July 7–11, 1997, Santa Barbara, California, ed. C. Campagnari, World Scientific, Singapore (1999) p. 155 [hep-ph/9709291];  
L. Wolfenstein, *Phys. Rev.* **D57** (1998) 6857.
- [12] M. Ciuchini, G. Degrossi, P. Gambino and G.F. Giudice, *Nucl. Phys.* **B534** (1998) 3.
- [13] A.J. Buras, P. Gambino, M. Gorbahn, S. Jäger and L. Silvestrini, *Phys. Lett.* **B500** (2001) 161.
- [14] For overviews, see E. Akhmedov, lectures given at NATO ASI 2000, June 26 – July 7, 2000, Cascais, Portugal, hep-ph/0011353;  
B. Kayser, lectures given at TASI 2000, June 4–30, 2000, Boulder, Colorado, hep-ph/0104147;  
V. Barger, talk given at PASCOS 99, Granlibakken, Tahoe City, California, December 10–16, 1999, MADPH-00-1168 [hep-ph/0005011];  
S.M. Bilenkii, C. Giunti and W. Grimus, *Prog. Part. Nucl. Phys.* **43** (1999) 1.
- [15] A. De Rujula, M.B. Gavela and P. Hernandez, *Nucl. Phys.* **B547** (1999) 21;  
K. Dick, M. Freund, M. Lindner and A. Romanino, *Nucl. Phys.* **B562** (1999) 29.
- [16] A.D. Sakharov, *JETP Lett.* **5** (1967) 24.
- [17] For an overview, see W. Buchmüller, lectures given at NATO ASI 2000, June 26 – July 7, 2000, Cascais, Portugal, DESY-00-194 [hep-ph/0101102].
- [18] V.A. Rubakov and M.E. Shaposhnikov, *Usp. Fiz. Nauk* **166** (1996) 493; *Phys. Usp.* **39** (1996) 461;  
A. Riotto and M. Trodden, *Annu. Rev. Nucl. Part. Sci.* **49** (1999) 35.

- [19] I.I. Bigi, talk given at BCP4, February 19–23, 2001, Ise-Shima, Japan, UND-HEP-01-BIG 02 [hep-ph/0104008].
- [20] S. Bergmann and Y. Nir, *J. High Energy Phys.* **9909** (1999) 031;  
Y. Nir, *Nuovo Cim.* **109A** (1996) 991;  
G. Blaylock, A. Seiden and Y. Nir, *Phys. Lett.* **B355** (1995) 555;  
L. Wolfenstein, *Phys. Rev. Lett.* **75** (1995) 2460.
- [21] X.-G. He, B.H. McKellar and S. Pakvasa, *Int. J. Mod. Phys.* **A4** (1989) 5011;  
W. Bernreuther and M. Suzuki, *Rev. Mod. Phys.* **63** (1991) 313;  
S.M. Barr, *Int. J. Mod. Phys.* **A8** (1993) 209;  
W. Bernreuther, PITHA-98-25 [hep-ph/9808453];  
V. Barger, T. Falk, T. Han, J. Jiang, T. Li and T. Plehn, *Phys. Rev.* **D64** (2001) 056007.
- [22] G. Valencia, *AIP Conf. Proc.* **539** (2000) 80;  
S. Pakvasa, UH-511-955-00, hep-ph/0002210;  
X.-G. He, H. Murayama, S. Pakvasa and G. Valencia, *Phys. Rev.* **D61** (2000) 071701.
- [23] S.L. Glashow, *Nucl. Phys.* **22** (1961) 579;  
S. Weinberg, *Phys. Rev. Lett.* **19** (1967) 1264;  
A. Salam, in *Elementary Particle Theory*, ed. N. Svartholm, Almqvist and Wiksell, Stockholm (1968).
- [24] N. Cabibbo, *Phys. Rev. Lett.* **10** (1963) 531.
- [25] M. Kobayashi and T. Maskawa, *Progr. Theor. Phys.* **49** (1973) 652.
- [26] R.D. Peccei, UCLA-98-TEP-21 [hep-ph/9807514].
- [27] L.-L. Chau and W.-Y. Keung, *Phys. Rev. Lett.* **53** (1984) 1802;  
H. Harari and M. Leurer, *Phys. Lett.* **B181** (1986) 123;  
H. Fritzsch and J. Plankl, *Phys. Rev.* **D35** (1987) 1732;  
F.J. Botella and L.-L. Chao, *Phys. Lett.* **B168** (1986) 97.
- [28] H. Fritzsch and Z.-Z. Xing, *Phys. Lett.* **B413** (1997) 396.
- [29] M. Schmidtler and K.R. Schubert, *Z. Phys.* **C53** (1992) 347.
- [30] A.J. Buras, M.E. Lautenbacher and G. Ostermaier, *Phys. Rev.* **D50** (1994) 3433.
- [31] L. Wolfenstein, *Phys. Rev. Lett.* **51** (1983) 1945.

- [32] C. Jarlskog, *Phys. Rev. Lett.* **55** (1985) 1039; *Z. Phys.* **C29** (1985) 491.
- [33] J. Bernabeu, G. Branco and M. Gronau, *Phys. Lett.* **B169** (1986) 243.
- [34] R. Aleksan, B. Kayser and D. London, *Phys. Rev. Lett.* **73** (1994) 18.
- [35] C. Jarlskog and R. Stora, *Phys. Lett.* **B208** (1988) 268.
- [36] L.L. Chau and W.-Y. Keung, *Phys. Rev. Lett.* **53** (1984) 1802.
- [37] For a review, see M. Neubert, in *Heavy Flavours II*, eds. A.J. Buras and M. Lindner, World Scientific, Singapore (1998) p. 239 [hep-ph/9702375].
- [38] M. Ciuchini *et al.*, *J. High Energy Phys.* **0107** (2001) 013.
- [39] CLEO Collaboration (B.H. Behrens *et al.*), *Phys. Rev.* **D61** (2000) 052001.
- [40] LEP Working Group on  $|V_{ub}|$ :  
<http://battagl.home.cern.ch/battagl/vub/vub.html>.
- [41] Particle Data Group, D.E. Groom *et al.*, *Eur. Phys. J.* **C15** (2000) 1.
- [42] A. Ali and D. London, *Eur. Phys. J.* **C18** (2001) 665;  
see also *Eur. Phys. J.* **C9** (1999) 687; *Phys. Rep.* **320** (1999) 79; hep-ph/0002167.
- [43] S. Plaszczynski and M.-H. Schune, LAL-99-67 [hep-ph/9911280].
- [44] Y. Grossman, Y. Nir, S. Plaszczynski and M.-H. Schune, *Nucl. Phys.* **B511** (1998) 69.
- [45] A. Höcker, H. Lacker, S. Laplace, F. Le Diberder, *Eur. Phys. J.* **C21** (2001) 225.
- [46] A.J. Buras and R. Buras, *Phys. Lett.* **B501** (2001) 223.
- [47] A.J. Buras and R. Fleischer, *Phys. Rev.* **D64** (2001) 115010.
- [48] F. De Fazio, DPT-00-46 [hep-ph/0010007].
- [49] K.G. Wilson, *Phys. Rev.* **179** (1969) 1499;  
K.G. Wilson and W. Zimmermann, *Comm. Math. Phys.* **24** (1972) 87;  
W. Zimmerman, in the proceedings of the 1970 Brandeis Summer Institute in Theoretical Physics, eds. S. Deser, M. Grisaru and H. Pendleton, MIT Press (1971) p. 369; *Ann. Phys.* **77** (1973) 570.
- [50] T. Inami and C.S. Lim, *Progr. Theor. Phys.* **65** (1981) 297.
- [51] G. Buchalla, A.J. Buras and M.K. Harlander, *Nucl. Phys.* **B349** (1991) 1.

- [52] F.J. Gilman and M.B. Wise, *Phys. Rev.* **D20** (1979) 2392;  
G. Altarelli, G. Curci, G. Martinelli and S. Petrarca, *Phys. Lett.* **B99** (1981) 141;  
A.J. Buras and P.H. Weisz, *Nucl. Phys.* **B333** (1990) 66.
- [53] W.A. Bardeen, A.J. Buras, D.W. Duke and T. Muta, *Phys. Rev.* **D18** (1978) 3998.
- [54] A.J. Buras, *Nucl. Phys.* **B434** (1995) 606.
- [55] G. Buchalla, A.J. Buras and M.E. Lautenbacher, *Rev. Mod. Phys.* **68** (1996) 1125.
- [56] A.J. Buras, in the proceedings of the Les Houches 1997 Summer School on Theoretical Physics: Probing the Standard Model of Particle Interactions, July 28 – September 5, 1997, Les Houches, France, eds. R. Gupta, A. Morel, E. de Rafael and F. David, North-Holland, Amsterdam (1998) [hep-ph/9806471].
- [57] A.J. Buras, M. Jamin, M.E. Lautenbacher and P.H. Weisz, *Nucl. Phys.* **B400** (1993) 37;  
A.J. Buras, M. Jamin and M.E. Lautenbacher, *Nucl. Phys.* **B400** (1993) 75 and **B408** (1993) 209.
- [58] M. Ciuchini, E. Franco, G. Martinelli and L. Reina, *Phys. Lett.* **B301** (1993) 263;  
*Nucl. Phys.* **B415** (1994) 403.
- [59] G. 't Hooft and M. Veltman, *Nucl. Phys.* **B44** (1972) 189;  
P. Breitenlohner and D. Maison, *Comm. Math. Phys.* **52** (1977) 11, 39, 55.
- [60] A.J. Buras, M. Misiak and J. Urban, *Nucl. Phys.* **B586** (2000) 397.
- [61] M. Ciuchini, E. Franco, V. Lubicz, G. Martinelli, I. Scimemi and L. Silvestrini, *Nucl. Phys.* **B523** (1998) 501;  
A.J. Buras, S. Jäger and J. Urban, *Nucl. Phys.* **B605** (2001) 600.
- [62] R. Fleischer, *Z. Phys.* **C58** (1993) 483.
- [63] R. Fleischer, *Z. Phys.* **C62** (1994) 81.
- [64] M. Bander, D. Silverman and A. Soni, *Phys. Rev. Lett.* **43** (1979) 242.
- [65] D. London and R.D. Peccei, *Phys. Lett.* **B223** (1989) 257;  
N.G. Deshpande and J. Trampetic, *Phys. Rev.* **D41** (1990) 895 and 2926;  
J.-M. Gérard and W.-S. Hou, *Phys. Rev.* **D43** (1991) 2909; *Phys. Lett.* **B253** (1991) 478.
- [66] G. Kramer, W.F. Palmer and H. Simma, *Nucl. Phys.* **B428** (1994) 77; *Z. Phys.* **C66** (1995) 429.

- [67] A. Ali, G. Kramer and C. Lü, *Phys. Rev.* **D58** (1998) 094009.
- [68] A. Ali, G. Kramer and C. Lü, *Phys. Rev.* **D59** (1999) 014005.
- [69] H. Simma and D. Wyler, *Phys. Lett.* **B272** (1991) 395.
- [70] B.F. Ward, *Phys. Rev.* **D51** (1995) 6253.
- [71] S.L. Glashow, J. Iliopoulos and L. Maiani, *Phys. Rev.* **D2** (1970) 1285.
- [72] A.J. Buras and R. Fleischer, *Phys. Lett.* **B341** (1995) 379.
- [73] R. Fleischer, *Phys. Lett.* **B341** (1994) 205.
- [74] R. Fleischer, *Phys. Rev.* **D60** (1999) 073008.
- [75] M. Ciuchini, E. Franco, G. Martinelli and L. Silvestrini, *Nucl. Phys.* **B501** (1997) 271.
- [76] C. Isola, M. Ladisa, G. Nardulli, T.N. Pham and P. Santorelli, *Phys. Rev.* **D64** (2001) 014029.
- [77] M. Ciuchini, E. Franco, G. Martinelli, M. Pierini and L. Silvestrini, *Phys. Lett.* **B515** (2001) 33.
- [78] L. Wolfenstein, *Phys. Rev.* **D52** (1995) 537;  
J.F. Donoghue, E. Golowich, A.A. Petrov and J.M. Soares, *Phys. Rev. Lett.* **77** (1996) 2178;  
B. Blok, M. Gronau and J.L. Rosner, *Phys. Rev. Lett.* **78** (1997) 3999 and **79** (1997) 1167;  
M. Neubert, *Phys. Lett.* **B424** (1998) 152;  
J.-M. Gérard and J. Weyers, *Eur. Phys. J.* **C7** (1999) 1;  
A. Falk, A. Kagan, Y. Nir and A. Petrov, *Phys. Rev.* **D57** (1998) 4290;  
D. Atwood and A. Soni, *Phys. Rev.* **D58** (1998) 036005.
- [79] A.J. Buras, R. Fleischer and T. Mannel, *Nucl. Phys.* **B533** (1998) 3.
- [80] R. Fleischer, *Int. J. Mod. Phys.* **A12** (1997) 2459.
- [81] N.G. Deshpande and X.-G. He, *Phys. Lett.* **B336** (1994) 471.
- [82] R. Fleischer, *Phys. Lett.* **B321** (1994) 259.
- [83] R. Fleischer, *Phys. Lett.* **B332** (1994) 419.
- [84] N.G. Deshpande and X.-G. He, *Phys. Rev. Lett.* **74** (1995) 26 [E: *ibid.*, p. 4099].



- [85] M. Gronau, O. Hernández, D. London and J. Rosner, *Phys. Rev.* **D52** (1995) 6374.
- [86] A.J. Buras and R. Fleischer, *Phys. Lett.* **B365** (1996) 390.
- [87] A.J. Buras and R. Fleischer, *Eur. Phys. J.* **C11** (1999) 93.
- [88] R. Fleischer, *Phys. Lett.* **B365** (1996) 399.
- [89] M. Bauer, B. Stech and M. Wirbel, *Z. Phys.* **C34** (1987) 103;  
M. Wirbel, B. Stech and M. Bauer, *Z. Phys.* **C29** (1985) 637.
- [90] M. Neubert and B. Stech, in *Heavy Flavours II*, eds. A.J. Buras and M. Lindner, World Scientific, Singapore (1998) p. 294 [hep-ph/9705292].
- [91] J. Schwinger, *Phys. Rev. Lett.* **12** (1964) 630;  
D. Farikov and B. Stech, *Nucl. Phys.* **B133** (1978) 315;  
N. Cabibbo and L. Maiani, *Phys. Lett.* **B73** (1978) 418 [E: *ibid.* **B76** (1978) 663].
- [92] J.D. Bjorken, *Nucl. Phys. (Proc. Suppl.)* **B11** (1989) 325;  
M. Dugan and B. Grinstein, *Phys. Lett.* **B255** (1991) 583;  
H.D. Politzer and M.B. Wise, *Phys. Lett.* **B257** (1991) 399.
- [93] A.J. Buras and L. Silvestrini, *Nucl. Phys.* **B548** (1999) 293.
- [94] Z. Luo and J.L. Rosner, *Phys. Rev.* **D64** (2001) 094001.
- [95] M. Diehl and G. Hiller, *J. High Energy Phys.* **0106** (2001) 067.
- [96] A.J. Buras and J.-M. Gérard, *Nucl. Phys.* **B264** (1986) 371;  
A.J. Buras, J.-M. Gérard and R. Rückl, *Nucl. Phys.* **B268** (1986) 16.
- [97] R. Fleischer, *Nucl. Phys.* **B412** (1994) 201.
- [98] M. Beneke, G. Buchalla, M. Neubert and C.T. Sachrajda, *Phys. Rev. Lett.* **83** (1999) 1914.
- [99] M. Beneke, G. Buchalla, M. Neubert and C.T. Sachrajda, *Nucl. Phys.* **B591** (2000) 313.
- [100] M. Beneke, G. Buchalla, M. Neubert and C.T. Sachrajda, *Nucl. Phys.* **B606** (2001) 245.
- [101] H.-n. Li and H.L. Yu, *Phys. Rev. Lett.* **74** (1995) 4388 and *Phys. Rev.* **D53** (1996) 2480;  
C.H. Chang and H.-n. Li, *Phys. Rev.* **D55** (1997) 5577;

- T.W. Yeh and H.-n. Li, *Phys. Rev.* **D56** (1997) 1615;  
H.Y. Cheng, H.-n. Li and K.C. Yang, *Phys. Rev.* **D60** (1999) 094005.
- [102] Y.Y. Keum, H.-n. Li and A.I. Sanda, *Phys. Lett.* **B504** (2001) 6; *Phys. Rev.* **D63** (2001) 054008.
- [103] Y.Y. Keum and H.-n. Li, *Phys. Rev.* **D63** (2001) 074006.
- [104] G. Buchalla, lectures given at TASI 2000, June 4–30, 2000, Boulder, Colorado, CERN-TH-2001-041 [hep-ph/0103166].
- [105] A.J. Buras, M. Jamin, and P.H. Weisz, *Nucl. Phys.* **B347** (1990) 491.
- [106] S. Herrlich and U. Nierste, *Nucl. Phys.* **B419** (1994) 292; *Phys. Rev.* **D52** (1995) 6505; *Nucl. Phys.* **B476** (1996) 27.
- [107] L. Lellouch, *Nucl. Phys. (Proc. Suppl.)* **B94** (2001) 142.
- [108] W.A. Bardeen, A.J. Buras and J.-M. Gérard, *Phys. Lett.* **B211** (1988) 343;  
J. Bijnens and J. Prades, *Nucl. Phys.* **B444** (1995) 523; *J. High Energy Phys.* **0001** (2000) 002;  
T. Hambye, G.O. Köhler and P.H. Soldan, *Eur. Phys. J.* **C10** (1999) 271.
- [109] S. Bertolini, J.O. Eeg, M. Fabbrichesi and E.I. Lashin, *Nucl. Phys.* **B514** (1998) 63.
- [110] J.M. Flynn and L. Randall, *Phys. Lett.* **B224** (1989) 221 [E: **B235** (1989) 412];  
G. Buchalla, A.J. Buras and M.K. Harlander, *Nucl. Phys.* **B337** (1990) 313.
- [111] L. Wolfenstein, *Phys. Rev. Lett.* **13** (1964) 562.
- [112] KTeV Collaboration (A. Alavi-Harati *et al.*), *Phys. Rev. Lett.* **83** (1999) 22;  
for the most recent update given in (4.7), see  
<http://kpsa.fnal.gov:8080/public/ktev.html>.
- [113] NA48 Collaboration (V. Fanti *et al.*), *Phys. Lett.* **B465** (1999) 335;  
for the most recent update given in (4.7), see <http://na48.web.cern.ch/NA48/>.
- [114] S. Bertolini, M. Fabbrichesi and J.O. Eeg, *Rev. Mod. Phys.* **72** (2000) 65;  
M. Jamin, HD-THEP-99-51 [hep-ph/9911390];  
M. Ciuchini and G. Martinelli, *Nucl. Phys. (Proc. Suppl.)* **B99** (2001) 27;  
T. Hambye and P.H. Soldan, *Nucl. Phys. (Proc. Suppl.)* **B96** (2001) 323;  
E. Pallante, A. Pich and I. Scimemi, *Nucl. Phys.* **B617** (2001) 441.
- [115] A.J. Buras and J.-M. Gérard, *Phys. Lett.* **B517** (2001) 129.

- [116] D. Rein and L.M. Segal, *Phys. Rev.* **D39** (1989) 3325;  
J.S. Hagelin and L.S. Littenberg, *Prog. Part. Nucl. Phys.* **23** (1989) 1;  
M. Lu and M.B. Wise, *Phys. Lett.* **B324** (1994) 461;  
S. Fajfer, *Nuovo Cim.* **A110** (1997) 397;  
C.Q. Geng, I.J. Hsu and Y.C. Lin, *Phys. Rev.* **D54** (1996) 877.
- [117] G. Buchalla and G. Isidori, *Phys. Lett.* **B440** (1998) 170.
- [118] A.F. Falk, A. Lewandowski and A.A. Petrov, *Phys. Lett.* **B505** (2001) 107.
- [119] G. Buchalla and A.J. Buras, *Nucl. Phys.* **B398** (1993) 285 and **B400** (1993) 225;  
M. Misiak and J. Urban, *Phys. Lett.* **B451** (1999) 161.
- [120] G. Buchalla and A.J. Buras, *Nucl. Phys.* **B548** (1999) 309 and **B412** (1994) 106.
- [121] S. Adler *et al.*, *Phys. Rev. Lett.* **84** (2000) 3768.
- [122] G. Buchalla and A.J. Buras, *Phys. Lett.* **B333** (1994) 221; *Phys. Rev.* **D54** (1996) 6782.
- [123] Y. Grossman and Y. Nir, *Phys. Lett.* **B398** (1997) 163.
- [124] V.F. Weisskopf and E.P. Wigner, *Z. Phys.* **63** (1930) 54 and **65** (1930) 18.
- [125] A.J. Buras, W. Słominski and H. Steger, *Nucl. Phys.* **B245** (1984) 369.
- [126] J. Urban, F. Krauss, U. Jentschura and G. Soff, *Nucl. Phys.* **B523** (1998) 40.
- [127] L. Lellouch and C.D. Lin (UKQCD Collaboration), *Phys. Rev.* **D64** (2001) 094501;  
J. Flynn and C.D. Lin, *J. Phys.* **G27** (2001) 1245;  
C.T. Sachrajda, *Nucl. Instrum. Meth.* **A462** (2001) 23.
- [128] E. Bagan, P. Ball, V.M. Braun and H.G. Dosch, *Phys. Lett.* **B278** (1992) 457;  
M. Neubert, *Phys. Rev.* **D45** (1992) 2451;  
S. Narison, *Phys. Lett.* **B322** (1994) 247.
- [129] CLEO Collaboration (D.E. Jaffe *et al.*), *Phys. Rev. Lett.* **86** (2001) 5000.
- [130] Y. Grossman, B. Kayser and Y. Nir, *Phys. Lett.* **B415** (1997) 90.
- [131] LEP *B* Oscillation Working Group, see  
[http://lepibosc.web.cern.ch/LEPBOSC/combined\\_results/](http://lepibosc.web.cern.ch/LEPBOSC/combined_results/).
- [132] R. Fleischer and T. Mannel, *Phys. Lett.* **B506** (2001) 311.
- [133] W. Buchmüller and D. Wyler, *Nucl. Phys.* **B268** (1986) 621.

- [134] A.B. Carter and A.I. Sanda, *Phys. Rev. Lett.* **45** (1980) 952; *Phys. Rev.* **D23** (1981) 1567;  
I.I. Bigi and A.I. Sanda, *Nucl. Phys.* **B193** (1981) 85.
- [135] R. Fleischer, *Eur. Phys. J.* **C10** (1999) 299.
- [136] Y. Nir and D. Silverman, *Nucl. Phys.* **B345** (1990) 301.
- [137] OPAL Collaboration (K. Ackerstaff *et al.*), *Eur. Phys. J.* **C5** (1998) 379.
- [138] CDF Collaboration (T. Affolder *et al.*), *Phys. Rev.* **D61** (2000) 072005.
- [139] ALEPH Collaboration (R. Barate *et al.*), *Phys. Lett.* **B492** (2000) 259.
- [140] BaBar Collaboration (B. Aubert *et al.*), *Phys. Rev. Lett.* **86** (2001) 2515.
- [141] Belle Collaboration (A. Abashian *et al.*), *Phys. Rev. Lett.* **86** (2001) 2509.
- [142] D. Hitlin (BaBar Collaboration), plenary talk given at ICHEP 2000, July 27 – August 2, 2000, Osaka, Japan, BABAR-PROC-00-14 [hep-ex/0011024].
- [143] H. Aihara (Belle Collaboration), plenary talk given at ICHEP 2000, July 27 – August 2, 2000, Osaka, Japan, hep-ex/0010008.
- [144] A.L. Kagan and M. Neubert, *Phys. Lett.* **B492** (2000) 115;  
J.P. Silva and L. Wolfenstein, *Phys. Rev.* **D63** (2001) 056001;  
Z.-Z. Xing, hep-ph/0008018;  
G. Eyal, Y. Nir and G. Perez, *J. High Energy Phys.* **0008** (2000) 028;  
G. Barenboim, F.J. Botella and O. Vives, *Phys. Rev.* **D64** (2001) 015007;  
H. Fritzsch and Z.Z. Xing, *Phys. Lett.* **B506** (2001) 109;  
Y.-L. Wu and Y.-F. Zhou, *Int. J. Mod. Phys.* **A16** (2001) 4547;  
G. Bhattacharyya, A. Datta and A. Kundu, *Phys. Lett.* **B514** (2001) 47.
- [145] S. Bergmann and G. Perez, *Phys. Rev.* **D64** (2001) 115009.
- [146] A. Ali and E. Lunghi, *Eur. Phys. J.* **C21** (2001) 683.
- [147] A.J. Buras, P.H. Chankowski, J. Rosiek and L. Ślawnianowska, *Nucl. Phys.* **B619** (2001) 434.
- [148] P. Ball *et al.*, Report of the *b*-decay Working Group of the Workshop *Standard Model Physics (and More) at the LHC*, CERN-TH/2000-101 [hep-ph/0003238].
- [149] M. Gronau, O.F. Hernández, D. London and J.L. Rosner, *Phys. Rev.* **D52** (1995) 6356 and 6374.

- [150] Y. Grossman and M.P. Worah, *Phys. Lett.* **B395** (1997) 241.
- [151] CLEO Collaboration (G. Bonvicini *et al.*), *Phys. Rev. Lett.* **84** (2000) 5940.
- [152] J. Nash (BaBar Collaboration), talk given at Lepton Photon 01, July 23–28, 2001, Rome, Italy.
- [153] BaBar Collaboration (B. Aubert *et al.*), *Phys. Rev.* **D65** (2002) 032001.
- [154] Belle Collaboration (K. Abe *et al.*), BELLE-CONF-0101.
- [155] BaBar Collaboration (B. Aubert *et al.*), *Phys. Rev. Lett.* **87** (2001) 201803.
- [156] H. Tajima (Belle Collaboration), Belle Preprint 2001-8, contributed to the proceedings of the XXXVIth Rencontres de Moriond session devoted to QCD and High Energy Hadronic Interactions, March 17–24, 2001, Bourg-Saint-Maurice, France [hep-ex/0105024].
- [157] I. Dunietz, H.R. Quinn, A. Snyder, W. Toki and H.J. Lipkin, *Phys. Rev.* **D43** (1991) 2193.
- [158] A.S. Dighe, I. Dunietz and R. Fleischer, *Eur. Phys. J.* **C6** (1999) 647.
- [159] A.S. Dighe, I. Dunietz and R. Fleischer, *Phys. Lett.* **B433** (1998) 147.
- [160] I. Dunietz, R. Fleischer and U. Nierste, *Phys. Rev.* **D63** (2001) 114015.
- [161] Ya.I. Azimov, V.L. Rappoport and V.V. Sarantsev, *Z. Phys.* **A356** (1997) 437;  
Y. Grossman and H.R. Quinn, *Phys. Rev.* **D56** (1997) 7259;  
J. Charles, A. Le Yaouanc, L. Oliver, O. Pène and J.-C. Raynal, *Phys. Lett.* **B425** (1998) 375;  
B. Kayser and D. London, *Phys. Rev.* **D61** (2000) 116012;  
H.R. Quinn, T. Schietinger, J.P. Silva, A.E. Snyder, *Phys. Rev. Lett.* **85** (2000) 5284.
- [162] D. London and A. Soni, *Phys. Lett.* **B407** (1997) 61.
- [163] R. Fleischer and T. Mannel, *Phys. Lett.* **B511** (2001) 240.
- [164] Belle Collaboration (K. Abe *et al.*), BELLE-CONF-0113.
- [165] CLEO Collaboration (R.A. Briere *et al.*), *Phys. Rev. Lett.* **86** (2001) 3718.
- [166] BaBar Collaboration (B. Aubert *et al.*), *Phys. Rev. Lett.* **87** (2001) 151801.

- [167] X.-G. He, J.P. Ma and C.-Y. Wu, *Phys. Rev.* **D63** (2001) 094004;  
H.-Y. Cheng and K.-C. Yang, *Phys. Rev.* **D64** (2001) 074004;  
S. Mishima, hep-ph/0107163;  
C.-H. Chen, Y.-Y. Keum and H.-n. Li, *Phys. Rev.* **D64** (2001) 112002.
- [168] Y. Grossman, G. Isidori and M.P. Worah, *Phys. Rev.* **D58** (1998) 057504.
- [169] R. Fleischer, *Phys. Lett.* **B459** (1999) 306.
- [170] M. Gronau, *Phys. Lett.* **B300** (1993) 163;  
R. Aleksan *et al.*, *Phys. Lett.* **B356** (1995) 95;  
F. DeJongh and P. Sphicas, *Phys. Rev.* **D53** (1996) 4930;  
P.S. Marrocchesi and N. Paver, *Int. J. Mod. Phys.* **A13** (1998) 251;  
A. Ali, G. Kramer and C.-D. Lü, in [68];  
B.F. Ward, in [70].
- [171] J.P. Silva and L. Wolfenstein, *Phys. Rev.* **D49** (1994) R1151; *Phys. Rev.* **D62** (2000) 014018.
- [172] CLEO Collaboration (D. Cronin-Hennessy *et al.*), *Phys. Rev. Lett.* **85** (2000) 515.
- [173] BaBar Collaboration (B. Aubert *et al.*), *Phys. Rev. Lett.* **87** (2001) 151802.
- [174] Belle Collaboration (K. Abe *et al.*), *Phys. Rev. Lett.* **87** (2001) 101801.
- [175] R. Fleischer, *Eur. Phys. J.* **C16** (2000) 87.
- [176] J. Dorfan (BaBar Collaboration), talk given at Lepton Photon 01, July 23–28, 2001, Rome, Italy;  
BaBar Collaboration (B. Aubert *et al.*), BABAR-CONF-01/05 [hep-ex/0107074].
- [177] M. Gronau and D. London, *Phys. Rev. Lett.* **65** (1990) 3381.
- [178] M. Gronau, D. Pirjol and T.-M. Yan, *Phys. Rev.* **D60** (1999) 034021.
- [179] S. Gardner, *Phys. Rev.* **D59** (1999) 077502.
- [180] CLEO Collaboration (D.M. Asner *et al.*), *Phys. Rev.* **D65** (2002) 031103.
- [181] Y. Grossman and H.R. Quinn, *Phys. Rev.* **D58** (1998) 017504.
- [182] J. Charles, *Phys. Rev.* **D59** (1999) 054007.
- [183] M. Gronau, D. London, N. Sinha and R. Sinha, *Phys. Lett.* **B514** (2001) 315.
- [184] H. Lipkin, Y. Nir, H. Quinn and A. Snyder, *Phys. Rev.* **D44** (1991) 1454.

- [185] A. Snyder and H. Quinn, *Phys. Rev.* **D48** (1993) 2139.
- [186] H. Quinn and J. Silva, *Phys. Rev.* **D62** (2000) 054002.
- [187] A. Deandrea, R. Gatto, M. Ladisa, G. Nardulli and P. Santorelli, *Phys. Rev.* **D62** (2000) 036001.
- [188] R. Enomoto and M. Tanabashi, *Phys. Lett.* **B386** (1996) 413;  
S. Gardner, H.B. O'Connell and A.W. Thomas, *Phys. Rev. Lett.* **80** (1998) 1834.
- [189] R. Enomoto, Y. Okada and Y. Shimizu, *Phys. Lett.* **B433** (1998) 109.
- [190] I. Bediaga, R.E. Blanco, C. Göbel and R. Mendez-Galain, *Phys. Rev. Lett.* **81** (1998) 4067.
- [191] A.J. Buras and R. Fleischer, *Phys. Lett.* **B360** (1995) 138.
- [192] R. Fleischer and T. Mannel, *Phys. Lett.* **B397** (1997) 269.
- [193] F. Würthwein, private communication;  
M. Tanaka (CDF Collaboration), *Nucl. Instrum. Meth.* **A462** (2001) 165.
- [194] R.G. Sachs, EFI-85-22 (unpublished);  
I. Dunietz and R.G. Sachs, *Phys. Rev.* **D37** (1988) 3186 [E: *ibid.* **D39** (1988) 3515];  
I. Dunietz, *Phys. Lett.* **B427** (1998) 179.
- [195] *The BaBar Physics Book*, eds. P. Harrison and H. Quinn, SLAC report 504 (1998).
- [196] M. Diehl and G. Hiller, *Phys. Lett.* **B517** (2001) 125.
- [197] R. Fleischer and I. Dunietz, *Phys. Lett.* **B387** (1996) 361.
- [198] For an analysis of the physics potential at the  $\Upsilon(5S)$  resonance, see S. Petrak, BABAR NOTE 507 (1999).
- [199] J.S. Hagelin, *Nucl. Phys.* **B193** (1981) 123;  
E. Franco, M. Lusignoli and A. Pugliese, *Nucl. Phys.* **B194** (1982) 403;  
L.L. Chau, *Phys. Rep.* **95** (1983) 1;  
M.B. Voloshin, N.G. Uraltsev, V.A. Khoze and M.A. Shifman, *Sov. J. Nucl. Phys.* **46** (1987) 112;  
A. Datta, E.A. Paschos and U. Türke, *Phys. Lett.* **B196** (1987) 382;  
A. Datta, E.A. Paschos and Y.L. Wu, *Nucl. Phys.* **B311** (1988) 35;  
R. Aleksan, A. Le Yaouanc, L. Oliver, O. Pene and J.C. Raynal, *Phys. Lett.* **B316** (1993) 567.

- [200] A. Stocchi, talk given at ICHEP 2000, July 27 – August 2, 2000, Osaka, Japan, LAL-00-55 [hep-ph/0010222].
- [201] A.J. Buras, in the proceedings of ICHEP 1996, July 25–31, 1996, Warsaw, Poland, eds. Z. Ajduk and A.K. Wroblewski, World Scientific, Singapore (1997) p. 243 [hep-ph/9610461].
- [202] M. Beneke, G. Buchalla and I. Dunietz, *Phys. Rev.* **D54** (1996) 4419.
- [203] M. Beneke, G. Buchalla, C. Greub, A. Lenz and U. Nierste, *Phys. Lett.* **B459** (1999) 631.
- [204] S. Hashimoto and N. Yamada (JLQCD Collaboration), talk given at BCP4, February 19–23, 2001, Ise-Shima, Japan, KEK-CP-108 [hep-ph/0104080]; S. Hashimoto, K. Ishikawa, T. Onogi, M. Sakamoto, N. Tsutsui and N. Yamada, *Phys. Rev.* **D62** (2000) 114502.
- [205] D. Becirevic, D. Meloni, A. Retico, V. Gimenez, V. Lubicz and G. Martinelli, *Eur. Phys. J.* **C18** (2000) 157.
- [206] M. Beneke and A. Lenz, *J. Phys.* **G27** (2001) 1219.
- [207] I. Dunietz, *Phys. Rev.* **D52** (1995) 3048.
- [208] R. Fleischer and I. Dunietz, *Phys. Rev.* **D55** (1997) 259.
- [209] R. Fleischer, *Phys. Rev.* **D58** (1998) 093001.
- [210] R. Fleischer, in the proceedings of the 2nd Conference on B Physics and CP Violation, March 24–28, 1997, Honolulu, Hawaii, eds. T.E. Browder, F.A. Harris and S. Pakvasa, World Scientific, Singapore (1998) p. 469 [hep-ph/9705404].
- [211] C.-W. Chiang and L. Wolfenstein, *Phys. Rev.* **D61** (2000) 074031.
- [212] Y. Grossman, *Phys. Lett.* **B380** (1996) 99.
- [213] R. Aleksan, I. Dunietz and B. Kayser, *Z. Phys.* **C54** (1992) 653.
- [214] M. Gronau and D. London, *Phys. Lett.* **B253** (1991) 483.
- [215] D. London, N. Sinha and R. Sinha, *Phys. Rev. Lett.* **85** (2000) 1807.
- [216] A. Falk and A. Petrov, *Phys. Rev. Lett.* **85** (2000) 252.
- [217] A. Dighe, I. Dunietz, H. Lipkin and J. Rosner, *Phys. Lett.* **B369** (1996) 144.



- [218] J. Rosner, *Phys. Rev.* **D42** (1990) 3732.
- [219] CDF Collaboration (T. Affolder *et al.*), *Phys. Rev. Lett.* **85** (2000) 4668.
- [220] See, for instance, D. Chang, *Nucl. Phys.* **B214** (1983) 435;  
G. Ecker and W. Grimus, *Nucl. Phys.* **B258** (1985) 328; *Z. Phys.* **C30** (1986) 293.
- [221] G. Barenboim, J. Bernabeu, J. Matias and M. Raidal, *Phys. Rev.* **D60** (1999) 016003.
- [222] P. Ball, J.-M. Frère and J. Matias, *Nucl. Phys.* **B572** (2000) 3.
- [223] P. Ball and R. Fleischer, *Phys. Lett.* **B475** (2000) 111.
- [224] D. Silverman, *Phys. Rev.* **D58** (1998) 095006.
- [225] M. Gronau and D. Wyler, *Phys. Lett.* **B265** (1991) 172.
- [226] CLEO Collaboration (M. Athanas *et. al.*), *Phys. Rev. Lett.* **80** (1998) 5493.
- [227] Belle Collaboration (K. Abe *et. al.*), *Phys. Rev. Lett.* **87** (2001) 111801.
- [228] D. Atwood, I. Dunietz and A. Soni, *Phys. Rev. Lett.* **78** (1997) 3257.
- [229] D. Atwood, I. Dunietz and A. Soni, *Phys. Rev.* **D63** (2001) 036005;  
D. Atwood, talk given at BCP4, February 19–23, 2001, Ise-Shima, Japan, AMES-HET-01-03 [hep-ph/0103345].
- [230] M. Gronau, *Phys. Rev.* **D58** (1998) 037301.
- [231] Z.-Z. Xing, *Phys. Rev.* **D58** (1998) 093005.
- [232] R. Fleischer and T. Mannel, *Phys. Rev.* **D57** (1998) 2752.
- [233] M. Gronau and J.L. Rosner, *Phys. Lett.* **B439** (1998) 171.
- [234] J. Jang and P. Ko, *Phys. Rev.* **D58** (1998) 111302.
- [235] I. Dunietz, *Phys. Lett.* **B270** (1991) 75.
- [236] M. Masetti, *Phys. Lett.* **B286** (1992) 160.
- [237] R. Fleischer and D. Wyler, *Phys. Rev.* **D62** (2000) 057503.
- [238] M. Galdón, R. Pérez Ochoa, M.A. Sanchis-Lozano, J.A. Valls, *Nucl. Phys. (Proc. Suppl.)* **B50** (1996) 311.

- [239] J.-F. Liu and K.-T. Chao, *Phys. Rev.* **D56** (1997) 4133;  
P. Colangelo and F. De Fazio, *Phys. Rev.* **D61** (2000) 034012.
- [240] FOCUS Collaboration (J.M. Link *et al.*), *Phys. Lett.* **B485** (2000) 62.
- [241] S. Bergmann, Y. Grossman, Z. Ligeti, Y. Nir and A.A. Petrov, *Phys. Lett.* **B486** (2000) 418.
- [242] E791 Collaboration (E.M. Aitala *et al.*), *Phys. Lett.* **B445** (1999) 449; *Phys. Rev. Lett.* **83** (1999) 32.
- [243] CLEO Collaboration (D. Cronin-Hennessy *et al.*), hep-ex/0102006.
- [244] CLEO Collaboration (R. Godang *et al.*) *Phys. Rev. Lett.* **84** (2000) 5038.
- [245] J. Tanaka (Belle Collaboration), talk given at BCP4, February 19–23, 2001, Ise-Shima, Japan, hep-ex/0104053.
- [246] C.C. Meca and J.P. Silva, *Phys. Rev. Lett.* **81** (1998) 1377.
- [247] J.P. Silva and A. Soffer, *Phys. Rev.* **D61** (2000) 112001.
- [248] M. Gronau, J. Rosner and D. London, *Phys. Rev. Lett.* **73** (1994) 21.
- [249] O. Hernández, D. London, M. Gronau and J. Rosner, *Phys. Lett.* **B333** (1994) 500; *Phys. Rev.* **D50** (1994) 4529;  
M. Gronau, O. Hernandez, D. London and J. Rosner, *Phys. Rev.* **D52** (1995) 6356.
- [250] CLEO Collaboration (R. Godang *et al.*), *Phys. Rev. Lett.* **80** (1998) 3456.
- [251] CLEO Collaboration (S. Chen *et al.*), *Phys. Rev. Lett.* **85** (2000) 525.
- [252] Belle Collaboration (K. Abe *et al.*), *Phys. Rev.* **D64** (2001) 071101.
- [253] R. Fleischer, *Eur. Phys. J.* **C6** (1999) 451.
- [254] M. Gronau and J. Rosner, *Phys. Rev.* **D57** (1998) 6843.
- [255] M. Neubert and J. Rosner, *Phys. Lett.* **B441** (1998) 403; *Phys. Rev. Lett.* **81** (1998) 5076.
- [256] M. Neubert, *J. High Energy Phys.* **9902** (1999) 014.
- [257] A.J. Buras and R. Fleischer, *Eur. Phys. J.* **C16** (2000) 97.
- [258] A. Falk, A. Kagan, Y. Nir and A. Petrov, in [78].

- [259] R. Fleischer, *Phys. Lett.* **B435** (1998) 221.
- [260] M. Gronau and J. Rosner, *Phys. Rev.* **D58** (1998) 113005.
- [261] M. Gronau and D. Pirjol, *Phys. Lett.* **B449** (1999) 321;  
K. Agashe and N. Deshpande, *Phys. Lett.* **B451** (1999) 215 and **B454** (1999) 359.
- [262] W.-S. Hou, J.G. Smith and Frank Würthwein, NTU-HEP-99-25 [hep-ex/9910014].
- [263] R. Fleischer and T. Mannel, TTP-97-22 [hep-ph/9706261].
- [264] D. Choudhury, B. Dutta and A. Kundu, *Phys. Lett.* **B456** (1999) 185;  
X.-G. He, C.-L.Hsueh and J.-Q. Shi, *Phys. Rev. Lett.* **84** (2000) 18.
- [265] Y. Grossman, M. Neubert and A. Kagan, *J. High Energy Phys.* **9910** (1999) 029.
- [266] R. Fleischer and J. Matias, *Phys. Rev.* **D61** (2000) 074004.
- [267] J. Matias, *Phys. Lett.* **B520** (2001) 131.
- [268] A. Khodjamirian, R. Rückl and C.W. Winhart, *Phys. Rev.* **D58** (1998) 054013;  
E. Bagan, P. Ball and V.M. Braun, *Phys. Lett.* **B417** (1998) 154;  
P. Ball, *J. High Energy Phys.* **9809** (1998) 005.
- [269] W.-S. Hou and K.-C. Yang, *Phys. Rev.* **D61** (2000) 073014.
- [270] M. Neubert, CLNS-00-1660 [hep-ph/0001334], presented at the ICTP Summer School in Particle Physics, June 7 – July 9, 1999, Trieste, Italy.
- [271] S.J. Brodsky and G. Lepage, *Phys. Lett.* **B87** (1979) 359 and *Phys. Rev.* **D22** (1980) 2157;  
R. Field *et al.*, *Nucl. Phys.* **B186** (1981) 429.
- [272] J.L. Rosner, *Phys. Rev.* **D64** (2001) 094002.
- [273] A. Khodjamirian, *Nucl. Phys.* **B605** (2001) 558.
- [274] A.L. Kagan, *Phys. Rev.* **D51** (1995) 6196.
- [275] D. Pirjol, *Phys. Rev.* **D60** (1999) 054020.
- [276] H. Lipkin, *Phys. Lett.* **B415** (1997) 186.
- [277] I. Dunietz, in the proceedings of the Workshop on *B* Physics at Hadron Accelerators, Snowmass, Colorado, eds. P. McBride and C. Shekhar Mishra, p. 83 (1993).
- [278] M. Gronau and J. Rosner, *Phys. Lett.* **B482** (2000) 71.

- [279] P. Ball and V.M. Braun, *Phys. Rev.* **D58** (1998) 094016.
- [280] P.Z. Skands, *J. High Energy Phys.* **0101** (2001) 008.
- [281] E. Jenkins and M.J. Savage, *Phys. Lett.* **B281** (1992) 331.
- [282] B. Grinstein, E. Jenkins, A.V. Manohar, M.J. Savage and M.B. Wise, *Nucl. Phys.* **B380** (1992) 369.
- [283] UKQCD Collaboration (L. Lellouch *et al.*), *Nucl. Phys. (Proc. Suppl.)* **B73** (1999) 357.
- [284] H. Georgi, *Weak Interactions and Modern Particle Theory* (Addison–Wesley Publishing Company, Redwood City, California, 1984).
- [285] C.-W. Chiang and L. Wolfenstein, *Phys. Lett.* **B493** (2000) 73.
- [286] M. Gronau, *Phys. Lett.* **B492** (2000) 297.
- [287] T. Hurth and T. Mannel, *Phys. Lett.* **B511** (2001) 196.
- [288] S.W. Bosch and G. Buchalla, *Nucl. Phys.* **B621** (2002) 459;  
see also M. Beneke, T. Feldmann and D. Seidel, *Nucl. Phys.* **B612** (2001) 25.
- [289] M. Gronau and J.L. Rosner, *Phys. Lett.* **B500** (2001) 247.
- [290] L.F. Abbott, P. Sikivie and M.B. Wise, *Phys. Rev.* **D21** (1980) 1393.
- [291] A.J. Buras and L. Silvestrini, *Nucl. Phys.* **B546** (1999) 299;  
A.J. Buras, G. Colangelo, G. Isidori, A. Romanino and L. Silvestrini, *Nucl. Phys.* **B566** (2000) 3.
- [292] A. Masiero and O. Vives, *Nucl. Phys. Proc. Suppl.* **B99** (2001) 228;  
S.A. Abel and J.M. Frère, *Phys. Rev.* **D55** (1997) 1623;  
A.L. Kagan and M. Neubert, *Phys. Rev. Lett.* **83** (1999) 4929;  
M. Brhlik, L.L. Everett, G.L. Kane, S.F. King and O. Lebedev, *Phys. Rev. Lett.* **84** (2000) 3041;  
R. Barbieri, R. Contino and A. Strumia, *Nucl. Phys.* **B578** (2000) 153;  
K.S. Babu, B. Dutta and R.N. Mohapatra, *Phys. Rev.* **D61** (2000) 091701;  
A. Masiero, M. Piai, A. Romanino and L. Silvestrini, *Phys. Rev.* **D64** (2001) 075005;  
M. Dine, E. Kramer, Y. Nir and Y. Shadmi, *Phys. Rev.* **D63** (2001) 116005.

- [293] T. Goto, N. Kitazawa, Y. Okada and M. Tanaka, *Phys. Rev.* **D53** (1996) 6662;  
Y. Grossman, Y. Nir and M.P. Worah, *Phys. Lett.* **B407** (1997) 307;  
A.L. Kagan and M. Neubert, in [144];  
M. Randhawa and M. Gupta, *Phys. Lett.* **B516** (2001) 446.
- [294] A.J. Buras, *Phys. Lett.* **B333** (1994) 476; *Nucl. Instr. Meth.* **A368** (1995) 1.
- [295] Y. Grossman, Y. Nir and R. Rattazzi, in [11].
- [296] A. Alavi-Harati *et al.*, *Phys. Rev.* **D61** (2000) 072006.
- [297] S. Bergmann and G. Perez, *J. High Energy Phys.* **0008** (2000) 034.
- [298] ALEPH Collaboration (R. Barate *et al.*), *Eur. Phys. J.* **C19** (2001) 213.
- [299] M. Misiak, talk given at the XXXVIth Rencontres de Moriond, March 10–17, 2001, Les Arcs, France [hep-ph/0105312].
- [300] Muon  $g - 2$  Collaboration (H.N. Brown *et al.*), *Phys. Rev. Lett.* **86** (2001) 2227.
- [301] T. Hurth, CERN-TH-2001-146 [hep-ph/0106050];  
T. Mannel, talk given at BCP4, February 19–23, 2001, Ise-Shima, Japan, TTP01-09 [hep-ph/0103310];  
C. Greub, talk given at the 8th International Symposium on Heavy Flavor Physics, July 25 – 29, 1999, Southampton, England, BUTP-99-22 [hep-ph/9911348];  
A. Ali, in the proceedings of the 7th International Symposium on Heavy Flavor Physics, July 7–11, 1997, Santa Barbara, California, ed. C. Campagnari, World Scientific, Singapore (1999) p. 196 [hep-ph/9709507].